IDENTIFICATION OF POINT PROCESS SYSTEMS WITH APPLICATION TO COMPLEX NEURONAL NETWORKS

by

Abdul Majeed Amjad

A thesis

Submitted to the Faculty of Science

of the University of Glasgow

for the degree of

Doctor of Philosophy

April 1989

This thesis is dedicated to

my parents

CONTENTS

ACKNOWLEDGEMENTS

I would like to express my deepest gratitude to my supervisors Mr. Peter Breeze and Dr. Jay Rosenberg of Statistics and Physiology Departments at the University of Glasgow, firstly, for suggesting the topics studied in this thesis, and secondly for their invaluable guidance, constant interest and continual encouragement, without which this thesis would have not been presented.

I would also like to thank Dr. David Halliday for many useful discussions which we had in the course of this project.

I wish to extend my thanks to Professor D. M. Titterington, Head of the Department, and to the staff members for providing me with every possible assistance, statistical or otherwise, in a very friendly environment. A word of special thanks to Mr. Tom Aitchison, whose consideration, affection and help was of great value, and also to Miss Mary Nisbet for her kindness in helping with the preparation of this thesis.

I would also like to express my appreciation to all my friends and fellow research students for making my stay here so enjoyable.

I am grateful to the Ministries of Education, Government of Pakistan and Government of Baluchistan, Pakistan, for their financial support.

Finally, I wish to express my heartfelt thanks to my family whose continuing understanding, encouragement and patience have carried me through my many years of study and research.

SUMMARY

The main aim of the thesis is to develop and apply statistical and computational techniques for the system identification of the complex interactions that occur between the components of neuronal networks within the central nervous system. An analysis of these interactions will provide a basis for understading the operations that the central nervous system uses to carry out particular tasks.

In order to work effectively, it is necessary for a statistician to become familiar with the background for understanding the physiological problems. In Chapter 1, a brief description of the neuromuscular control system followed by a more detailed discussion of the muscle spindle, a particular component of the neuromuscular control system we are interested in, is given. The next section describes the problems we will be studying in this thesis. The final part of this chapter presents the basic data sets mainly obtained on the muscle spindle under different experimental conditions, and which will form the experimental material for our studies.

Chapter 2 presents a review of the general theory of point processes. A formal definition of point process is given. Some standard assumptions, e.g., stationarity, orderliness, and strong mixing, are described on the basis of which the theory is developed, and finally certain point process parameters in both time and frequency domains are defined.

In Chapter 3 we introduce a univariate point process. Certain parameters are defined in both the time and frequency domain. The estimates and their asymptotic properties are discussed.

Construction of asymptotic confidence intervals for certain parameters in both time and frequency domains is carried out and illustrated by using the data sets described in Chapter 1. The main object of this chapter is, firstly, to emphasize the importance of the estimation of the power spectrum as it is a fundamental parameter in multivariate point process analysis, and secondly, to compare the methods available in both domains. A variety of procedures for estimating the power spectrum are discussed. In a comparison of the methods in both domains, it is shown by a number of illustrations that the frequency domain procedures are more informative and effective than the time domain ones.

In Chapter 4, introducing a bivariate stationary point process, we define certain parameters useful for measuring the association and timing relation between two processes in both domains. The main aim of this chapter is again to compare the procedures in both domains. Estimation of these parameters is discussed by extending the procedures given in Chapter 3. Examining the asymptotic properties of the estimates, approximate asymptotic confidence intervals for certain parameters are constructed and illustrated by using simulated data followed by the spindle data. The problem of identification of a point process system is introduced and, considering each input to and output from the spindle as realisations of a bivariate point process, a linear model relating the output to the input is developed. This model is a special case of the Volterra expansion for point processes introduced by Brillinger. Parameters related to this model e.g., coherence and phase provide a powerful tool for measuring the strength of association and timing relation between two processes. A comparison of these parameters with the corresponding time domain parameters e.g. the cross-intensity function, again shows that the frequency domain methods reveal some extra features of the processes. The results obtained in both domains suggest that the output discharges from the spindle are independent in the absence of any input. The activation of any of the static gamma inputs is seen to impose a coupling between the two discharges over roughly the same range of frequencies. The effect of each input, however, is seen to differ in that each input imposes a different time delay between the output discharges. The phase parameter provides useful information for such a comparison.

The usefulness of the frequency domain procedures is further extended to the situation when the system is assumed to receive many inputs and give rise to sevaral outputs. Chapter 5 mainly deals with such situations. This chapter presents an extensive development of the wide range of applicability of a Fourier-based approach to measures of association and related problems. In order to answer the question if the association between two processes is because of a direct connection or if it is a consequence of a common input, and the extended question how the association and timing relation between a pair of outputs is altered by the presence of a number of inputs, the idea of partial parameters is introduced. Certain partial parameters in the frequency domain are defined and derived, and their estimation is considered. A point process linear model relating a single output to two inputs is developed, and the identification of the muscle spindle (assumed to be acted upon by two static gamma inputs) is carried out. The model suggests that the two inputs jointly increase the linear predictability of the sensory discharges from the same muscle spindle. The model is further extended to a more general one in order to include a number of inputs. This may be an ideal model in the identification of the muscle spindle in a more realistic situation when it is acted upon by several inputs. Parameters related to this model are defined, their estimation procedures are discussed. Certain tests of significance are also developed and demonstrated by using the spindle data.

The final part of this chapter considers a further complicated situation when the system receives a multiple-input and gives rise to a multiple-output. The idea is to study the picture of the spindle under normal and real conditions. For this purpose, a linear regression-type multivariate point process model is introduced and developed. Various measures of inter-relationships between the inputs and the outputs are defined. The partial parameters of higher order are also discussed. The estimates and their asymptotic properties are examined, and finally these procedures are demonstrated by a large number of examples using simulated as well as real data on the spindle. The model, in our case, seems to work effectively. Some examples, however, give a possible indication of non-linear structure present in the processes.

In Chapter 6 we extend the linear point process system identification techniques to the systems which are assumed to be non-linear. The simplest non-linear case is quadratic. Certain third order (quadratic) time domain parameters, e.g., the third order product density, conditional density, and cumulant density, are defined and their estimates are considered. It is shown by a simulated study that all the three parameters give different informations about the non-linearities. The application of these parameters is demonstrated by using the real data on muscle spindle. The third order parameters are further extended to order-4. The aim is to have more insight into the processes under investigation. Estimates of the fourth order product density are considered. Asymptotic confidence intervals are constructed and illustrated. In the frequency domain, the third order spectrum is defined and illustrated. A quadratic model relating a single output to a single input is introduced and developed which leads to the quadratic coherence, a measure of quadratic effects that the input has on the output. The estimation and application of the quadratic coherence is demonstrated. The final section of this chapter extends the quadratic model in order to include a second input. The model is solved under the assumption that the inputs are two independent Poisson processes, and which leads to a simple solution for the identification of a non-linear system with two inputs (independent Poisson processes). The results obtained in both domains reveal significant non-linear features of the muscle spindle.

Chapter 7, considering the situations and problems for future work, gives a list of possible ways in which the work of this thesis may be extended.

CHAPTER 1

NEUROPHYSIOLOGY : A BRIEF DESCRIPTION

1.1 INTRODUCTION

Many biological systems have the important feature that under normal conditions they are acted upon by several inputs simultaneously, and in response may give rise to several outputs. This feature of biological systems plays a crucial role in its function. The muscle spindle, for example, is one particularly important component of the neuromuscular control system which is thought to provide information to the other parts of the nervous system that is important in the control of movement and maintenance of posture. The spindle, under normal conditions, is acted upon by a continuous change in the length of the muscle which occurs as a consequence of movement. In addition to the length change, the output activity from the spindle is further modified by several other input processes which are initiated from within the central nervous system.

The pattern of the activity of the components of the central nervous system reveals a certain degree of randomness associated with the signals transmitted by these components. In fact, it has been recognised by many statisticians that the field of neurophysiology provides a rich source of problems and data relating to stochastic processes (Brillinger, 1975c; Brillinger et al, 1976; Feinberg, 1974; Sampath and Srinivasan, 1977).

To give the necessary background for an understanding of the physiological problems, we first present a brief description of the neuromuscular control system followed by a more detailed discussion of one of its components, the muscle spindle, which is the one we are mainly interested in, and is also the source of data for our studies.

The final part of this Chapter provides a brief summary of the basic data sets which will be used as experimental material for the analysis in the subsequent Chapters.

1.2 NEUROMUSCULAR CONTROL SYSTEM

The neuromuscular control system may be considered as all those parts of the nervous and muscular systems which initiate and control movements and maintain posture. Anatomically and functionally this system has further been divided into two parts,

a. Central nervous system

b. Peripheral nervous system.

a. CENTRAL NERVOUS SYSTEM (BRAIN)

The central nervous system consists of the brain and the spinal cord. The human brain contains a complicated network of perhaps ten billion highly specialised cells called **neurones** or nerve cells. Like other cells, the neurone is bounded by a thin membrane and has a cell body called a **soma**. A number of extensions of the cell, projected from the soma, are called the dendrites and the axon. Normally, a cell gives rise to a single axon but this axon may give off side branches and characteristically divides up into a number of smaller branches just before terminating. A cell body is about 30 micra across and the dendrites perhaps 200 to 300 μm long. The length of axon from one nerve cell to the next varies from 50 μm to several meters long. The nerve cells are not isolated but rather interconnected in a very characteristic way. The points of connections, called synapses, are of particular importance, for it is at this point where the information flows from one cell to another. So the neurones form neuronal networks, and it is the characteristics of these networks that determine the behaviour of the nervous system. Fig.1.2.1 illustrates a schematic diagram of a small network of three neurones.

Cell bodies are clustered in certain areas in the brain while other regions consist of axons running from one group of neurones to another. In these regions large numbers of closely packed axons run parallel to form structures called fibre tracks. Similar

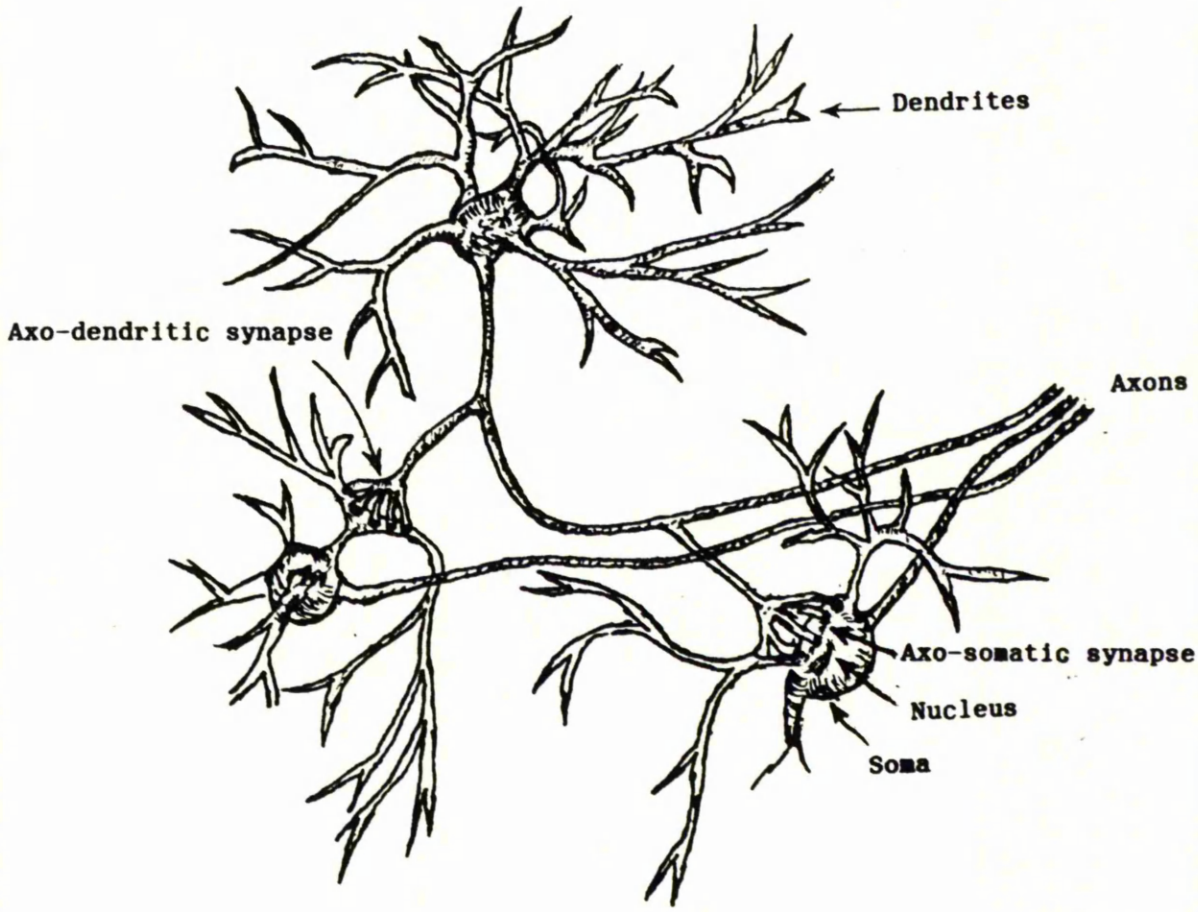

Fig.1.2.1

Schematic diagram showing a small network of three neurones.

tracks run outside of brain to muscles where they are referred to as nerves.

The neurone is the basic unit of the animal involved in the transmission of information. One way the information is transmitted through the dendrites and axon is via changes in electrical activity. An abrupt pulse-like change in the membrane potential is usually called a nerve impulse or action potential. This can be elicited in the nerve fibre by almost any factor that suddenly increases the permeability to certain ions, for example, electrical stimulation, mechanical compression, application of chemicals to the membrane, etc. The nerve impulse is approximately 100 mv in amplitude and 1 msec in duration. Because of this relatively short duration impulses are often referred to as spikes. Spikes are propagated along the axon with a velocity which depends in part on the diameter of the axon. A neurone cell can generate propagated impulses repetitively to produce a train of spikes with mean frequency which may vary from pulse every few seconds to several hundred pulses per second. When a pulse reaches the synapse it provokes the release of a transmitter substance which alters the permeability of the dendrites of the next cell to certain ions. The resulting flow of ions generates a small electric current which moves down the dendrites to the soma. If the synapse is excitatory the spike activity of the second cell is increased, if inhibitory it is decreased.

b. PERIPHERAL NERVOUS SYSTEM

The peripheral nervous system, at the level of spinal cord, has a sequence of organisationally identical repeating units called "segmental levels" of the spinal cord. Fig.1.2.2 illustrates the components of the peripheral neuromuscular system at one segmental level. A large number of classes of nerve cells lie within the spinal cord in groups or nuclei, which may have as many as 2000 cells. One of

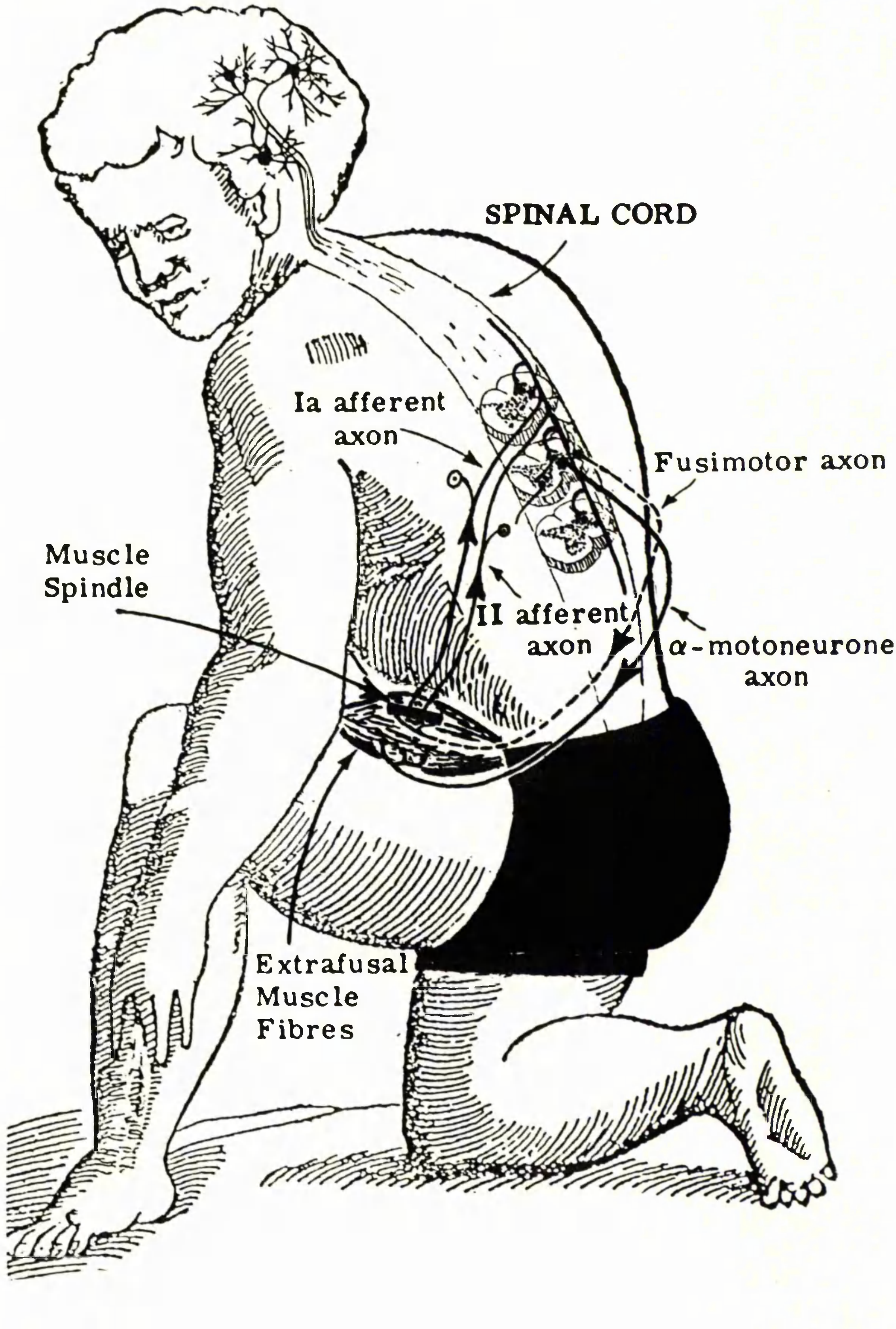

Fig.1.2.2

Diagram of some of the path-ways connecting a muscle spindle to the spinal cord. Some of the interactions between, and distribution of, the neuronal circuits within the spinal cord are also illustrated.

these groups is known as "α-motoneurone" . Diameters of the cell-bodies and the axons of these neurones range from 25 to 100 μm and from 8 to 20 μm, respectively. The axons of these neurones leave the spinal cord to innervate the load-bearing or "extrafusal" muscle fibres forming the main mass of the muscles responsible for generating forces or changes of length. These axons normally conduct impulses from their cell-bodies to the extrafusal muscle fibres at a velocity ranging from 50 tO 120 m/sec. Once the axon of an α-motoneurone reaches a muscle, it divides into a number of fine branches. These terminal branches end on specialised areas of the extrafusal fibres called the "motor endplate". When an impulse reaches the junction between the axon and the muscle fibre, a sequence of electro-chemical events occurs which leads to the contraction of the muscle fibres. Each terminal branch of the α-motoneurone innervates a single extrafusal fibre of one muscle. All of the extrafusal fibres that are innervated by one α-motoneurone lie within the same muscle. The α-motoneurone and all the extrafusal fibres that it innervates are jointly called a "motor unit", the size of which and the number of motor units within a muscle vary from muscle to muscle depending on the function of that muscle.

Lying in parallel with the extrafusal fibres and the tendons, are a number of physiological transducers, also called "muscle receptors", which are very sensitive to imposed length changes or forces acting on the muscle. The nerves attached to these receptors, called "sensory nerves", normally transmit pulse-coded information in the form of spike trains to the groups of nerve cells lying within the spinal cord. After entering the spinal cord each sensory axon divides up into a number of branches which make synaptic-contact with a large number of cells over several segmental levels of the spinal cord. Each cell within the spinal cord receives input information from a large number of sensory axons coming from different receptors in the same muscle as well as from the receptors attached to different muscles. The electro-chemical events, which occur at the synapses as a consequence of all incoming spike trains from the receptors, then modify the on-going activity of these inter-related cells.

A further detail of the organisation of the spinal cord may be found in Shepherd (1974).

1.3 THE MUSCLE SPINDLE

One particularly important class of muscle receptors is known as the "muscle spindle". The muscle spindle is believed to have a critical role in the initiation of movement and the maintenance of posture. Most skeletal muscles, which are concerned with posture or movements, contain a number of muscle spindles lying parallel with the extrafusal fibres. They are composed of a number of highly specialised muscle fibres, called "intrafusal fibres", which lie parallel to each other and are contained partially within a fluid-filled capsule of connective tissue (Boyd,1962). These intrafusal fibres are much shorter than the extrafusal muscle fibres. They have been divided into three different categories,

1. The Dynamic Nuclear-Bag Fibres (Db_1),
2. The Static Nuclear-Bag Fibres (Sb_2),
3. The Nuclear-Chain Fibres (C).

The mechanical properties of these intrafusal fibres differ, and hence respond distinctly to length changes imposed on the parent muscle (Bessou and Pages, 1975, Boyd, 1980).

The information regarding the imposed length changes on the intrafusal fibres from the spindle to the spinal cord is transmitted by the two types of the sensory axons closely attached with the muscle spindle. These are the primary or group Ia , and the secondary or the group II sensory axons. The organisation of both sensory axons within the muscle spindle differs in that the terminal branches of the Ia sensory axon form spirals around the central region of each of the three types, Db_1, Ds_2, and C whereas the the terminal branches of the II sensory axons, lying to either side of the Ia ending, are associated with the nuclear-chain fibre (C), some of them, however, may lie on the static-bag fibre. Both the Ia and II sensory axons conduct impulses at a different conduction velocity. In the case of the Ia sensory axon, it ranges from 72 to 120 m/sec, whereas in the II sensory axons it is in the range 24-72 m/sec. When a muscle is held at a fixed length, the sensory axons from the muscle spindle generate impulses at a constant rate depending on the length at which the muscle is held (Matthews, and Stein, 1969). The rate, however, is increased with an increase in the muscle length.

Each muscle spindle is innervated by a single Ia sensory axon, but may have several II axons. The changes in activity in the Ia sensory axon in part reflect the responses to imposed length changes in all the three types of intrafusal fibres, whereas the activity in the II sensory axons reflect, mainly, changes in the nuclear-chain fibres. Both the sensory axons are found to project largely to different groups of cells within the spinal cord (Johansson,1981).

In addition, the intrafusal fibres are activated by another group of axons, called "gamma motoneurones" or "fusimotor axons" , which lie within the spinal cord in the neighbourhood of the α-motoneurones. The cell-bodies of these neurones are considerably smaller than those of the α-motoneurones. These motoneurones generate impulses at a velocity ranging from 10 to 50 m/sec, and innervate only the intrafusal fibres. Each gamma-motoneurone may innervate intrafusal fibres lying in different muscle spindles within the same muscle. These motoneurones have been divided into two types, the gamma-dynamic and gamma-static axons (Matthews, 1962, Emonet-Denand et al, 1977). The gamma-dynamic axons innervate the dynamic nuclear-bag fibres, whereas the gamma-static axons innervate either the nuclear-chain fibres or the static nuclear-bag fibres, or both (Boyd, 1980). A single muscle spindle may be innervated by as many as six gamma-motoneurones. Fig.1.3.1 summarises the main features of the muscle spindle. Fig.1.3.1a is a schematic diagram of the sensory and motor innervation of the muscle spindle. The spirals of the primary sensory ending are clearly seen wrapped round all the intrafusal fibres, whereas the terminals of the secondary sensory ending are largely restricted to the chain fibres. Fig.1.3.1b is a simplified diagram of the normal innervation of the muscle spindle. The Ia and II sensory axons and a single gamma-motoneurone of a muscle spindle is illustrated in Fig.1.2.2.

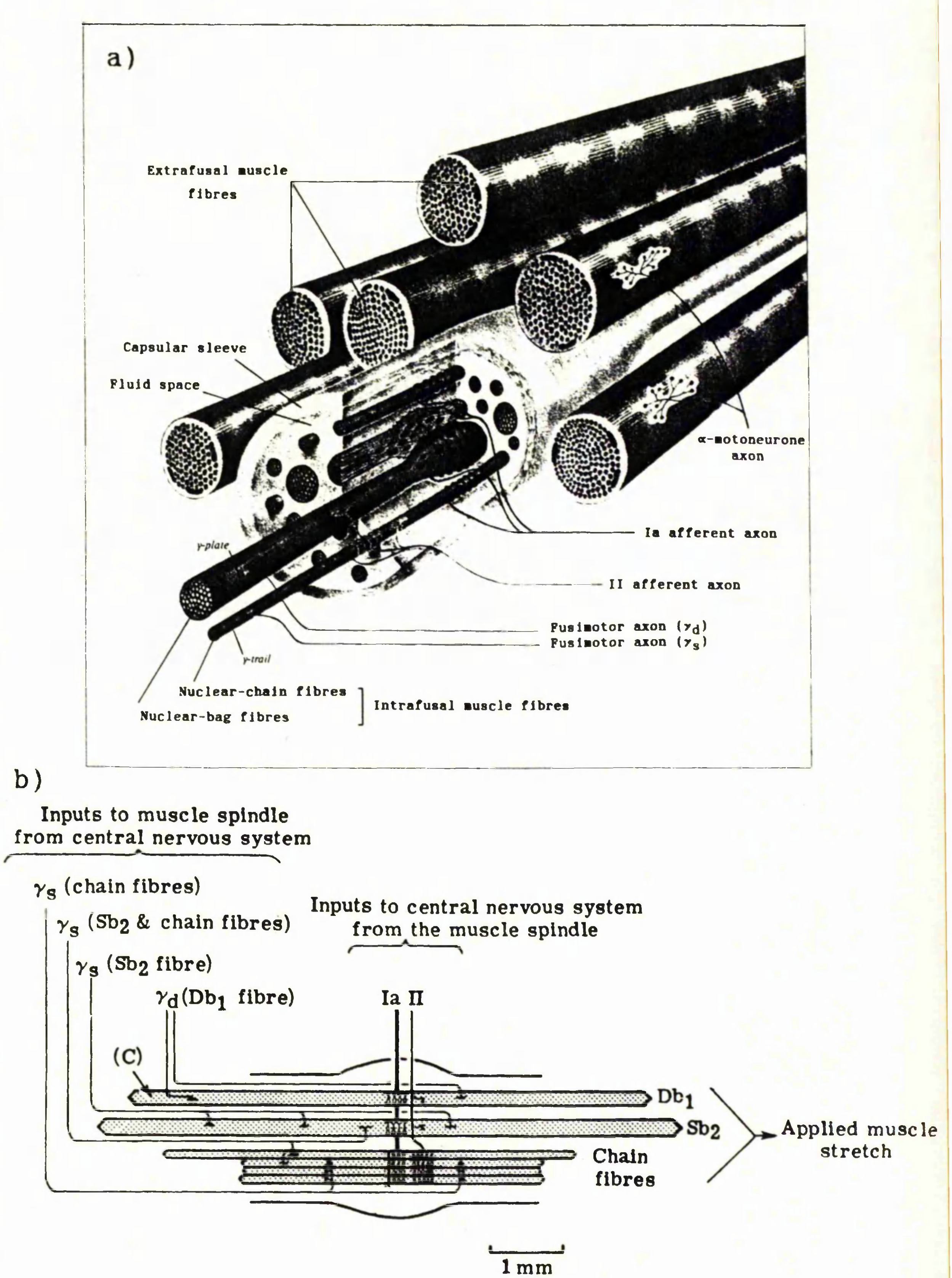

Fig.1.3.1

a) A schematic diagram of the sensory and motor innervation of the muscle spindle. The spirals of the primary sensory ending are seen wrapped round all the intrafusal fibres, whereas the terminals of the secondary sensory ending are restricted to the chain fibres

b) Simplified diagram of the normal innervation of the muscle spindle.

1.4 THE PROBLEMS

The study of the behaviour of the small networks of neurones frequently requires the determination of the measure of strength of association between component neurones, an assessment of the timing relation between them, and the identification of which of the neurones may interact directly or, are influenced by the common inputs.

Most of the identification techniques which have been recently applied to the muscle spindle data are based on the models involving length input, ℓ, and primary sensory neurone responses (e.g, Maclain et al, 1977; Rigas,1983) or involving fusimotor activity and primary sensory axons (Rigas,1983). Although the inherently multi-variable nature of the spindle is of considerable importance in terms of the role that it plays within the neuromuscular control system, only a few of the published studies have attempted to consider more than one input process (e.g., Matthews, 1981).

In order to answer to a wide range of questions relating to the identification of the muscle spindle in its more real situation, i.e., with multiple-input and multiple-output, one needs a framework of mathematical, statistical, and computational procedures related to multivariate analysis.

The object of this section of the Chapter is to outline the problems and questions to be answered in a further study of the neuromuscular control system.

The short duration with almost the same amplitude of the action potentials or spikes, compared with the intervals (random) between the times of occurance of these spikes and the variety of the observable patterns, provides the basis for considering a spike train as a realization of a stochastic point process along a line. Such a process is described fully by an ordered sequence of the realised times

$$\cdots < \tau_{-2} < \tau_{-1} < \tau_0 < \tau_1 < \tau_2 < \cdots$$

of occurance of the spikes (Cox and Lewis, 1966). Therefore the muscle spindle may be considered as a hybrid stochastic system involving continuous time series (random changes in the length of the muscle) and point processes (fusimotor inputs to and sensory outputs from the spindle). The problems we will consider include

A. Quantify the behaviour of the spindle by studying the Ia and II sensory responses from the same muscle spindle when it is assumed to be acted upon by different combinations of the fusimotor inputs and the length change.

B. Extend the linear point process model with single-input and single-output to the case when the spindle is assumed to receive two point process inputs. The aim is to study the characteristics of the sensory responses to the simultaneous activation of two fusimotor inputs, and to investigate the input-output relations.

C. Extend the linear model to a general one for the case when the muscle spindle is assumed to be acted upon by several, "r", point process inputs.

D. Develop a general multivariate regression-type point process linear model and measure the association and timing relation between any two of the sensory outputs, the Ia and the II's discharges, from the same spindle in the presence of 'r' fusimotor inputs in order to answer the question whether the association between these outputs is because of a direct connection between them or if it is a consequence of common inputs, and how the timing relation between these outputs are influenced by the presence of a number of inputs.

E. Extend the linear model to a non-linear (quadratic) one in order to include the non-linearities that have an important influence on the behaviour of the muscle spindles within the neuromuscular control system.

1.5 TYPICAL DATA SETS OBTAINED FROM MAMMALIAN MUSCLE SPINDLE

The data sets in this study were mainly obtained from a muscle spindle lying within the tenuissimus muscle in the hindlimb of deeply anaesthetized cats. This was done by isolating a muscle spindle within the parent muscle and dissecting the selected nerves, the fusimotor axons from the spinal cord and the primary and sensory nerves to the spinal cord. The parent muscle was clamped in a muscle puller to allow muscle length to be experimentally controlled. Fine silver wire electrodes insulated except for the tip were attached to the dissected nerve endings. The fusimotor axons were stimulated with voltage pulses, and the resulting primary and secondary responses in the form of sequences of pulses from the spindle were recorded. During the whole experiment the spindle and its blood supply were kept intact.

Under different experimental conditions the following data sets were obtained to form the experimental material for our studies. Some of the basic statistical characteristics of these data are also presented.

1. The Ia and II spontaneous discharges recorded from the same muscle spindle

In the absence of the fusimotor activity and the length change the Ia and II sensory axons generate nerve impulses at relatively constant rates (Matthews and Stein, 1969) depending on the length at which the parent muscle is held. The discharge from the sensory axons under these conditions is referred to as the spontaneous discharge of the spindle.

Fig.1.5.1a represents some simple graphical measures corresponding to the Ia spontaneous discharge. Fig.1.5.1a is the interval histogram (h=2msec) between the spikes shown in Fig.1.5.1c. Some of the basic statistics of the Ia discharge are also indicated in the figure. Fig.1.5.1b represents the scatter diagram of the adjacent intervals between the spikes, and reveals a small dispersion confirming the regularity of the Ia spontaneous discharge.

2. The Ia and the II discharges when a length change ℓ is imposed on the parent muscle.

Fig.1.5.2 gives some basic statistical characteristics of the Ia discharge when the length of the parent muscle is varied (illustrated in Fig.1.5.2e) through a servo-controlled muscle puller. Figs. 1.5.2a,b are the inter-spike-interval histogram and scatter plot of the Ia discharge, respectively, whereas Fig.1.5.2c is the $\log_{10}$ of the empirical survivor function (Cox and Lewis, 1968), and is given by

$$\log_{10} R_N(x)=\log_{10}\{\text{Proportion of the spike-intervals longer than } x\}$$

and gives evidence of a non-Poisson behaviour of the Ia

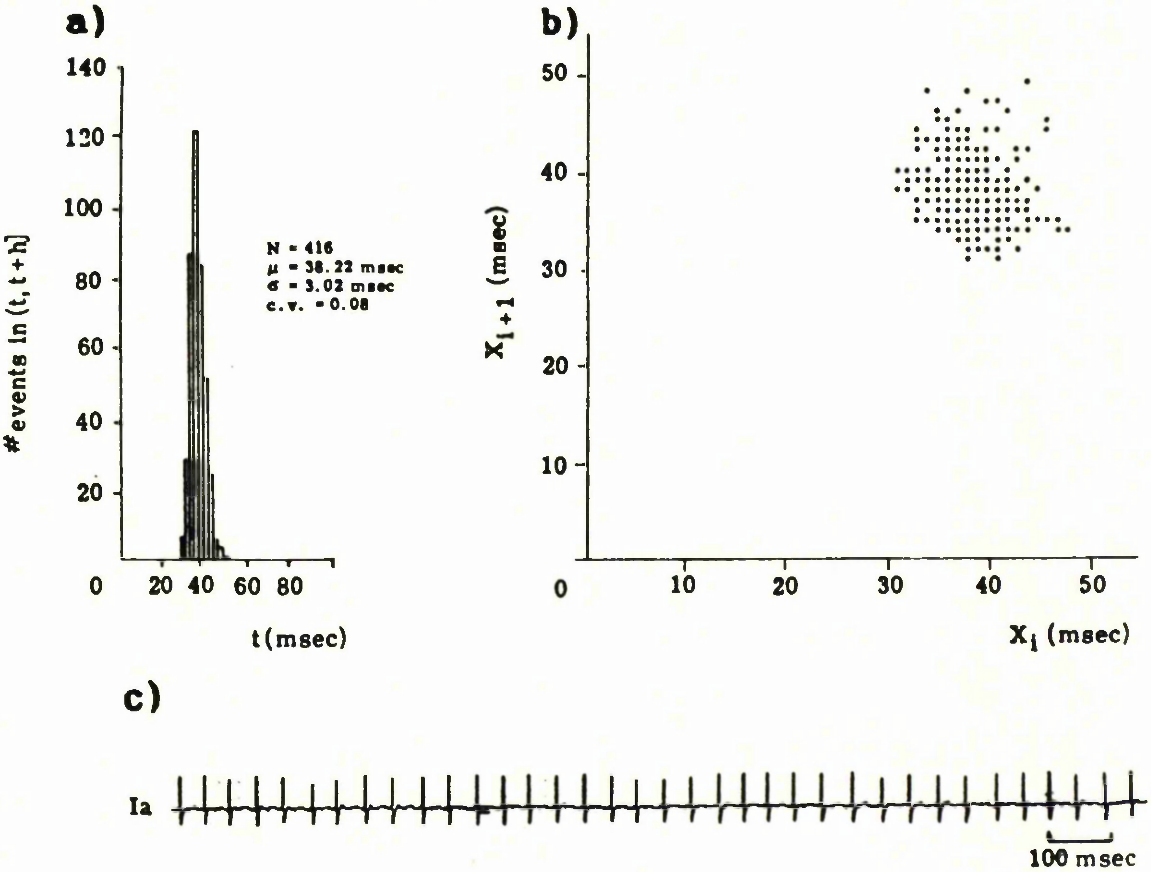

Fig.1.5.1 Basic statistics of the spontaneous Ia discharge

a) Histogram of the inter-spike intervals of the Spontaneous Ia discharge computed with h=2 msec.
b) Scatter plot of the adjacent inter-spike intervals of the Ia discharge
c) A realised sequence of spikes of the spontaneous Ia discharge.

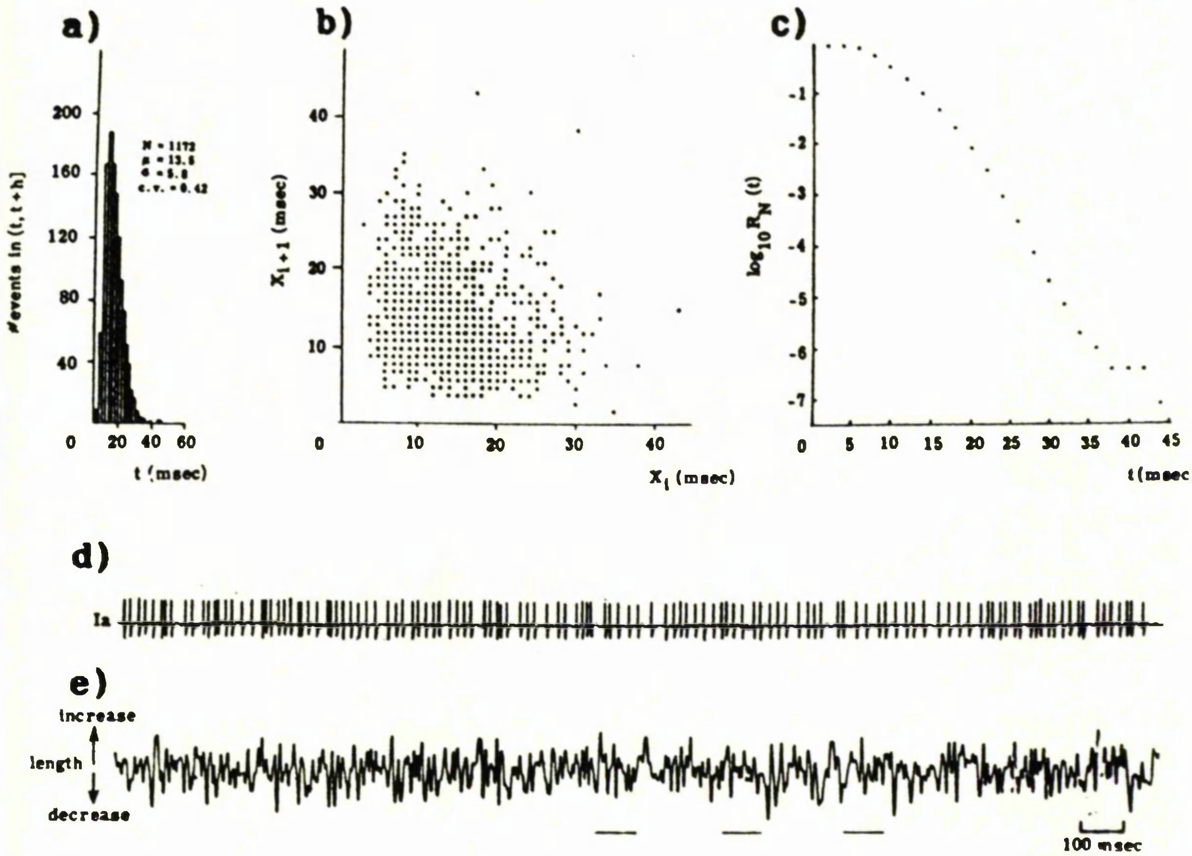

Fig.1.5.2 Basic statistics of the Ia discharge in the presence of a length change

a) Histogram (h=2msec) of the inter-spike intervals of the Ia discharge in the presence of a length change
b) Scatter plot of the adjacent inter-spike intervals of the Ia discharge
c) Log_{10} of the empirical survivor function
d) A realised sequence of spikes of the Ia discharge in the presence of a length change
e) A section of the continuous random length change with time imposed on the parent muscle

discharge. A comparison between Fig.1.5.1c and Fig.1.5.2d also suggests a loss of regularity in the Ia discharge.

3. The Ia and II discharges recorded from the same muscle spindle in the presence of a static gamma input, $_1\gamma_s$, alone

This data set consists of the Ia and II responses when one of the static fusimotor axons ($_1\gamma_s$) to the same muscle spindle is stimulated from the output of a Geiger counter placed close to a radioactive source. Fig.1.5.3c is the interval histogram of the static gamma input, and suggests an exponential distribution (i.e., a Poisson process). The insert in this figure gives a sequence of the spikes of the gamma input. Fig.1.5.3a is the histogram of the inter-spike intervals of the Ia discharge in the presence of $_1\gamma_s$, and clearly reveals that the fusimotor activity completely destroys the regularity of the Ia discharge as compared with Fig.1.5.1.

4. The Ia and II discharges from the same muscle spindle when it is activated by a second static gamma, $_2\gamma_s$, input.

5. The Ia and II discharges from the same muscle spindle in the presence of a concurrent and independent random stimulation of both static gamma inputs, $_1\gamma_s$ and $_2\gamma_s$.

6. The Ia and II discharges from the same muscle spindle when both the static gamma inputs, $_1\gamma_s$ and $_2\gamma_s$ are applied concurrently and independently in the presence of a length change ℓ.

Fig.1.5.3b gives the interval histogram of the Ia discharge (the insert gives a sequence of the Ia spikes) in the presence of a random length change and a static gamma input, $_1\gamma_s$.

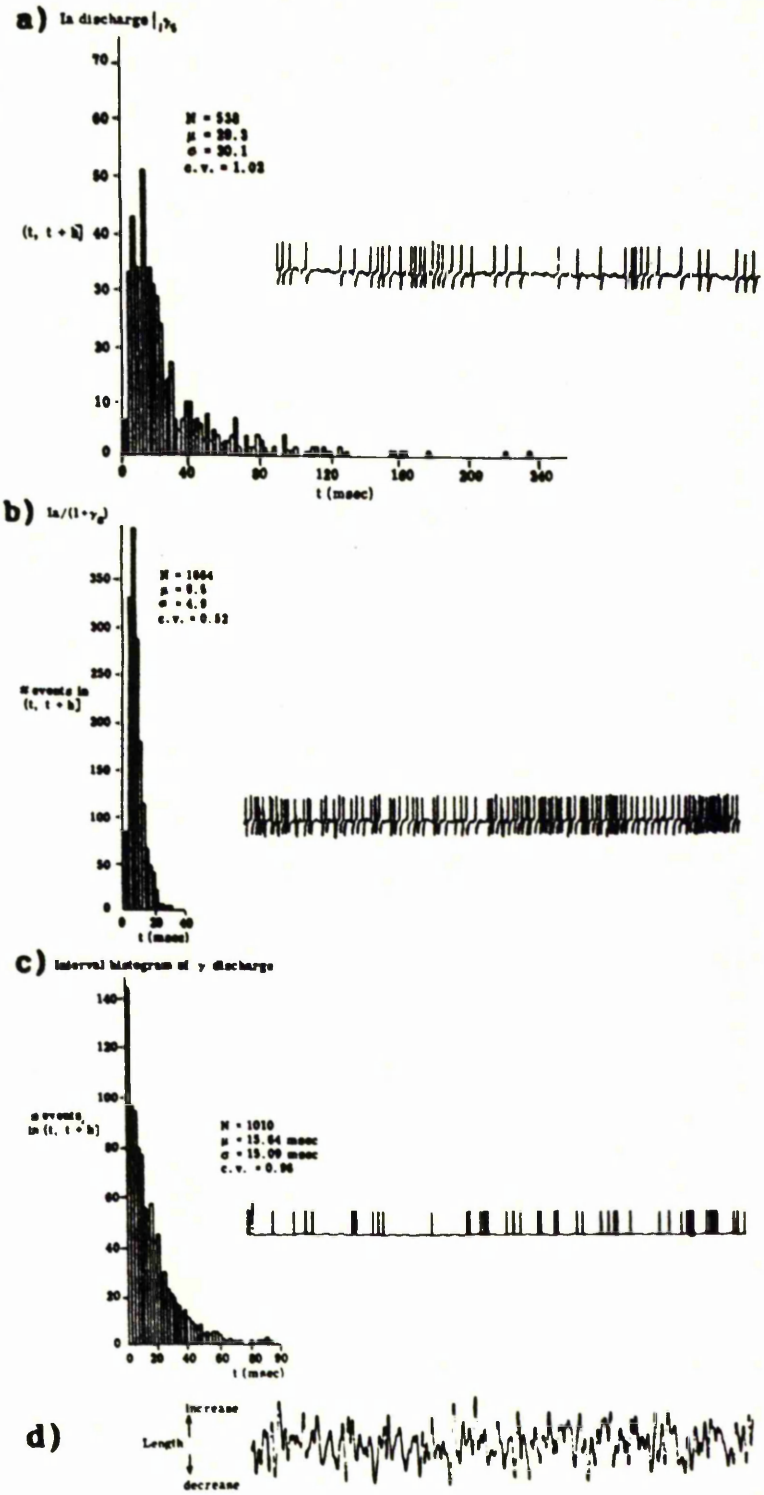

Fig.1.5.3 Basic statistics of the Ia discharge under different conditions

Histogram (h=2msec) of the inter-spike intervals of

(a) Ia discharge in the presence of a static gamma input, $_1\gamma_s$.

b) Ia discharge in the presence of $_1\gamma_s$ when a length change (a section of which is shown in Fig.d) is also imposed on the parent muscle.

c) Static gamma input, $_1\gamma_s$.

The insert in each figure gives a sequence of the spikes of the corresponding discharge.

This figure, as compared with Fig.1.5.3.a, suggests that the mechanism of the spindle responds differently to the fusimotor axon applied alone and along with a length input.

7. Single unit EMG recorded from the soleus muscle, an extension of the ankle, in the presence of a random stimulation of synergist medial gastronemius nerve at group I threshold.

In addition to the above data, a number of simulated studies will also be carried out which form the basis for understanding and interpreting the results obtained from the real data.

CHAPTER 2

STOCHASTIC POINT PROCESSES

2.1 INTRODUCTION

The analysis of the data and the related problems described in Chapter 1 require a formal framework of mathemetical, statistical and computational procedures involving both the time series and point processes. These subjects are a particular case of what is known as stochastic processes, and have been discussed by Doob(1953), Bartlett(1966), and Cramer and Leadbetter(1967).

The literatures concerning these two subjects are large and rapidly growing, and have developed comparatively independently of each other with the exception of Bartlett(1966) and Brillinger(1972). The main theory and applications in the case of time series are given in Jenkins and Watts(1968), Box and Jenkins(1970), Koopmans(1974), Bloomfield(1976), and Brillinger(1981) whereas, that in the case of point processes can be found in Cox and Lewis(1966), Lewis(1972), Brillinger(1975a), Cox and Isham(1980), Daley and Vere-Jones(1988).

Although there are many similarities between the two subjects, and in certain cases the parameters of one subject have direct analogues in the study of the other, there are situations when unique methods are only applicable to one but not to the other. An extensive discussion and a vast comparison of both the time series and point processes can be seen in Brillinger(1978).

In this chapter we present the general theory of point processes in order to form the basis for the statistical analysis of the data described in chapter 1.

We start with a brief description of the history of the point processes.

2.2 HISTORICAL NOTES ON POINT PROCESSES

A stochatic point process may be defined as a random, non-negative integer-valued measure, and often refers to isolated events occurring in time or space. Subject areas leading to the collection of point process data include queues, neuronal electrical activity, heartbeats, radioactivity, accident or failure processes, seismology and many others. A wide variety of examples are given in Lewis(1972).

The early history (1620-1742) of the study of point processes is known to begin with construction of life tables in the analysis of populations. Such a table corresponds to the superposition of many independent point processes, each with a single point at the time of death of an individual. This early history is discussed in more detail in Westgaard(1968).

The next era of point processes is related to the most important processes known as Poisson processes, and starts with the discovery of the Poisson distributuion credited to de Moivre and Poisson around 18th century. The poisson process was introduced over a long period. In 1868 Boltzman introduced the expression $\exp\{-\mu h\}$ for a probability of no events in an interval of duration h, and in 1910 Bateman determined the counting distributions by solving a set of differential equations (Height,1967). In 1909 Erlang applied the theory of Point processes to traffic problems, and then to communication problems to build better telephone systems by determining the optimal number of circuits. He is also known to have initiated the study of queuing systems involving input and output point processes which correspond to times of arrival and departure of customers. The queueing theory was further developed by Khinchine, Palm and many others (ref: Bhat, 1969).

Another class of point processes with a long history of study is known as Renewal processes in which the successive intervals between the events are independent and non-negative variables. The credit for the first serious investigation of these processes has been given to Herbelot (e.g., Lotka, 1957).

The late 1930's saw the beginning of substantial developments in the modelling of point processes by physicists to study radioactive decay and particle bombardment experiments.

A class of point correlation functions was introduced by Yvon in 1935 to study the dependency properties of certain point processes. Later, Ramakrishnan(1950) introduced multidimensional product densities to study the higher order dependencies of point processes.

Another form of point processes called the branching processes is described in Kendall(1975). Recent developments of point processes with applications to physiological and seismology problems may be found in Brillinger(1975b, 1986, 1988).

2.3 DEFINITION OF POINT PROCESS

Let $\underline{N}(t)=\{N_1(t), \cdots,\}$ $t \in \mathbf{R}$, be an r-vector random variable.

We say that $\underline{N}(t)$ is an r-vector valued stochastic point process if the individual components, $N_1(t)$, $N_2(t)$, $\cdots$, $N_r(t)$ are random non-negative integer-valued measures (Brillinger, 1975b).

More generally, suppose that $\underline{N}(I,s)$, $I \in B_{\mathbf{R}}$, $s \in S$, where $B_{\mathbf{R}}$ is the σ-algebra of Borel sets of the real line and (S, B_s, P) is the basic probability space, and let N_a $(a=1,2,\ldots r)$ be the a^{th} component of $\underline{N}$, then $N_a(I,s)$ gives the number of events of the process N_a that fall in the interval I for the realisation s. Since we refer to one realisation s, we suppress the dependence of N_a on s.

It is convenient for the development of the theory of point processes if we consider the following differential notation

$$d\underline{N}(t)=\#\{\underline{N} \text{ event in } (t,\ t+dt]\} \qquad -\infty<t<\infty$$

where $\#(\cdot)$ denotes the number of events of process $\underline{N}$ in a small interval of length dt.

2.4 ASSUMPTIONS

In the development of the theory of point processes we further set down some assumptions as follows:-

2.4.1 STATIONARITY

A point process is assumed to be stationary if its probabilistic structure does not change with time.

We say that the point process N_a $(a=1,2,\ldots,r)$ is "simple stationary" if the probability distribution of the number of events $N(t,\ t+h]$ is the same as that of the number of events $N(t+h,\ t+h+\tau]$ $\forall\ t,\tau,h\geq 0$.

We say that the point process N_a is " second-order stationary" (weakly stationary), if the joint probability distribution of the number of events $N(t,\ t+h_1]$ and $N(t+h_2,\ t+h_3]$ is the same as that of the number of events $N(t+\tau,\ t+h_1+\tau]$ and $N(t+h_2+\tau,\ t+h_3+\tau]$.

We say that the point process N_a is "completely stationary" (strong stationary) if the joint probability distribution of the number of events in any arbitrary number of intervals is invariant under translation. The verification of complete stationarity is quite impracticable, expect for small number of intervals.

The above definition can easily be extended to the case of an r-vector valued point process for which it is required that the joint probability distribution of the variate $\{N_{a_1}(I_1),\ \cdots,\ N_{a_\ell}(I_\ell)\}$ is invariant under translation, for $a_1,\cdots,a_\ell=1,\cdots,r$; $\ell=1,2,\cdots$

2.4.2 ORDERLINESS

A point process N_a is said to be orderly if

$$\Pr\{N(t,\ t+h]\geq 1\} = o(h)$$

i.e., the probability of two or more events occurring in the interval (t, t+h] tends to zero as $h\to 0$. This condition, in practice , prevents the occurrence of multiple events in small intervals.

Extending the definition of the orderliness, an r vector-valued point process $\underline{N}(t)$ is said to be orderly if the superposition of the component (marginal) point processes results in an orderly process. The process $\underline{N}(t)$ is called marginally orderly if the marginal processes are orderly. Thus orderliness implies marginally orderly; however a marginally orderly process need not be orderly (Cox and Lewis, 1972, Srinivasan, 1974).

2.4.3 STRONG MIXING

We also assume that the process N_a is strong mixing with (e.g., Brillinger, 1975b)

$$g(u) = \sup\{|\Pr\{AB\}-\Pr\{A\}\Pr\{B\}| : A\in B_{N(-\infty,t]}\ ,\ B\in B_{N(t+u,\infty)}\}$$

tending to zero as $u\to\infty$.

This condition can also be applied to the r vector-valued case by which the events of one component process, N_a, well-separated in time from ~~the~~ the events of the other component, N_b, of the process $\underline{N}$ are independent, for $a,b=1,\cdots,r$.

2.5 POINT PROCESS PARAMETERS

In this section we define certain parameters related to an r vector-valued stationary point process which provide useful tools in the analysis of a multivariate point process.

2.5.1 THE PRODUCT DENSITY FUNCTION OF ORDER-ℓ

Let $\underline{N}(t)=\{N_1(t), \cdots, N_r(t)\}$ be an r vector-valued stationary point process satisfying the conditions of orderliness and (strong) mixing. The product density of order-ℓ may be defined as

$$P_{a_1 \ldots a_\ell}(u_1, \cdots, u_{\ell-1}) = \text{Lim}_{\,h_1, \ldots, h_\ell \to 0} \Pr\{N_{a_1} \text{event in } (t+u_1,\ t+u_1+h_1],$$

$$N_{a_2} \text{event in } (t+u_2,\ t+u_2+h_2],\ \cdots,\ \text{and}$$

$$N_{a_\ell} \text{event in } (t,\ t+h_\ell]\}/h_1 h_2 \cdots h_\ell \qquad (2.5.1)$$

for $u_1, \cdots, u_{\ell-1}$, 0 distinct ; $a_1, \cdots, a_\ell = 1, \cdots, r$; $\ell = 1, 2, \cdots$ Under the condition of orderliness, expression (2.5.1) may be written as

$$P_{a_1 \ldots a_\ell}(u_1, \cdots, u_{\ell-1}) du_1 \cdots du_{\ell-1} dt$$

$$= E\{dN_{a_1}(t+u_1) \cdots dN_{a_{\ell-1}}(t+u_{\ell-1}) dN_{a_\ell}(t)\} \qquad (2.5.2)$$

where $dN_a(t)$ is defined in Section 2.3.

Particular cases of above definition are

$$P_a dt = E\{dN_a(t)\}$$

$$P_{ab}(u) du dt = E\{dN_a(t+u) dN_b(t)\}$$

$$P_{abc}(u,v)dudvdt = E\{dN_a(t+u)dN_b(t+v)dN_c(t)\}$$

for $u,v,0$ distinct; $a,b,c=1,2,\cdots,r$.

The product density of order-1, P_a, is called the mean intensity of the process a.

The above definition may be extended to include a number of singularities which occur within a process if the restriction on $u_1,\cdots,u_{\ell-1},0$ of being distinct is not imposed. It follows from the general definition I.3 of Appendix I, for example, that

$$E\{dN_a(t+u)dN_a(t)\} = \{P_{aa}(u)+\delta(u)P_a\}dudt$$

$$E\{dN_a(t+u)dN_a(t+v)dN_a(t)\} = \{P_{aaa}(u,v)+\delta(u-v)P_{aa}(v)+\delta(u)P_{aa}(v) +\delta(v)P_{aa}(u-v)+\delta(u)\delta(v)P_a\}dudvdt$$

where $\delta(\cdot)$ denotes the Dirac delta function.

2.5.2 THE CUMULANT DENSITY FUNCTION OF ORDER-ℓ

In addition to the product densities of order ℓ, we define the cumulant density function of order-ℓ of the stationary point process $\underline{N}$ as

$$q_{a_1\ldots a_\ell}(u_1,\cdots,u_{\ell-1})du_1\cdots du_{\ell-1}dt$$

$$= \mathrm{cum}\{dN_{a_1}(t+u_1),\cdots,dN_{a_{\ell-1}}(t+u_{\ell-1}),dN_{a_\ell}(t)\} \qquad (2.5.3)$$

for all $u_1,\cdots,u_{\ell-1},0$ distinct; $a_1,\cdots,a_\ell=1,\cdots,r$; $\ell=1,2,\cdots$

The singularities in the cumulants which occur within a process may also be accounted for in the same manner as that in the case of product densities (see definition I.3 of Appendix I).

The cumulant densities are connected directly with the product densities through the relations such as

$$q_a = P_a$$

$$q_{ab}(u) = P_{ab}(u)-P_aP_b$$

$$q_{abc}(u,v) = P_{abc}(u,v)-P_{ab}(u-v)P_c-P_{ac}(u)P_b-P_{bc}(v)P_a+2P_aP_bP_c$$

for $a,b,c=1,2,\cdots,r$; $u,v,0$ distinct.

The cumulant density functions provide useful measures of joint statistical dependences, and together with the product density functions are discussed in Ramakrishnan(1950). The cumulants and their properties in the case of ordinary random variables are presented in Definition I.2 of Appendix I.

2.5.3 THE SPECTRUM OF ORDER-ℓ

Let $\underline{N}(t)$ be an r vector-valued stationary point process satisfying the conditions of orderliness and (strong) mixing. Further, suppose that the ℓth order cumulant function given by expression (2.5.3) exists and satisfies the assumption I.2 of Appendix I. We define the spectrum of order ℓ as

$$f_{a_1\ldots a_\ell}(\lambda_1,\cdots,\lambda_{\ell-1})$$

$$= (2\pi)^{-\ell+1}\int\cdots\int\exp\left[-i\sum_{j=1}^{\ell-1}\lambda_j u_j\right]q_{a_1\ldots a_\ell}(u_1,\cdots,u_{\ell-1})du_1\cdots du_{\ell-1}$$

for $-\infty<\lambda_j<\infty$,$j=1,\cdots,\ell-1;a_1,\cdots,a_\ell=1,\cdots,r$; $\forall$ a_j distinct; $\ell=2,3,\cdots$, where i denotes $[-1]^{1/2}$.

CHAPTER 3

UNIVARIATE POINT PROCESSES

3.1 INTRODUCTION

Univariate point processes have been diccussed by many authors, see, for example, Cox and Lewis(1966), Brillinger(1975a). The field of neurophysiology provides a rich source of data which can be analysed within the framework of point process theory. The theory provides two parallel approaches to work with, i.e., the time domain approach and the frequency domain approach. Both domains, though mathematically equivalent, have certain advantages as well as disadvantages over each other. Methods in both domains taken together, however, provide a powerful collection of analysis techniques.

In this chapter certain parameters of a univariate point process in both domains are defined. Their estimation procedures and the properties of these estimates are discussed. Asymptotic confidence intervals of the parameters of interest are constructed, and finally, applications of these procedures to the data sets obtained on the muscle spindle are demonstrated.

The main aim of this chapter is to compare the procedures available in the both domains as well as, by the application of these procedures, to investigate the characteristics of the outputs from the muscle spindle, the Ia and the II discharges, when it is acted upon by various stimuli.

3.2 ANALYSIS IN THE TIME DOMAIN

This section deals with the definition, estimation, and application of certain parameters of a univariate point process in the time domain.

As defined in Chapter 2, a stochastic point process is a random, non-negative integer-valued measure with realisation as a sequence of events occuring in time or space. Let $\{N(t)\}$ be a univariate point process defined in time. A convenient way to develop the theory is to consider the differential process $\{dN(t)\}$ defined as

$$dN(t) = \#\{\text{events in } (t,t+dt]\}$$

where $\#\{A\}$ denotes the number of events in set A. With this differential notation, certain parameters useful in analysing univariate point processes in the time domain are defined in the following section.

3.2.1 TIME DOMAIN PARAMETERS

Time domain point process parameters directly analogous to the product moment functions of ordinary time series are provided by the product densities. In this section the product densities up to order-2 and some important functions derived from them which are useful in analysing a point process are discussed.

THE MEAN INTENSITY

A principal descriptor of a point process provided by its mean rate is called the product density of order-1 or the mean intensity. This parameter provides a measure of the intensity with which events occur. In general, it is a function of time but if the process is stationary it is a constant quantity and is defined as

$$P_N = \mathrm{Lim}_{h \to 0} \text{ Prob}\{ \text{ Event of process N in } (t,t+h]\}/h \qquad (3.2.1)$$

Further, if the process is orderly (Khintchine, 1960), we have

$$P_N = E\{dN(t)\}/dt \qquad (3.2.2)$$

THE SECOND ORDER PRODUCT DENSITY FUNCTION

The product density of order-2 of a stationary point process provides a measure of the intensity with which events separated by 'u' time units occur, and is given by

$$P_{NN}(u) = \text{Lim}_{h_1,h_2 \to 0} \text{ Prob}\{N \text{ event in } (t,t+h_1] \text{ and } N \text{ event in } (t+u,t+u+h_2]\}/h_1h_2 \qquad u \neq 0 \qquad (3.2.3)$$

Under the condition of orderliness,

$$P_{NN}(u) = E\{dN(t+u)dN(t)\}/dudt \qquad u \neq 0 \qquad (3.2.4)$$

Clearly, $P_{NN}(u)$ is an even function of u.

Under the (strong) mixing condition i.e increments of the processes well separated in time are independent, it follows that

$$\text{Lim}_{u \to \infty} P_{NN}(u) = P_N^2 \qquad (3.2.5)$$

THE AUTO-INTENSITY FUNCTION (AIF)

Another important function which describes the second order properties of a stationary point process is the autointensity function, and is defined as

$$m_{NN}(u) = \text{Lim}_{h \to 0} \text{ Prob}\{N \text{ event in } (t+u,t+u+h] | N \text{ event at } t\}/h \qquad (3.2.6)$$

$$m_{NN}(u) = E\{dN(t+u) | dN(t)=1\}/du \qquad u \neq 0 \qquad (3.2.7)$$

This function gives the measure of intensity with which the events occur at time u given that there is an event at the origin. From the definition of conditional probability, it follows that expression (3.2.6) can be written as

$$m_{NN}(u) = P_{NN}(u)/P_N \qquad u \neq 0 \qquad (3.2.8)$$

and under the (strong) mixing condition, it reduces to

$$\text{Lim}_{u\to\infty}\ m_{NN}(u) = P_N \qquad (3.2.9)$$

Expression (3.2.9) suggests that the function $m_{NN}(u)$ contains information about the mean intensity of the process. In practice $m_{NN}(u)$ should fluctuate around the mean rate of the process for large values of u.

THE AUTO-COVARIANCE FUNCTION (ACF)

The autocovariance function at lag u which describes the covariance structure between the increments separated by 'u' time units is defined as

$$\text{cov}\{dN(t+u),dN(t)\} = E\{dN(t+u)dN(t)\}-E\{dN(t+u)\}E\{dN(t)\}$$

$$= [P_N\delta(u)+q_{NN}(u)]dudt \qquad -\infty<u<\infty \qquad (3.2.10)$$

Where $\delta(.)$ is the Dirac delta function being added in order to take into account of the singularity at u=0 because of the fact that $\text{Var}[dN(t)]=P_N dt$ (Lewis, 1970). The function $q_{NN}(u)=P_{NN}(u)-P_N^2$ is the second order cumulant function and is assumed to be continuous at u=0.

Further, under the (strong) mixing condition,

$$\text{Lim}_{u\to\infty}\ q_{NN}(u) = 0 \qquad (3.2.11)$$

3.2.2 ESTIMATION OF THE PARAMETERS

We now turn to the problem of estimating the parameters described in the previous section. Under the condition of stationarity, the product density and the cumulant density functions depend on one less parameter than in the general case. This reduction has the important implication that plausible estimates of the parameters can be based on a single realization of the process.

Suppose that the process N is observed throughout the time (0,T]. Let τ_1 , τ_2 , τ_3 , . . . , $\tau_{N(T)}$ be the observed times of the total number of N(T) events which occurred in (0,T]. Consider the interval (0,T] divided into T/h intervals of length h. The number of times the event

" Point of process N in a small interval of length h"

occurred is N(T). A natural estimate of the mean intensity P_N is

$$\hat{P}_N = N(T)/T \qquad (3.2.12)$$

The value of this estimate is the reciprocal of the obvious estimate of the mean interval between events of the process.

The obvious estimates of the product density and autointensity functions are given by

$$\hat{P}_{NN}(u) = J_{NN}{}^{(T)}(u)/hT \qquad (3.2.13)$$

$$\hat{m}_{NN}(u) = J_{NN}{}^{(T)}(u)/hN(T) \qquad (3.2.14)$$

[Brillinger(1976a)]

where

$$J_{NN}{}^{(T)}(u) = \#\{(k,j) \text{ such that } u-(h/2) < \tau_k - \tau_j < u+(h/2)\} \qquad (3.2.15)$$

for j,k=1,2,3, ..., where h is a binwidth parameter, to be taken as small. The symbol #{A} denotes the number of counts in set A.

The variate $J_{NN}{}^{(T)}(u)$ counts the number of the events which fall in a bin of width h and midpoint u (Cox & Lewis,1966). This variate may also be explained by considering the record length T divided into small intervals $[(2h\ell-h)/2,\ (2h\ell+h)/2]$ $\ell=1,2,\ldots,L$ where L is the integral part of $(2T-h)/2h$ and then computing the number of differences $\tau_k-\tau_j$ which fall in each of these intervals.

Now as

$$J_{NN}^{(T)}(u) = J_{NN}^{(T)}(-u)$$

we need only the computation of (3.2.15) for $k \geq j$.

Finally, an estimate of $q_{NN}(u)$ can simply be obtained by inserting the respective estimates in expression (3.2.11) i.e

$$\hat{q}_{NN}(u) = \hat{P}_{NN}(u)-\hat{P}_N^2 \qquad u\neq 0 \qquad (3.2.16)$$

In the next section we discuss the asymptotic properties of these estimates.

3.2.3 PROPERTIES OF THE ESTIMATES

Suppose that the process N is given for $0 \leq t \leq T$. Then as $T\to\infty$, the variates $J_{NN}^{(T)}(u_\ell)$;$u_\ell=h\ell$, $\ell=1,2,\ldots,$ are asymptotically independent Poisson random variables with mean $hTP_{NN}(u_\ell)$ (Brillinger,1976a,b). which implies that

$$\hat{P}_{NN}(u) \sim (hT)^{-1}Po[hTP_{NN}(u)]$$

where $Po[\alpha]$ denotes a Poisson random variable with mean α.

Similarly,

$$\hat{m}_{NN}(u) \sim (hTP_N)^{-1}Po[hTP_{NN}(u)].$$

Furthermore, if $h\to 0$ but $hT\to\infty$ as $T\to\infty$,

$$J_{NN}^{(T)}(u) \sim N[hTP_{NN}(u)\ ,\ hTP_{NN}(u)] \qquad (3.2.17)$$

where $N[\alpha,\beta]$ denotes a normal random variable with mean α and variance β, Since under the above conditions a Poisson distribution may be well approximated by a normal distribution. It follows from (3.2.17) that as $h \to 0$, $hT \to \infty$, approximately

$$\hat{P}_{NN}(u) \sim N[P_{NN}(u)\ ,\ P_{NN}(u)/hT] \qquad (3.2.18)$$

With similar arguments it can be shown that

$$\hat{m}_{NN}(u) \sim N[m_{NN}(u)\ ,\ m_{NN}(u)/hTP_N] \qquad (3.2.19)$$

3.2.4 CONFIDENCE INTERVALS FOR THE AUTO-INTENSITY FUNCTION

The parameter $m_{NN}(u)$ may be used to assess the correlation structure between the increments of the process N. The limiting distribution of $m_{NN}(u)$ [expression 3.2.9] suggests that a confidence interval for $m_{NN}(u)$, under the null hypothesis that the increments are independent (Poisson process), can easily be constructed which may provide a useful tool for such an assessment.

A variety of procedures for the construction of an approximate 95% confidence interval for $m_{NN}(u)$, under the null hypothesis of independent increments, are considered as follows

Method 1

Under the (strong) mixing condition,

$$\text{Lim}_{u \to \infty}\, m_{NN}(u) = P_N$$

suggests that if the increments of the process are independent, the asymptotic distribution of $\hat{m}_{NN}(u)$ becomes

$$\hat{m}_{NN}(u) \sim N[P_N \, , \, 1/hT] \tag{3.2.20}$$

and which implies that an approximate 95% confidence interval under the hypothesis of independence, can simply be set up as

$$\hat{P}_N \pm 1.96 \, [1/hT]^{½} \tag{3.2.21}$$

Method 2

Applying a variance stablizing transformation for a Poisson variate, i.e., if X is a Poisson variate with mean α then

$$(X)^{½} \sim N[(\alpha)^{½} \, , \, 1/4] \qquad \text{(Kendall \& Stuart,1966)}$$

implies that the variate $[\hat{m}_{NN}(u)]^{½}$ will approximately be normal with mean $[m_{NN}(u)]^{½}$ and variance $1/4hTP_N$. Hence an approximate 95% confidence interval for $[m_{NN}(u)]^{½}$, under the hypothesis of independent increments of the process, becomes

$$(\hat{P}_N)^{½} \pm 1.96[(4hT\hat{P}_N)^{-1}]^{½}$$

or for convenience, simply

$$(\hat{P}_N)^{½} \pm [hN(T)]^{-½} \tag{3.2.22}$$

Then we obtain a confidence interval for $m_{NN}(u)$ by squaring the end points of the confidence interval for $[m_{NN}(u)]^{½}$.

Method 3

A third method of constructing the confidence interval may be achieved by using a modified estimate of $m_{NN}(u)$ which is based on a smoothed version of $J_{NN}^{(T)}(u)$. Following Cox(1965) and Brillinger(1976a), the modified estimate of $m_{NN}(u)$ is given by

$$\tilde{m}_{NN}(u) = 1/hN(T)[\Sigma w_i J_{NN}^{(T)}(u-ih)] \qquad (3.2.23)$$

where w_i are the smoothing weights which satisfy the condition $\Sigma w_i=1$. The distribution of this new estimate can be seen as asymptotically normal with mean $m_{NN}(u)$ and variance $(hTP_N)^{-1}m_{NN}(u)\Sigma w_i^2$. Hence applying again a square root transformation, we can construct an improved asymptotic 95% confidence interval for $[m_{NN}(u)]^{1/2}$ under the hypothesis of independence as

$$(\hat{P}_N)^{½} \pm \{[hN(T)]^{-1}\Sigma w_i^2\}^{½} \qquad (3.2.24)$$

For example, with a "Hanning window" (Tukey, 1977) as a smoothing scheme, the estimate (3.2.23) is seen to have the form

$$\tilde{m}_{NN}(u) = 1/hN(T)[0.25J_{NN}^{(T)}(u-h) + 0.5J_{NN}^{(T)}(u) + 0.25J_{NN}^{(T)}(u+h)] \qquad (3.2.25)$$

whereas the confidence interval (3.2.24) becomes as

$$(\hat{P}_N)^{½} \pm \{ 0.375[hN(T)]^{-1} \}^{½} \qquad (3.2.26)$$

3.2.5 APPLICATIONS

We now apply the above-mentioned procedures for estimating the autointensity function (AIF) and the asymptotic confidence interval for it to our spindle data sets in order to investigate the characteristics of the sensory axons when the muscle spindle is acted upon by various inputs.

Fig.3.2.1 and Fig.3.2.2 are the various estimates of the AIF of the Ia and II spontaneous discharges whereas Fig.3.2.3 and Fig.3.2.4 allow a comparison of AIF's of the Ia and II discharges when different stimuli are applied to the spindle. The record duration of each sample is T=60,000 msec. The lag value 'u' in each figure ranges from 0 to 512 msec.

Fig.3.2.1a and Fig.3.2.2a give the estimate $J_{NN}^{(T)}(u)$ of the Ia and II discharge respectively, computed with a binwidth h=1 msec. This histogram-like estimate, usually called the autocorrelation histogram (ACH), is commonly used by neurophysiologists (Bryant et al,1973). Both figures (Fig.3.2.1a and Fig.3.2.2a) suggest a periodic behaviour of the discharge of Ia and II sensory axons when no input stimulus is applied to the spindle. The periodicity of the II discharge, however, is seen to be more pronounced than that of the Ia. The endings for this typical data recorded with the muscle at a fixed length are firing pulses at the rate of about 10.5 and 26.3 pulses per second, respectively.

Fig.3.2.2b and Fig.3.2.3b are estimates of the AIF of the Ia & II spontaneous discharges which are calculated by using expression (3.2.14). The dotted line in each figure corresponds to the mean rate of the Ia and the II discharges while the horizontal solid lines below and above this line are approximate 95% asymptotic confidence intervals based on expression (3.2.21) of Method 1. Again, a periodicity in both discharges is clear. In the case of Ia discharge

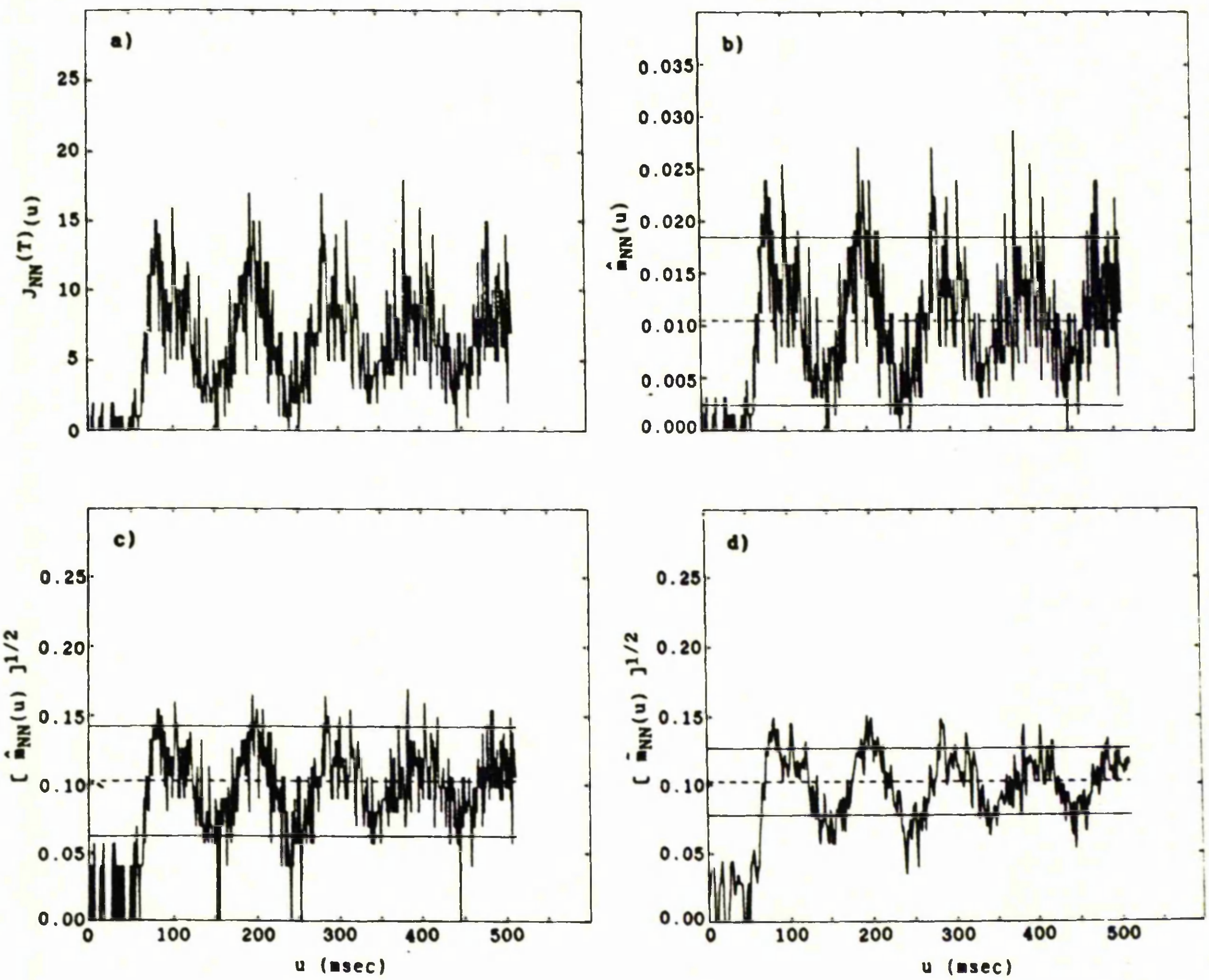

Fig.3.2.1 Illustration of the AIF of the Ia spontaneous discharge

a) Estimate $J_{NN}^{(T)}(u)$ with a binwidth h=1 msec.
b) Estimate of $m_{NN}(u)$ based on $J_{NN}^{(T)}(u)$ illustrated in (a).
c) Square root of the estimate of $m_{NN}(u)$ illustrated in (b).
d) Square root of the smoothed estimate of $m_{NN}(u)$ with a "Hanning window" as a smoothing scheme.

The dotted line in (b) corresponds to the mean rate $\hat{P}_N$ whereas that in (c) and (d) corresponds to the square root of $\hat{P}_N$ of the Ia spontaneous discharge. The horizontal lines below and above the dotted line are the approximate 95% confidence limits for the AIF under the hypothesis that the impulses of the Ia discharge are independent.

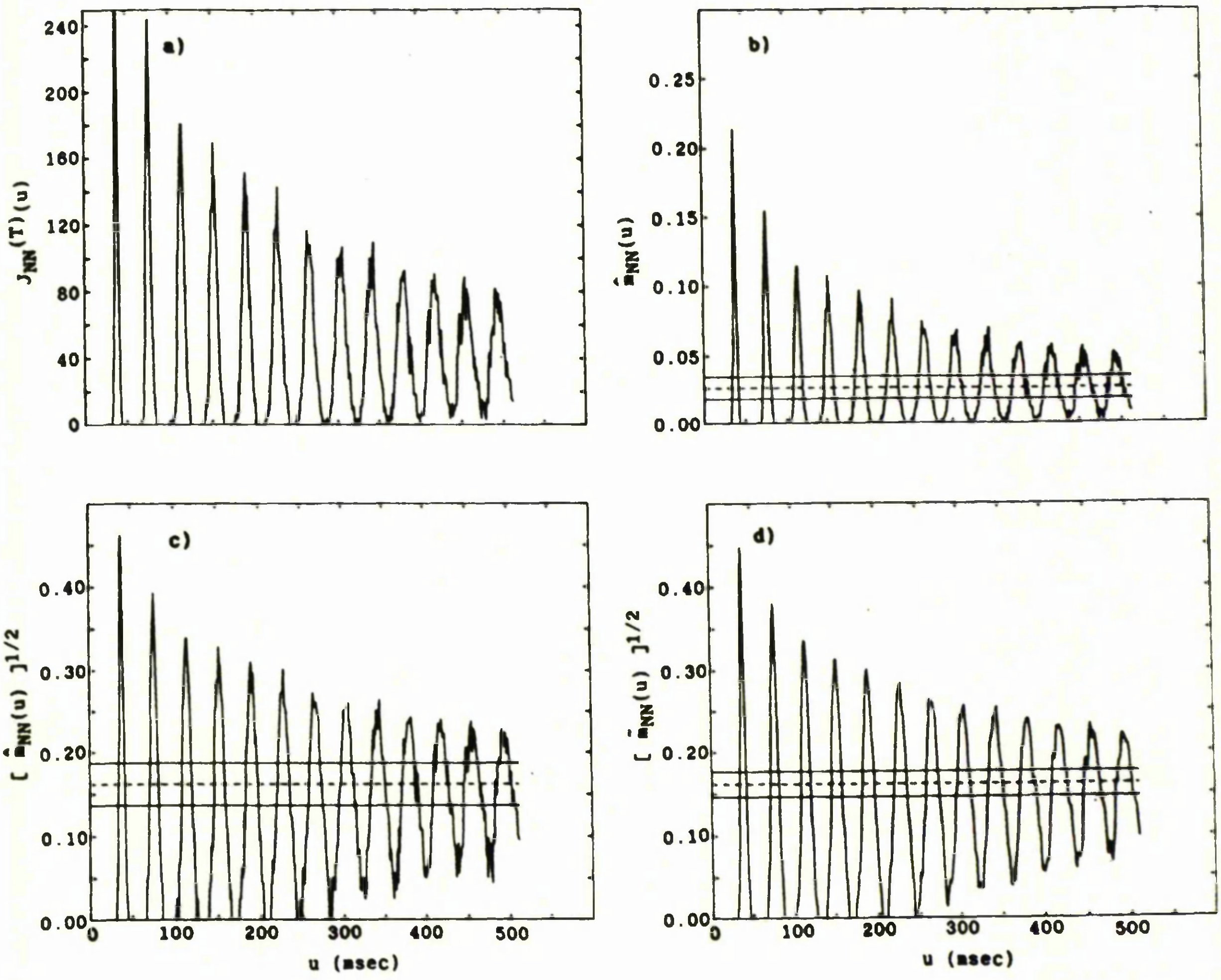

Fig.3.2.2 Illustration of the AIF of the II spontaneous discharge

a) Estimate of $J_{NN}^{(T)}(u)$ with a binwidth h=1 msec.
b) Estimate of $m_{NN}(u)$ based on $J_{NN}^{(T)}(u)$ illustrated in (a).
c) Square root of the estimate of $m_{NN}(u)$ illustrated in (b).
d) Square root of the smoothed estimte of $m_{NN}(u)$ with a "Hanning window" as a smoothing scheme.

The dotted line in (b) corresponds to the mean rate $\hat{P}_N$ whereas that in (c) and (d) corresponds to the square root of $\hat{P}_N$ of the II spontaneous discharge. The horizontal lines below and above the dotted line are the approximate 95% confidence limits for the AIF under the hypothesis that the impulses of the II discharge are independent.

(Fig.3.2.1b), however, there appears to be a greater variability in the estimate than in the case of the II discharge (Fig.3.2.2b). The values outside the confidence interval give evidence of significant autocorrelation between the increments of the process.

Figs3.2.1c and Fig.3.2.2c give the square root of the estimates of the AIF of both discharges (estimated by Method 2). Clearly this transformation improves the properties of the estimate as well as the symmetry of the function. The confidence intervals, constructed by using expression (3.2.22), again reveal the same autocorrelation structure between the increments of the process.

Finally, following Method 3, the improved and better estimates of the AIF of Ia & II spontaneous discharges are presented in Fig.3.2.1d and Fig.3.2.2d. These figures are the square roots of the estimates given in expression (3.2.25) with a "Hanning window" as a smoothing scheme, and reveal the same features as before.

Figs.3.2.3a-f give a comparison of the AIF's of the Ia discharge when the muscle spindle is acted upon by various prescribed stimuli. Fig.3.2.3a is the square root of the smoothed AIF of the Ia spontaneous discharge which reveals a periodicity with a period of about 90 msec. Fig.3.2.3b-d correspond to the Ia response to a single input length change 'ℓ', a random fusimotor input '${}_1\gamma_s$' and a second fusimotor input '${}_2\gamma_s$' respectively, whereas Fig.3.2.3e is the AIF of the Ia discharge in the presence of both fusimotor inputs '${}_1\gamma_s$' and '${}_2\gamma_s$' which are applied simultaneously but independently. Figure 3.2.3f is the AIF of the Ia discharge when all the three inputs are being applied concurrently and independently.

One striking feature of the Figs.3.2.3b-f is the loss of periodicity and an increase in the mean rate of the Ia discharge. Further, the Ia pulses occurring more than about 50 msec apart now become independent of each other i.e. the process then behaves as a

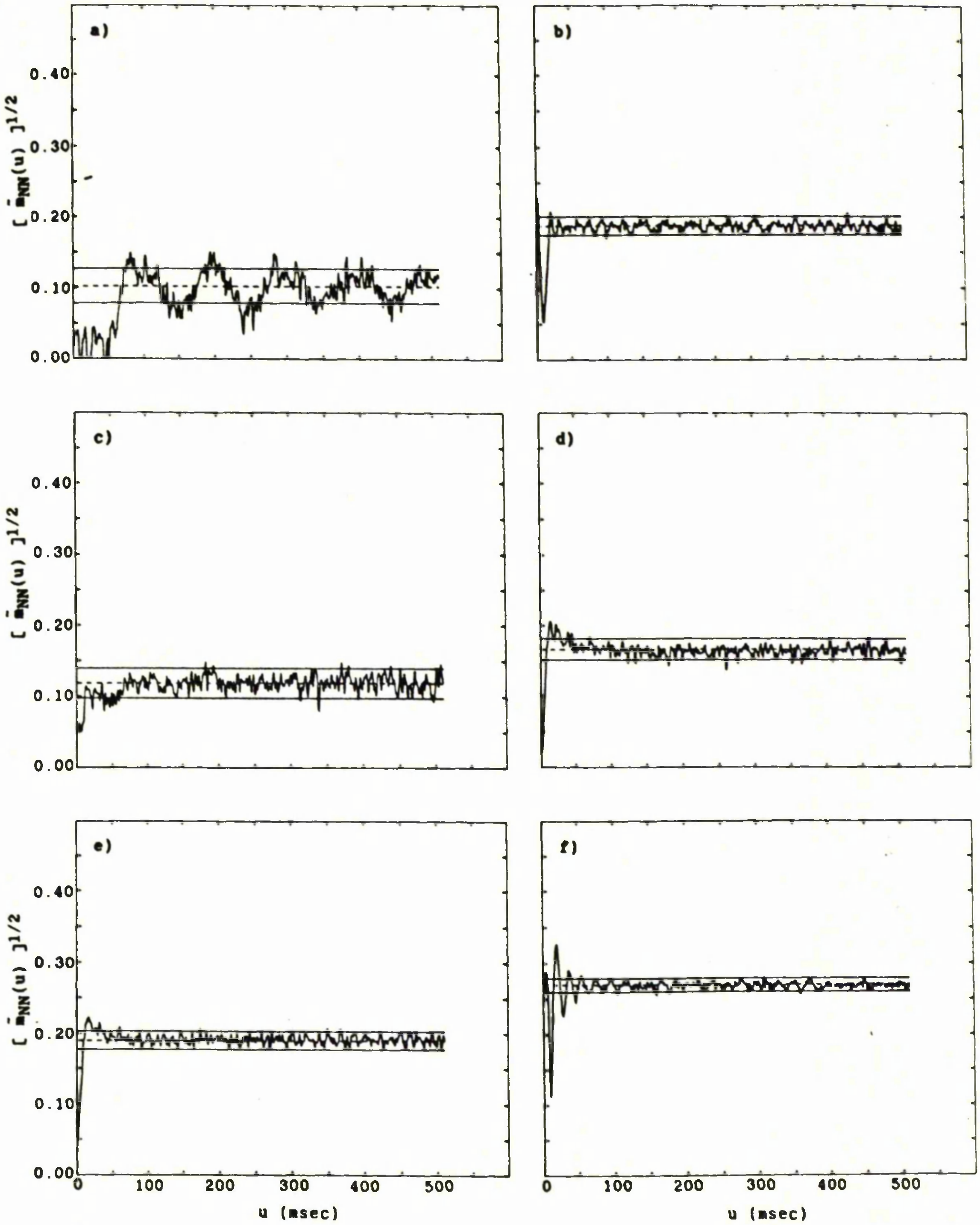

Fig.3.2.3 Square root of the smoothed estimtes of the AIF of

a) Ia spontaneous discharge
b) Ia discharge in the presence of a length change 'ℓ'
c) Ia discharge in the presence of a static gamma input '${}_1\gamma_s$'
d) Ia discharge in the presence of a 2nd static gamma input '${}_2\gamma_s$'
e) Ia discharge in the presence of both '${}_1\gamma_s$' and '${}_2\gamma_s$'
f) Ia discharge in the presence of 'ℓ' , '${}_1\gamma_s$' , and '${}_2\gamma_s$' .

The dotted line in each figure represents the square root of the mean rate of the corresponding discharge whereas the solid lines below and above this dotted line are the 95% approximate confidence limits for the respective AIF under the hypothesis of independence. The smoothing of the estimates is done by a "Hanning window".

Poisson process. Fig.3.2.3e clearly reveals a combined effect of both fusimotor inputs. Similarly Fig.3.2.3f can also be seen as a weighted combination of the three inputs but we can also see a possible periodicity with a higher rate and which we expect to see more clearly in the frequency domain.

The effect of these stimuli on the discharge of the secondary sensory axon, II, is presented in Figs.3.2.4a-f which give the square roots of the smoothed estimates of the AIF's of the II discharge in the presence of the same input stimuli as discussed for the Ia discharge.

Figs.3.2.4a-c give clear evidence of a strong periodic behaviour of the II discharge revealing that the presence of the length change or '${}_1\gamma_s$', alone does not affect this periodicity.

Figs.3.2.4(d-e) give the square root of the smoothed estimates of the AIF's of the II response to the second static gamma, ${}_2\gamma_s$, alone, and to both static gammas activated concurrently and independently, respectively. Again a periodicity in the II discharge is clear. However, the pulses occuring about 250 msec apart seem to become independent, and after that the process starts behaving like a Poisson process with the same mean rate of II discharge. Thus ${}_2\gamma_s$ alone or in the presence of the other gamma stimulus affects the regularity of the II sensory response by shortening the span of the dependence between the pulses.

Fig.3.2.4f corresponds to the square root of the estimate of the smoothed AIF of the II discharge when the spindle is acted upon by all the three stimuli, an imposed length change 'ℓ', a static gamma '${}_1\gamma_s$' and a second static gamma '${}_2\gamma_s$', applied concurrently and independently. The figure describes how the presence of these inputs alters the II response. The regularity of the response has disappeared and the rate of the discharge has been increased. A

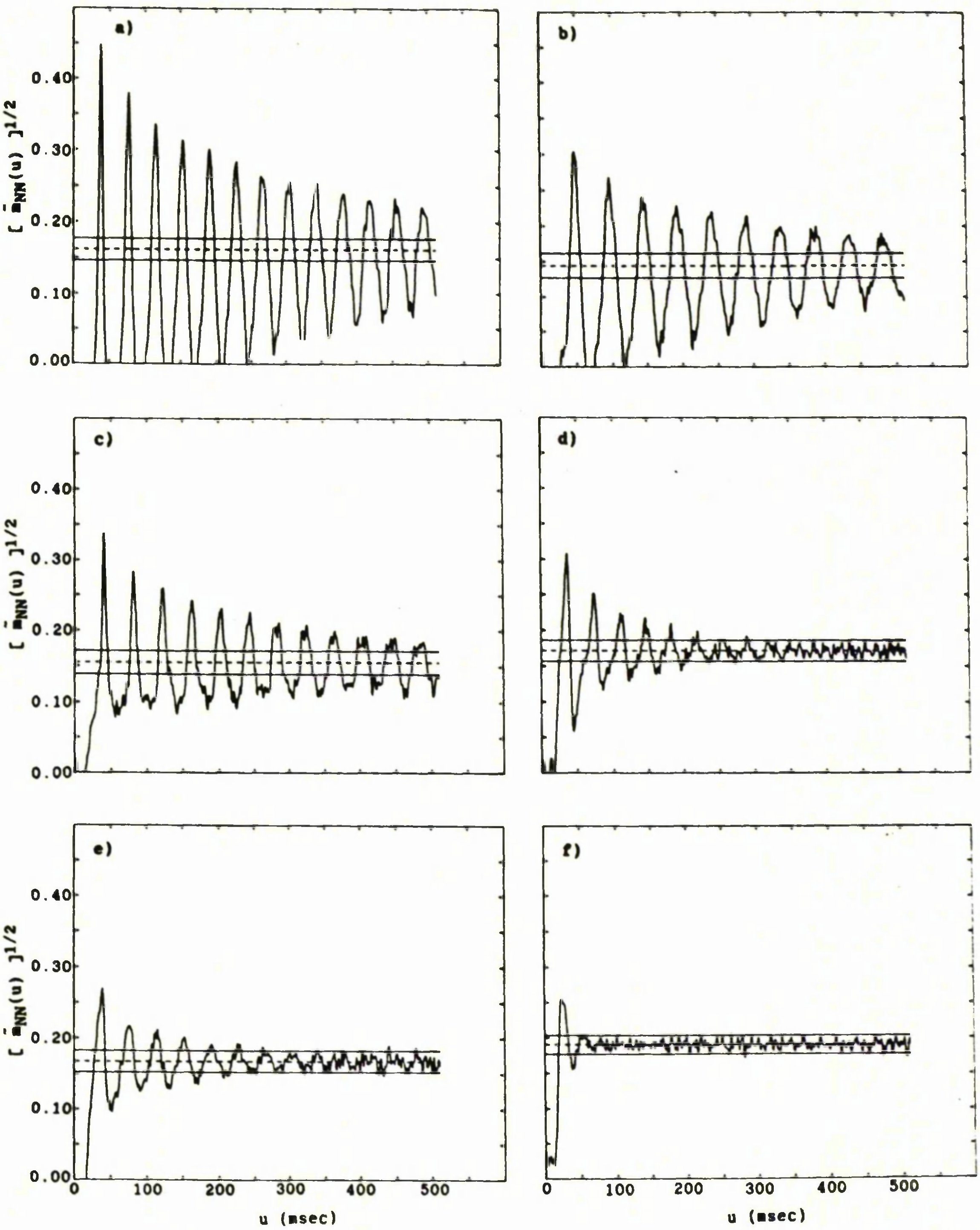

Fig.3.2.4 Square root of the smoothed estimates of the AIF of

a) II spontaneous discharge
b) II discharge in the presence of a length change 'ℓ'
c) II discharge in the presence of a static gamma input '$_1\gamma_s$'
d) II discharge in the presence of a 2nd static gamma input '$_2\gamma_s$'
e) II discharge in the presence of both '$_1\gamma_s$' and '$_2\gamma_s$'
f) II discharge in the presence of 'ℓ', '$_1\gamma_s$', and '$_2\gamma_s$'

The dotted line in each figure represents the square root of the mean rate of the corresponding II discharge whereas the solid lines below and above this dotted line are the 95% approximate confidence limits for the respective AIF under the hypothesis of independence. The smoothing of the estimates is done by a "Hanning window".

peak at about u=20 msec suggests an excitation and after that at about u=38 msec, a possible inhibition after which the estimate simply behaves as the mean intensity of a Poisson process.

Finally, from the above, we may conclude that in the absence of any stimulus the discharges of the both Ia and II sensory axons are periodic at a rate which depends on the length of the parent muscle at which it is held. The presence of any one of the input stimuli destroys the periodicity of the Ia discharge, whereas the periodicity of the II discharge is not affected at all. Further, a combination of the imposed lenth change 'ℓ' and both static gamma stimuli alters the II response and produces a higher discharge rate.

3.3 ANALYSIS IN THE FREQUENCY DOMAIN

In the theory of stationary time series, parallel with the time domain analysis, it is valuable to consider frequency domain analysis. Methods available in the frequency domain can easily be extended to the stationary point process case. Many of these methods are seen to be a direct analogue of time series.

It is sometimes assumed that time and frequency domain methods give equivalent representations of a data set, because they are mathematically equivalent and contain the same information about the process, and consequently it is sufficient to use only one of these representations (Tukey,1978 ; Koopmans,1983). But because of the finite amount of data mathematical equivalence does not imply equivalent representation (Tukey,1978). The need for both methods, however, depends on the complexity of the system under investigation.

We emphasize the frequency domain analysis not only because these methods often reveal more features about the process and give better understanding to physiologists but also because we find them to be more sensitive.

3.3.1 FREQUENCY DOMAIN PARAMETERS

The fundamental parameter of a stationary point process is the power spectrum (PS) which, by the analogy with time series, is defined as the Fourier transform of the autocovariance function. A detailed discussion on the Fourier transform and its properties can be found in Brigham(1974) or Bracewell(1986).

Suppose N(t) is a stationary point process satisfying the conditions of orderliness and mixing. Let P_N and $q_{NN}(u)$ be the mean rate and the cumulant function of N. Further, $q_{NN}(u)$ satifies the following condition

$$\int_{-\infty}^{+\infty} |q_{NN}(u)|du < \infty \qquad (3.3.1)$$

Then the power spectrum of the point process N is defined as (e.g. Bartlett, 1963 ; Brillinger and Tukey, 1984),

$$f_{NN}(\lambda) = (2\pi)^{-1}\int \exp(-i\lambda u)\operatorname{cov}\{dN(t+u),dN(t)\}]/dt \qquad -\infty<\lambda<\infty \qquad (3.3.2)$$

$$f_{NN}(\lambda) = P_N/2\pi + (2\pi)^{-1}\int \exp(-i\lambda u)q_{NN}(u)du \qquad -\infty<\lambda<\infty \qquad (3.3.3)$$

The parameter λ is the frequency in radians. The power spectrum is proportional to the variance of the component of frequency λ of the process N, and may be interpreted as reflecting the power in each frequency component of the process (Brillinger et al, 1976).

One important manner in which the power spectrum of a point process satisfying condition (3.3.1) differs from that of an ordinary time series follows from the Riemann-Lebesque Lemma (Katznelson,1968 ; Papoulis,1962) i.e

$$\operatorname{Lim}_{\lambda\to\infty} f_{NN}(\lambda) = P_N/2\pi \neq 0$$

This constant value corresponds to the power spectrum of the Poisson process since in the case of the Poisson process

$$q_{NN}(u) = 0$$

However, the power spectrum is similar to that of an ordinary time series in that it is a symmetric and non-negative function of λ.

The inverse relation to the definition (3.3.3) may be provided by

$$q_{NN}(u) = \int \exp(+i\lambda u)[f_{NN}(\lambda) - P_N/2\pi]d\lambda \qquad (3.3.4)$$

3.3.2 ESTIMATION OF THE POWER SPECTRUM

By the analogy with stationary time series, the estimate of the power spectrum may be based on any of the methods described by, for example, Tukey(1959), Parzen(1961), Bloomfield(1976), Brillinger(1981) and Priestley(1987) in the case of time series and Bartlett(1963), Cox and Lewis(1966), Brillinger(1975a) and Rigas(1983) in the case of point processes.

Following the 'direct' method (Brillinger, 1975a; and Rigas, 1983), the periodogram-based estimate of the power spectrum of a point process may be obtained in two alternative ways.

(a) An estimate based on the periodogram of the entire record length.

(b) An estimate based on the periodograms of disjoint sections of the record length.

3.3.3 THE PERIODOGRAM OF A POINT PROCESS

Suppose that the process N is observed in (0,T] with τ_1, τ_2, ... , $\tau_{N(T)}$ the observed times of occurrence, then by analogy with time series, the periodogram of the point process N is defined by Bartlett(1963) and Brillinger and Tukey(1984) as

$$I_{NN}^{(T)}(\lambda) = (2\pi T)^{-1}|d_N^{(T)}(\lambda)|^2 \qquad -\infty\angle\lambda\angle\infty \qquad (3.3.5)$$

where $d_N^{(T)}(\lambda)$ is the finite Fourier-Stieltjes transform of the counting process N(t) and is given by

$$d_N^{(T)}(\lambda) = \int_0^T \exp(-i\lambda t)dN(t) \qquad (3.3.6)$$

The spectral representation may be used to relate the point process to the associated time series (Brillinger, 1975a ; Rigas, 1983), and which implies that the spectrum of the series

$$X(t) = \{N(t+h)-N(t)\}/h$$

is closely related to the spectrum of the point process N when h=1 and $|\lambda|<\pi$. This suggests that (3.3.6) can be approximated by

$$d_N^{(T)}(\lambda) = \sum_{t=0}^{T-1} \exp(-i\lambda t)\{N(t+1)-N(t)\} \tag{3.3.7}$$

The difference $\{N(t+1)-N(t)\}$ takes on values 0 when no events have occurred and the value 1 when there is an event in $(t,t+1]$. Hence, in practice, considering the point process a 0-1 time series, sampled at equally spaced intervals of one unit of time, the expression (3.3.7) becomes

$$d_N^{(T)}(\lambda) = \sum_{j=1}^{N(T)} \exp(-i\lambda\tau_j) \tag{3.3.8}$$

The power spectrum may now, alternatively, be defined as

$$f_{NN}(\lambda) = \operatorname{Lt}_{T\to\infty} (2\pi T)^{-1} \text{ ave.}|d_N^{(T)}(\lambda)|^2 \qquad \lambda\neq 0$$

Brillinger and Tukey(1984)

where "ave." denotes the average value.

3.3.4 PERIODOGRAM AS AN ESTIMATE OF THE SPECTRUM

The periodogram given by

$$I_{NN}^{(T)}(\lambda) = (2\pi T)^{-1}|d_N^{(T)}(\lambda)|^2$$

has the same symmetry and non-negativity as the power spectrum of a point process given by (3.3.3). Further, for the variate $d_N^{(T)}(\lambda)$, λ of the form $2\pi s/T$, s an integer, and for $0<\lambda_1<\lambda_2<\ldots<\lambda_k$, the variates

$d_N^{(T)}(\lambda_1)$, $d_N^{(T)}(\lambda_2)$, ... , $d_N^{(T)}(\lambda_k)$ are asymptotically independent and distributed as

$$d_N^{(T)}(\lambda) \sim N^C[0\ ,\ 2\pi T f_{NN}(\lambda)] \qquad \text{Brillinger(1975a, 1983)}$$

where $N^C[\alpha,\beta]$ denotes a complex normal random variable with mean α and variance β, which suggests that the periodogram, $I_{NN}^{(T)}(\lambda)$, is an obvious estimate of the power spectrum.

3.3.5 PROPERTIES OF THE PERIODOGRAM

Let N(t) be a stationary point process defined on (0,T]. Suppose the second order cumulant exists and satisfies the following condition,

$$\int |q_{NN}(u)|\,du < \infty$$

Then we have,

$$\text{(i)}\quad E\{I_{NN}^{(T)}(\lambda)\} = \frac{1}{2\pi T}\int \left[\frac{\sin(\lambda-\alpha)T/2}{(\lambda-\alpha)/2}\right]^2 f_{NN}(\alpha)\,d\alpha + \frac{P_N^2}{2\pi T}\left[\frac{\sin\lambda T/2}{\lambda/2}\right] \qquad (3.3.9)$$

$$\text{(ii)}\quad \operatorname{cov}\{I_{NN}^{(T)}(\lambda), I_{NN}^{(T)}(\mu)\} = \left\{\left[\frac{\sin(\lambda+\mu)T/2}{T(\lambda+\mu)/2}\right]^2 + \left[\frac{\sin(\lambda-\mu)T/2}{T(\lambda-\mu)/2}\right]^2\right\} f_{NN}^2(\lambda)$$

$$+\ O(T^{-1}) \qquad \lambda \neq \mu \qquad (3.3.10)$$

$$\text{(iii)}\quad \operatorname{var}\{I_{NN}^{(T)}(\lambda)\} = f_{NN}^2(\lambda) + O(T^{-1}) \qquad (3.3.11)$$

Proof:- The proof is given in Theorem I.2 and I.3 of Appendix I.

Now, for $\lambda \neq 0$, the final term in (3.3.9) is small and we see that $E[I_{NN}^{(T)}(\lambda)]$ is a weighted average of $f_{NN}(\lambda)$ with weights concentrated in the neighbourhood of λ.

Further, the function

$$\frac{1}{2\pi T}\left[\frac{\sin(\lambda-\alpha)T/2}{(\lambda-\alpha)/2}\right]^2$$

in expression (3.3.9) becomes a delta function as $T\to\infty$ (Populis, 1962) which implies that

$$\operatorname{Lim}_{T\to\infty} E\{I_{NN}^{(T)}\} = f_{NN}(\lambda) \tag{3.3.12}$$

i.e., the periodogram, $I_{NN}^{(T)}(\lambda)$, is an asymptotically unbiased estimate of the spectrum.

Under the condition of the above theorem and with $\lambda=2\pi r/T$, $\mu=2\pi s/T$ for r,s integers such that r, s, r+s $\not\equiv$ 0 (mod T), we have (Rigas, 1983),

$$\begin{aligned} &\operatorname{cov}\{I_{NN}^{(T)}(\lambda), I_{NN}^{(T)}(\mu)\} = O(T^{-1}) \\ &\operatorname{var}\{I_{NN}^{(T)}(\lambda)\} = f_{NN}^2(\lambda) + O(T^{-1}) \end{aligned} \tag{3.3.13}$$

This suggests that the periodogram is not a consistent estimate of the spectrum in that no matter how large the record length, T, is taken, the variance of this estimate tends to remain at a constant level $f_{NN}^2(\lambda)$. From expression (3.3.13), it is also clear that adjacent periodogram ordinates are uncorrelated for large value of T. Finally, the variates $I_{NN}^{(T)}(\lambda_j)$, $\lambda_j=2\pi j/T$, j=1,2,... are seen to be asymptotically independent $f_{NN}(\lambda_j)\chi^2_2/2$ random variables from the fact that $d_N^{(T)}(\lambda_j)$, $\lambda_j=2\pi j/T$, $j=1,2,\ldots$ are asymptotically independent normal variates.

The above result leads to the consideration of the construction of a consistent estimate of the spectrum of a stationary point process by smoothing the periodogram.

3.3.6 CONSISTENT ESTIMATES OF THE SPECTRUM

In this section we consider a variety of methods for a consistent estimate of the power spectrum of a stationary point process.

Method 1 Smoothed periodogram : a consistent estimate of the spectrum

From the previous section we have that (2m+1) adjacent ordinates of the periodogram $I_{NN}^{(T)}(\lambda+2\pi j/T)$, $j=0,\pm1,\pm2,\ldots,\pm m$ are approximately independent $f_{NN}(\lambda)\chi^2_2/2$ variates, which suggests an estimate of the power spectrum having the following form

$$
\begin{aligned}
f_{NN}^{(T)}(\lambda) &= \sum_{j=-m}^{+m} w_j I_{NN}^{(T)}\left[\lambda+\frac{2\pi j}{T}\right] && \lambda\neq 0 \\
&= \left[\sum_{j=1}^{m} w_j\right]^{-1} \sum_{j=1}^{m} w_j I_{NN}^{(T)}\left[\frac{2\pi j}{T}\right] && \lambda=0
\end{aligned}
\qquad (3.3.14)
$$

where w_j, $j=0,\pm1,\pm2,\ldots,\pm m$ are the weights which satisfy the following condition

$$\Sigma w_j = 1 \qquad \text{for } j=-m,\ldots,+m$$

and where $m/T\to 0$ as $T\to\infty$

It can easily be shown that this estimate is asymptotically unbiased with variance

$$\mathrm{var}\{f_{NN}^{(T)}(\lambda)\} = f_{NN}^2(\lambda)\sum_{j=-m}^{+m} w_j^2 + O(T^{-1}) \qquad \lambda\neq 0$$

(3.3.15)

$$= \Big[\sum_{j=1}^{m} w_j\Big]^{-2} f_{NN}^2(\lambda)\sum_{j=1}^{m} w_j^2 + O(T^{-1}) \qquad \lambda=0$$

and the covariance structure given by

$$\mathrm{cov}\{f_{NN}^{(T)}(\lambda), f_{NN}^{(T)}(\mu)\} = O(T^{-1}) \qquad \text{(Rigas,1983)}$$

Therefore, for $\lambda\neq 0$ and T large the variance of the estimate (3.3.14) is seen to be proportional to Σwj^2. Now Σwj^2 can be minimised subject to the constraint $\Sigma w_j=1$ with the choice of

$$w_j = 1/(2m+1)$$

i.e., a choice of equal weights leading to an estimate of the following form

$$f_{NN}^{(T)}(\lambda) = \frac{1}{2m+1}\sum_{j=-m}^{+m} I_{NN}^{(T)}(\lambda+\frac{2\pi j}{T}) \qquad \lambda\neq 0$$

(3.3.15)

$$= \frac{1}{m}\sum_{j=1}^{m} I_{NN}^{(T)}(2\pi j/T) \qquad \lambda=0$$

having variance

$$\mathrm{var}\{f_{NN}^{(T)}(\lambda)\} = f_{NN}^2(\lambda)/(2m+1) + O(T^{-1}) \qquad \lambda\neq 0$$

(3.3.16)

$$= f_{NN}^2(\lambda)/m + O(T^{-1}) \qquad \lambda=0$$

and

$$\mathrm{cov}\{f_{NN}^{T}(\lambda), f_{NN}^{(T)}(\mu)\} = O(T^{-1})$$

The asymptotic distribution of $f_{NN}^{(T)}(\lambda)$ is clearly a weighted combination of independent Chi-Squared variates. In practice, this may be approximated by a multiple θx^2_ν of a Chi-Squared distribution (Box,1954) whose mean and degrees of freedom are determined by equating first and second order moments. i.e.,

$$\text{mean} = \theta.\nu = \Sigma m_j = 1 \qquad\qquad \theta=1/\nu$$

$$\text{Variance} = \theta^2.2\nu = \Sigma w_j^2 = 1/(2m+1), \text{ hence } \nu=2(2m+1)$$

Therefore $f_{NN}^{(T)}(\lambda)$ is seen to be distributed approximately as,

$$f_{NN}^{(T)}(\lambda) \sim x^2_{2(2m+1)}/2(2m+1)$$

The estimate (3.3.15) is a simple average of the periodogram ordinates in the neighbourhood of λ. The bias of this estimate is generally greater than that of $I_{NN}^{(T)}(\lambda)$ which may increase as m gets larger. However, the variance of this estimate is 1/(2m+1) times that of the unsmoothed periodogram, so a compromise value of m will have to be found in order to get an acceptable level of stability with minimum bias (e.g. Brillinger, 1981).

METHOD 2

Following the definition of the power spectrum of a stationary point process (expression 3.3.3), an estimate of the spectrum may be given by

$$f_{NN}^{(T)}(\lambda) = \frac{\hat{P}_N}{2\pi} + \int k_T(u)\hat{q}_{NN}(u)\exp(-i\lambda u)du \qquad (3.3.17)$$

$$= \frac{\hat{P}_N}{2\pi} + b\sum k_T(u_j)\hat{q}_{NN}(u_j)\exp(-i\lambda u_j)$$

for $u_j = bj$; $j = 0, \pm 1, \pm 2, \ldots$. The parameter b is a binwidth. The function $k_T(u)=k(b_T u)$ is called a convergence factor, taper or data window which improves the convergence properties of the Fourier transform (Harris,1978 ; Brillinger,1981). The function k(u) is assumed to be even, of bounded variation, which vanishes for $|u|\geq 1$ and takes value 1 at u=0 (Parzen,1957). The scale parameter b_T is called the bandwidth of the estimate and is assumed to tend to 0 as $T\to\infty$ in such a way that $b_T T\to\infty$ (Brillinger, 1981).

Further, the Fourier transform of k(u) given by

$$K(\alpha) = (2\pi)^{-1}\int k(u)\exp(-i\alpha u)du$$

is assumed to be real valued, even, of bounded variation satisfying the following conditions

$$\int K(\alpha)d\alpha = 1 \qquad \text{and} \qquad \int |K(\alpha)|d\alpha < \infty$$

The expression (3.3.17) may be written as (Parzen,1957)

$$f_{NN}^{(T)}(\lambda) = \frac{\hat{P}_N}{2\pi} + \int_{-T}^{T} k(b_T u)\hat{q}_{NN}(u)\exp(-i\lambda u)du$$

or in terms of spectral estimates,

$$f_{NN}^{(T)}(\lambda) = (b_T)^{-1}\int K[b_T^{-1}(\lambda-\alpha)]I_{NN}^{(T)}(\alpha)d\alpha \qquad (3.3.18)$$

$$\cong \frac{2\pi}{b_T T}\sum_s K\left[b_T^{-1}(\lambda - \frac{2\pi s}{T})\right]I_{NN}^{(T)}(\frac{2\pi s}{T})$$

We now discuss the properties of the proposed estimate.

PROPERTIES OF $f_{NN}^{(T)}(\lambda)$

From Theorem I.4 of Appendix I, it follows that

i) $$\lim_{T\to\infty} E\{f_{NN}^{(T)}(\lambda)\} = f_{NN}(\lambda)$$

ii) $$\lim_{T\to\infty} b_T T \operatorname{cov}\{f_{NN}^{(T)}(\lambda), f_{NN}^{(T)}(\mu)\}$$

$$= 2\pi[\delta\{\lambda-\mu\}+\delta\{\lambda+\mu\}]f_{NN}^2(\lambda)\int K^2(\alpha)d\alpha$$

where

$\delta\{\lambda\}=1$ if $\lambda\equiv 0 \pmod{2\pi}$ and is zero otherwise

and

iii) $$\lim_{T\to\infty} b_T T \operatorname{var}\{f_{NN}^{(T)}(\lambda)\} = 2\pi\, f_{NN}^2(\lambda)\int K^2(\alpha)d\alpha \qquad (3.3.19)$$

This implies that $f_{NN}^{(T)}(\lambda)$ is an asymptotically unbiased estimate of $f_{NN}(\lambda)$ as well as is a consistent one since $\operatorname{var}[f_{NN}^{(T)}(\lambda)]\to 0$ as $b_T T\to\infty$. Further, it follows that $f_{NN}^{(T)}(\lambda)$ and $f_{NN}^{(T)}(\mu)$ for $\lambda,\mu,\lambda\pm\mu\neq 0$ are asymptotically independent normal variates.

METHOD 3 **A consistent estimate of the PS based on disjoint segments**

A further way of obtaining a consistent estimate of the power spectrum of a point process is obtained by splitting up the whole record length, T, into disjoint sections and averaging the spectral estimates over these sections (Brillinger and Tukey, 1984).

One computational advantage of this procedure is that it does not require large storage space for large data sets particularly when analysing multivariate point process data. We, in practice, also found this method fastest. Emphasizing these advantages, we base our multivariate point process analysis on this procedure.

Suppose that $N(t)$ is observed on $(0,T]$ and the entire record is divided into L disjoint sections each of which has duration of length R so that $T=LR$.

We define the periodogram of the jth section at frequency λ by

$$I_{NN}^{(R)}(\lambda,j) = (2\pi R)^{-1}|d_N^{(R)}(\lambda,j)|^2 \qquad (3.3.19A)$$

where

$$d_N^{(R)}(\lambda,j) = \sum_{t=jR}^{(j+1)R} \exp(-i\lambda t)\Big[N(t+1)-N(t)\Big] \quad ; \quad j=0,1,\ldots,L-1$$

An estimate $f_{NN}^{(LR)}(\lambda)$ of the power spectrum may be obtained by simply averaging these periodograms over L sections, i.e.,

$$f_{NN}^{(LR)}(\lambda) = \frac{1}{L}\sum_{j=0}^{L-1} I_{NN}^{(R)}(\lambda,j) \qquad \lambda\neq 0 \qquad (3.3.20)$$

The asymptotic 1st and 2nd order properties of the estimate $f_{NN}^{(LR)}(\lambda)$ are examined as follows,

PROPERTIES OF $f_{NN}^{(LR)}(\lambda)$

Let N(t) be a stationary bivariate point process defined on (0,T]. Suppose that the 2nd order cumulant function $q_{NN}(u)$ exists and satisfies the condition

$$\int |u|\,|q_{NN}(u)|\,du < \infty$$

then

$$\text{i)} \qquad \underset{T\to\infty}{\mathrm{Lt}}\; E\{f_{NN}^{(LR)}(\lambda)\} = f_{NN}(\lambda) \qquad \lambda\neq 0$$

$$\text{ii)} \qquad \underset{T\to\infty}{\mathrm{Lt}}\; \mathrm{var}\{f_{NN}^{(LR)}(\lambda)\} = (L)^{-1}f_{NN}^{2}(\lambda) \qquad \lambda\neq 0 \qquad (3.3.21)$$

Proof:-

The proof follows from the previous result that the periodogram ordinates are asymptotically independent variates distributed with variance $f_{NN}^{2}(\lambda)$ {Expressions (3.3.11) and (3.3.13)} and the fact that $L\to\infty$, $L/T\to 0$ as $T\to\infty$.

It also follows that $f_{NN}^{(LR)}(\lambda_1), \ldots, f_{NN}^{(LR)}(\lambda_J)$ are asymptotically normal variates.

The smoothness of the estimate may further be improved by applying a "Hanning window" of the form

$$\hat{f}_{NN}^{(LR)}(\lambda_k) = 0.25f_{NN}^{(LR)}(\lambda_{k-1})+0.5f_{NN}^{(LR)}(\lambda_k)+0.25f_{NN}^{(LR)}(\lambda_{k+1})$$

This estimate can easily be seen to be asymptotically unbiased and normally distributed with variance

$$\mathrm{var}\{\hat{f}_{NN}^{(LR)}(\lambda)\} = 0.375(L)^{-1}f_{NN}^{2}(\lambda)$$

A comparison of expression (3.3.16), (3.3.19) and (3.3.21) shows that the limiting distribution of $f_{NN}^{(T)}(\lambda)$ given by Method 2 is consistent with that of Method 1 and 3 for large m and L, if we make the identification (Brillinger, 1981)

$$(2m+1)^{-1} = \frac{2\pi}{b_T T} \int K^2(\alpha)d\alpha = (L)^{-1} \qquad (3.3.22)$$

We, so far, have proposed a variety of procedures for the estimation of the PS of a stationary point process. All are based on the periodogram of the point process and give an estimate which is asymtotically unbiased as well as consistent. A direct use of the expression (3.3.17) has the disadvantage that it may give negative value of the estimate even if $K(\alpha) \geq 0$ (Brillinger, 1975a).

In the next section we consider the problem of constructing confidence intervals for $f_{NN}(\lambda)$.

3.3.7 CONFIDENCE INTERVALS FOR THE SPECTRUM

The power spectrum (PS) of a point process provides a useful tool in the frequency domain to detect any periodicities present in the process as well as to assess the correlation structure between the increments of the process. An asymptotic confidence interval (marginal) for $f_{NN}(\lambda)$ at a given frequency λ plays an important role for such an assessment. In this section we discuss a variety of ways of constructing asymptotic confidence intervals. These intervals are to be interpreted at each frequency i.e., in the sense of marginal inference rather than a simultaneous one.

From the previous section, we find that each procedure for the estimation of the spectrum of a point process gives an estimate whose limiting distribution approaches a normal distribution, e.g, $f_{NN}^{(T)}(\lambda)$ given by Method 2 is such that,

$$f_{NN}^{(T)}(\lambda) \sim N[f_{NN}(\lambda), f_{NN}^2(\lambda)2\pi(b_T T)^{-1}\int K^2(\alpha)d\alpha]$$

Now applying the result of Rao(1984,P/385) for variance stabilizing transformations, we find that

$$\log_e[f_{NN}^{(T)}(\lambda)] \sim N[\log_e f_{NN}(\lambda),\ 2\pi(b_T T)^{-1}\int K^2(\alpha)d\alpha]$$

Therefore, an approximate 95% confidence interval for $\log_e[f_{NN}(\lambda)]$ at a given frequency λ can easily be constructed as

$$\log_e[f_{NN}^{(T)}(\lambda)] \pm 1.96[2\pi(b_T T)^{-1}\int K^2(\alpha)d\alpha]^{\frac{1}{2}}$$

Under the hypothesis that the process is Poisson with the same mean rate, this interval becomes

$$\log_e(\hat{P}_N/2\pi) \pm 1.96[2\pi(b_T T)^{-1}\int K^2(\alpha)d\alpha]^{\frac{1}{2}} \qquad (3.3.23)$$

With large degrees of freedom, the confidence interval for method 1 is seen to be

$$\log_e(\hat{P}_N/2\pi) \pm 1.96[2m+1]^{-1/2} \qquad (3.3.24)$$

and for method 3,

$$\log_e(\hat{P}_N/2\pi) \pm 1.96[L]^{-1/2} \qquad (3.3.25)$$

We now turn to the applications of the methods demonstrated above to the same data sets obtained on the muscle spindle.

3.3.8 APPLICATIONS

Fig. 3.3.1a illustrates the periodogram of the II spontaneous discharge. This estimate is based on expression (3.8.1). The evaluation of expression (3.8.3) is carried out by using the fast Fourier transform (FFT) algorithm (Gentleman and Sande, 1966) at discrete frequencies of the form $\lambda_n=2\pi n/T$ radians/msec or 1000n/T Hz. with $n=0,1,2,\ldots,(T-1)/2$ and $T=2^{15}$ msec.

From the Nyquist criterion (Nyquist, 1928), a sampling interval of 1 msec gives the Nyquist frequency of 500 Hz. This also ensures that in our case there is no problem of aliasing over the range of frequencies of interest. Aliasing is a kind of phenomenon by which all the "power" at frequencies higher than the Nyquist frequency is superimposed on the section of the spectral density function lying between zero and the Nyquist frequency (Blackman and Tukey, 1959; Ramirez, 1974).

The figure (Fig.3.3.1a) has been plotted at frequencies from 0 to 200 Hz. The first peak which is very sharp and fairly large in magnitude occurs, as expected from the time domain analysis, at a frequency of about 26.25 Hz., which suggests a strong periodic component at that frequency. Other relatively smaller peaks occur at the frequencies which are multiples of the fundamental frequency. Further, a lack of smoothness and erratic behaviour of the estimate at larger frequencies can also be seen which is an obvious consequence of the asymptotic properties of the periodogram ordinates.

Fig. 3.3.1b represents the logarithm to base e of the estimate of the spectrum of the II discharge and is obtained by smoothing the periodogram illustrated in fig. 3.3.1a with m=31 i.e., using expression (3.3.15) of method 1. The dotted line corresponds to $\log_e$ of the estimated asymptotic value of the spectrum i.e., the spectrum of a Poisson process with the same mean rate. The solid lines are an approximate 95% confidence interval for the asymptotic value of the estimate, and are obtained by using expression (3.3.24). Again the sharp peaks give the evidence of the presence of a strong periodic component in the process at frequency of 26.25 Hz. These peaks seem to die off near the frequncy 200 Hz. and after this frequency the estimate starts staying within the confidence interval revealing the behaviour of a poisson process with the same mean rate.

Figures 3.3.2 and 3.3.3 illustrate the application of Method 3 and correspond to the log to the base e of the estimated auto spectra of the Ia and II discharges under different conditions of the input stimuli. The dotted lines are $\log_e(\hat{P}_N/2\pi)$ where $\hat{P}_N$ is the estimate of the mean intensity. The solid lines correspond to approximate 95% confidence intervals under the hypothesis of being a

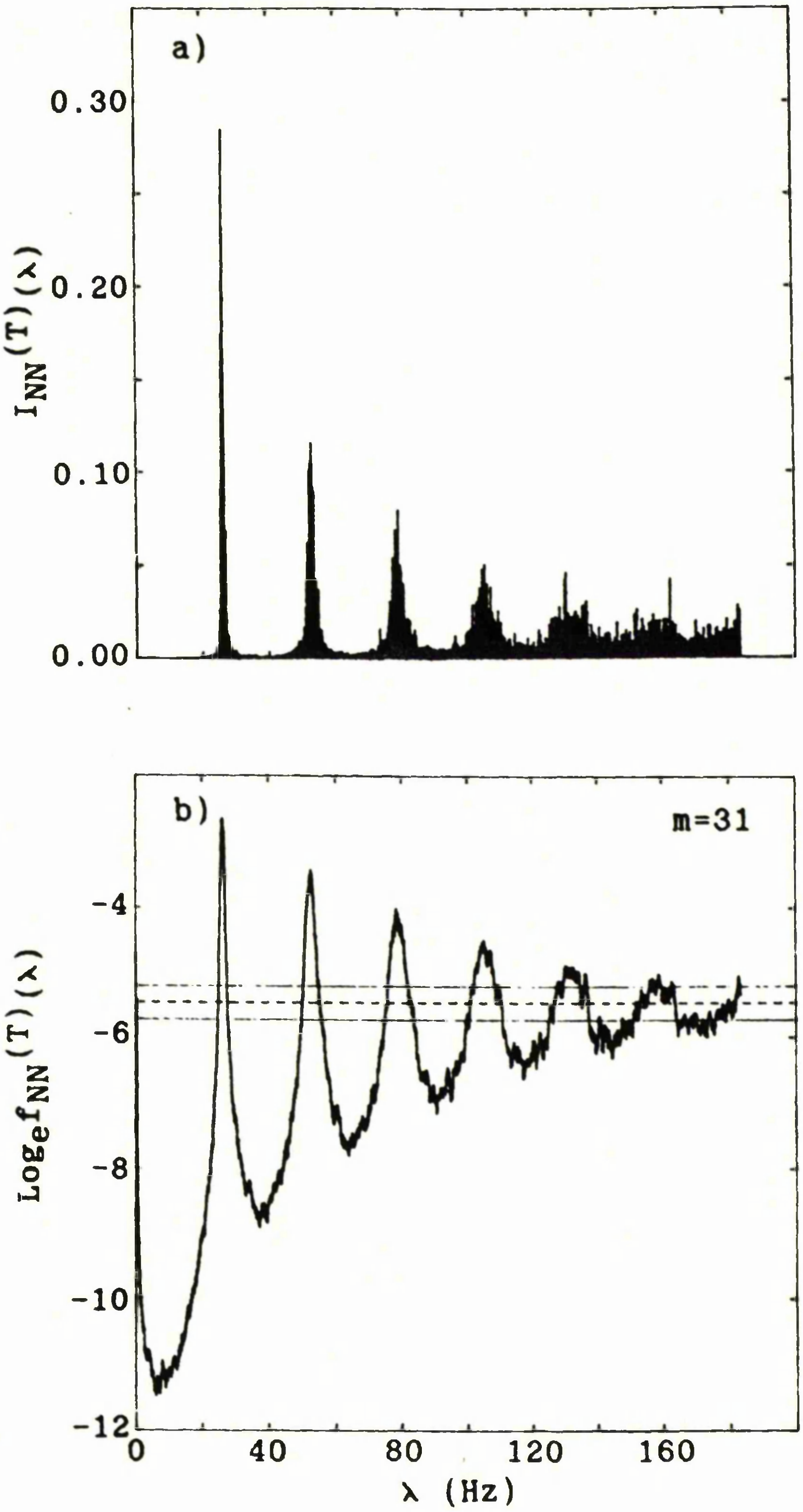

Fig.3.3.1 Illustration of the periodogram and the auto-spectrum

a) Periodogram of the II spontaneous discharge, and is based on the entire record length $T=2^{15}$ msec.
b) Log to the base e of the estimated auto-spectrum of the II spontaneous discharge. The estimate of the spectrum is based on the periodogram illustrated in (a).

The dotted line in (b) corresponds to $\log_e(\hat{P}_N/2\pi)$, and the solid lines below and above this line represent an approximate 95% confidence interval for the spectrum at a given frequency under the hypothesis of Poisson process.

Poisson process and are based on expression (3.3.25).

Applying this Method, the whole record of length T=60000 msec is divided into L=58 disjoint sections each with length of R=1024 msec. The periodogram ordinates at frequencies of the form $\lambda_k=2\pi k/R$, k=1,2,... for each section are obtained by using expression (3.3.19A) and then are averaged over these sections to get an estimate of the auto spectrum $f_{NN}(\lambda)$ at frequency $2\pi k/R$ radians/msec or 1000k/R Hertz.

Each set of plots in both figures 3.3.2 and 3.3.3 gives a comparison between the estimates of the autospectra of the Ia and II discharges, respectively when the spindle is acted upon by different stimuli. It can be seen how the discharge of both sensory axons is influenced by an activation of these stimuli.

Fig. 3.3.2a corresponds to the estimate of $\log_e[f_{IaIa}(\lambda)]$ when no input is present. A depression at low frequencies can clearly be seen which lasts until a significant peak at frequency 10 Hz occurs suggesting a possible periodic component at that frequency, and after this frequency the process seems to behave like a Poisson process with the same mean rate. Figs. 3.3.2b-d correspond to the estimate of $\log_e[f_{IaIa}(\lambda)]$ when a single input 'ℓ' (length change), $_1\gamma_s$, and $_2\gamma_s$ is applied to the spindle, respectively. A common feature of these figures is the loss of any periodicity and an increase in the mean rate of the Ia discharge. However, a comparison between these figures also reveals how each input alone affects the Ia discharge in a different way over a different range of frequencies e.g the effect of $_2\gamma_s$ (fig. 3.3.2d) is seen to be at low frequencies in the range 0-10 Hz. whereas the effect of length change 'ℓ' (fig. 3.3.2b) is in the range 10-55 Hz. In contrast, the effect of $_1\gamma_s$ (fig. 3.3.2c) is different from that of 'ℓ' and $_2\gamma_s$. The estimate in this figure behaves like a Poisson process at almost all frequencies except at a very few at the beginning suggesting that the

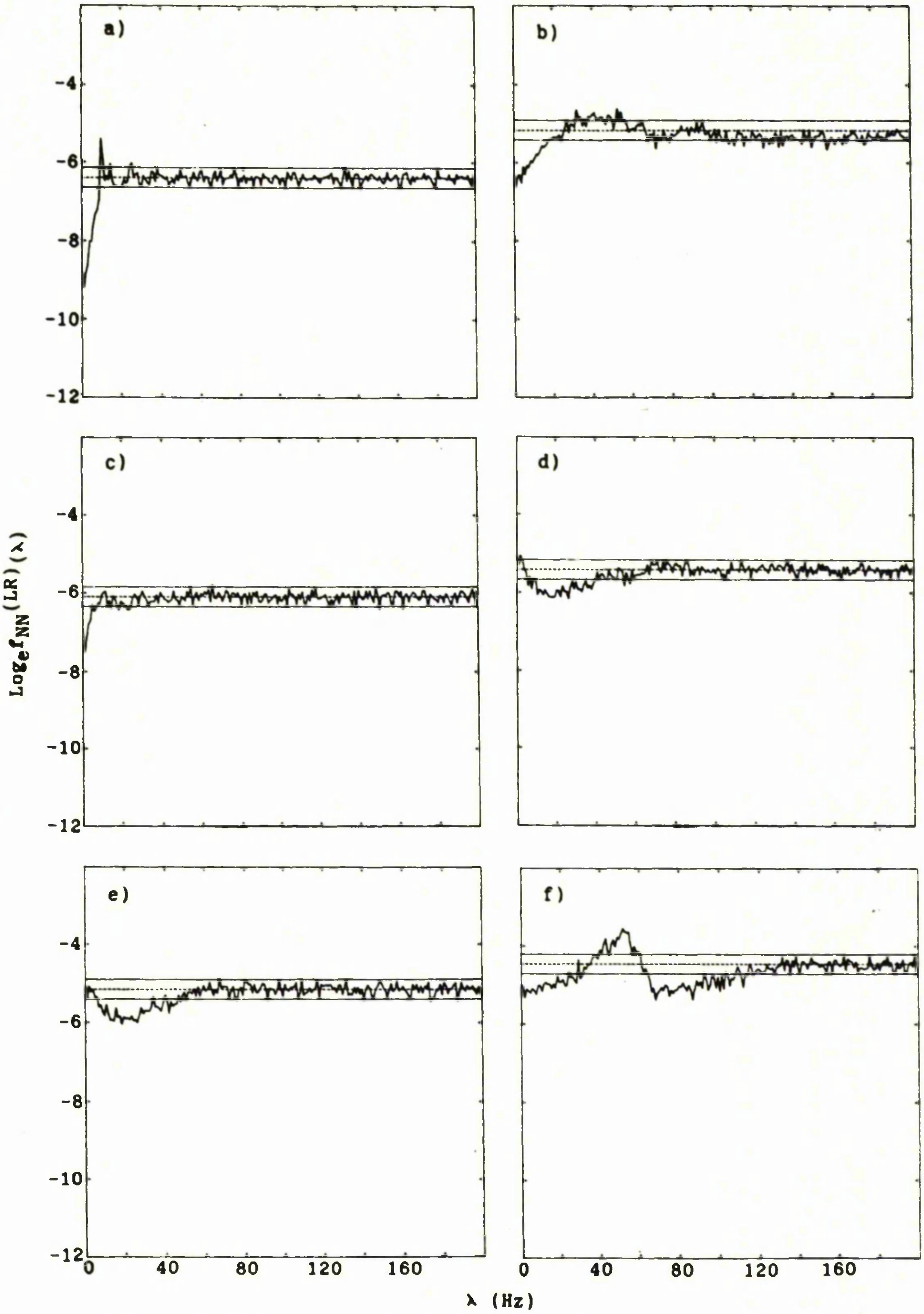

Fig.3.3.2 Log to the base e of the estimated auto-spectrum of

a) Ia spontaneous discharge
b) Ia discharge in the presence of a length change, ℓ
c) Ia discharge in the presence of a static gamma input, ${}_1\gamma_s$
d) Ia discharge in the presence of a 2nd static gamma input, ${}_2\gamma_s$
e) Ia discharge in the presence of both ${}_1\gamma_s$ and ${}_2\gamma_s$
f) Ia discharge in the presence of ℓ, ${}_1\gamma_s$, and ${}_2\gamma_s$

The estimates are based on the periodograms of disjoint segments (L=58, R=1024msec). The dotted line in each figure gives $\log_e(\hat{P}_N/2\pi)$ where $\hat{P}_N$ is the mean rate of the corresponding Ia discharge. The horizontal solid lines represent an approximate 95% confidence interval for the spectrum at a given frequency under the hypothesis of Poisson process.

activation of $_1\gamma_s$ alone not only destroys the regularity of the Ia discharge but also breaks down the dependence between the pulses of the discharge. These additional features about the Ia discharge which were not reflected in the time domain analysis (Fig.3.2.3) demonstrate the effectiveness and usefulness of the frequency domain analysis. Fig. 3.3.2e, which gives the estimate $\log_e f_{IaIa}{}^{(T)}(\lambda)$ when both static gamma inputs are activated concurrently and independently, can be seen as a weighted combination of Figs. 3.3.2c and 3.3.2d revealing the joint effect of both gamma static motoneurons. Finally, Fig.3.3.2f which is the estimate of $\log_e[f_{IaIa}(\lambda)]$ when all the inputs i.e., 'ℓ', $_1\gamma_s$ and $_2\gamma_s$ are applied to the spindle has quite different features in it. A combined effect of all these inputs can clearly be seen at low frequencies in the range of 0-30 Hz. The effect of the length change, is, however, seen to be stronger at frequencies 40-50 Hz. resulting in a periodicity at about 50 Hz., and which is consistent with the corresponding time domain figure3.2.3f.

Figure 3.3.3 gives a similar comparison between the estimated spectra of the II discharge under the same input conditions. Based on procedure 3, these figures have been plotted over the same range of frequencies with the same periodogram length of the segments as in Fig. 3.3.2.

Fig. 3.3.3a is the estimate of $\log_e[f_{II,II}(\lambda)]$ in the absense of any input. which reveals exactly the same features as the Fig. 3.3.1b based on procedure 1. However, a slight difference between these two estimates is an obvious consequence of a different approach and can be attributed to the fact that they are based on different periodogram lengths and smoothing schemes. A extensive discussion on this point can be seen in Rigas(1983, Chapter 3). Priestley(1987,chap.6) discusses a variety of window functions in the context of continuous time series.

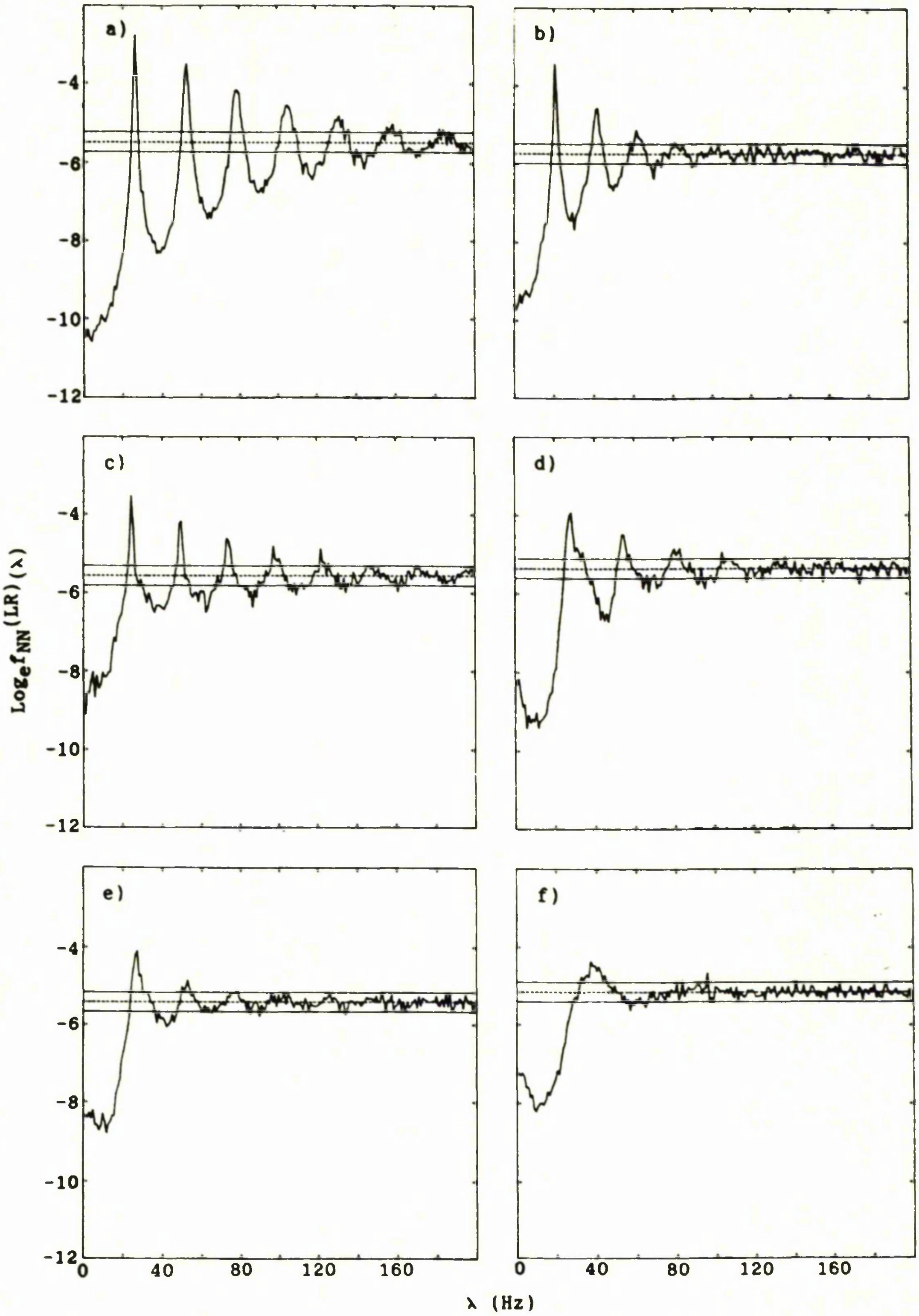

Fig.3.3.3 Log to the base e of the estimated spectrum of

a) II spontaneous discharge
b) II discharge in the presence of a length change, ℓ
c) II discharge in the presence of a static gamma input, $_1\gamma_s$
d) II discharge in the presence of a 2nd static gamma input, $_2\gamma_s$
e) II discharge in the presence of both $_1\gamma_s$ and $_2\gamma_s$
f) II discharge in the presence of ℓ, $_1\gamma_s$, and $_2\gamma_s$

The estimates are based on the periodograms of disjoint segments (L=58, R=1024msec). The dotted line in each figure gives $\log_e(\hat{P}_N/2\pi)$ where $\hat{P}_N$ is the mean rate of the corresponding II discharge. The horizontal solid lines represent an approximate 95% confidence interval for the spectrum at a given frequency under the hypothesis of Poisson process.

Comparing Fig. 3.3.3a with the other figures b-f we see that the regularity of the II discharge is not affected by the presence of any of the inputs. A slight change in the mean rate, however, suggests a possible excitatory or inhibitory effect due to the inputs being applied.

From the above analysis, we may conclude that the presence of any of the gamma static motoneurons destroys the regularity of the Ia discharge but the presence of the length change alongwith these motoneurons helps in maintaining this regularity by increasing the rate of the discharge.The regularity of the II spontaneous discharge, however, remains unaffected by the presence of these inputs. We also see that both estimation procedures are consistent with each other and reveal not only the same features but some more in the frequency domain than that obtained in time domain analysis.

3.4 SUMMARY AND CONCLUSIONS

In this chapter a univariate stationary point process was introduced. Certain parameters were defined in both the time and frequency domains. A variety of procedures for estimating these parameters was discussed. Large sample properties of these estimates were examined, and asymptotic confidence intervals for certain parameters of interest were constructed. The applications of these procedures were demonstrated by applying them to the muscle spindle data described in Chapter 1.

A close comparison of these procedures and their applications in both domains emphasized the use of the frequency domain methods, since they were found to reveal more about the process under investigation. However, the time domain methods together with the frequency domain ones proved quite helpful in promoting a better understanding, and drawing conclusions about the characteristics of the underlying process.

We summarise the important features of the procedures of both domains we discussed in this chapter.

1. The auto intensity-function (AIF) may be considered as a useful time domain measure of the inter-relationships between the events of a univariate point process.
   Method 3 for constructing asymptotic confidence intervals for this parameter improves the large sample properties as well as the symmetry of the estimate.
2. The power spectrum of a point process reveals useful information about the frequency content of the process.
   The asymptotic confidence intervals for the spectrum provide a useful tool in detecting the periodicities as well as any Poisson behaviour of the process.

3. An estimate of the spectrum may be based on a variety of procedures. Based on method 3, an estimate may be obtained by averaging the periodogram ordinates over a number of disjoint segments of the whole record. One may also use overlapping segments in the case of a short amount of data to form a (shingled) estimate (Brillinger, 1974a, 1983). A discussion and application of this modification in the case of ordinary time series may be found in Welch(1972).

One of the main advantages of method 3 is that it requires less storage space, a computationally desirable property, as well as this, it is also found to be faster than the other mentioned methods. However, there is a difficulty that it does not give an estimate at $\lambda=0$ (Brillinger, 1981).

Emphasizing method 3, we estimated the spectrum, mainly, based on the disjoint sections in order to form a basis for the multivariate point process analysis (Chapters 4, 5, and 6).

CHAPTER 4

BIVARIATE POINT PROCESSES

4.1 INTRODUCTION

The procedures discussed in the previous Chapter for analysing a univariate stationary point process in both time and frequency domains may be extended to the bivariate case. Comparative studies of both domains again emphasize the usefulness of the frequency domain methods.

In this Chapter certain parameters of a bivariate stationary point process in both domains are defined. Estimates of these parameters are considered and their large sample properties are examined. Asymptotic confidence intervals for certain parameters are constructed and illustrated. Certain tests of significance useful for investigating interesting features of the processes are developed and applied to the data sets.

The main aim of this Chapter is again to compare the methods of both domains as well as to apply them to the data sets in order to have more insight into the processes under investigation.

The muscle spindle receives a number of point process-like inputs and gives rise to at least two other point process-like outputs, the Ia and II discharges. It becomes desirable to consider it as a point process system and identify the properties of this system.

The second part of this Chapter considers the problems of identification of a linear time-invariant point process system. A single-input single-output linear model is introduced and developed. The objective of this model is to identify the system (muscle spindle) by relating the outputs, the Ia and II discharges, to each of the input point processes, and measuring the relationship between the input and output.

We start with the analysis in the time domain and discuss certain parameters of a bivariate stationary point process.

4.2 PARAMETERS IN THE TIME DOMAIN

Let $\underline{N}(t)=\{N_1(t),\ N_2(t)\}$ be a real-valued stationary bivariate point process defined on the real line with differential increment at t given by $\{dN_1(t),\ dN_2(t)\} = \{N_1(t,\ t+dt],\ N_2(t,t+dt]\}$. Further suppose that $\underline{N}(t)$ satisfies the assumptions of orderliness and (strong) mixing.

We define the following parameters which are useful for analysing a bivariate point process in the time domain.

THE SECOND ORDER CROSS-PRODUCT DENSITY

The second order cross-product density of a stationary bivariate point process provides a measure of the intensity with which the events of the processes N_1 and N_2 separated by 'u' time units occur simultaneously, and is defined as

$$P_{21}(u)=\text{Lim}_{\,h_1,h_2\to 0}\ \Pr\{N_1 \text{ event in } (t,t+h_1] \text{ and } N_2 \text{ event in } (t+u,t+u+h_2]\}/h_1h_2 \qquad (4.2.1)$$

Since the process is orderly, the expression (4.2.1) may be written as (Khintchine,1960),

$$P_{21}(u) = E[dN_2(t+u)dN_1(t)]/dudt$$

It is also clear from (4.2.1) that

$$P_{21}(u) = P_{12}(-u) \qquad (4.2.2)$$

i.e. the cross-product density function is not an even function. Further, under the (strong) mixing condition, it follows from (4.2.1) that

$$\mathrm{Lim}_{u\to\infty}\ P_{21}(u) = P_2P_1 \tag{4.2.3}$$

where P_1 and P_2 are the mean intensities of the processes N_1 and N_2 respectively.

THE SECOND ORDER CROSS-INTENSITY FUNCTION (CIF)

A related useful function called the cross intensity function provides a measure of the intensity with which an event of process N_2 occurs at time t+u given that there is an N_1 event at time t and is defined by

$$m_{21}(u) = \mathrm{Lim}_{h\to 0}\ \Pr\{N_2 \text{ event in } (t+u,\ t+u+h] \mid N_1 \text{ event at } t\}/h$$

$$= E\{dN_2(t+u) \mid dN_1(t)=1\}/du$$

$$= P_{21}(u)/P_1 \qquad \text{(using stationarity)}$$

It follows from expression (4.2.2) that $m_{21}(u)$ is not an even function. Under a (strong) mixing condition, it also follows that,

$$\mathrm{Lim}_{u\to\infty}\ m_{21}(u) = P_2 \tag{4.2.4}$$

which implies that the function $m_{21}(u)$, in practice, should fluctuate closely around the mean intensity P_2 for large u.

CROSS-COVARIANCE FUNCTION (CCF)

Another useful function which measures the covariance structure between the increments of the two processes separated by 'u' time units is called the cross covariance function and is defined as

$$\mathrm{Cov}\{dN_2(t+u),\ dN_1(t)\} = \mathrm{cum}\{dN_2(t+u), dN_1(t)\}$$

$$\mathrm{Cov}\{dN_2(t+u),\ dN_1(t)\} = E\{[dN_2(t+u)-P_2du][dN_1(t)-P_1dt]\}$$

$$= [P_{21}(u)-P_2P_1]dudt \qquad (4.2.5)$$

The function $q_{21}(u)=P_{21}(u)-P_2P_1$ is called the second-order cumulant function and under a (strong) mixing condition it tends to 0 as $u\to\infty$.

4.2.1 ESTIMATION OF THE PARAMETERS

We now turn to the problem of estimating the parameters defined above.

Let $\underline{N}(t)=\{N_1(t),\ N_2(t)\}$ be a stationary bivariate point process satisfying (strong) mixing and orderliness conditions. Further, let $\underline{N}(t)$ be observed on the interval $(0,T]$ with r_j $[j = 1,2,\ldots,N_1(T)]$ and s_k $[k=1,2,\ldots,N_2(T)]$ the observed times of the events of the processes N_1 and N_2 respectively, where $N_k(T)$ $[k=1,2]$ is the number of events of process N_k occurring in $(0,T]$.

The parameters $P_{21}(u)$ and $m_{21}(u)$ may be estimated (Brillinger, 1976a,b) by

$$\hat{P}_{21}(u)=J_{21}^{(T)}(u)/hT \qquad (4.2.6)$$

$$\hat{m}_{21}(u)=J_{21}^{(T)}(u)/hN_1(T) \qquad (4.2.7)$$

where

$$J_{21}^{(T)}(u) = \#\{(s_k,r_j);\ \text{such that } u-(h/2)<s_k-r_j<u+(h/2)\} \qquad (4.2.8)$$

where h is a binwidth. The symbol $\#\{A\}$ denotes the number of events in set A.

The variate $J_{21}^{(T)}(u)$, like $J_{NN}^{(T)}(u)$ in the case of a univariate point process defined in chapter 3, is a histogram-type estimate and counts the number of differences $(s_k - r_j)$ which fall in a bin of width h centred on u.

Finally, the cumulant function $q_{21}(u)$ can simply be estimated by substituting the respective estimates in the expression (4.2.5) i.e.,

$$\hat{q}_{21}(u) = \hat{P}_{21}(u) - \hat{P}_2\hat{P}_1$$

In the next section we discuss the properties of the estimates described above.

4.2.2 <u>PROPERTIES OF THE ESTIMATES</u>

Let $\underline{N}(t)=\{N_1(t), N_2(t)\}$ $0<t<T$ be a stationary, orderly bivariate point process satisfying a strong mixing condition. Then the variates $J_{21}^{(T)}(u_j)$, $u_j=hj$; $j=1,2,\ldots,$ given by expression (4.2.8) are asymptotically independent Poisson with mean $(hT)P_{21}(u_j)$, $j=1,2,\ldots,$ as $T\to\infty$ (Brillinger, 1976a). This implies that for large T

$$\hat{P}_{21}(u) \sim (hT)^{-1} \, Po[(hT)P_{21}(u)] \qquad (4.2.9)$$

and

$$\hat{m}_{21}(u) \sim (hTP_1)^{-1} \, Po[(hT)P_{21}(u)] \qquad (4.2.10)$$

where $Po[\alpha]$ denotes a Poisson random variable with mean α.
Further, if $h\to0$, $T\to\infty$ in such a way that $hT\to\infty$, then the estimates given in (4.2.9) and (4.2.10) will be approximately normal (Brillinger, 1976a), i.e.,

$$\hat{P}_{21}(u) \sim N[P_{21}(u), \, P_{21}(u)/hT] \qquad (4.2.11)$$

$$\hat{m}_{21}(u) \sim N[m_{21}(u),\ m_{21}(u)/hTP_1] \tag{4.2.12}$$

The variance of $\hat{m}_{21}(u)$ may be stabilised by applying a square root transformation (Kendall & Stuart, 1966), i.e., under the same limiting conditions the distribution of the transformed variate $[\hat{m}_{21}(u)]^{1/2}$ is seen to be as

$$[\hat{m}_{21}(u)]^{1/2} \sim N\{[m_{21}(u)]^{1/2},\ [4hTP_1]^{-1}\} \tag{4.2.13}$$

4.2.3 <u>CONFIDENCE INTERVAL FOR THE CROSS-INTENSITY</u>

As the auto-intensity function (AIF) proves a useful tool in assessing the auto-covariance structure between the increments of a univariate point process, similarly the cross-intensity function (CIF) may be used as a measure of the association between two point processes. Approximate confidence intervals for the cross-intensity function at a given lag value under the hypothesis that the processes are independent can easily be constructed. The limiting form of $m_{21}(u)$ given in expression (4.2.4) suggests that in the case that the increment of N_1 is independent of the increment of the N_2 process, u time units apart, the CIF, $m_{21}(u)$, will be

$$m_{21}(u)=P_2$$

We may examine this hypothesis by constructing an approximate 95% confidence interval for the asymptotic value of $[m_{21}(u)]^{½}$ based on expression (4.2.13) of the form,

$$[\hat{P}_2]^{1/2} \pm 1.96[4hT\hat{P}_1]^{-1/2}$$

or for convenience,

$$[\hat{P}_2]^{1/2} \pm [hN_1(T)]^{-1/2} \tag{4.2.14}$$

Values of the estimate $[\hat{m}_{21}(u)]^{1/2}$ lying outside the confidence interval at a given lag u may suggest a departure from the hypothesis that the increments of the process N_1 are independent of that of the process N_2 at that lag. The CIF may also be used to assess the timing relations between the processes as well as the nature of the association i.e., whether the effects of one process on the other are excitatory or inhibitory.

4.2.4 APPLICATIONS

Before applying the above methods to our real data sets, we start with a simulation study. We generate bivariate point process data set with excitatory effects (see chapter 1) and a known time delay between them using the following scheme.

Let I, ϵ_1 and ϵ_2 be three independent Poisson processes with r_i $[i=1,2,...,N_I(T)]$, s_j $[j=1,2,...,N_{\epsilon 1}(T)]$ and t_k $[k=1,2,...,N_{\epsilon 2}(T)]$ the times of the events of the processes I,ϵ_1 and ϵ_2 respectively. We construct two more processes N_1 & N_2 by superposing the above processes in the following manner

$$N_1(t) = I+\epsilon_1$$
$$N_2(t) = I^d+\epsilon_2$$

where '+' sign denotes a superposition (Cox & Lewis,1972) and I^d represents the process I delayed by 'd' units of time.

Generating N_1 and N_2 as above with d=10 msec, we estimate the CIF of the two processes. Figure (4.2.1b) demonstrates the application of the cross-intensity function of this data set, the estimate of which is based on expression (4.2.7).

In our example the variate $J^{(T)}{}_{21}(u)$ is calculated with a binwidth of h=1 msec. The computation of this variate is carried out by applying a new algorithm (Halliday, 1986) which is faster than the previous algorithms given in Brillinger(1976b) and Rigas(1983). This algorithm takes the advantage of the fact that the times of the events are always stored in ascending order, and the range of the lag values of interest is usually very short as compared with the record length. A direct cross-comparison between the events of the two processes, therefore, does not require any pooling of the processes, and so un-necessary comparisons within the processes are avoided. It is described in Section II.1 of Appendix II.

Figure 4.2.1a corresponds to the square root of the cross-intensity function (CIF) of the two independent Poisson processes ϵ_1 and ϵ_2. The dotted line represents the estimate $[\hat{P}_2]^{1/2}$ while the solid horizontal lines are approximate 95% confidence limits at a given lag u, and are based on the expression (4.2.14) under the hypothesis of the two processes being independent. The independence hypothesis is strongly supported. It is clearly seen how these confidence limits help in assessing the hypothesis of no association between the two processes.

Fig. 4.2.1b is the square root of $\hat{m}_{21}(u)$, the CIF of the computer simulated point process data N_1 & N_2. It clearly demonstrates the application and interpretation of the CIF. As expected, a large, sharp, and well-defined peak occurs at u=10 msec suggesting a strong association between the processes at this lag with an N_1 event having, on the average, an excitatory effect on the N_2 event occuring about 10 msec later.

Figure 4.2.1c represents the square root of the estimated CIF of real physiological data where the process N_2 corresponds to a single unit EMG (discharge) recorded from the soleus

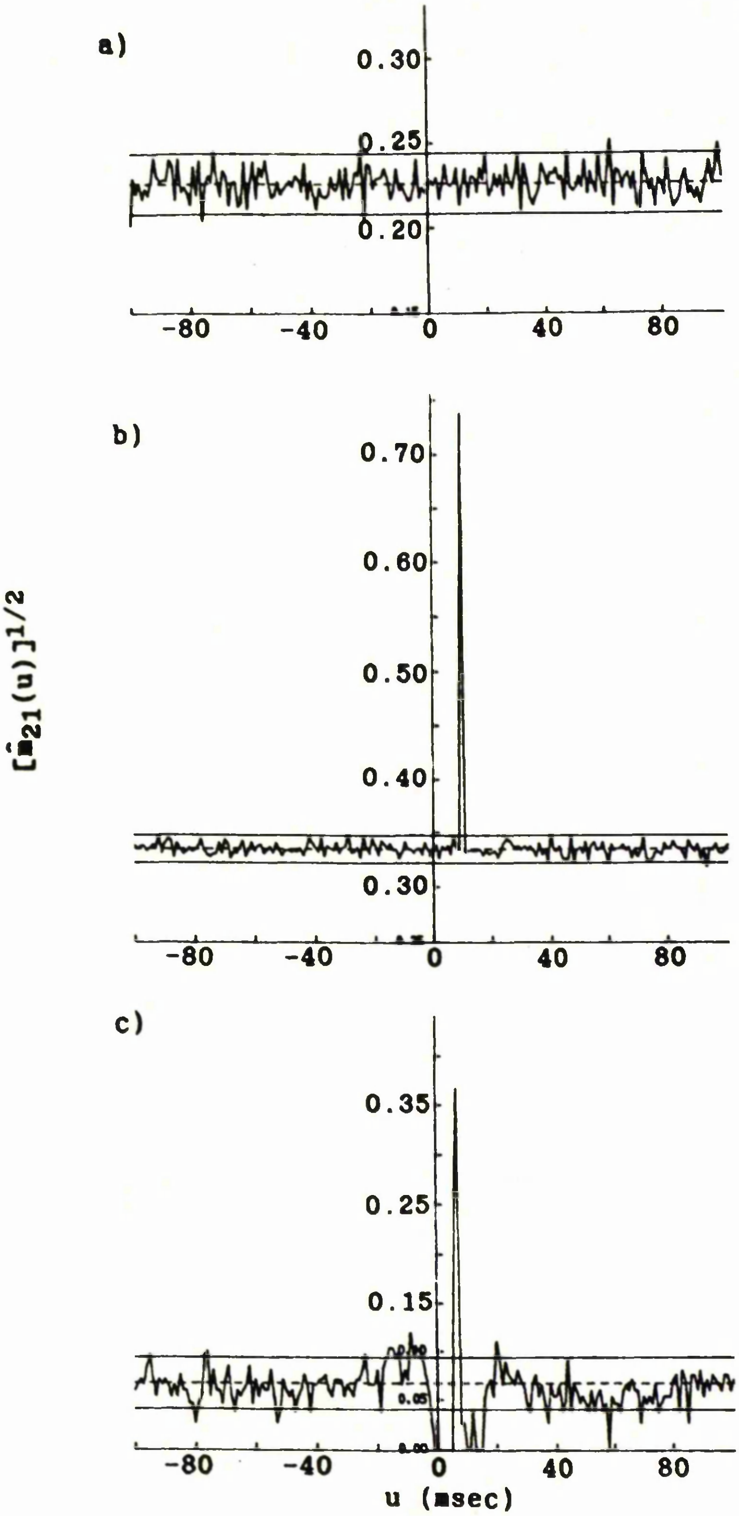

Fig.4.2.1 Square root of the estimated cross-intensity function of

a) two independent Poisson processes
b) computer simulated data dominated by a pure delay
c) real data corresponding to a single unit EMG (N_2) when a random stimulation (N_1) of Medial Gastronemius nerve is applied at group I threshold

The dotted line in each figure represents the square root of the corresponding mean rate $\hat{P}_2$. The horizontal solid lines below and above this line give an approximate 95% confidence interval for $[m_{21}(u)]^{½}$ under the hypothesis of N_1 and N_2 being independent.

muscle during a random stimulation (process N_1) of the Medial Gastrocnemius nerve at group I threshold (see chapter 1). The figure clearly reveals similar features to those seen in the simulated data, except for a dip at the origin which shows an inhibitory effect of N_1 on N_2 i.e there is no N_2 spike occurring immediately after an N_1 spike. The large and well defined peak at u=7 msec suggests that the random stimulation excites the group I fibres after about 7 msec. This delay is consistent with the known conduction velocities of both discharges.

Application of the CIF also provides useful information in assessing changes in the relationship between two processes brought about by the presence of the other processes. Figures 4.2.2a-b are examples of the CIF between a static fusimotor '${}_1\gamma_s$' and a Ia ending (Fig. 4.2.2a) and a II ending (Fig. 4.2.2b) from the same spindle. Fig. (4.2.2a) reveals a strong association between ${}_1\gamma_s$ and the Ia over the range of lags 12-24 msec with an average delay of 14-16 sec, whereas Fig(4.2.2b) suggests a possible significant, though not very strong, association between ${}_1\gamma_s$ and the II ending. The ill-defined peak in the estimate about lag 20-30 msec, however, does not allow one to estimate accurately the time delay between ${}_1\gamma_s$ and the II discharge. A comparison between both figures (4.2.2a) and (4.2.2b) also suggests that the association between the ${}_1\gamma_s$ and the Ia is stronger than that between the ${}_1\gamma_s$ and the II ending.

Figures 4.2.2c-d demonstrate how these CIF's are altered in the presence of other processes. For example, when a second fusimotor input, '${}_2\gamma_s$', is activated, the span of the association between ${}_1\gamma_s$ and the Ia is seen to have been reduced from 12-24 msec to 10-16 msec (Fig. 4.2.2c) with a shorter delay of about 12-14 msec between the two processes. On the other hand the presence of the ${}_2\gamma_s$ does not seem to alter the coupling between ${}_1\gamma_s$ and the II discharge

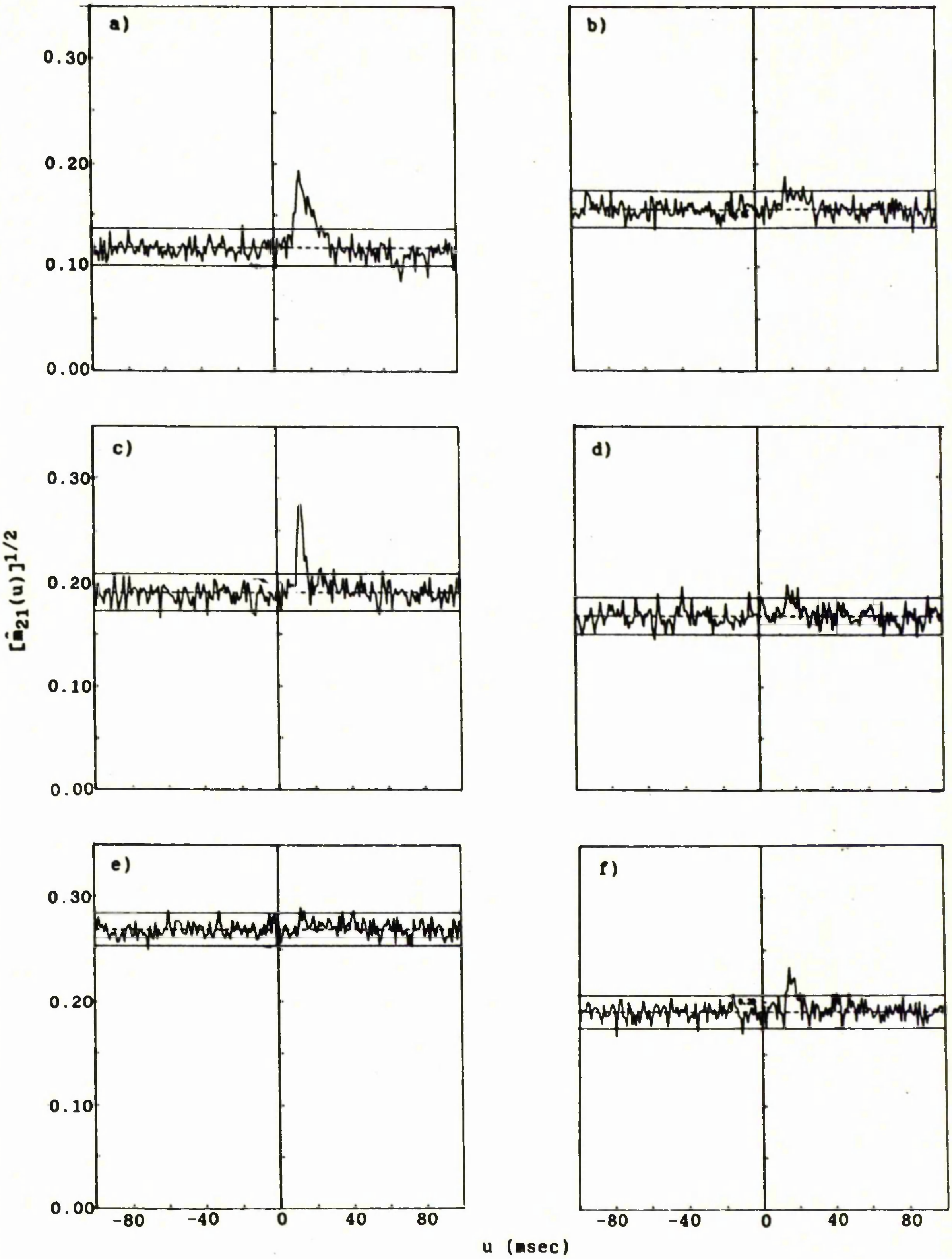

Fig.4.2.2 Square root of the estimated CIF between

a) Ia discharge and a static gamma input $_1\gamma_s$
b) II discharge and the static gamma input $_1\gamma_s$
c) Ia discharge and $_1\gamma_s$ in the presence of a second gamma $_2\gamma_s$
d) II discharge and $_1\gamma_s$ in the presence $_2\gamma_s$
e) Ia discharge and $_1\gamma_s$ in the presence of $_2\gamma_s$ and a length change
f) II discharge and $_1\gamma_s$ in the presence of $_2\gamma_s$ and a length change

The dotted line in each figure represents the square root of the mean rate of the corresponding output discharge whereas the solid horizontal lines give an approximate 95% confidence interval for $[m_{21}(u)]^{\frac{1}{2}}$ under the hypothesis of N_1 and N_2 being independent.

(Fig.4.2.2d), though there is a slight increase in the rate of the II discharge. Futher, a comparison of Figs. (4.2.2c) and (4.2.2d) reveals that the strength of coupling between ${}_1\gamma_s$ and the Ia discharge remains greater than that between ${}_2\gamma_s$ and the II discharge.

In addition, during the presence of a length change, 'ℓ', (Figs. 4.2.2e-f), the '${}_1\gamma_s$' activity is seen to become completely uncoupled from the Ia ending (Fig. 4.2.2e), although the rate of the Ia discharge is more than doubled. The coupling between ${}_1\gamma_s$ and the II ending is little changed (Fig. 4.2.2f).

This example suggests that within the same muscle spindle the Ia sensory axon becomes uncoupled from '${}_1\gamma_s$' by the presence of a dynamic length change 'ℓ' and responds to a combination of the '${}_2\gamma_s$' and 'ℓ' , whereas the II ending is largely unaffected by the activation of 'ℓ' and remains coupled to the fusimotor input ${}_1\gamma_s$.

The interpretation of the above results is consistent with the known differences in the behaviour of the Ia and II sensory endings of the muscle spindle examined separately in response to dynamically imposed length changes (e.g Matthews, 1981), with the additional information that the II ending, in the presence of the length change 'ℓ', still responds primarily to the fusimotor inputs.

Finally, we apply the CIF to the Ia and II sensory discharges from the same muscle spindle, in order to see any significant effects that the input stimuli may have on the coupling between these discharges. Figure 4.2.3 illustrates how the coupling between the output processes, the Ia and II, is affected by the presence of various input conditions imposed on the spindle. Fig. 4.2.3a clearly suggests that in the absence of any input, the two outputs, are independent of each other. The presence of a dynamic length change 'ℓ' imposed on the spindle, induces a dependence between the Ia and II discharges (Fig. 4.2.3b), in which the Ia discharge

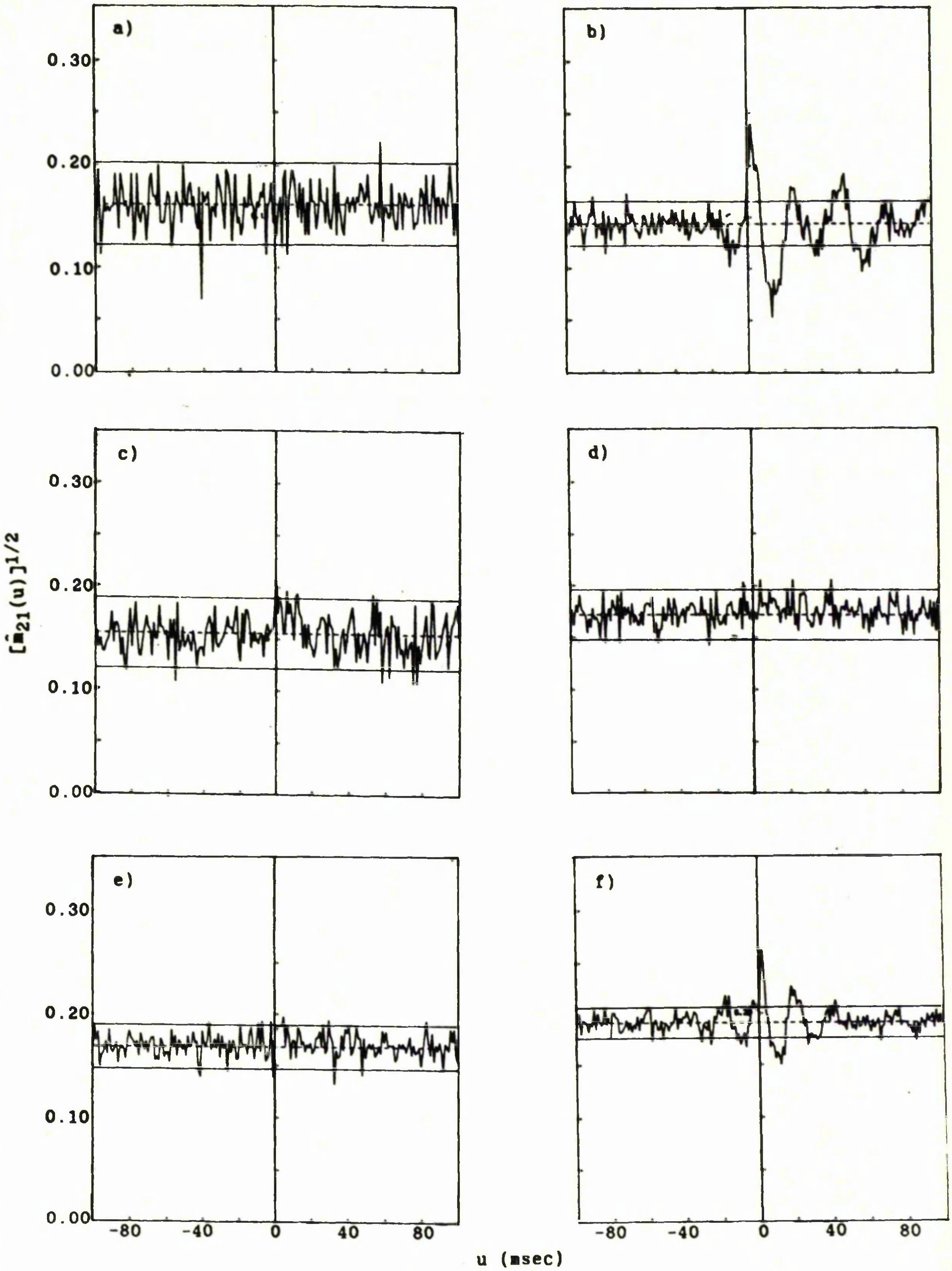

Fig.4.2.3 Square root of the estimated CIF between

a) Ia and II spontaneous discharges
b) Ia and II discharges in the presence of a length change ℓ
c) Ia and II discharges in the presence of a static gamma ${}_1\gamma_s$
d) Ia and II discharges in the presence of a second gamma ${}_2\gamma_s$
e) Ia and II discharges in the presence of both ${}_1\gamma_s$ and ${}_2\gamma_s$
f) Ia and II discharges in the presence of ${}_1\gamma_s$, ${}_2\gamma_s$ and ℓ

The dotted line in each figure gives $[\hat{P}_{Ia}]^{1/2}$ whereas the solid horizontal lines are an approximate 95% confidence interval for $[m_{IaII}(u)]^{1/2}$ under the hypothesis of independent discharges.

discharge becomes coupled with the II discharge in a periodic way. This suggests a possible periodic response of the II ending associated with the Ia ending. The effects of the fusimotor inputs (Fig. 4.2.3c-e) on the association between the Ia and II endings are not revealed clearly, although a small tendency for the Ia & II to become coupled can possibly be seen at low lags. The final figure (4.2.3f) which corresponds to the estimate $[\hat{m}_{II,Ia}(u)]^{1/2}$ in the presence of all the three inputs reveals the same features as the Fig. (4.2.3b) except that there is an increase in the mean rate of the II discharge.

Therefore, we turn to the frequency domain analysis in order to develop certain parameters which may provide additional useful information regarding any distinguishable effects of these inputs on the relationship between the outputs.

4.3 PARAMETERS IN THE FREQUENCY DOMAIN

Let $\underline{N}(t)=\{N_1(t),N_2(t)\}$ be a stationary bivariate point process defined on the real line which satisfies the conditions of mixing and orderliness. Let P_1 and P_2 be the mean intensities of the component processes N_1 and N_2, respectively. Further, suppose that the cross-cumulant function $q_{21}(u)$ as defined in section 4.2 exists and satisfies the condition,

$$\int_{-\infty}^{+\infty}|q_{21}(u)|du<\infty$$

The cross spectrum of the bivariate process $\underline{N}(t)$ is defined as the Fourier transform of the cross cumulant function, i.e.

$$f_{21}(\lambda) = (1/2\pi)\int_{-\infty}^{+\infty}\exp(-i\lambda u)q_{21}(u)du \qquad -\infty<\lambda<\infty \qquad (4.3.1)$$

This parameter is proportional to the covariance of the component of frequency λ of the process N_1 with the corresponding component of the process N_2. Since the cumulants measure the statistical dependence between the processes, the cross spectrum $f_{21}(\lambda)$ may be interpreted as measuring the association of the processes N_1 and N_2 at frequency λ (Brillinger et al 1976), i.e., $f_{21}(\lambda)=0$ indicates no linear relationship at frequency λ.

The inverse relation of expression (4.3.1) is given by

$$q_{21}(u) = \int_{-\infty}^{+\infty}\exp(+i\lambda u)f_{21}(\lambda)d\lambda \qquad -\infty<u<\infty$$

The cross spectrum, in general, is a complex-valued function, and may be written in the form

$$f_{21}(\lambda) = [\mathrm{Re}\ f_{21}(\lambda)] + i\ [\mathrm{Im}\ f_{21}(\lambda)]$$

where $\mathrm{Re}\ f_{21}(\lambda)$ and $\mathrm{Im}\ f_{21}(\lambda)$ are the real and imaginary parts of $f_{21}(\lambda)$. Since $\underline{N}(t)$ is real-valued, so is $q_{21}(u)$. Further, as $q_{21}(u)=q_{12}(-u)$, the cross spectrum $f_{21}(\lambda)$ has the property

$$f_{21}(\lambda) = \overline{f_{21}(-\lambda)} = \overline{f_{12}(\lambda)} = f_{12}(-\lambda)$$

where for example $\overline{f_{12}(\lambda)}$ is the complex conjugate of $f_{12}(\lambda)$.

It follows from the the Riemann-Lebesque Lemma (Katznelson,1968; Papoulis,1962) that

$$\mathrm{Lim}_{\lambda\to\infty}\ f_{21}(\lambda) = 0$$

For further details, see for example, Cox & Lewis (1966) and Brillinger (1975a). Brillinger (1975c) and Brillinger et al (1976) also discuss point process parameters with applications to neurophysiological data.

In the next section we discuss the estimation procedures for the cross spectrum defined above.

4.3.1 ESTIMATION OF THE CROSS SPECTRUM

The procedures dicussed in chapter 3 for the estimation of the auto-spectrum of a univariate point process may be extended to the case of a bivariate point process.

Following procedure 3 of Section 3.3.6, an estimate of the cross spectrum may be based on the cross-periodograms of disjoint sections of the entire record length.

4.3.2 THE CROSS–PERIODOGRAM OF A BIVARIATE POINT PROCESS

Let $\underline{N}(t)=\{N_1(t),N_2(t)\}$ be a stationary bivariate and orderly point process satisfying a (strong) mixing condition. Suppose it is observed on the interval (0,T]. Futher, let the events of the component processes N_1 and N_2 have occurred at times r_j ; $j=1,2,3,\dots,N_1(T)$ and s_k ; $k=1,2,\dots,N_2(T)$, respectively. The cross-periodogram is defined as

$$I_{21}^{(T)}(\lambda)=(1/2\pi T)[d_2^{(T)}(\lambda)\overline{d_1^{(T)}(\lambda)}] \qquad -\infty<\lambda<\infty$$

where $d_1^{(T)}(\lambda)$ and $d_2^{(T)}(\lambda)$ are the finite Fourier-Stieltjes transforms of the processes N_1 and N_2 ,respectively, and are given by

$$d_1^{(T)}(\lambda) = \int_0^T \exp(-i\lambda r)dN_1(r) \equiv \sum_{j=1}^{N_1(T)} \exp(-i\lambda r_j) \tag{4.3.2}$$

$$d_2^{(T)}(\lambda) = \int_0^T \exp(-i\lambda s)dN_2(s) \equiv \sum_{k=1}^{N_2(T)} \exp(-i\lambda s_k) \tag{4.3.3}$$

and $\overline{d_1^{(T)}(\lambda)}$ denotes the complex conjugate of $d_1^{(T)}(\lambda)$.

The cross-periodogram $I_{21}^{(T)}(\lambda)$ is a complex function with the property

$$I_{21}^{(T)}(\lambda) = \overline{I_{21}^{(T)}(-\lambda)} = I_{12}^{(T)}(-\lambda)$$

From Theorems I.2 and I.3 of Appendix I, it follows that the cross-periodogram is an asymptotically unbiased estimate of the cross spectrum $f_{21}(\lambda)$. Under the conditions of the Theorems I.2 and I.3, it, further, follows that

$$\mathrm{Var}[I_{21}^{(T)}(\lambda)] = f_{22}(\lambda)f_{11}(\lambda)+O(T^{-1})$$

and

$$\mathrm{Cov}[I_{21}^{(T)}(\lambda),I_{21}^{(T)}(\mu)] = O(T^{-1}) \qquad \lambda \neq \pm\mu$$

which suggests that the periodogram ordinates at distinct frequencies are asymptotically independent. Further, the variance of $I_{21}^{(T)}(\lambda)$ remains at a constant level for all values of T as $T\to\infty$, which implies that the cross-periodogram is not a consistent estimate of the cross spectrum. Hence, smoothing procedures are required in order to improve the properties of this estimate.

4.3.3 A CONSISTENT ESTIMATE OF THE CROSS-SPECTRUM

Based on the cross-periodograms of disjoint segments, a consistent estimate of the cross-spectrum may be obtained as follows

Suppose that the bivariate point process $\underline{N}(t)$ is observed on $(0,T]$. Let the record length, T, be split into L disjoint sections each with duration R such that T=LR. We set,

$$d_k^{(R)}(\lambda,j) = \int_{jR}^{(j+1)R} \exp(-i\lambda t)\,dN_k(t) \qquad -\infty<\lambda<\infty$$

$$= \sum_{t=jR}^{(j+1)R} \exp(-i\lambda t)[N_k(t+1)-N_k(t)] \qquad \begin{matrix} k=1,2 \\ j=0,1,\ldots,L-1 \end{matrix}$$

and define the cross-periodogram of the jth section at frequency λ by

$$I_{21}^{(R)}(\lambda,j) = (1/2\pi R)[d_2^{(R)}(\lambda,j)\overline{d_1^{(R)}(\lambda,j)}] \qquad (4.3.4)$$

An estimate of the cross spectrum $f_{21}(\lambda)$ may now be obtained by averaging the periodograms over L sections at frequency λ i.e.,

$$f_{21}^{(T)}(\lambda) = (1/L)\sum_{j=0}^{L-1} I_{21}^{(R)}(\lambda,j) \qquad \lambda\neq 0 \qquad (4.3.5)$$

4.3.4 PROPERTIES OF THE ESTIMATE OF THE CROSS SPECTRUM

Let $\underline{N}(t)=\{N_1(t), N_2(t)\}$ be a bivariate stationary point process which satisfies the conditions of mixing and orderliness. Suppose the second order cross-cumulant function $q_{21}(u)$ exists and satisfies the condition

$$\int |u||q_{21}(u)|du<\infty$$

Let the estimate of the cross-spectrum $f_{21}(\lambda)$ be given by expression (4.3.5), then

$$\operatorname{Lim}_{T\to\infty} E[f_{21}^{(T)}(\lambda)]=f_{21}(\lambda) \qquad \text{and}$$

$$\operatorname{Lim}_{T\to\infty} \operatorname{Cov}\{f_{21}^{(T)}(\lambda),f_{21}^{(T)}(\mu)\}=[\delta\{\lambda-\mu\}f_{22}(\lambda)f_{11}(\lambda) +\delta\{\lambda+\mu\}f_{21}(\lambda)f_{21}(-\lambda)]/L$$

where $\delta\{\lambda\}=1$ if $\lambda=0$, and 0 otherwise. Further,

$$\operatorname{Lim}_{T\to\infty} \operatorname{Var}[f_{21}^{(T)}(\lambda)]=[f_{22}(\lambda)f_{11}(\lambda)]/L \qquad (4.3.6)$$

Proof:-

The proof follows from Theorem I.4 of Appendix I and setting

$$(L)^{-1} = \frac{2\pi}{b_T T}\int K^2(\alpha)d\alpha$$

Under the limiting condition that as $T\to\infty$, $L\to\infty$, but $(L/T)\to 0$, the estimate $f_{21}^{(T)}(\lambda)$ is normal with variance given in expression (4.3.6). An appropriate choice of L can reduce the variability of the estimate $f_{21}^{(T)}(\lambda)$ to an acceptable level of bias in the estimate.

As described at the beginning of this section, the cross-spectrum $f_{21}(\lambda)$ may be interpreted as reflecting the covariance between the harmonics at frequency λ of two processes. One disadvantage of the use of covariance as a measure of association is that it is not bounded, which means that although $f_{21}(\lambda)=0$ indicates the absence of a linear relationship at frequency λ, there are no values indicating a perfect relationship.

Given the limitations of the covariance based measure of association, in many situations, one turns to a regression type of analysis, which in the frequency domain leads naturally to measures of association based on the Fourier transforms of the processes (Brillinger,1986). One frequency domain measure of association, analogous to correlation-squared and called coherence, provides a normalized measure of the strength of association between two processes.

4.4 COHERENCE: A FREQUENCY-DOMAIN MEASURE OF ASSOCIATION

The coherence, $|R_{21}(\lambda)|^2$, between processes N_1 and N_2 at frequency λ may be defined as the limiting correlation-squared between the Fourier-Stieltjes transforms $d_1^{(T)}(\lambda)$ and $d_2^{(T)}(\lambda)$ as given in expressions (4.3.2) and (4.3.3), i.e.,

$$\text{Coherence} = |R_{21}(\lambda)|^2 = \text{Lim}_{T\to\infty} |\text{corr}[d_2^{(T)}(\lambda), d_1^{(T)}(\lambda)]|^2$$

where "corr" denotes complex correlation. By definition,

$$|R_{21}(\lambda)|^2 = \text{Lim}_{T\to\infty} \left| \frac{\text{Cov}[d_2^{(T)}(\lambda), d_1^{(T)}(\lambda)]}{\{\text{Var}[d_2^{(T)}(\lambda)]\text{Var}[d_1^{(T)}(\lambda)]\}^{1/2}} \right|^2$$

Now as

$$\mathrm{Cov}[d_2^{(T)}(\lambda), d_1^{(T)}(\lambda)] = \mathrm{cum}[d_2^{(T)}(\lambda), \overline{d_1^{(T)}(\lambda)}]$$

$$= E[d_2^{(T)}(\lambda)\overline{d_1^{(T)}(\lambda)}] - E[d_2^{(T)}(\lambda)]E[\overline{d_1^{(T)}(\lambda)}]$$

$$= \int_0^T\!\!\int \exp\{-i\lambda(s-r)\}q_{21}(s-r)drds$$

Setting s-r=u and v=r, we obtain

$$= \int_{-T}^{T}(T-|u|)\exp(-i\lambda u)q_{21}(u)du$$

$$= \int_{-T}^{T}(T-|u|)\exp(-i\lambda u)\left[\int_{-\infty}^{\infty}\exp(i\alpha u)f_{21}(\alpha)d\alpha\right]du$$

$$= \int_{-\infty}^{+\infty}\left[\int_0^T(T-u)\exp\{-i(\lambda-\alpha)u\}du + \int_0^T(T+u)\exp\{-i(\lambda-\alpha)u\}du\right]f_{21}(\alpha)d\alpha$$

$$= \int_{-\infty}^{\infty}[2/(\lambda-\alpha)^2][1-\cos(\lambda-\alpha)T]f_{21}(\alpha)d\alpha$$

$$= \int_{-\infty}^{\infty}\left[\frac{\sin(\lambda-\alpha)T/2}{(\lambda-\alpha)/2}\right]^2 f_{21}(\alpha)d\alpha \ .$$

With similar arguments, it can be shown that

$$\mathrm{Var}[d_k^{(T)}(\lambda)] = \int_{-\infty}^{\infty}\left[\frac{\sin(\lambda-\alpha)T/2}{(\lambda-\alpha)/2}\right]^2 f_{kk}(\alpha)d\alpha \qquad ; \quad k=1,2$$

The function

$$\frac{1}{2\pi T}\left[\frac{\sin(\lambda-\alpha)T/2}{(\lambda-\alpha)/2}\right]^2$$

tends to a delta fuction as $T\to\infty$ (Papoulis, 1962), which implies that

$$|R_{21}(\lambda)|^2 = \frac{|f_{21}(\lambda)|^2}{f_{11}(\lambda)f_{22}(\lambda)} \tag{4.4.1}$$

It can easily be shown that

$$0\leq|R_{21}(\lambda)|^2\leq 1$$

Hence the coherence is essentially a normalised cross spectrum which provides an absolute measure of association on a scale from 0 to 1 . The value $|R_{21}(\lambda)|^2=0$ indicates that the processes are independent whereas the value 1 signifies a perfect linear association. The coherence gives the range of frequencies over which the processes are associated.

4.4.1 ESTIMATION OF THE COHERENCE

An estimate of the coherence may be obtained simply by inserting the respective estimates in expression (4.4.1), i.e.,

$$|R_{21}^{(T)}(\lambda)|^2 = \frac{|f_{21}^{(T)}(\lambda)|^2}{f_{11}^{(T)}(\lambda)f_{22}^{(T)}(\lambda)} \qquad \lambda\neq 0 \tag{4.4.2}$$

4.4.2 PROPERTIES OF THE ESTIMATE OF THE COHERENCE

The estimate of coherence, $|R_{21}^{(T)}(\lambda)|^2$, may be interpreted as the point process analogue of the sample multiple correlation coefficient (i.e., a squared correlation coefficient in the case of simple linear regression theory). It possesses the same properties as the ordinary sample multiple correlation coefficient (Brillinger,1981), and these are discussed in Chapter 5.

4.4.3 A TEST FOR ZERO COHERENCE

Although $|R_{21}(\lambda)|^2$ lies between 0 and 1, with 0 occurring in the case of independence, the estimate $|R_{21}^{(T)}(\lambda)|^2$ for processes that are independent will have value greater than 0. To account for this sampling variability we may set up the following test to assess the hypothesis of independence at a given frequency λ.

From expression (5.5.15) of Chapter 5, it follows that under the hypothesis $|R_{21}(\lambda)|^2=0$, the estimate of coherence given by expression (4.4.2) is distributed as a Beta random variable with parameters 1 and L-1. In order to obtain a 100α per cent point for $|R_{21}^{(T)}(\lambda)|^2$ at frequency λ, it follows from the expression (5.5.17) that

$$z = 1-(1-\alpha)^{1/L-1} \tag{4.4.3}$$

is such that, under the hypothesis $|R_{21}(\lambda)|^2=0$,

$$\Pr[\,|R_{21}^{(T)}(\lambda)|^2 \leq z\,] = \alpha$$

i.e., we reject the hypothesis at frequency λ if $|R_{21}^{(T)}(\lambda)|^2 \geq z$.

4.4.4 ASYMPTOTIC CONFIDENCE INTERVAL FOR THE COHERENCE

In order to assess the possible closeness of an estimate to a parameter, it is desirable to provide a confidence interval for the parameter based on the estimate. Asymptotic distributions of the estimates may be used in this connection.

Theorem 5.5.1 implies that $|R_{21}^{(T)}(\lambda)|^2$ is an asymptotically unbiased estimate of the coherence, which is asymptotically normal with variance given by

$$\lim_{T\to\infty} \mathrm{Var}[|R_{21}^{(T)}(\lambda)|^2] = (2/L)|R_{21}(\lambda)|^2\,[1-|R_{21}(\lambda)|^2]^2 \quad (4.4.4)$$

An estimate of the variance of $|R_{21}^{(T)}(\lambda)|^2$ at frequency λ may be obtained by substituting the estimate $|R_{21}^{(T)}(\lambda)|^2$ in expression (4.4.4). Hence an approximate 95% confidence interval for $|R_{21}(\lambda)|^2$ at frequency λ may be constructed as

$$|R_{21}^{(T)}(\lambda)|^2 \pm 1.96\left[\frac{|R_{21}^{(T)}(\lambda)|^2[1-|R_{21}^{(T)}(\lambda)|^2]^2}{L/2}\right]^{1/2} \quad (4.4.5)$$

An alternative way of constructing an approximate confidence interval for the coherence at frequency λ may be obtained by considering a variance stabilizing transformation. Experience with variance stabilizing transformations (e.g, Kendall and Stuart, 1966) suggests that it is often possible to choose a transformation so that the transformed variate is more nearly normal than the untransformed one. A Hyperbolic Tangent transformation

$$\tanh^{-1}|R_{21}^{(T)}(\lambda)|$$

can be seen to improve the normality of the estimate with a stabilized variance (Brillinger, 1981) given by

$$\lim_{T\to\infty} \mathrm{Var}[\tanh^{-1} |R_{21}^{(T)}(\lambda)|] = 1/2L \qquad \lambda\neq 0 \qquad (4.4.6)$$

Hence an approximate 95% confidence interval for $\tanh^{-1}|R_{21}(\lambda)|$ at frequency λ may be given by

$$\tanh^{-1}|R_{21}^{(T)}(\lambda)| \pm 1.96[2L]^{-\frac{1}{2}} \qquad \lambda\neq 0 \qquad (4.4.7)$$

and with a back transformation, the corresponding 95% confidence interval for $|R_{21}(\lambda)|^2$ becomes

$$\left[\frac{\exp[c(\lambda)-k]-1}{\exp[c(\lambda)-k]+1}\right]^2 \leq |R_{21}(\lambda)|^2 \leq \left[\frac{\exp[c(\lambda)+k]-1}{\exp[c(\lambda)+k]+1}\right]^2 \qquad (4.4.8)$$

where

$$c(\lambda) = \ln\left\{\frac{1+|R_{21}^{(T)}(\lambda)|}{1-|R_{21}^{(T)}(\lambda)|}\right\} \qquad \lambda\neq 0$$

and

$$k = 2.77/\sqrt{L}$$

Similar results in the case of ordinary time series can found in Brillinger(1981), Bloomfield(1976) and Jenkins and Watts(1968).

4.4.5 A TEST FOR EQUALITY OF TWO COHERENCES

Some times it is desired to test whether two independent bivariate point processes have the same correlation structure, i.e., whether the coherences of both bivariate processes are equal at all frequencies. A statistical test for such a hypothesis may be set up based either on the transformed variate $\tanh^{-1} |R_{21}^{(T)}(\lambda)|$ or the untransformed one, i.e., a test of the null hypothesis

$$|R_{ab}(\lambda)|^2 = |R_{cd}(\lambda)|^2$$

is equivalent to the test that

$$\tanh^{-1}|R_{ab}(\lambda)|=\tanh^{-1}|R_{cd}(\lambda)|.$$

Now as

$$\tanh^{-1}|R_{ab}^{(T)}(\lambda)| \sim N[\tanh^{-1}|R_{ab}(\lambda)|,\ 1/2L]$$

and

$$\tanh^{-1}|R_{cd}^{(T)}(\lambda)| \sim N[\tanh^{-1}|R_{cd}(\lambda)|,\ 1/2L]$$

therefore, under the null hypothesis,

$$\tanh^{-1}|R_{ab}(\lambda)|-\tanh^{-1}|R_{cd}(\lambda)| \sim N[0,\ 1/L]$$

There is no covariance term since the estimates of both coherences are from independent experiments (i.e., independent bivariate point processes). The case with a significant covariance structure will be discussed in chapter 5.

We reject the hypothesis of equal coherences at frequency λ if

$$\left| \tanh^{-1}|R_{ab}^{(T)}(\lambda)|-\tanh^{-1}|R_{cd}^{(T)}(\lambda)| \right| \geq 1.96[L]^{-½}$$

4.5 IDENTIFICATION OF A POINT PROCESS SYSTEM

A point process system may be considered as a collection of (1) a space of input step functions $N_1(t)$, (2) a space of output step functions $N_2(t)$, and (3) an operator 'S' which carries input functions over into output functions. A point process system is called time-invariant if the bivariate process $\underline{N}(t)=\{N_1(t),\ N_2(t)\}$ is stationary for stationary $N_1(t)$. A system is said to be stochastic if it incorporates random features. A system is said to have a refractory period if there exists a time interval immediately following an output event, during which time there can be no further output, for example, refractoriness in neuronal discharges is similar to dead times in a Geiger counter.

By the identification of a point process system, we mean the determination of the characteristics of the system, i.e, the operator, from the information available in the realizations of the input and output processes. For a stochastic system a complete identification is not possible, and the best we can hope for is to determine the average properties of the quantities or parameters that characterize the system 'S'.

4.5.1 SINGLE-INPUT SINGLE-OUTPUT POINT PROCESS LINEAR MODEL

The muscle spindle may be thought of as a point process system which is assumed to receive inputs in the form of point processes and gives rise to at least two point process outputs, the Ia and II discharges. We begin with a single input - single output point process description

$$N_1(t)\ \text{————}\ \boxed{\begin{array}{c}\text{muscle}\\ \text{spindle}\end{array}}\ \text{————}\ N_2(t)$$

and develop a simple linear point process model to represent the following key characteristic of the system

$$\mu_1(t) = \text{Lim}_{h\to 0} \Pr\{N_2 \text{ event in } (t, t+h] | N_1\}/h$$

$$= E\{dN_2(t) | N_1\}/dt \tag{4.5.1}$$

Suppose that in the absence of any input, $N_1(.)\equiv 0$, and that $\mu_1(t)$ exists and is equal to a constant

$$\mu_1(t) = \alpha_0 \tag{4.5.2}$$

The system here is seen to emit events at rate α_0.

Next, if the input corresponds to a single event at time u, the expression (4.5.2) may be altered to

$$\mu_1(t) = \alpha_0+\alpha_1(t-u) \tag{4.5.3}$$

where $\alpha_1(t-u)$ represents the effect on the output process of a single event at time u.

Similarly, if a number of input events occurred at times $u_1,u_2,\ldots$, the expression (4.5.3) becomes

$$\mu_1(t) = \alpha_0 + \alpha_1(t-u_1) + \alpha_1(t-u_2)+\ldots$$

i.e., $$\mu_1(t) = \alpha_0+\int_{-\infty}^{\infty}\alpha_1(t-u)dN_1(u)$$

$$E\{dN_2(t) | N_1\} = \left[\alpha_0+ \int\alpha_1(t-u)dN_1(u)\right]dt \tag{4.5.4}$$

The model (4.5.4) may be seen as a point process analogue of the linear time invariant systems considered for ordinary time series. By analogy with the terminology of the cross spectral analysis of ordinary time series, $\alpha_1(u)$ is called the average impulse response function (Brillinger, 1974b) and its Fourier transform given by

$$A(\lambda) = \int \exp(-i\lambda u)\alpha_1(u)du \qquad -\infty < \lambda < \infty$$

is called the transfer function of the point process system.

4.5.2 SOLUTION OF THE MODEL

The solution to the model (4.5.4) for α_0 and $\alpha_1(.)$, in the least square sense, may be obtained by minimizing the mean squared error (M.S.E) given by

$$E\left[dN_2(t)-[\alpha_0+\int \alpha_1(t-u)dN_1(u)]dt\right]^2$$

or as follows;

Taking the expected value of equation (4.5.4) with respect to N_1, we have

$$E\{\ E[dN_2(t)|N_1]\ \} = \left[\alpha_0+\int \alpha_1(t-u)E[dN_1(u)]\right]dt$$

$$\text{i.e.,} \qquad P_2 = \alpha_0+P_1\int \alpha_1(u)du$$

which implies that

$$\alpha_0 = P_2-P_1\int \alpha_1(u)du \tag{4.5.5}$$

where P_1 and P_2 are the mean intensities of the input and ouput processes, respectively.

Similarly, multiplying equation (4.5.4) by $dN_1(t-u)$ and taking the expected value with respect to N_1, we obtain

$$E\left[E\{dN_2(t)|N_1\}dN_1(t-u)\right] = \left[\alpha_0 E\{dN_1(t-u)\} + \int \alpha_1(t-v)E\{dN_1(v)dN_1(t-u)\}\right]dt$$

$$P_{21}(u) = P_1\alpha_0 + \int \alpha_1(t-v)\left[P_{11}(v-t+u) + P_1\delta(v-t+u)\right]dv$$

where $\delta(.)$ is the Dirac delta function. Substituting the value of α_0 from (4.5.5) and simplifying, we obtain

$$q_{21}(u) = P_1\alpha_1(u) + \int \alpha_1(u-v)q_{11}(v)dv \qquad (4.5.6)$$

where $q_{11}(.)$ is the cumulant function of the input N_1 and $q_{21}(.)$ is the cross cumulant function between output, N_2, and input, N_1. From expression (4.8.5), it follows that if the input is a Poisson process then the impulse response function becomes

$$\alpha_1(u) = q_{21}(u)/P_1$$

However, in general, the solution to the equation (4.5.6) for $\alpha_1(u)$ requires some form of deconvolution, which may be avoided by taking the Fourier transform of (4.5.6), i.e.,

$$\frac{1}{2\pi}\int \exp(-i\lambda u)q_{21}(u)du = \frac{1}{2\pi}\int \exp(-i\lambda u)\left[\int \alpha_1(u-v)q_{11}(v)dv + P_1\alpha_1(u)\right]du$$

$$f_{21}(\lambda) = \frac{1}{2\pi}\int \exp(-i\lambda u)\left[\int \alpha_1(u-v)\{q_{11}(v)+P_1\delta(v)\}dv\right]du$$

which gives after some manipulations

$$f_{21}(\lambda)=A(\lambda)f_{11}(\lambda) \tag{4.5.7}$$

where $f_{11}(\lambda)$, $f_{21}(\lambda)$ and $A(\lambda)$ are the auto-spectrum of N_1, cross-spectrum between N_1 and N_2 and the transfer function of the system, respectively.

Expression (4.5.7) shows that $A(\lambda)$ may be identified by

$$A(\lambda)=f_{21}(\lambda)/f_{11}(\lambda) \qquad f_{11}(\lambda)\neq 0 \tag{4.5.8}$$

The impulse response function, $\alpha_1(u)$, may now be determined by the inverse Fourier transform of (4.5.8), i.e.,

$$\alpha_1(u) = \int \exp(i\lambda u)A(\lambda)d\lambda$$

4.5.3 MEAN SQUARED ERROR OF THE MODEL

In order to obtain the mean squared error (MSE) of the linear point process model, expression (4.5.4) suggests that we define the following process

$$d\epsilon(t)= dN_2(t)- \left[\alpha_0 + \int \alpha_1(t-u)dN_1(u)\right]dt$$

where $d\epsilon(t)$ is an error process with stationary increments. Clearly $E[d\epsilon(t)]=0$.

The product density of $d\epsilon(.)$ at times t and t' is given by

$$[P_{\epsilon\epsilon}'(t-t')+P_{\epsilon}\delta(t-t')]dtdt' = E\{d\epsilon(t)d\epsilon(t')\}$$

$$= E\left[dN_2(t)-\left\{\alpha_0+\int\alpha_1(t-u)dN_1(u)\right\}dt\right]\left[dN_2(t')-\left\{\alpha_0+\int\alpha_1(t'-v)dN_1(v)\right\}dt'\right]$$

Substituting the value of α_0 from expression (4.5.5) and simplifying, we obtain

$$P_{\epsilon\epsilon}(t-t')+P_{\epsilon}\delta(t-t')=q_{22}(t-t')+P_2\delta(t-t')-\int\alpha_1(t-u)q_{21}(t'-u)du$$

$$-\int\alpha_1(t'-v)q_{21}(t-v)dv$$

$$+\iint\alpha_1(t-u)\alpha_1(t'-v)\left[q_{11}(u-v)+\delta(u-v)\right]dudv$$

Setting t-t'=w, we have

$$q_{\epsilon\epsilon}(w) = \left[q_{22}(w)+P_2\delta(w)\right]-\int\alpha_1(w+v)q_{21}(v)dv-\int\alpha_1(v)q_{21}(w+v)dv$$

$$+\iint\alpha_1(u)\alpha_1(v)\left[q_{11}(w-u+v)+P_1\delta(w-u+v)\right]dudv \qquad (4.5.9)$$

Expression (4.5.9), by taking the Fourier transform, may be written in terms of frequency domain parameters as

$$f_{\epsilon\epsilon}(\lambda) = f_{22}(\lambda) - A(\lambda)\overline{f_{21}(\lambda)} - \overline{A(\lambda)}f_{21}(\lambda) + A(\lambda)\overline{A(\lambda)}f_{11}(\lambda) \qquad (4.5.10)$$

which gives after substituting $A(\lambda)$ from expression (4.5.8)

$$f_{\epsilon\epsilon}(\lambda) = \left[f_{22}(\lambda) - \frac{|f_{21}(\lambda)|^2}{f_{11}(\lambda)}\right]$$

$$= f_{22}(\lambda)\left[1 - |R_{21}(\lambda)|^2\right] \qquad (4.5.11)$$

where $f_{\epsilon\epsilon}(\lambda)$ is the spectrum of the error process $\epsilon(t)$, and is a non-negative function of λ. Expression (4.5.11) suggests that the value of $f_{\epsilon\epsilon}(.)$, based on the linear model, at frequency λ depends on the coherence parameter in that $f_{\epsilon\epsilon}(\lambda)$ is zero if the coherence between the processes N_1 and N_2 is 1. This result gives another interpretation of the coherence as a measure of the degree of linear predictability of the process N_2 by the process N_1.

Related to the complex valued function $A(\lambda)$, the transfer function, are two additional parameters, the GAIN and the PHASE which give useful information about the relationship between the input and the output processes.

4.5.4 THE GAIN AND THE PHASE

The gain $G(\lambda)$ at frequency λ may be defined as the absolute value of the transfer function, i.e.,

$$G(\lambda) = |A(\lambda)|$$

$$= \frac{1}{f_{11}(\lambda)}\left[\{\text{Re } f_{21}(\lambda)\}^2 + \{\text{Im } f_{21}(\lambda)\}^2\right]^{\frac{1}{2}} \qquad (4.5.12)$$

The gain function may also be used as a measure of association between the input and the output processes. A value of $G(\lambda)=0$ indicates a lack of linear relationship.

The phase $\Phi_{21}(\lambda)$ is defined as the argument of the transfer function, i.e.,

$$\Phi_{21}(\lambda) = \arg\{A(\lambda)\}$$

and since $f_{11}(\lambda)\neq 0$, the phase may also be written as

$$\Phi_{21}(\lambda) = \arg\{f_{21}(\lambda)\}$$

$$= \tan^{-1}\left[\frac{\text{Im } f_{21}(\lambda)}{\text{Re } f_{21}(\lambda)}\right] \qquad (4.5.13)$$

The phase may be interpreted as representing the phase difference between the harmonics of the processes N_1 and N_2 at frequency λ. Expression (4.5.13) suggests that the phase is an odd function of frequency, so $\Phi_{21}(\lambda)=0$ at $\lambda=0$.

4.5.5 ESTIMATION OF THE TRANSFER FUNCTION, GAIN, AND PHASE

Estimates of the transfer function, the gain and the phase may be obtained by inserting the respective estimates in expressions (4.5.8), (4.5.12) and (4.5.13), respectively, i.e.,

$$A^{(T)}(\lambda)=f_{21}{}^{(T)}(\lambda)/f_{11}{}^{(T)}(\lambda) \qquad \lambda\neq 0 \qquad (4.5.14)$$

$$G^{(T)}(\lambda)=|f_{21}{}^{(T)}(\lambda)|/f_{11}{}^{(T)}(\lambda) \qquad \lambda\neq 0 \qquad (4.5.15)$$

$$\Phi_{21}{}^{(T)}(\lambda)=\tan^{-1}\left[\frac{\text{Im } f_{21}{}^{(T)}(\lambda)}{\text{Re } f_{21}{}^{(T)}(\lambda)}\right] \qquad \lambda\neq 0 \qquad (4.5.16)$$

4.5.6 ASYMPTOTIC PROPERTIES OF THE ESTIMATES

Let $\underline{N}(t)=\{N_1(t),N_2(t)\}$ be a bivariate stationary point process defined on (0,T]. Suppose that the estimates $A^{(T)}(\lambda)$, $G^{(T)}(\lambda)$ and $\Phi_{21}{}^{(T)}(\lambda)$ are given by expressions (4.5.14), (4.5.15) and (4.5.16), and that $f_{11}(\lambda)\neq 0$, then from Rigas(1983)

$$\lim_{T\to\infty} E[A^{(T)}(\lambda)]=A(\lambda) \qquad \lambda\neq 0$$

$$\lim_{T\to\infty} E\{\ln G^{(T)}(\lambda)\}=\ln G(\lambda) \qquad \lambda\neq 0$$

$$\lim_{T\to\infty} E\{\Phi_{21}{}^{(T)}(\lambda)\}=\Phi_{21}(\lambda) \qquad \lambda\neq 0$$

$$\lim_{T\to\infty} \text{Cov}\{A^{(T)}(\lambda),A^{(T)}(\mu)\}=0 \qquad \lambda\pm\mu\neq 0 \ ; \ 0<\lambda,\mu<\pi$$

$$\lim_{T\to\infty} \text{Cov}\{\ln G^{(T)}(\lambda),\ln G^{(T)}(\mu)\}=0 \qquad \lambda\pm\mu\neq 0 \ ; \ 0<\lambda,\mu<\pi$$

$$\lim_{T\to\infty} \text{Cov}\{\Phi_{21}{}^{(T)}(\lambda),\Phi_{21}{}^{(T)}(\mu)\}=0 \qquad \lambda\pm\mu\neq 0 \ ; \ 0<\lambda,\mu<\pi \qquad (4.5.17)$$

$$\operatorname{Lim}_{T\to\infty} \operatorname{Var}\{A^{(T)}(\lambda)\} = \frac{f_{22}(\lambda)}{Lf_{11}(\lambda)}\left[1-|R_{21}(\lambda)|^2\right] \qquad \lambda\neq 0$$

$$\operatorname{Lim}_{T\to\infty} \operatorname{Var}\{\ln G^{(T)}(\lambda)\} = \frac{1}{2L}\left[|R_{21}(\lambda)|^{-2} -1\right] \qquad \lambda\neq 0 \qquad (4.5.18)$$

$$\operatorname{Lim}_{T\to\infty} \operatorname{Var}\{\Phi_{21}{}^{(T)}(\lambda)\} = \frac{1}{2L}\left[|R_{21}(\lambda)|^{-2} -1\right] \qquad \lambda\neq 0 \qquad (4.5.19)$$

The estimates $A^{(T)}(\lambda)$, $\ln G^{(T)}(\lambda)$ and $\Phi_{21}{}^{(T)}(\lambda)$ are asymptotically normal which follows from the fact that $f_{21}{}^{(T)}(\lambda_1)$, $f_{21}{}^{(T)}(\lambda_2), \ldots$ are asymptotically complex normal (Brillinger, 1972; Rigas, 1983).

4.5.7 CONFIDENCE INTERVALS FOR THE PHASE AND THE GAIN

The asymptotic normality of the estimates of the phase and the logarithm of the gain allow one to construct approximate confidence intervals for the corresponding parameters. Hence, from the above results, approximate 95% confidence intervals for $\Phi_{21}(\lambda)$ and $\log_e G(\lambda)$ at frequency λ can be obtained, respectively, by

$$\Phi_{21}{}^{(T)}(\lambda) \pm e(\lambda) \qquad \lambda\neq 0 \qquad (4.5.20)$$

$$\ln G^{(T)}(\lambda) \pm e(\lambda) \qquad \lambda\neq 0 \qquad (4.5.21)$$

where

$$e(\lambda) = 1.96\left[\frac{|R_{21}{}^{(T)}(\lambda)|^{-2} -1}{2L}\right]^{1/2}$$

In the next section we discuss the usefulness of the phase parameter in some more detail since it provides information regarding the delays between two processes. This information, particularly in a physiological context, has a significant importance because it helps in determining the pattern of communication between the nerve cells.

In practice, for point process systems dominated delays, the sampled phase curve would fluctuate about a straight line passing through the origin ($\lambda=0$). The fluctuation becomes larger as the coherence gets smaller, and the behaviour of the phase as a function of frequency becomes more erratic.

4.6 PHASE: A FREQUENCY DOMAIN MEASURE OF TIMING RELATIONS

In the time domain analysis (section 4.5), the cross-intensity function (CIF) was seen to provide information about the timing relations between two processes. A parallel approach in the frequency domain for such information may be based on the phase parameter.

Suppose, for example, that $[r_j, s_k]$ represent the event times for the bivariate process $\{N_1(t), N_2(t)\}$. If the process N_2 is a lagged version of the process N_1 with lag τ, i.e.,

$$s_k = r_k + \tau \qquad k=1,2,\dots,N_1(T)$$

then following Brillinger and Tukey(1984), the cross spectrum, $f_{21}(\lambda)$, between the processes N_1 and N_2 is given by

$$f_{21}(\lambda) = \text{Lim}_{T\to\infty} E[\Sigma\exp\{-i\lambda(r_k+\tau)\}\Sigma\exp\{i\lambda r_k\}]$$

$$= \exp\{-i\lambda\tau\}f_{11}(\lambda)$$

which implies that

$$\Phi_{21}(\lambda) = -\tau\lambda \qquad (4.6.1)$$

Expression (4.6.1) shows that in the case of a pure delay, the phase $\Phi_{21}(\lambda)$ is a linear function of frequency λ with $(-\tau)$ being the slope of the line $\Phi_{21}(\lambda)=-\tau\lambda$. If $\tau=0$, the processes N_1 and N_2 would be synchronous, and one could expect the sample phase to be close to zero. Since the variance of the estimate of the phase at any frequency depends on the coherence at that frequency (expression 4.5.19), the phase will not be well-determined at any frequency λ at which $|R_{21}^{(T)}(\lambda)|^2 \leq z$, where z refers to expression (4.4.3).

4.6.1 ESTIMATION OF THE TIME DELAY

Expressions (4.5.17) and (4.5.19), and the asympototic normality of the sampled phase, $\Phi_{21}^{(T)}(\lambda)$, suggest that the delay 'τ' between the processes N_1 and N_2 may be well estimated as the slope of the least squares line relating $\Phi_{21}^{(T)}(\lambda)$ to λ, and passing through the origin. However, the dependence of the variance of $\Phi_{21}^{(T)}(\lambda)$ on the coherence (expression 4.5.19) suggests that in the case of a non-constant coherence we need to fit a weighted least squares line (see Weisberg, 1985) over the range of frequencies $[\lambda_1, \lambda_n]$ where the coherence is significantly different from zero, and λ_n is such that

$$|R_{21}^{(T)}(\lambda)|^2 \leq z \quad \text{for} \quad \lambda \geq \lambda_n$$

A simple procedure to fit such a weighted least squares line is described as follows:

Let $\Phi_{21}^{(T)}(\lambda_j)=\Phi_j$ be the sampled phase evaluated at discrete frequencies of the form $\lambda_j=2\pi j/R$, $j=1,2,\ldots,n$ where n corresponds the frequency after which $|R_{21}^{(T)}(\lambda)|^2 \leq z$. In practice, as we will see (e.g. Fig.4.7.1c), some values of the coherence in the range $[\lambda_1, \lambda_n]$ may occur to be non-significant. For large n, these few values may be either droped from the least sequares fit, or by using weighted least sequares, these may be given less importance (weight).

In order to fit a weighted least squares line, we define a simple linear regression model (through the origin) of the form

$$\phi_j = \beta\lambda_j + \epsilon_j$$

where $\beta=-\tau$. The expressions (4.5.17) and (4.5.19) lead to the validity of the standard assumptions

$$\epsilon_j \sim N\{0,\sigma_j^2\} \qquad \text{and } \operatorname{cov}\{\epsilon_j, \epsilon_k\} \cong 0$$

where

$$\sigma_j^2 = \sigma^2 w_j = \operatorname{Var}\{\phi_{21}^{(T)}(\lambda_j)\} = (1/2L)\{|R_{21}(\lambda_j)|^{-2} -1\}$$

The weighted least squares estimate of β is seen to be

$$\hat{\beta} = \frac{\Sigma w_j \phi_j \lambda_j}{\Sigma w_j \lambda_j^2} \tag{4.6.2}$$

and an estimate of its variance as

$$\hat{\operatorname{var}}(\hat{\beta}) = \frac{\hat{\sigma}^2}{\Sigma w_j \lambda_j^2}$$

where

$$\hat{\sigma}^2 = \frac{\Sigma w_j (\phi_j - \hat{\beta}\lambda_j)^2}{n-1}$$

A plausible choice of w_j may be given by (e.g., Weisberg,1985 Pp.85)

$$w_j = 1/\hat{\sigma}_j^2$$

where

$$\hat{\sigma}_j^2 = (1/2L)\{|R_{21}^{(T)}(\lambda_j)|^{-2} - 1\}$$

4.6.2 CONFIDENCE INTERVAL FOR THE TIME DELAY

Applying standard regression theory, a 95% confidence interval for τ may be set up as

$$-\hat{\beta} \pm t_{(n-1;0.975)}[\hat{\text{var}}(\hat{\beta})]^{\frac{1}{2}} \qquad (4.6.3)$$

where $t_{(n-1;0.975)}$ denotes the upper 97.5% point of a t-distribution with n-1 degrees of freedom. For large n, $t(\cdot;\cdot)$ in expression (4.6.3) may be approximated by a standard normal variate, which leads to

$$-\hat{\beta} \pm 1.96[\hat{\text{var}}(\hat{\beta})]^{\frac{1}{2}} \qquad (4.6.4)$$

The above confidence intervals for τ may also be used to test for synchrony. The confidence interval will support the hypothesis of synchrony if it contains the value zero.

4.7 APPLICATIONS

We now turn to the application of the frequency domain procedures discussed above (Sections 4.3-4.6) and apply them to the same data sets as we considered in the time domain analysis (Section 4.2.4). The main aim of using the same data is to compare these methods and their effectiveness with those of the time domain. We also hope to get some more insight into the system (muscle spindle) under investigation.

Figs. 4.7.1a,b correspond to the estimates of the coherence and the phase of the computer generated data with a known time delay of 10 msec (see Section 4.2.4). Both estimates have been plotted against the frequencies of the form (1000j/R) Hz., with R=1024, j=1,2,..., over the range (0, 100) Hz. The dotted line in the coherence plot at each frequency corresponds to the value of z (see Section 4.4.3) i.e., the 95% point of the null distribution under the hypothesis of the processes being independent at that frequency. It is clear from the Fig.4.7.1a that, over the whole range of frequencies, both processes are coupled.

The plot of the estimate of the phase with the phase values restricted in some interval is called the constrained phase . The fundamental range of the phase is the interval $[-\pi, \pi]$ (Bloomfield, 1976; Brillinger, 1981). However, this range of restriction may be altered depending on the form of $\Phi_{21}(\lambda)$ at hand. For example, the estimate of phase considered in Fig.4.11.1b is constrained to lie within the interval $(-3\pi/2, \pi/2)$ using the following expression

$$\text{Let } D_{21}^{(T)}(\lambda) = \text{Im } f_{21}^{(T)}(\lambda)/\text{Re } f_{21}^{(T)}(\lambda) \quad \lambda \neq 0, \text{ then}$$

$$\Phi_{21}^{(T)}(\lambda) = \begin{cases} \tan^{-1}[D_{21}^{(T)}(\lambda)] & \text{if Re } f_{21}^{(T)}(\lambda) \geq 0 \\ \tan^{-1}[D_{21}^{(T)}(\lambda)]-\pi & \text{if Re } f_{21}^{(T)}(\lambda) < 0 \\ -\pi/2 & \text{if Re } f_{21}^{(T)}(\lambda)=0, \text{ Im } f_{21}^{(T)}(\lambda) < 0 \\ +\pi/2 & \text{if Re } f_{21}^{(T)}(\lambda)=0, \text{ Im } f_{21}^{(T)}(\lambda) \geq 0 \\ \text{arbitrary } (0) & \text{if Re } f_{21}^{(T)}(\lambda)=0, \text{ Im } f_{21}^{(T)}(\lambda)=0 \end{cases}$$

It is clear from the phase plot (Fig.4.7.1b) that the estimate of the phase can be approximated by a straight line passing through the

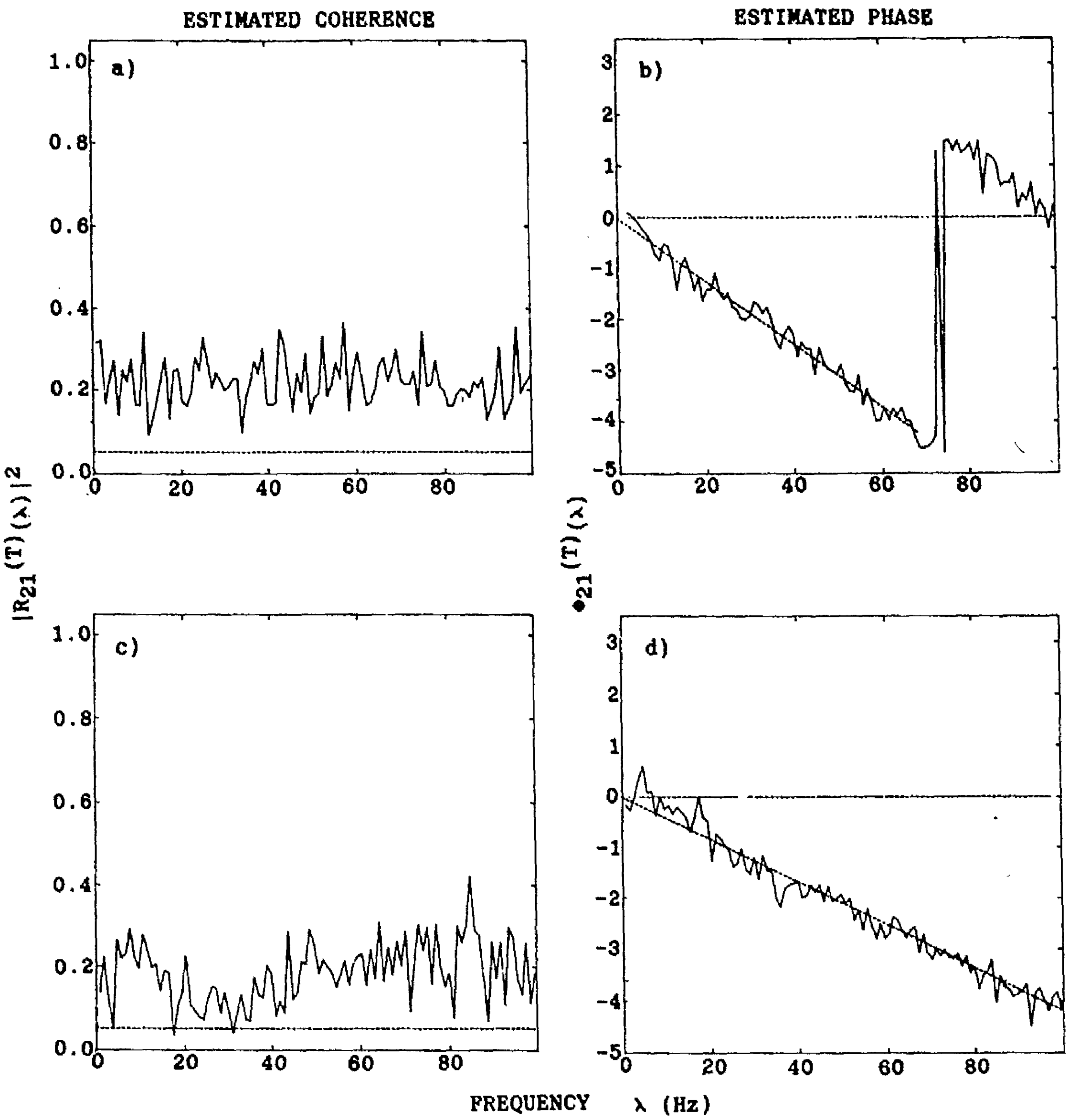

Fig.4.7.1 Illustration of the coherence and phase

a) Estimates of the coherence and b) the phase of the computer simulated data dominated by a pure delay

c) Estimates of the coherence and d) the phase of the real data corresponding to a single unit EMG (process N_2), when a random stimulation (process N_1) of Medial Gastrocnemius is applied at group I threshold

The dotted line in the coherence plots represents the upper limit of the 95% confidence interval (marginal) for the coherence under the hypothesis that the two processes are independent. The slopes of the fitted least squares lines (dotted) on the phase curves correspond to the estimated time delays.

origin over a range of frequencies at which the coherence is non-zero. A fitted least squares line (dotted line in Fig.4.7.1b) based on the method described in Section 4.6.1 gives an estimate of the time delay $\hat{\tau}$=9.9 msec with a 95% confidence interval of (9.7, 10.1) msec, which is consistent with the corresponding time domain estimate using the cross-intensity function (Fig.4.2.1b).

Figs.4.7.1c,d corresponds to the estimates of coherence and phase of the real physiological data we analysed in the time domain (Section 4.2.4). The coherence plot (Fig.4.7.1c) reveals that the output process N_2 is coupled with the input process over the entire range of frequencies, whereas the estimate of the phase (Fig.4.7.1d) shows that, over this range of frequencies, N_2 is delayed, on the average, by an amount of 6.7 msec with a 95% confidence interval, for the delay, of (6.6, 6.8) msec.

Fig.4.7.2 demonstrates the application of coherence to the spindle data. The individual estimates of coherences (Figs4.7.2a-f) correspond to the cross-intensities shown in Fig.4.2.3a-f. The coherence figures seem to reveal additional features by giving a range of frequencies over which the coupling between the two processes occurs. For example, comparing Fig.4.7.2b with Fig.4.7.2f, it is seen that the presence of the length change 'ℓ' imposes a coupling between the Ia and II discharges over a different range of frequencies from the one over which the Ia and II are coupled in the presence of the fusimotor activity, and which suggests that at fairly high frequencies the discharge from the two endings is controlled by the length change without regard to the presence of the fusimotor activity. This feature of the data was not reflected in the time domain figures (Fig.4.2.3b and Fig.4.2.3f). A comparison of Fig.4.7.2f with Figs.4.7.2c-e also reveals that the imposed length change 'ℓ' weakens the effects of the fusimotor axons on the coupling

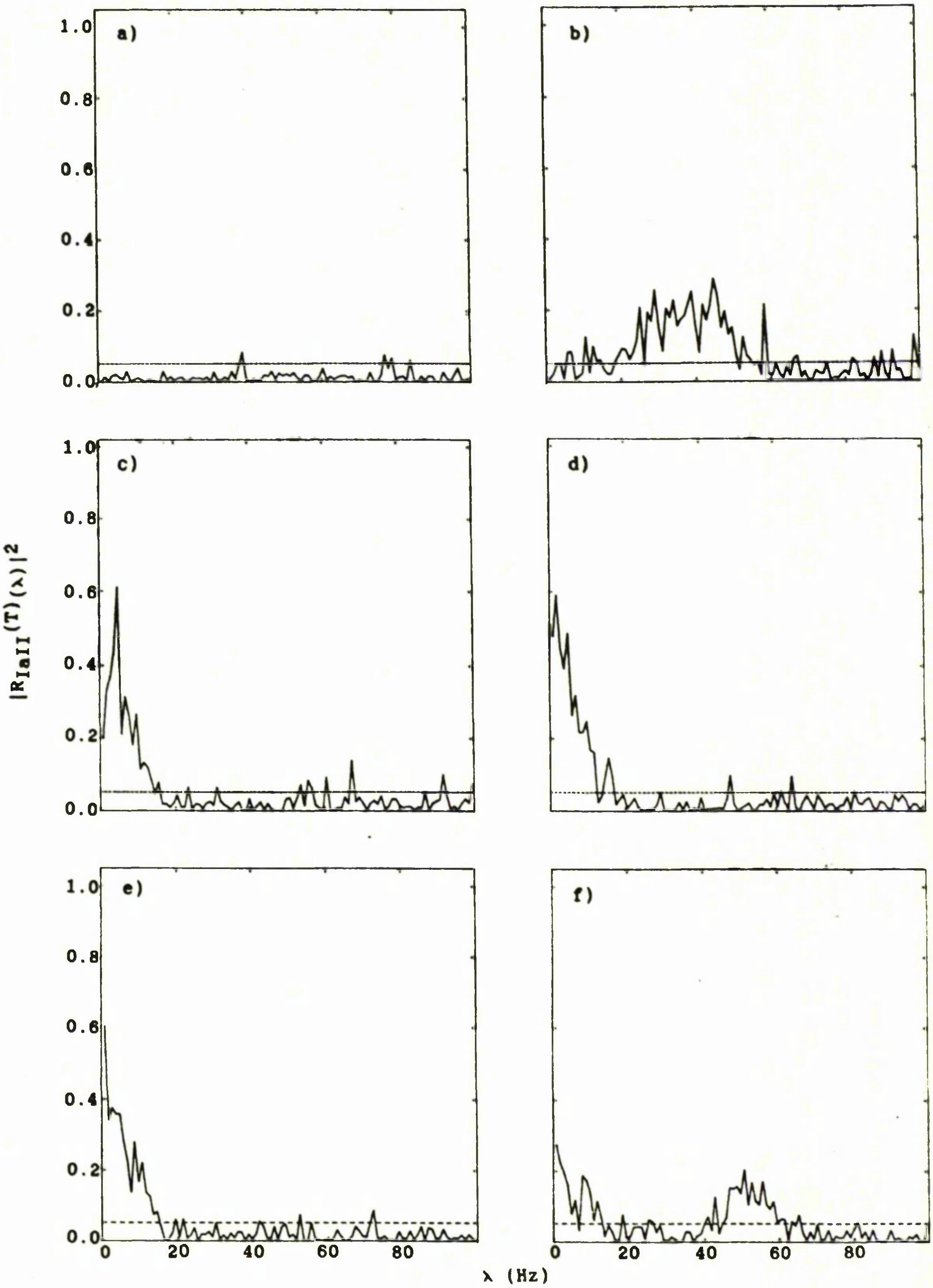

Fig.4.7.2 Estimate of coherence between

a) Ia and II spontaneous discharges
b) Ia and II discharges in the presence of a length change ℓ
c) Ia and II discharges in the presence of a static gamma $_1\gamma_s$
d) Ia and II discharges in the presence of a second gamma $_2\gamma_s$
e) Ia and II discharges in the presence of both $_1\gamma_s$ and $_2\gamma_s$
f) Ia and II discharges in the presence of ℓ, $_1\gamma_s$, and $_2\gamma_s$

The dotted line in each plot gives the upper limit of the 95% confidence interval (marginal) for the coherence under the hypothesis that the processes are independent.

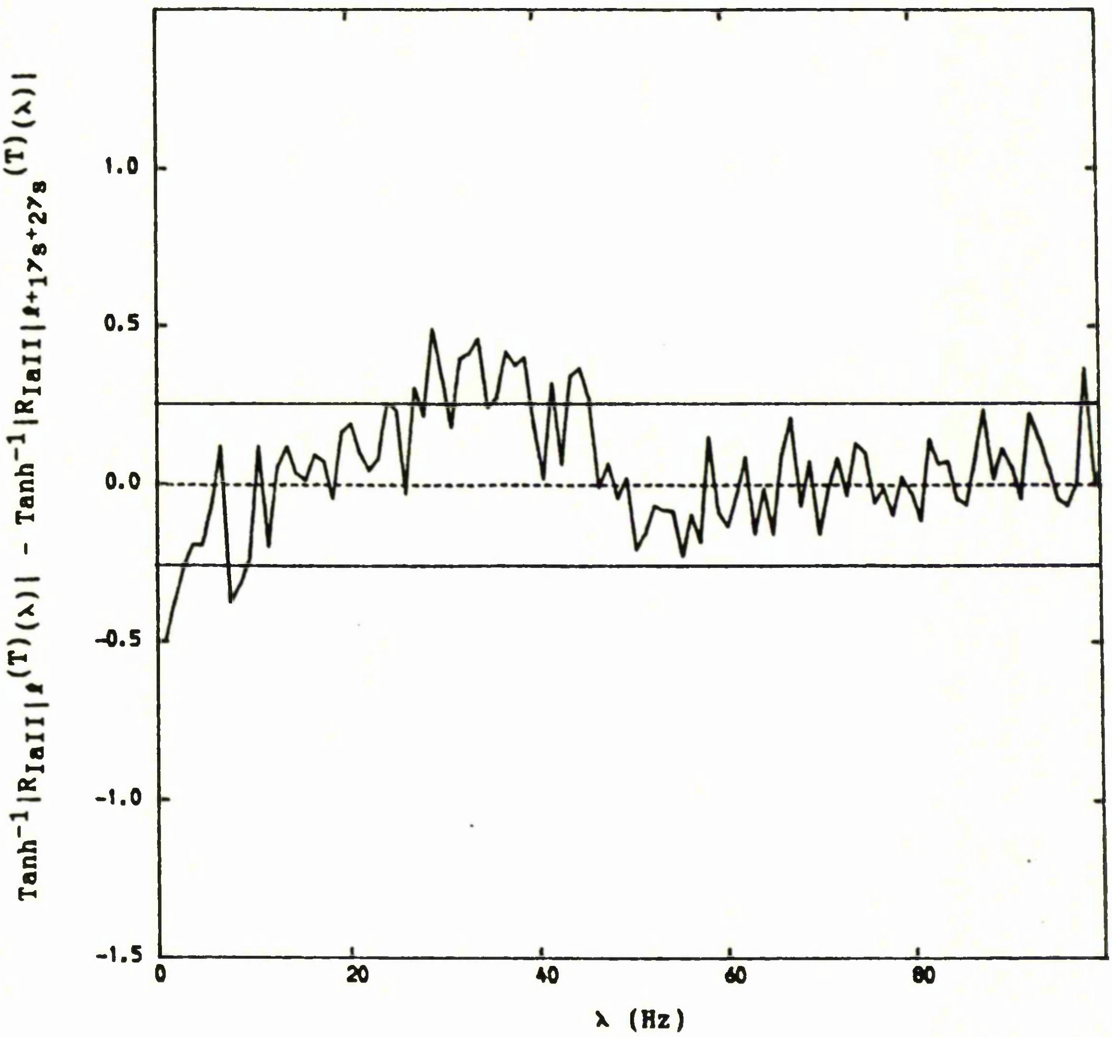

Fig.4.7.3 Test for the equality of two coherences

The curve shown in the plot corresponds to the difference of the inverse hyperbolic-tangent transform of the moduli of the two coherences illustrated in Figs.4.7.2b,f. The solid horizontal lines below and above the dotted line represent the critical values at approximately 5% level of significance for a two sided test of the hypothesis that the two moduli are equal at a given frequency λ.

between the Ia and II endings. This can also be seen more formally by applying the test for the equality of two coherences developed in section 4.4.5. Fig.4.7.3 represents the difference of the moduli of the two coherences illustrated in Figs.4.7.2b,f. The solid lines below and above the dotted line, against any frequency λ, correspond to the critical values for the difference at approximately 5% level of significance under the hypothesis that the two moduli are equal at that frequency. A value lying outside these limits at any frequency indicates that the difference between the strength of association of the two processes may plausibly be significant at that frequency. It is clear from the figure that the activity of fusimotor axons reduces the strength of coupling, which was due to the presence of the length change alone (Fig.4.7.2b), over the range of frequencies 30-40 Hz. So the coupling between the Ia and II endings in the presence of all the three inputs, 'ℓ', '$_1\gamma_s$' and '$_2\gamma_s$', (Fig.4.7.2f) may possibly be a consequence of the combined effects of these inputs.

It is also of interest, in the light of recent work by Edgley and Jankowska(1987) to examine how the phase relation between the Ia and II endings in the presence of the fusimotor inputs is altered by the changes in these inputs. Figs.4.7.4b,d,f give a comparison of the phases {restricted in the range $[-\pi, \pi]$} between the Ia and II endings under different conditions of the fusimotor inputs. Figs.4.7.4a,c,e are the estimates of the corresponding coherences. The delay estimated from the phase between the Ia and II discharges, computed in the presence of '$_1\gamma_s$' (the slope of the dotted line in Fig.4.7.4b) is 2.3 $\pm$ 2.2 msec (a phase lead of the Ia over II) over the range of frequencies where the coupling between the Ia and the II is non-zero (Fig.4.7.4a). This small difference in the phase between the Ia and II responses at the level of input to the spinal cord, where their activity was recorded, occurred in spite of a large

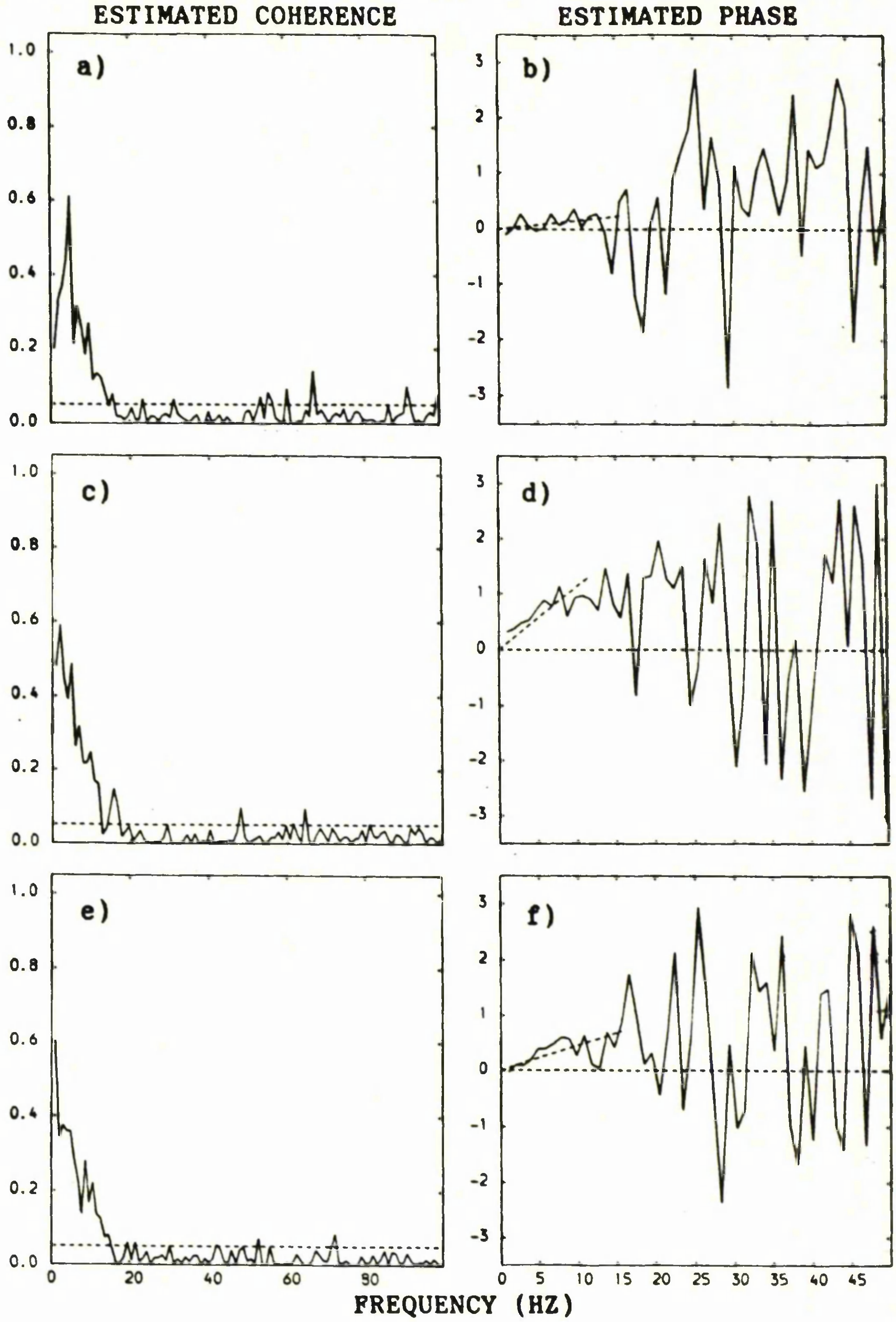

Fig.4.7.4 Timing realtions between the Ia and II discharges

a) Estimates of the coherence and b) phase between the Ia and II discharges in the presence of a static gamma input $_1\gamma_s$
c) Estimates of the coherence and d) phase between the Ia and II discharges in the presence of a second gamma input $_2\gamma_s$
e) Estimates of the coherence and f) phase between the Ia and II discharges when both gamma inputs are present

The dotted line in the coherence plots gives the upper limit of the 95% confidence interval (marginal) for the coherence at a given frequency under the hypothesis that the two discharges are independent. The slope of the fitted least squares line (dotted) on the phase curves, over the range of frequencies where the corresponding coherence is significant, represents the estimated lead of the Ia over II discharge.

difference in their respective conduction velocities. On the other hand the Ia lead in the presence of '$_2\gamma_s$' alone (Fig.4.7.4d) is seen to have been significantly increased over the range of frequencies where the Ia II coupling is significant (Fig.4.7.4c). The lead in this case happens to be 18.0 ± 3.9 msec which is substantially greater than one would expect on the basis of conduction velocity difference alone. The stimulation of both fusimotor axones, applied concurrently and independently, is seen to impose a phase lead (Fig.4.7.4f) of 7.3 ± 2.2 msec of the Ia over II.

Figs.4.7.5a-c illustrate the applications of the confidence intervals, respectively, for the coherence, phase and $\log_e$\{gain\} between the Ia discharge and the fusimotor input '$_2\gamma_s$'. The horizontal dotted line in the coherence plot (Fig.4.7.5a) at each frequency represents the upper limit of the 95% confidence interval under the hypothesis that the processes are independent at that frequency. The dotted curves below and above the estimate (solid curve) at a given frequency are the approximate 95% confidence limits for the coherence at that frequency, and are computed from expression (4.4.8). The dotted curves in the phase and gain plots are based on the expressions (4.5.20) and (4.5.21), respectively. The confidence limits in each of the plots are clearly seen to become wider as the coherence gets smaller indicating how the reliability of the estimate at any frequency depends on the coherence at that frequency.

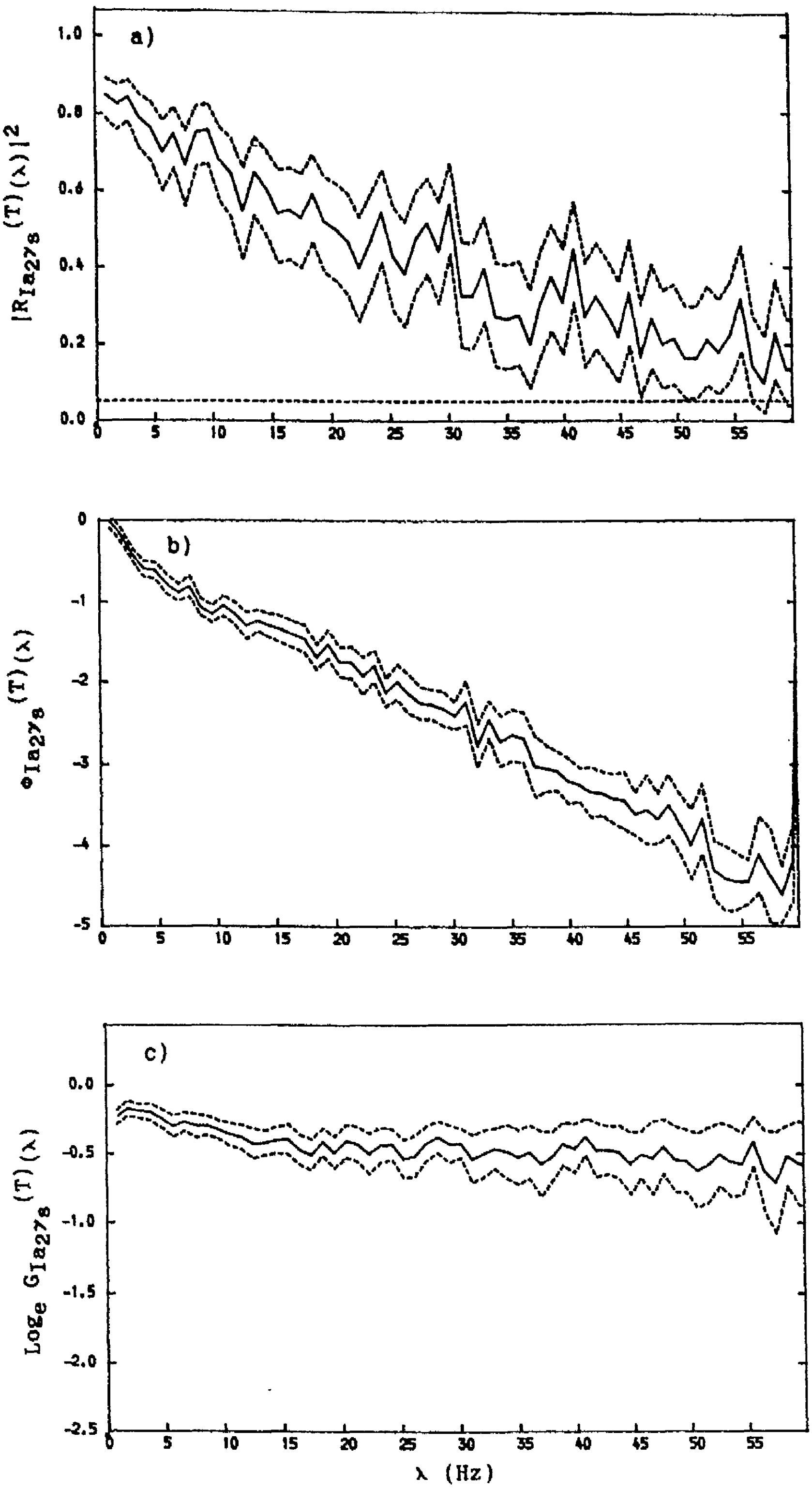

Fig.4.7.5 Illustration of the asymptotic confidence intervals

a) Estimated coherence (solid curve) between the Ia discharge and the $_{2}\gamma_s$
b) Estimated phase (solid curve) between the Ia discharge and the $_{2}\gamma_s$
c) Estimated $\log_e$ gain (solid curve) between the Ia discharge and the $_{2}\gamma_s$

The dotted curves above and below the estimates in each figure represent approximate 95% confidence interval (marginal) for the respective parametes.

4.8 SUMMARY AND CONCLUSIONS

In this chapter we presented a bivariate stationary point process. Certain parameters useful for measuring the association and timing relations between the processes were defined in both time and frequency domains. Estimation procedures for these parameters were discussed, their asymptotic distributions were examined, and confidence intervals for certain parameters were constructed. Certain tests of significance in the assessment of association and timing relation between the processes were developed. The applications of these procedures were demonstrated by a number of illustrations using simulated data followed by the real data obtained on the muscle spindle.

We also considered the problem of identification of a point process system and introduced a simple linear point process model by relating single input to single output. Based on the mean squared error criterion, the model seemed fairly approperiate in the application to the spindle data.

The frequency domain methods again seemed to reveal some additional features about the processes which were not reflected by the time domain ones, and this confirms the usefullness of the frequency domin.

Following is a brief summary of the main features of the procedures and their applications we demonstrated in this chapter.

1. The cross-intensity function, a time domain parameter and a simple extension of the auto-intensity function, may be used as a time domain measure of association. But it has certain disadvantages, as discussed by Brillinger(1986), that it is the point process analogue of covariance, and consequently may be expected to have the same limitations i.e., first it

is dimensional and secondly it is not bounded, which means that one can not measure the extent to which the processes are associated.

2. The coherence, a frequency domain measure of association, possesses the desirable properties, i.e., it is bounded in [0,1], the two extremes of the linear association. Further, as a frequency domain measure, it provides a range of frequencies over which the processes are associated.
3. The cross-intensity function may also be used as a measure of the timing relation between two processes. A sharp peak in the estimate of CIF indicates a possible time delay between the processes. But, as we have found in the examples, a well-defined peak may not appear in the estimate all the time. Further, as the estimate of the time delay is based on perhaps a single point (the peak point), one may easily lead to a less reliable estimate of the delay.
4. The phase, a frequency domain measure of the timing relation between two processes, provides with a better properties of the estimated delay. Further, based on the standard regression theory, the phase allows one to construct a confidence interval for the delay.

The above advantages of the frequency domain methods clearly suggest a further use of these methods and their extensions to analyse multivariate point processes, to be considered in Chapter 5.

CHAPTER 5

MULTIVARIATE POINT PROCESSES

5.1 INTRODUCTION

The usefulness of the frequency domain methods, discussed in Chapters 3 and 4, leads to a further consideration of a wide range of questions relating to a more realistic situation when the system (the muscle spindle) involves multiple-input and multiple-output. Of particular is the question of whether the association between a pair of outputs is a consequence of a common input or of a direct connection, and the extended question of how the association and timing relation between a pair of outputs is influenced by the presence of a number of inputs.

The main aim of this Chapter is to provide a formal framework of techniques to find the answers to these questions.

Introducing the idea of partial parameters, we start with the definition and derivation of certain point process partial parameters in the frequency domain, and discuss their estimation procedures.

A point process linear model with two inputs and a single output is introduced and developed. The identification of the muscle spindle, when it is assumed to be acted upon by two point process inputs, ${}_1\gamma_s$ and ${}_2\gamma_s$, is carried out by using this model.
A further extension of this model to the more general case with "r" inputs is considered. Estimates of the parameters related to this general model, and the properties of these estimates are examined. Certain tests of significance are also set up and demonstrated by a number of illustrations.

In the final part of this Chapter, we consider a point process system with multiple-input and multiple-output and develop a general linear regression-type multivariate point process model. The idea is to identify the muscle spindle in more realistic situation under which it operates. Certain ordinary and partial parameters, measuring the input-output relations, are defined. Estimates and their asymptotic properties are discussed. The appropriateness of this model will become apparent in the applications of these procedures to both simulated and real data.

5.2 THE PARTIAL CROSS-SPECTRUM

In dealing with relations between point processes it is often desirable to investigate whether the association between two processes, say, $N_1(t)$ and $N_2(t)$ is due to a direct connection between them or if it is a consequence of a third process $N_3(t)$. The answer to this question leads to the introduction of the partial parameters. The frequency domain methods are easily extended to develop such parameters. One of these parameters is called the partial cross-spectrum which measures the association between the components of two processes, N_1 and N_2, at a given frequency after the influence of a third, N_3, has been removed.

In order to develop an explicit expression for the partial cross-spectrum we proceed as follows:

Consider a linear time invariant point process system with two inputs $M_1(t)$ and $M_2(t)$ and a single output $N(t)$. A graphical representation of this situation may be given as

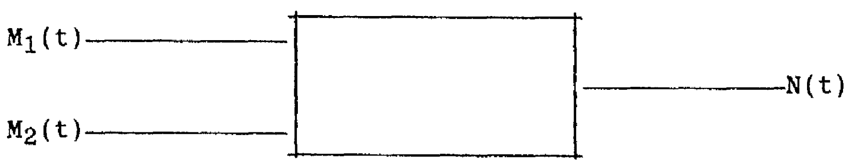

By the analogy with ordinary time series (Tick, 1963; Jenkins and Watts, 1968), the processes N and M_1 are first predicted from process M_2 based on the linear models

$$E\{dN(t)|M_2\} = \{\alpha_0 + \int \alpha_{NM_2}(t-u)dM_2(u)\}dt$$

and

$$E\{dM_1(t)|M_2\} = \{\alpha_0' + \int \alpha_{M_1M_2}(t-u)dM_2(u)\}dt$$

Now consider the following error processes with stationary increments

$$d\epsilon_1(t)=dN(t)-\left[\alpha_0+\int \alpha_{NM_2}(t-u)dM_2(u)\right]dt \qquad (5.2.1)$$

$$d\epsilon_2(t)=dM_1(t)-\left[\alpha_0'+\int \alpha_{M_1M_2}(t-u)dM_2(u)\right]dt \qquad (5.2.2)$$

Clearly $E\{d\epsilon_1(t)\}=E\{d\epsilon_2(t)\}=0$. Further, from Section 4.4.2 of Chapter 4, it follows that

$$\alpha_0 = P_N - P_{M_2}\int \alpha_{NM_2}(u)du$$

$$\alpha_0' = P_{M_1} - P_{M_2}\int \alpha_{M_1M_2}(u)du$$

and

$$A_{NM_2}(\lambda) = \int \exp(-i\lambda u)\alpha_{NM_2}(u)du = \frac{f_{NM_2}(\lambda)}{f_{M_2M_2}(\lambda)} \qquad (5.2.3)$$

$$A_{M_1M_2}(\lambda) = \int \exp(-i\lambda u)\alpha_{M_1M_2}(u)du = \frac{f_{M_1M_2}(\lambda)}{f_{M_2M_2}(\lambda)} \qquad (5.2.4)$$

The cross cumulant density function between the processes $\epsilon_1(\cdot)$ and $\epsilon_2(\cdot)$ at two time instants t and t' may be defined as the partial cross-cumulant density between N and M_1 after the linear time

invariant effects of process M_2 have been removed.
Denoted by $q_{NM_1.M_2}(t-t')$, it is given as

$$q_{NM_1.M_2}(t-t') = E\{d\epsilon_1(t)d\epsilon_2(t')\} - E\{d\epsilon_1(t)\}E\{d\epsilon_2(t')\} \qquad (5.2.5)$$

Substituting $d\epsilon_1(t)$ and $d\epsilon_2(t')$ from expressions (5.2.1) and (5.2.2) into (5.2.5), and after some algebraic manipulation, we obtain

$$\begin{aligned} q_{NM_1.M_2}(t-t') = q_{NM_1}(t-t') &- \int\alpha_2(t'-v)q_{NM_2}(t-v)dv \\ &- \int\alpha_1(t-v)q_{M_1M_2}(t'-v)dv \\ &+ \iint\alpha_1(t-w)\alpha_2(t'-v)\left[q_{M_2M_2}(w-v)+P_{M_2}\delta(w-v)\right]dwdv \end{aligned}$$

where $\delta(\cdot)$ is the Dirac delta function.
Setting $t-t'=u$, we obtain

$$\begin{aligned} q_{NM_1.M_2}(u) = q_{NM_1}(u) - \int\alpha_2(w)q_{NM_2}(u+w)dw &- \int\alpha_1(w)q_{M_1M_2}(u-w)dw \\ + \iint\alpha_1(v)\alpha_2(w)\left[q_{M_2M_2}(u+w-v)+P_{M_2}\delta(u+w-v)\right]dwdv \end{aligned}$$

The Fourier transform of the above expression leads to the corresponding frequency domain representation given by

$$\begin{aligned} f_{NM_1.M_2}(\lambda) = f_{NM_1}(\lambda) - \overline{A_2(\lambda)}f_{NM_2}(\lambda) &- A_1(\lambda)\overline{f_{M_1M_2}(\lambda)} \\ &+ A_1(\lambda)\overline{A_2(\lambda)}f_{M_2M_2}(\lambda) \end{aligned} \qquad (5.2.6)$$

Substituting $A_1(\cdot)$ and $A_2(\cdot)$ from expressions (5.2.3), (5.2.4) and simplifying, we obtain

$$f_{NM_1.M_2}(\lambda) = f_{NM_1}(\lambda) - \frac{f_{NM_2}(\lambda)f_{M_2M_1}(\lambda)}{f_{M_2M_2}(\lambda)} \tag{5.2.7}$$

which is the required partial cross-specrum between the processes N and M_1 having the linear effects of the process M_2 been removed.

More generally for an r vector-valued stationary point process $\underline{N}(t)=\{N_1(t), \ldots, N_r(t)\}$, the partial cross spectrum of order 1 between processes N_a and N_b after removing the linear effects of N_c is given by

$$f_{N_aN_b.N_c}(\lambda) = f_{N_aN_b}(\lambda) - \frac{f_{N_aN_c}(\lambda)f_{N_cN_b}(\lambda)}{f_{N_cN_c}(\lambda)} \tag{5.2.8}$$

for a,b,c= 1, 2, $\cdots$, r ; c≠a, c≠b.

In the case a=b but a≠c, the partial spectrum is called the auto-partial spectrum of order 1 of process N_a after removing the linear effects of N_c.

The partial cross-spectrum of order 1, $f_{N_aN_b.N_c}(\lambda)$, may be interpreted as measuring the association between two processes at frequency λ after removing the influence of a third process. The value $f_{N_aN_b.N_c}(\lambda)=0$ would suggest that there is no direct connection between processes N_a and N_b. However, as the value of this parameter is not bounded above, enabling us to signify the strength of direct connection between the processes. This disadvantage leads to the necessity of providing a normalised measure of partial association. The partial coherence provides such a measure. We discuss this parameter in more detail in the next section.

5.3 COHERENCE: A FREQUENCY DOMAIN MEASURE OF PARTIAL ASSOCIATION

The partial coherence of order 1, i.e, between N_a and N_b after removing the linear effects of process N_c may be defined as the limiting correlation-squared between the Fourier-Stieltjes transforms of processes N_a and N_b after removing their best linear predictors based on process N_c (for a,b,c=1,2,...,r ; c≠a, c≠b).

Suppose that the r vector valued stationary process $\underline{N}(t)$ is observed in (0,T]. The Fourier-Stieltjes transform of the generalised expressions of (5.2.1) and (5.2.2) may be written as

$$d_{\epsilon_a}{}^{(T)}(\lambda) = d_{N_a}{}^{(T)}(\lambda) - A_{N_a}(\lambda) d_{N_c}{}^{(T)}(\lambda)$$

$$d_{\epsilon_b}{}^{(T)}(\lambda) = d_{N_b}{}^{(T)}(\lambda) - A_{N_b}(\lambda) d_{N_c}{}^{(T)}(\lambda)$$

For a,b,c = 1, 2, ···, r ; c≠a, c≠b.

The partial coherence, $|R_{N_aN_b.N_c}(\lambda)|^2$, between N_a and N_b with the linear effects of process N_c having been removed is defined, suppressing the dependence on λ, as

$$|R_{N_aN_b.N_c}|^2 = \text{Lim}_{\,T\to\infty} \left| \text{corr}\left\{ d_{\epsilon_a}{}^{(T)} \;,\; d_{\epsilon_b}{}^{(T)} \right\} \right|^2$$

$$= \text{Lim}_{\,T\to\infty} \left| \text{corr}\left\{ d_{N_a}{}^{(T)} - \frac{f_{N_aN_c}}{f_{N_cN_c}} d_{N_c}{}^{(T)} \;,\; d_{N_b}{}^{(T)} - \frac{f_{N_bN_c}}{f_{N_cN_c}} d_{N_c}{}^{(T)} \right\} \right|^2$$

where "corr" denotes complex correlation.

Now as

$$\text{Cov}\left\{d_{N_a}(T) - \frac{f_{N_aN_c}}{f_{N_cN_c}}\ d_{N_c}(T)\ ,\ d_{N_b}(T) - \frac{f_{N_bN_c}}{f_{N_cN_c}}\ d_{N_c}(T)\right\}$$

$$= \text{Cov}\left\{d_{N_a}(T), d_{N_b}(T)\right\} - \frac{f_{N_bN_c}}{f_{N_cN_c}} \text{Cov}\left\{d_{N_a}(T), d_{N_c}(T)\right\}$$

$$- \frac{f_{N_aN_c}}{f_{N_cN_c}} \text{Cov}\left\{d_{N_c}(T), d_{N_b}(T)\right\} + \frac{f_{N_aN_c}\ f_{N_bN_c}}{f_{N_cN_c}^{\ 2}} \text{Cov}\left\{d_{N_c}(T), d_{N_c}(T)\right\}$$

substituting the values of the individual covariances on the right hand side of the above expression derived in Section (4.4), and taking limit as $T\to\infty$ and simplifying, we find

$$\text{Lim}_{\ T\to\infty} \left[\frac{1}{2\pi T} \text{Cov}\left\{d_{N_a}(T) - \frac{f_{N_aN_c}}{f_{N_cN_c}} d_{N_c}(T), d_{N_b}(T) - \frac{f_{N_bN_c}}{f_{N_cN_c}} d_c(T)\right\}\right]$$

$$= f_{N_aN_b} - \frac{f_{N_aN_c}\ f_{N_cN_b}}{f_{N_cN_c}}$$

$$= f_{N_aN_b \cdot N_c}$$

Similarly for the variance

$$\text{Var}\left\{d_{N_a}(T) - \frac{f_{N_aN_c}}{f_{N_cN_c}} d_{N_c}(T)\right\} = \text{Var}\left\{d_{N_a}(T)\right\} - \frac{f_{N_aN_c}}{f_{N_cN_c}} \text{Cov}\left\{d_{N_a}(T), d_{N_c}(T)\right\}$$

$$- \frac{f_{N_aN_c}}{f_{N_cN_c}} \text{Cov}\left\{d_{N_c}(T), d_{N_a}(T)\right\} + \frac{f_{N_aN_c}^{\ 2}}{f_{N_cN_c}^{\ 2}} \text{Var}\left\{d_{N_c}(T)\right\}$$

we find that

$$\operatorname{Lim}_{T\to\infty} \frac{1}{2\pi T}\operatorname{Var}\left\{d_a(T) - \frac{f_{N_aN_c}}{f_{N_cN_c}} d_c(T)\right\} = f_{N_aN_a} - \frac{f_{N_aN_c}\, f_{N_cN_a}}{f_{N_cN_c}}$$

$$= f_{N_aN_a . N_c}$$

Therefore the partial coherence at frequency λ is seen to be

$$|R_{N_aN_b . N_c}(\lambda)|^2 = \frac{|f_{N_aN_b . N_c}(\lambda)|^2}{f_{N_aN_a . N_c}(\lambda) f_{N_bN_b . N_c}(\lambda)} \quad . \qquad (5.3.1)$$

Expression (5.3.1) shows that the partial coherence is essentially a normalised partial cross-spectrum, and satifies the property

$$0 \leq |R_{N_aN_b . N_c}(\lambda)|^2 \leq 1$$

Substituting the values of partial spectra in expression (5.3.1), we may write the partial coherence of order-1 in terms of zero-order partial coherencies (ordinary), suppressing the dependence of λ, as

$$|R_{N_aN_b . N_c}|^2 = \frac{\left|\frac{f_{N_aN_b}}{[f_{N_aN_a}\, f_{N_bN_b}]^{1/2}} - \frac{f_{N_aN_c}\, f_{N_cN_b}}{[f_{N_aN_a}\, f_{N_cN_c}]^{1/2}\, [f_{N_cN_c}\, f_{N_bN_b}]^{1/2}}\right|^2}{\left[1 - |R_{N_aN_c}|^2\right]\left[1 - |R_{N_cN_b}|^2\right]}$$

$$= \frac{|R_{N_aN_b} - R_{N_aN_c}\, R_{N_cN_b}|^2}{\left[1 - |R_{N_aN_c}|^2\right]\left[1 - |R_{N_cN_b}|^2\right]} \qquad (5.3.2)$$

5.3.1 ESTIMATION OF THE PARTIAL COHERENCE

An estimate of the partial coherence of order 1 may be obtained by inserting estimates of the ordinary coherencies in expression (5.3.2) i.e.,

$$|R_{N_aN_b.N_c}^{(T)}(\lambda)|^2 = \frac{|R_{N_aN_b}^{(T)}(\lambda) - R_{N_aN_c}^{(T)}(\lambda)R_{N_cN_b}^{(T)}(\lambda)|^2}{\left[1-|R_{N_aN_c}^{(T)}(\lambda)|^2\right]\left[1-|R_{N_cN_b}^{(T)}(\lambda)|^2\right]} \qquad (5.3.3)$$

The properties of this estimate will be discussed in Section 5.6.5 in a more general case where the partial coherence of order-r i.e., the coherence between two point processes after removing the linear effects of r other processes, is required in order to assess the connectivity between these two processes in the presence of r other processes. We now turn to the two-input single-output point process system and develop a linear model relating the output to the inputs.

5.4 TWO-INPUTS SINGLE-OUTPUT POINT PROCESS LINEAR MODEL

In this section we consider the situation where the point process system receives two inputs and in response gives rise to a single output. The main purpose of studying this situation is to investigate the characteristics of the muscle spindle when the response of the sensory axones, Ia and II, is recorded in the presence of the two gamma fusimotor axons, '$_1\gamma_s$' and '$_2\gamma_s$'. A graphical representation of this situation is given at the start of Section 5, e.g.,

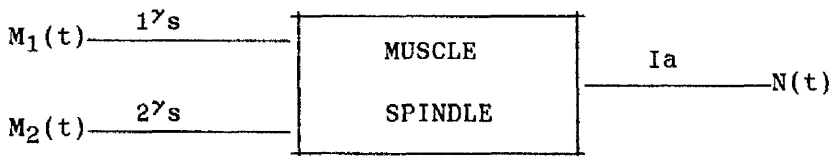

5.4.1 THE MODEL

Extending the simple linear point process model discussed in Section (4.5.1) of Chapter 4, we now develop the following linear model relating N(t) to $M_1(t)$ and $M_2(t)$, and assuming that both $M_1(t)$ and $M_2(t)$ act on N(t) additively and independently,

$$E\{dN(t)|M_1,M_2\} = \left[\alpha_0+\int\alpha_1(t-u)dM_1(u)+\int\alpha_2(t-u)dM_2(u)\right]dt, \qquad (5.4.1)$$

where the quantity $E\{dN(t)|M_1,M_2\}$ has the interpretation

$$\Pr\{N \text{ event in } (t,\ t+dt]|\text{the events in the } M_1 \text{ and } M_2 \text{ processes}\}$$

The constant α_0 would represent the mean rate of N in the case M_1 and M_2 are inactive. The functions $\alpha_1(\cdot)$ and $\alpha_2(\cdot)$ are the impulse response functions corresponding to the processes M_1 and M_2, respectively.

5.4.2 <u>SOLUTION OF THE MODEL</u>

Equation (5.4.1) may be solved for α_0, $\alpha_1(\cdot)$ and $\alpha_2(\cdot)$ using the same methods as used in the case of the simple linear point process model (Section 4.5.2), i.e.,

Take the expected value of (5.4.1) with respect to M_1 and M_2 and obtain

$$P_N = \alpha_0 + P_{M_1}\int\alpha_1(u)du + P_{M_2}\int\alpha_2(u)du$$

which implies that

$$\alpha_0 = P_N - P_{M_1}\int\alpha_1(u)du - P_{M_2}\int\alpha_2(u)du \tag{5.4.2}$$

Now multiplying (5.4.1) by $dM_1(t-u)$ and taking expected values with respect to the pair (M_1, M_2), we obtain

$$P_{NM_1}(u) = \alpha_0 P_{M_1} + \int\alpha_1(t-v)\left[P_{M_1M_1}(v-t+u)+P_{M_1}\delta(v-t+u)\right]dv$$

$$+ \int\alpha_2(t-v)P_{M_2M_1}(v-t+u)dv$$

Substituting the value of α_0 from expression (5.4.2) and simplifying

$$P_{NM_1}(u) = P_N P_{M_1} - P_{M_1}{}^2 \int\alpha_1(v)dv - P_{M_2}P_{M_1}\int\alpha_2(v)dv$$

$$+ \int\alpha_1(w)\left[P_{M_1M_1}(u-w)+P_{M_1}\delta(u-w)\right]dw + \int\alpha_2(w)P_{M_2M_1}(u-w)dw$$

A further simplification of the above expression reduces to

$$q_{NM_1}(u) = P_{M_1}\alpha_1(u) + \int \alpha_1(w) q_{M_1M_1}(u-w)dw + \int \alpha_2(w) q_{M_2M_1}(u-w)dw \quad (5.4.3)$$

where $q_{NM_1}(\cdot)$ and $q_{M_2M_1}(\cdot)$ are the cross-cumulant functions between processes N and M_1, and between M_2 and M_1.

Similarly multiplying (5.4.1) by $dM_2(t-u)$, taking expected values with respect to the pair (M_1, M_2), and substituting the value of α_0 and simplifying, we obtain

$$q_{NM_2}(u) = P_{M_2}\alpha_2(u) + \int \alpha_1(w) q_{M_1M_2}(u-w)dw + \int \alpha_2(w) q_{M_2M_2}(u-w)dw \quad (5.4.4)$$

From expressions (5.4.3) and (5.4.4), it follows that in the case the inputs M_1 and M_2 are independent Poisson processes, the impulse response functions $\alpha_1(\cdot)$ and $\alpha_2(\cdot)$ may be identified as

$$\alpha_1(u) = q_{NM_1}(u)/P_{M_1}$$

$$\alpha_2(u) = q_{NM_2}(u)/P_{M_2}$$

The solution for $\alpha_1(\cdot)$ and $\alpha_2(\cdot)$, in general, requires some form of deconvolution, which can be avoided by taking the Fourier transform of (5.4.3) and (5.4.4) , i.e.,

$$\frac{1}{2\pi}\int \exp(-i\lambda u) q_{NM_1}(u)du = \frac{1}{2\pi}\int \exp(-i\lambda u) \Big[\alpha_1(u)P_{M_1} + \int \alpha_1(w) q_{M_1M_1}(u-w)dw$$

$$+ \int \alpha_2(w) q_{M_2M_1}(u-w)dw\Big]du$$

and

$$\frac{1}{2\pi}\int \exp(-i\lambda u) q_{NM2}(u) du = \frac{1}{2\pi}\int \exp(-i\lambda u)\left[\alpha_2(u) P_{M_2} + \int \alpha_1(w) q_{M_1M_2}(u-w) dw \right.$$

$$\left. + \int \alpha_2(w) q_{M_2M_2}(u-w) dw \right] du$$

which implies that

$$f_{NM_1}(\lambda) = \int \exp(-i\lambda v)\alpha_1(v) dv \left[\frac{P_{M_1}}{2\pi} + \frac{1}{2\pi}\int \exp(-i\lambda w) q_{M_1M_1}(w) dw\right]$$

$$+ \int \exp(-i\lambda v)\alpha_2(v) dv \left[\frac{1}{2\pi}\int \exp(-i\lambda w) q_{M_2M_1}(w) dw\right]$$

and

$$f_{NM_2}(\lambda) = \int \exp(-i\lambda v)\alpha_1(v) dv \left[\frac{1}{2\pi}\int \exp(-i\lambda w) q_{M_1M_2}(w) dw\right]$$

$$+ \int \exp(-i\lambda v)\alpha_2(v) dv \left[\frac{P_{M_2}}{2\pi} + \frac{1}{2\pi}\int \exp(-i\lambda w) q_{M_2M_2}(w) dw\right]$$

or

$$f_{NM_1}(\lambda) = A_1(\lambda) f_{M_1M_1}(\lambda) + A_2(\lambda) f_{M_2M_1}(\lambda) \qquad (5.4.5)$$

$$f_{NM_2}(\lambda) = A_1(\lambda) f_{M_1M_2}(\lambda) + A_2(\lambda) f_{M_2M_2}(\lambda) \qquad (5.4.6)$$

Solving (5.4.5) and (5.4.6) simultaneously for $A_1(\cdot)$ and $A_2(\cdot)$, we obtain

$$A_1(\lambda) = \frac{f_{NM_1}(\lambda) f_{M_2M_2}(\lambda) - f_{NM_2}(\lambda) f_{M_2M_1}(\lambda)}{f_{M_1M_1}(\lambda) f_{M_2M_2}(\lambda) - |f_{M_2M_1}(\lambda)|^2} \qquad (5.4.7)$$

and

$$A_2(\lambda) = \frac{f_{NM_2}(\lambda)f_{M_1M_1}(\lambda) - f_{NM_1}(\lambda)f_{M_1M_2}(\lambda)}{f_{M_1M_1}(\lambda)f_{M_2M_2}(\lambda) - |f_{M_2M_1}(\lambda)|^2} \qquad (5.4.8)$$

A further simplification of (5.4.7) and (5.4.8) leads to

$$A_1(\lambda) = \frac{f_{NM_1.M_2}(\lambda)}{f_{M_1M_1.M_2}(\lambda)} \qquad (5.4.9)$$

and

$$A_2(\lambda) = \frac{f_{NM_2.M_1}(\lambda)}{f_{M_2M_2.M_1}(\lambda)} \qquad (5.4.10)$$

Thus the transfer funtion $A_1(\cdot)$ is seen to be ratio of the partial cross-spectrum between processes N and M_1 to the partial auto-spectrum of process M_1 allowing for the process M_2 whereas $A_2(\cdot)$ is the ratio of the partial cross-spectrum between N and M_2 to the partial auto-spectrum of M_2 allowing for the process M_1.

5.4.3 MEAN SQUARED ERROR OF THE MODEL

The computation of the mean squared error of the model given in (5.4.1) may be carried out if we define the following error process with stationary increments

$$d\epsilon(t) = dN(t) - \left\{\alpha_0 + \int \alpha_1(t-u)dM_1(u) + \int \alpha_2(t-u)dM_2(u)\right\}dt$$

Clearly $E\{d\epsilon(t)\}=0$. Now the cumulant density function of the process $\epsilon(\cdot)$ at two instants t and t' is given as

$$q_{\epsilon\epsilon}(t-t')dtdt' = E\{d\epsilon(t)d\epsilon(t')\} - E\{d\epsilon(t)\}E\{d\epsilon(t') \ .$$

Substituting the values of $d\epsilon(t)$ and $d\epsilon(t')$ and simplifying, we get

$$\begin{aligned}
q_{\epsilon\epsilon}(t-t') &= P_{NN}(t-t') + P_N\delta(t-t') - \alpha_0 P_N - \int \alpha_1(t'-v)P_{NM_1}(t-v)dv \\
&- \int \alpha_2(t'-v)P_{NM_2}(t-v)dv - \alpha_0 P_N + \alpha_0^2 + \alpha_0 P_{M_1}\int \alpha_1(t'-v)dv \\
&+ \alpha_0 P_{M_2}\int \alpha_2(t'-v)dv - \int \alpha_1(t-u)P_{NM_1}(t'-u)du \\
&+ \alpha_0 P_{M_1}\int \alpha_1(t-u)du + \iint \alpha_1(t-u)\alpha_1(t'-v)\left[P_{M_1M_1}(u-v)+P_{M_1}\delta(u-v)\right]dudv \\
&+ \iint \alpha_1(t-u)\alpha_2(t'-v)P_{M_1M_2}(u-v)dudv - \int \alpha_2(t-u)P_{NM_2}(t'-u)du \\
&+ \alpha_0 P_{M_2}\int \alpha_2(t-u)du + \iint \alpha_2(t-u)\alpha_1(t'-v)P_{M_2M_1}(u-v)dudv \\
&+ \iint \alpha_2(t-u)\alpha_2(t'-v)\left[P_{M_2M_2}(u-v)+P_{M_2}\delta(u-v)\right]dudv \ .
\end{aligned}$$

Substituting the value of α_0 from expression (5.4.2) and simplifying, we obtain

$$q_{\epsilon\epsilon}(t-t') = P_{NN}(t-t') - P_N^2 + P_N\delta(t-t') - \int\alpha_1(t'-v)\left[P_{NM_1}(t-v)-P_NP_{M_1}\right]dv$$

$$- \int\alpha_2(t'-v)\left[P_{NM_2}(t-v)-P_NP_{M_2}\right]dv - \int\alpha_1(t-u)\left[P_{NM_1}(t'-u)-P_NP_{M_1}\right]du$$

$$- \int\alpha_2(t-u)\left[P_{NM_1}(t'-u)-P_NP_{M_1}\right]du$$

$$+ \iint\alpha_2(t-u)\alpha_1(t'-v)P_{M_2M_1}(u-v)dudv - P_{M_2}P_{M_1}\iint\alpha_2(w)\alpha_1(t'-v)dwdv$$

$$+ \iint\alpha_1(t-u)\alpha_2(t'-v)P_{M_1M_2}(u-v)dudv - P_{M_2}P_{M_1}\iint\alpha_2(w)\alpha_1(t-u)dwdu$$

$$+ \iint\alpha_1(t-u)\alpha_1(t'-v)\left[P_{M_1M_1}(u-v)+P_{M_1}\delta(u-v)\right]dudv$$

$$- P_{M_1}{}^2\iint\alpha_1(w)\alpha_1(t-u)dwdu$$

$$+ \iint\alpha_2(t-u)\alpha_2(t'-v)\left[P_{M_2M_2}(u-v)+P_{M_1}\delta(u-v)\right]dudv$$

$$- P_{M_2}{}^2\iint\alpha_2(w)\alpha_2(t-u)dwdu$$

Therefore

$$q_{\epsilon\epsilon}(t-t') = q_{NN}(t-t')+P_N\delta(t-t') - \int\alpha_1(t'-v)q_{NM_1}(t-v)dv$$

$$- \int\alpha_2(t'-v)q_{NM_2}(t-v)du - \int\alpha_1(t-u)q_{NM_1}(t'-u)du$$

$$- \int \alpha_2(t-u) q_{NM_2}(t'-u) du + \iint \alpha_2(w)\alpha_1(t'-v) q_{M_2M_1}(t-w-v) dwdv$$

$$+ \iint \alpha_1(t-u)\alpha_2(w) q_{M_1M_2}(u-t'+w) dwdu$$

$$+ \iint \alpha_1(t-u)\alpha_1(w) \left[q_{M_1M_1}(u-t'+w) + P_{M_1}\delta(u-t'+w) \right] dwdu$$

$$+ \iint \alpha_2(t-u)\alpha_2(w) \left[q_{M_2M_2}(u-t'+w) + P_{M_2}\delta(u-t'+w) \right] dwdu$$

Hence

$$q_{\epsilon\epsilon}(t-t') = q_{NN}(t-t') + P_N\delta(t-t') - \int \alpha_1(w) q_{NM_1}(t-t'+w) dw$$

$$- \int \alpha_2(w) q_{NM_2}(t-t'+w) dw - \int \alpha_1(w) q_{NM_1}(t'-t+w) dw$$

$$- \int \alpha_2(w) q_{NM_2}(t'-t+w) dw + \iint \alpha_2(w)\alpha_1(s) q_{M_2M_1}(t-t'+w) dwds$$

$$+ \iint \alpha_1(s)\alpha_2(w) q_{M_1M_2}(t-t'+w-s) dwds$$

$$+ \iint \alpha_1(s)\alpha_2(w) \left[q_{M_1M_1}(t-t'+w-s) + P_{M_1}\delta(t-t'+w-s) \right] dwds$$

$$+ \iint \alpha_1(s)\alpha_2(w) \left[q_{M_2M_2}(t-t'+w-s) + P_{M_2}\delta(t-t'+w-s) \right] dwds$$

Setting $t-t'=u$, $w=v$, and since $q_{k\ell}(u)=q_{\ell k}(-u)$, we have

$$q_{\epsilon\epsilon}(u) = q_{NN}(u) + P_N\delta(u) - \int \alpha_1(v) q_{NM_1}(u+v) dv - \int \alpha_2(v) q_{NM_2}(u+v) dv$$

$$- \int \alpha_1(v) q_{M_1N}(u-v)dv - \int \alpha_2(v) q_{M_2N}(u-v)dv$$

$$+ \iint \alpha_2(s)\alpha_1(v) q_{M_2M_1}(u+v-s)dvds + \iint \alpha_1(s)\alpha_2(v) q_{M_1M_1}(u+v-s)dvds$$

$$+ \iint \alpha_1(s)\alpha_1(v) \left[q_{M_1M_1}(u+v-s) + P_{M_1}\delta(u+v-s) \right] dvds$$

$$+ \iint \alpha_2(s)\alpha_1(v) \left[q_{M_2M_2}(u+v-s) + P_{M_2}\delta(u+v-s) \right] dvds$$

The Fourier transform of the above expression leads to the corresponding frequency domain representation

$$f_{\epsilon\epsilon}(\lambda) = f_{NN}(\lambda) - \overline{A_1(\lambda)} f_{NM_1}(\lambda) - \overline{A_2(\lambda)} f_{NM_2}(\lambda) - A_1(\lambda) f_{M_1N}(\lambda)$$

$$- A_2(\lambda) f_{M_2N}(\lambda) + A_2(\lambda)\overline{A_1(\lambda)} f_{M_2M_1}(\lambda) + A_1(\lambda)\overline{A_2(\lambda)} f_{M_1M_2}(\lambda)$$

$$+ A_1(\lambda)\overline{A_1(\lambda)} f_{M_1M_1}(\lambda) + A_2(\lambda)\overline{A_2(\lambda)} f_{M_2M_2}(\lambda)$$

Substituting the values of $A_1(\cdot)$ and $A_2(\cdot)$ from (5.4.7) and (5.4.8), and after some further algebraic manipulation, the above expression reduces to

$$f_{\epsilon\epsilon}(\lambda) = f_{NN}(\lambda) - A_1(\lambda) f_{M_1N}(\lambda) - A_2(\lambda) f_{M_2N}(\lambda)$$

$$= f_{NN}(\lambda) \left[1 - \frac{A_1(\lambda) f_{M_1N}(\lambda)}{f_{NN}(\lambda)} - \frac{A_2(\lambda) f_{M_2N}(\lambda)}{f_{NN}(\lambda)} \right] \qquad (5.4.11)$$

Expression (5.4.11) may also be written as

$$f_{\epsilon\epsilon}(\lambda) = f_{NN}(\lambda)\left[\ 1 - |R_{N.M_1M_2}(\lambda)|^2\ \right] \tag{5.4.12}$$

where

$$|R_{N.M_1M_2}(\lambda)|^2 = \frac{A_1(\lambda)f_{M_1N}(\lambda)}{f_{NN}(\lambda)} + \frac{A_2(\lambda)f_{M_2N}(\lambda)}{f_{NN}(\lambda)} \tag{5.4.13}$$

Substituting the values of $A_1(\cdot)$ and $A_2(\cdot)$ from (5.4.7) and (5.4.8) and suppressing the dependence on λ, expression (5.4.13) becomes

$$|R_{N.M_1M_2}|^2 = \frac{f_{M_1N}}{f_{NN}}\left[\frac{f_{NM_1}f_{M_2M_2}-f_{NM_2}f_{M_2M_1}}{f_{M_1M_1}f_{M_2M_2}-|f_{M_1M_2}|^2}\right] + \frac{f_{M_2N}}{f_{NN}}\left[\frac{f_{NM_2}f_{M_1M_1}-f_{NM_1}f_{M_1M_2}}{f_{M_1M_1}f_{M_2M_2}-|f_{M_1M_2}|^2}\right]$$

$$= \frac{|f_{NM_1}|^2f_{M_2M_2}-f_{NM_2}f_{M_2M_1}f_{M_1N}-f_{NM_1}f_{M_1M_2}f_{M_2N}+|f_{NM_2}|^2f_{M_1M_1}}{f_{NN}[f_{M_1M_1}f_{M_2M_2}-|f_{M_1M_2}|^2}$$

$$= \frac{|R_{NM_1}|^2-R_{NM_2}R_{M_2M_1}R_{M_1N}-R_{NM_1}R_{M_1M_2}R_{M_2N}+|R_{NM_2}|^2}{1-|R_{M_1M_2}|^2}$$

$$= \frac{|R_{NM_1}|^2+|R_{NM_2}-R_{NM_1}R_{M_1M_2}|^2-|R_{NM_1}|^2|R_{M_1M_2}|^2}{1-|R_{M_1M_2}|^2} \tag{5.4.14}$$

From expression (5.3.2), this implies that

$$|R_{NM_2}-R_{NM_1}R_{M_1M_2}|^2 = |R_{NM_2.M_1}|^2 \,[1-|R_{NM_1}|^2]\,[1-|R_{M_1M_2}|^2] \quad .$$

Substituting this value in (5.4.14) and simplifying, we get

$$|R_{N.M_1M_2}|^2 = |R_{NM_1}|^2 + |R_{NM_2.M_1}|^2 \left\{ 1 - |R_{NM_1}|^2 \right\} \qquad (5.4.15)$$

The quantity $|R_{N.M_1M_2}(\lambda)|^2$ is called the multiple coherence at frequency λ between the output point process N and the input point processes M_1 and M_2. This parameter may be seen as a direct analogue of the multiple correlation coefficient-squared for the ordinary multiple regression model (see for example Draper and Smith, 1981).

Expression (5.4.12) shows that the minimum of the mean squared error of the linear model (5.4.1) depends on the multiple coherence $|R_{N.M_1M_2}(\lambda)|^2$ in that the error spectrum $f_{\epsilon\epsilon}(\lambda)$ would be zero if the multiple coherence is 1. Further, from expression (5.4.12), $0 \le f_{\epsilon\epsilon}(\lambda) \le f_{NN}(\lambda)$, then $0 \le |R_{N.M_1M_2}(\lambda)|^2 \le 1$, giving an interpretation of $|R_{N.M_1M_2}(\lambda)|^2$ as a measure of the adequacy of the model (5.4.1) in terms of linear predictability of the point process N from the point processes M_1 and M_2.

Related to the complex quantities $A_1(\lambda)$ and $A_2(\lambda)$ we further define two additional real-valued partial parameters called the 'partial gain' and the 'partial phase', which provide useful information about the relationship between output and each input after the allowance for the other input has been made.

5.4.4 THE PARTIAL GAIN AND THE PARTIAL PHASE OF ORDER 1

The partial gains $G_{NM_1.M_2}(\lambda)$ and $G_{NM_2.M_1}(\lambda)$ at frequency λ may be defined as the absolute values of $A_1(\lambda)$ and $A_2(\lambda)$, respectively, i.e.,

$$G_{NM_1.M_2}(\lambda) = |A_1(\lambda)| = \frac{|f_{NM_1.M_2}(\lambda)|}{f_{M_1M_1.M_2}(\lambda)} \qquad (5.4.16)$$

$$G_{NM_2.M_1}(\lambda) = |A_2(\lambda)| = \frac{|f_{NM_2.M_1}(\lambda)|}{f_{M_2M_2.M_1}(\lambda)} \qquad (5.4.17)$$

A value, for example, $G_{NM_1.M_2}(\lambda) = 0$ indicates no direct connection between the processes N and M_1, and all the association between them is possibly due to the fact that both are associated with the process M_2.

The partial phases $\Phi_{NM_1.M_2}(\lambda)$ and $\Phi_{NM_2.M_1}(\lambda)$ at frequency λ may be defined as the arguments of $A_1(\lambda)$ and $A_2(\lambda)$, respectively, i.e.,

$$\Phi_{NM_1.M_2}(\lambda) = \arg\{A_1(\lambda)\} = \arg\{f_{NM_1.M_2}(\lambda)\} \qquad (5.4.18)$$

$$\Phi_{NM_2.M_1}(\lambda) = \arg\{A_2(\lambda)\} = \arg\{f_{NM_2.M_1}(\lambda)\} \qquad (5.4.19)$$

The partial phase, for example, $\Phi_{NM_1.M_2}(\lambda)$ measures the phase shift (at frequency λ) between processes N and M_1 after allowing for phase shifts in each of these processes induced by their common association with process M_2. This parameter may also be used to assess the timing relations between two processes after the linear effects of the third process have been removed.

5.4.5 ESTIMATION OF THE MULTIPLE COHERENCE

An estimate of $|R_{N.M_1M_2}(\lambda)|^2$ at frequency λ may be obtained by substituting estimates of the partial coherences at that frequency in expression (5.4.15), i.e.,

$$|R_{N.M_1M_2}{}^{(T)}(\lambda)|^2 = |R_{NM_1}{}^{(T)}(\lambda)|^2 + |R_{NM_2.M_1}{}^{(T)}(\lambda)|^2 \left\{1 - |R_{NM_1}{}^{(T)}(\lambda)|^2\right\} \quad \lambda \neq 0 \tag{5.4.20}$$

where the estimation of the basic spectra needed in order to estimate the above coherences is based on disjoint segments of the whole record length (see Chapter 3).

5.4.6 PROPERTIES OF THE ESTIMATE OF THE MULTIPLE COHERENCE

The density function of the estimate of the multiple coherence in a general case of r vector-valued process as an input to a linear time-invariant point process system with a single ouput process is given in Section 5.5.4, which implies that in the case $|R_{N.M_1M_2}(\lambda)|^2=0$, the estimate $|R_{N.M_1M_2}{}^{(T)}(\lambda)|^2$ has a Beta distribution with parameters 2, and L-2, where L is the number of disjoint segments into which the entire record length is split.

In order to test the hypothesis $|R_{N.M_1M_2}(\lambda)|^2=0$ at frequency λ, it follows from the general result given in Section 5.5.5 that under this hypothesis

$$\frac{L-2}{2}\left[\frac{|R_{N.M_1M_2}{}^{(T)}(\lambda)|^2}{1-|R_{N.M_1M_2}{}^{(T)}(\lambda)|^2}\right] \sim F_{\{4,2(L-2)\}}$$

where $F_{\{n_1,n_2\}}$ denotes the F-distribution with n_1 and n_2 degrees of freedom. Which suggests that the hypothesis of zero multiple coherence at frequency λ should be rejected at 100(1-α)% level if

$$|R_{N.M_1M_2}{}^{(T)}(\lambda)|^2 \geq \frac{2C_\alpha}{L + 2(C_\alpha - 1)} \qquad (5.4.21)$$

where C_α is the upper 100α percent point of an F-distribution with 4 and 2(L-2) degrees of freedom.

In the next section we apply the above procedures to our spindle data sets i.e., the Ia and II response to both gamma static inputs, in order to see how these inputs, collectively, contribute to predicting each of the outputs, (the Ia and II discharges) and to see how the activation of a dynamic length change affects this predictability.

5.4.7 APPLICATIONS OF THE MULTIPLE COHERENCE

Since both stimuli, ${}_1\gamma_s$ and ${}_2\gamma_s$, are applied to the spindle concurrently and independently, expression (5.4.15) for the multiple coherence between each of the outputs, the Ia and II discharges, and both '${}_1\gamma_s$' and '${}_2\gamma s$' is seen to reduce to

$$|R_{N.M_1M_2}(\lambda)|^2 = |R_{NM_1}(\lambda)|^2 + \frac{|R_{NM_2}(\lambda)|^2 - |R_{NM_1}(\lambda)|^2\ |R_{NM_2}(\lambda)|^2}{[\ 1 - |R_{NM_1}(\lambda)|^2\ ]}$$

i.e., $$|R_{N.M_1M_2}(\lambda)|^2 = |R_{NM_1}(\lambda)|^2 + |R_{NM_2}(\lambda)|^2 \quad . \qquad (5.4.22)$$

Therefore the estimate of $|R_{N.M_1M_2}(\lambda)|^2$ may be obtained by inserting the corresponding estimates of ordinary coherences in (5.4.22).

Fig.5.4.1 and Fig.5.4.2 illustrate the application of multiple coherence. Figs.5.4.1a,c are the estimates of ordinary coherences between the Ia discharge and the '${}_1\gamma_s$', and between the Ia discharge and the '${}_2\gamma_s$', respectively when no length change is imposed on the spindle. Figs.5.4.1b,d correspond to the same estimates between the same processes but when a length change is also applied to the parent muscle containing the spindle. Figs.5.4.1e,f are the estimates of multiple coherence between the Ia and both static gamma axons with (Fig5.4.1f) and without (Fig5.4.1e) the length change activity. The horizontal dotted lines in these estimates are based on expression (5.4.21) and give the upper limit of an approximate 95% confidence interval for the multiple coherence at a given frequency λ under the hypothesis of M_1 and M_2 being jointly independent of N.

A comparison of Fig5.4.1e (multiple coherence) with Figs.5.4.1a,c (ordinary coherences) reveals that in the absence of the length change both inputs, jointly, increase the linear predictability

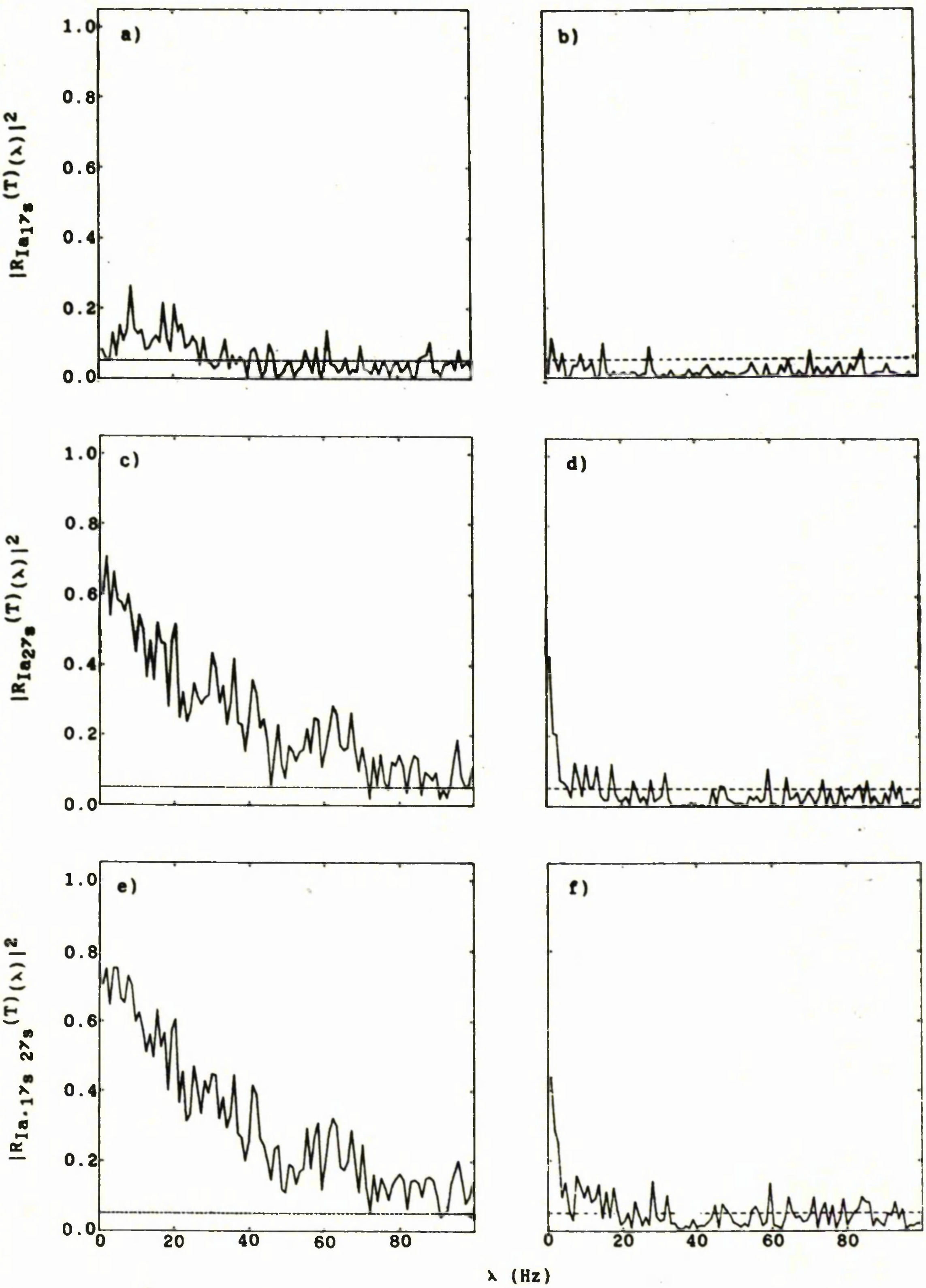

Fig.5.4.1 Illustration of the multiple coherence

a,b) Estimated coherences between the Ia discharge and ${}_1\gamma_s$ in the absence (a) and presence (b) of a length change ℓ

c,d) Estimated coherences between the Ia discharge and ${}_2\gamma_s$ in the absence (c) and presence (d) of ℓ

e,f) Estimated multiple coherences of the Ia discharge with the ${}_1\gamma_s$ and ${}_2\gamma_s$ in the absence (e) and presence (f) of ℓ

The horizontal dotted line in each figure represents the upper limit of the 95% confidence interval (marginal) for the respective estimate of the coherences under the hypothesis of zero coherence.

of the Ia discharge. The presence of the length change, hewever is seen to reduce this predictability (Fig.5.4.1) over almost the whole range of frequencies. The length change is also seen to impose virtual independence between the Ia discharge and each static gamma axon (Fig.5.4.1b,d).

Fig 5.4.2 gives the corresponding estimates and comparisons as Fig.5.4.1 but in this case the output from the spindle is the II discharge. A comparison of each estimate in Figs.5.4.2a,c, respectively, with the corresponding estimate in Fig.5.4.1b,d suggests that the length signal does not affect the coupling between the II discharge and each of the static gamma axons. The multiple coherence between the II discharge and both gammas with (Fig.5.4.2f) and without (Fig.5.4.2e) the activation of the length change reveal that the linear predictability of the II discharge from both gammas is increased in both cases only at low frequencies (as compared with Fig.5.4.2b,d and with Figs.5.4.2a,c, respectively). It is interesting to note that the presence of the length change enhances the coupling between the static gamma axon and the spindle II discharge.

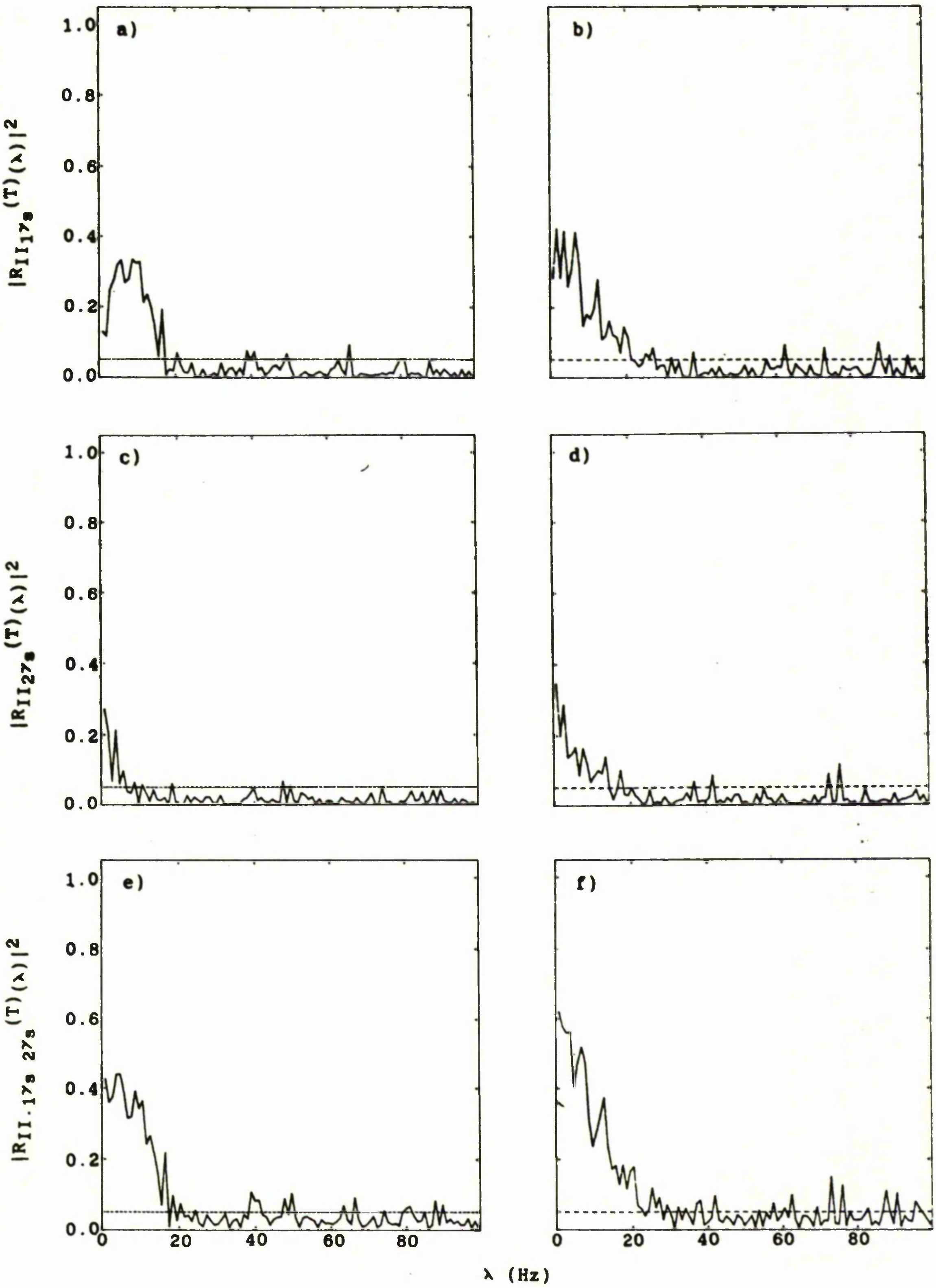

Fig.5.4.2 Illustration of the multiple coherence

a,b) Estimated coherences between the II discharge and ${}_1\gamma_s$ in the absence (a) and presence (b) of a length change ℓ

c,d) Estimated coherences between the II discharge and ${}_2\gamma_s$ in the absence (c) and presence (d) of ℓ

e,f) Estimated multiple coherences of the II discharge with the ${}_1\gamma_s$ and ${}_2\gamma_s$ in the absence (e) and presence (f) of ℓ

The horizontal dotted line in each figure represents the upper limit of the 95% confidence (marginal) interval for the respective estimate of the coherences under the hypothesis of zero coherence.

5.5 MULTIPLE-INPUT SINGLE-OUTPUT POINT PROCESS SYSTEMS

The linear point process model with two inputs and a single output, discussed in Section (5.4), may be extended to a general linear model in order to include a number of point process inputs which are applied to the system simultaneously. The object in developing this model in our case is to study the characteristics of the muscle spindle in a more realistic situation when it is acted upon by a number of fusimotor axons, and also to see how these inputs are useful in predicting separately each of the outputs, the Ia and II discharges, from the same spindle.

Let $\underline{M}(t)=\{M_1(t),\ M_2(t),\ \ldots,\ M_r(t)\}$ be a stationary r vector-valued point process being applied to the system, and N(t) be the output point process from the system. A simple graphical representation of this situation may be given as

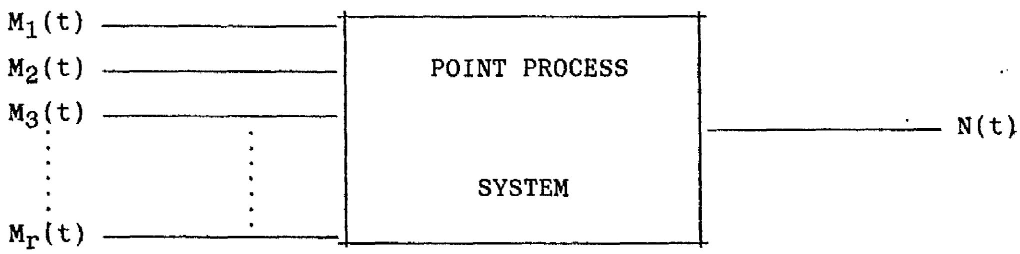

5.5.1 GENERAL LINEAR POINT PROCESS MODEL

Assuming no interactions occur between the components of the input process $\underline{M}(t)$, then the extension of the model (4.8.3) leads to a general linear model, relating N(t) to the $\underline{M}(t)$, of the form

$$E\{dN(t)|\underline{M}\} = \left\{\alpha_0+\int\alpha_1(t-u)dM_1(u)+\int\alpha_2(t-u)dM_2(u)+\ldots+\int\alpha_r(t-u)dM_r(u)\right\}dt \tag{5.5.1}$$

The quantity $E\{dN(t)|\underline{M}\}$ may be interpreted as

$$Pr\{\ N \text{ event in } (t,\ t+dt]|M_1,\ M_2,\ \ldots,\ M_r\}$$

The constant α_0 represents the mean rate of N(t) in the case that $\underline{M}(t)$ is inactive. The function $\alpha_j(\cdot)$ j=1,2,...,r is the impulse response function corresponding to the jth component of $\underline{M}(t)$.

Before we proceed on to the solution of above model (5.5.1) we set down some matrix notation

IN THE TIME DOMAIN

$$\mathbf{P}_{\underline{M}} = \begin{bmatrix} p_{M_1} \\ p_{M_2} \\ \vdots \\ p_{M_r} \end{bmatrix} \qquad \alpha_{\underline{M}}(\cdot) = \begin{bmatrix} \alpha_1(\cdot) \\ \alpha_2(\cdot) \\ \vdots \\ \alpha_r(\cdot) \end{bmatrix} \qquad \mathbf{P}_{\underline{M}N}(\cdot) = \begin{bmatrix} p_{M_1N}(\cdot) \\ p_{M_2N}(\cdot) \\ \vdots \\ p_{M_rN}(\cdot) \end{bmatrix}$$

$$\mathbf{P}_{N\underline{M}}(\cdot) = \begin{bmatrix} p_{NM_1}(\cdot) & p_{NM_2}(\cdot) & \ldots & p_{NM_r}(\cdot) \end{bmatrix}$$

$$\mathbf{P}_{\underline{MM}}(\cdot) = \begin{bmatrix} p_{M_1M_1}(\cdot) & p_{M_1M_2}(\cdot) & \ldots & p_{M_1M_r}(\cdot) \\ p_{M_2M_1}(\cdot) & p_{M_2M_2}(\cdot) & \ldots & p_{M_2M_r}(\cdot) \\ \vdots & \vdots & \ddots & \vdots \\ p_{M_rM_1}(\cdot) & p_{M_rM_2}(\cdot) & \ldots & p_{M_rM_r}(\cdot) \end{bmatrix}$$

$$\mathbf{D}_{\underline{M}} = \text{diag}\begin{bmatrix} p_{M_1} & p_{M_2} & \ldots & p_{M_r} \end{bmatrix}$$

IN THE FREQUENCY DOMAIN

$$F_{\underline{M}N}(\cdot) = \begin{bmatrix} f_{M_1N}(\cdot) \\ f_{M_2N}(\cdot) \\ \vdots \\ f_{M_rN}(\cdot) \end{bmatrix} \qquad A_{\underline{M}}(\cdot) = \begin{bmatrix} A_1(\cdot) \\ A_2(\cdot) \\ \vdots \\ A_r(\cdot) \end{bmatrix}$$

$$F_{N\underline{M}}(\cdot) = \begin{bmatrix} f_{NM_1}(\cdot) & f_{NM_2}(\cdot) & \cdots & f_{NM_r}(\cdot) \end{bmatrix}$$

$$F_{\underline{M}\underline{M}}(\cdot) = \begin{bmatrix} f_{M_1M_2}(\cdot) & f_{M_1M_2}(\cdot) & \cdots & f_{M_1M_r}(\cdot) \\ f_{M_2M_1}(\cdot) & f_{M_2M_1}(\cdot) & \cdots & f_{M_2M_r}(\cdot) \\ \vdots & \vdots & \ddots & \vdots \\ f_{M_rM_1}(\cdot) & f_{M_rM_2}(\cdot) & \cdots & f_{M_rM_r}(\cdot) \end{bmatrix}$$

Equation (5.2.1) may now be written as

$$E\{dN(t)|\underline{M}\} = \left\{\alpha_0 + \int \alpha_{\underline{M}}^T(t-u)d\underline{M}(u)\right\}dt \qquad (5.5.2)$$

where '$\alpha_{\underline{M}}^T(\cdot)$' denotes the transpose of $\alpha_{\underline{M}}(\cdot)$.

5.5.2 SOLUTION OF THE MODEL

Following the same arguments as used in Section 5.4.2 for the linear model (5.4.1), we solve (5.5.2) for α_0, $\alpha_1(\cdot)$, $\alpha_2(\cdot)$, ..., $\alpha_r(\cdot)$ as follows

Take the expected value of (5.5.2) with respect to $\underline{M}$

$$E\Big[E\{dN(t)|\underline{M}\}\Big] = E\Big[\left\{\alpha_0 + \int \alpha_{\underline{M}}^T(t-u)d\underline{M}(u)\right\}dt\Big]$$

to obtain

$$P_N = \alpha_0 + \int \alpha_{\underline{M}}^T(u) P_{\underline{M}} du \qquad (5.5.3)$$

Now multiplying (5.5.2) by $d\underline{M}^T(t-u)$ and taking the expected value with respect to $\underline{M}$, we obtain

$$E\left[E\{dN(t)|\underline{M}\} d\underline{M}^T(t-u)\right] = \left[\alpha_0 E\{d\underline{M}^T(t-u)\} + \int \alpha_{\underline{M}}^T(t-v) E\{d\underline{M}(v) d\underline{M}^T(t-u)\right] dt$$

$$P_{N\underline{M}}(u) = \alpha_0 P_{\underline{M}}^T + \int \alpha_{\underline{M}}^T(t-v) \left[P_{\underline{MM}}(v-t+u) + \delta(v-t+u) D_{\underline{M}}\right] dv$$

where $\delta(\cdot)$ is the Dirac delta function. Substitution of the value of α_0 from expression (5.5.3) and some algebraic manipulation leads to

$$Q_{N\underline{M}}(u) = \int \alpha_{\underline{M}}^T(v) \left[Q_{\underline{MM}}(u-v) + \delta(u-v) D_{\underline{M}}\right] dv \qquad (5.5.4)$$

where $Q_{N\underline{M}}(\cdot)$ is a (1 x r) vector with entries $q_{NM_1}(\cdot)$, ..., $q_{NM_r}(\cdot)$ and $Q_{\underline{MM}}(\cdot)$ an rxr cumulant matrix of $\underline{M}(\cdot)$ corresponding to$P_{\underline{MM}}(\cdot)$. From (5.5.4) we see that if the components of $\underline{M}(t)$ are independent Poisson processes with mean rates P_{M_1}, P_{M_2}, ..., P_{M_r}, respectively, then the impulse response function $\alpha_{\underline{M}}(\cdot)$ may be identified by

$$\alpha_{\underline{M}}^T(u) = Q_{N\underline{M}}(u) D_{\underline{M}}^{-1} \qquad (5.5.5)$$

The solution of the equation (5.5.4) for $\alpha_{\underline{M}}(\cdot)$, in general, requires some form of deconvolution which may be avoided by taking the Fourier transform of (5.5.4), i.e.,

$$\frac{1}{2\pi}\int \exp(-i\lambda u) Q_{N\underline{M}}(u) du = \frac{1}{2\pi}\int \exp(-i\lambda u)\left\{\int \alpha_{\underline{M}}^T(v)\left[Q_{\underline{MM}}(u-v) + \delta(u-v) D_{\underline{M}}\right] dv\right\} du$$

$$F_{N\underline{M}}(\lambda) = \left[\int \exp(-i\lambda v)\alpha_{\underline{M}}^{T}(v)\,dv\right]\left[\frac{1}{2\pi}\int \exp(-i\lambda w)\left\{Q_{\underline{M}\underline{M}}(w)+\delta(w)D_{\underline{M}}\right\}dw\right]$$

i.e.,
$$F_{N\underline{M}}(\lambda) = A_{\underline{M}}^{T}(\lambda)F_{\underline{M}\underline{M}}(\lambda) \tag{5.5.6}$$

which implies

$$A_{\underline{M}}^{T}(\lambda) = F_{N\underline{M}}(\lambda)[F_{\underline{M}\underline{M}}(\lambda)]^{-1} \tag{5.5.7}$$

Let "M_a" denote a typical component of $\underline{M}(t)$ and " $\mathbf{M_a'}$ " be the set of all the components of $\underline{M}(t)$ excluding the "M_a". Let $A_a(\lambda)$ be a typical element of the vector $A_{\underline{M}}(\lambda)$, then, generalising expression (5.4.9) or (5.4.10), $A_a(\lambda)$ can be seen to be

$$A_a(\lambda) = \frac{f_{NM_a.M_a'}(\lambda)}{f_{M_aM_a.M_a'}(\lambda)} \quad ; \quad a = 1, 2, \cdots, r$$

for example,

$$A_1\ (\lambda) = \frac{f_{NM_1.M_2M_3...M_r}(\lambda)}{f_{M_1M_1.M_2M_3...M_r}(\lambda)}$$

5.5.3 MEAN SQUARED ERROR OF THE MODEL

In order to compute the mean squared error of the model (5.5.1), we define the following error process with stationary increments

$$d\epsilon(t)=dN(t)-\left[\alpha_0+\int \alpha_{\underline{M}}^T(t-u)d\underline{M}(u)\right]dt$$

Clearly $E\{d\epsilon(t)\}=0$. The cumulant density of the process $\epsilon(\cdot)$ at two time instants t and t' is given by

$$\left\{q_{\epsilon\epsilon}(t-t')+P_\epsilon\delta(t-t')\right\}dtdt'=E\left\{d\epsilon(t)d\epsilon(t')\right\} - E\left\{d\epsilon(t)\right\}E\left\{d\epsilon(t')\right\}$$

$$= P_{NN}(t-t') + P_N\delta(t-t') - P_N\alpha_0 - \int P_{N\underline{M}}(t-v)\alpha_{\underline{M}}(t'-v)dv$$

$$- \alpha_0 P_N + \alpha_0\alpha_0 + \int \alpha_0 P_{\underline{M}}^T\alpha_{\underline{M}}(t'-v)dv$$

$$- \int \alpha_{\underline{M}}^T(t-u)P_{\underline{M}N}(u-t')du + \int \alpha_{\underline{M}}^T(t-u)P_{\underline{M}}\alpha_0 du$$

$$+ \iint \alpha_{\underline{M}}^T(t-u)\left[P_{\underline{\underline{MM}}}(u-v)+\delta(u-v)D_{\underline{M}}\right]\alpha_{\underline{M}}(t'-v)dudv$$

Substituting the value of α_0 from expression (5.2.3) and simplifying, we obtain

$$q_{\epsilon\epsilon}(t-t') = q_{NN}(t-t')+\delta(t-t')P_N - \int Q_{N\underline{M}}(t-v)\alpha_{\underline{M}}(t'-v)dv$$

$$- \int \alpha_{\underline{M}}^T(t-u)Q_{\underline{M}N}(u-t')du$$

$$+ \iint \alpha_{\underline{M}}^T(t-u)\left[Q_{\underline{\underline{MM}}}(u-v)+\delta(u-v)D_{\underline{M}}\right]\alpha_{\underline{M}}(t'-v)dudv$$

Setting t-u=p, t'-v=q, and t-t'=u, we obtain

$$q_{\epsilon\epsilon}(u) = q_{NN}(u)+\delta(u)P_N - \int Q_{N\underline{M}}(u+q)\alpha_{\underline{M}}(q)dq - \int \alpha_{\underline{M}}^T(p)Q_{\underline{M}N}(u-p)dp$$

$$+ \iint \alpha_{\underline{M}}^T(p)\left[Q_{\underline{M}\underline{M}}(u-p+q)+\delta(u-p+q)D_{\underline{M}}\right]\alpha_{\underline{M}}(q)dpdq \qquad (5.5.8)$$

The Fourier transform of (5.5.8) is seen to lead to the frequency domain representation

$$f_{\epsilon\epsilon}(\lambda) = f_{NN}(\lambda) - F_{N\underline{M}}(\lambda)\overline{A_{\underline{M}}(\lambda)} - A_{\underline{M}}^T(\lambda)F_{\underline{M}N}(\lambda)$$

$$+ A_{\underline{M}}^T(\lambda)F_{\underline{M}\underline{M}}(\lambda)\overline{A_{\underline{M}}(\lambda)} \qquad (5.5.9)$$

Substitution of $A_{\underline{M}}(\lambda)$ from (5.5.7) into (5.5.9) gives the minimum of the mean squared error

$$f_{\epsilon\epsilon}(\lambda) = f_{NN}(\lambda) - F_{N\underline{M}}(\lambda)[F_{\underline{M}\underline{M}}(\lambda)]^{-1}F_{\underline{M}N}(\lambda)$$

$$= f_{NN}(\lambda)\left[1 - |R_{N.\underline{M}}(\lambda)|^2\right] \qquad (5.5.10)$$

where

$$|R_{N.\underline{M}}(\lambda)|^2 = \frac{F_{N\underline{M}}(\lambda)[F_{\underline{M}\underline{M}}(\lambda)]^{-1}F_{\underline{M}N}(\lambda)}{f_{NN}(\lambda)} \qquad (5.5.11)$$

5.5.4 THE MULTIPLE COHERENCE OF ORDER-r

The quantity given in expression (5.5.11) is the multiple coherence (order r) between the process N and the r vector-valued process $\underline{M} = \{M_1, M_2, \ldots, M_r\}$ and is a direct analogue of the multiple correlation coefficient-squared of the ordinary general linear model with the property.

$$0 \leq |R_{N.\underline{M}}(\lambda)|^2 \leq 1$$

Further, from expression (5.5.10), it is seen that the error spectrum reduces to zero at frequency λ if $|R_{N.\underline{M}}(\lambda)|^2=1$ suggesting that a plausible measure of the adequacy of the general linear point process model (5.5.2) may be based on the multiple coherence, the closer the value of the multiple coherence to 1, the higher would be the linear predictability of process N from processes $M_1, M_2, \ldots, M_r$.

Extending the result given in expression (5.4.15), $|R_{N.\underline{M}}(\lambda)|^2$ may also be written in terms of partial coherences, suppressing the dependence on λ, as

$$\begin{aligned}
|R_{N.\underline{M}}|^2 = {} & |R_{NM_1}|^2 + |R_{NM_2.M_1}|^2\left[1-|R_{NM_1}|^2\right] \\
& + |R_{NM_3.M_1M_2}|^2\left[1-|R_{NM_1}|^2\right]\left[1-|R_{NM_2.M_1}|^2\right] + \cdots \\
& + |R_{NM_r.M_1M_2M_3\ldots M_{r-1}}|^2\left[1-|R_{NM_1}|^2\right]\left[1-|R_{NM_2.M_1}|^2\right] \\
& \left[1-|R_{NM_3.M_1M_2}|^2\right] \cdots \left[1-|R_{NM_{r-1}.M_1M_2M_3\ldots M_{r-2}}|^2\right] \qquad (5.5.12)
\end{aligned}$$

where the higher order partial coherences may be written in terms of the lower order partial coherences in the same manner as in expression (5.3.2).

ESTIMATION OF $|R_{N.\underline{M}}(\lambda)|^2$

An estimate of the multiple coherence $|R_{N.\underline{M}}(\lambda)|^2$ may be obtained by inserting the matrix-valued spectral estimates in expression (5.5.11) or estimates of the partial coherences in expression (5.5.12) i.e., for example,

$$|R_{N.\underline{M}}^{(T)}(\lambda)|^2 = \frac{F_{N\underline{M}}^{(T)}(\lambda)[F_{\underline{MM}}^{(T)}(\lambda)]^{-1}F_{\underline{M}N}^{(T)}(\lambda)}{f_{NN}^{(T)}(\lambda)} \qquad \lambda\neq 0 \qquad (5.5.13)$$

where

$$F_{N\underline{M}}^{(T)}(\lambda) = [\ f_{NM_k}^{(T)}(\lambda)\ ] \qquad k=1,2,\ldots,r$$

$$F_{\underline{MM}}^{(T)}(\lambda) = [\ f_{M_jM_k}^{(T)}(\lambda)\ ] \qquad j,k=1,2,\ldots,r$$

$$F_{\underline{M}N}^{(T)}(\lambda) = [\ f_{M_jN}^{(T)}(\lambda)\ ] \qquad j=1,2,\ldots,r$$

The above estimation is based on disjoint sections of the whole record length and has been discussed in Chapter 3.

PROPERTIES OF $|R_{N.\underline{M}}^{(T)}(\lambda)|^2$

By analogy with ordinary multiple regression theory, the density function of the estimate $|R_{N.\underline{M}}^{(T)}(\lambda)|^2$ is the same as that of the multiple correlation coefficient-squared between a random variable Y and an r-vector valued random variable $\underline{X}$. Extending the case of random variables Y and $\underline{X}$ (Goodman,1963) to point processes, the density of $|R_{N.\underline{M}}^{(T)}(\lambda)|^2$ is given by

$$\left[1-|R_{N.\underline{M}}(\lambda)|^2\right] {}_2F_1(L,L,r;|R_{N.\underline{M}}(\lambda)|^2|R_{N.\underline{M}}^{(T)}(\lambda)|^2)\frac{\Gamma(L)}{\Gamma(L-r)\Gamma(r)}$$

$$\left[|R_{N.\underline{M}}^{(T)}(\lambda)|^2\right]^{r-1}\left[1-|R_{N.\underline{M}}^{(T)}(\lambda)|^2\right]^{L-r-1} \qquad (5.5.14)$$

where ${}_2F_1$ is a generalised hypergeometric function (see Abramowitz and Stegun,1964).

In the case $|R_{N.\underline{M}}(\lambda)|^2=0$, expression (5.5.14) reduces to

$$\frac{\Gamma(L)}{\Gamma(L-r)\Gamma(r)}\left[|R_{N.\underline{M}}^{(T)}(\lambda)|^2\right]^{r-1}\left[1-|R_{N.\underline{M}}^{(T)}(\lambda)|^2\right]^{L-r-1} \quad \lambda\neq 0 \qquad (5.5.15)$$

which is a Beta density function with parameters r and L-r.

5.5.5 A TEST FOR ZERO MULTIPLE COHERENCE

In order to test whether the estimated multiple coherence at a given frequency is significantly different from zero, a statistical test may easily be developed. Expression (5.5.15) shows that in the case that $|R_{N.\underline{M}}(\lambda)|^2=0$, the estimate of the multiple coherence given by (5.5.13) has a Beta distribution with parameters r and L-r, and with distribution fuction

$$\Pr\left[|R_{N.\underline{M}}^{(T)}|^2\leq z\right]=\frac{\Gamma(L)}{\Gamma(L-r)\Gamma(r)}\int_0^z\left[|R_{N.\underline{M}}^{(T)}|^2\right]^{r-1}\left[1-|R_{N.\underline{M}}^{(T)}|^2\right]^{L-r-1}d|R_{N.\underline{M}}^{(T)}|^2$$

A series expansion of the right hand side of the above equation leads to (Abramowitz and Stegun,1964,Pp.944)

$$\Pr\left[|R_{N.\underline{M}}^{(T)}|^2\leq z\right] = f(z) \qquad (5.5.16)$$

where

$$f(z) = 1-\ (1-z)^{L-1}\sum_{j=0}^{r-1}\begin{bmatrix}L-1\\ j\end{bmatrix}\left[\frac{z}{1-z}\right]^j$$

Therefore the 100α% point of the pdf of $|R_{N.\underline{M}}^{(T)}|^2$ at frequency λ under the hypothesis $|R_{N.\underline{M}}(\lambda)|^2=0$ is give by

$$z = f^{-1}(\alpha) \tag{5.5.17}$$

such that

$$\Pr\left[|R_{N.\underline{M}}^{(T)}(\lambda)|^2 \angle f^{-1}(\alpha)\right] = \alpha$$

An alternative way for testing this hypothesis follows from the relation of the Beta and the F distributions (e.g. Mood et al, 1963), which implies that the statistic

$$\frac{L-r}{r}\left[\frac{|R_{N.\underline{M}}^{(T)}(\lambda)|^2}{1 - |R_{N.\underline{M}}^{(T)}(\lambda)|^2}\right]$$

has the F-distribution with 2r and 2(L-r) degrees of freedom under the hypothesis $|R_{N.\underline{M}}(\lambda)|^2=0$. This implies that the hypothesis should be rejected at frequency λ if

$$|R_{N.\underline{M}}^{(T)}(\lambda)|^2 \geq \frac{rC_\alpha}{L + r(C_\alpha-1)} \tag{5.5.18}$$

where C_α is the 100α% point of an F-distribution with 2r and 2(L-r) degrees of freedom.

5.5.6 A TEST FOR EQUALITY OF TWO COHERENCES

In Chapter 4 we developed a procedure to test whether the coherences between two pairs of point processes are equal when both pairs are assumed to be independent of each other. This assumption seems appropriate when both pairs of processes are realized from two independent experiments.

In this section we develop a similar test but for a general situation where the processes may not be independent and so neither are the estimates of the coherences. In a physiological context, one may wish to investigate whether the Ia discharge is coupled with the '${}_1\gamma_s$' more strongly than with the '${}_2\gamma_s$' when both these input gammas are applied simultaneously.

In order to test the equality of such two coherences we first develop the variance-covariance structure between the estimates of the coherences in the following Theorem.

THEOREM 5.5.1

Let $\underline{N}(t) = \{N_1(t), N_2(t), \cdots, N_r(t)\}$ be an r-vector valued stationary and orderly point process satisfying a (strong) mixing condition. Further, suppose that $\underline{N}(t)$ is realised in (0, T]. The estimate of the coherence between two components a and b of $\underline{N}$ is given by

$$|R_{ab}^{(T)}(\lambda)|^2 = \frac{|f_{ab}^{(T)}(\lambda)|^2}{f_{aa}^{(T)}(\lambda)f_{bb}^{(T)}(\lambda)} \qquad \lambda \neq 0$$

$a,b = N_1, N_2, \cdots, N_r$

where the spectral estimates $f_{ab}^{(T)}(\cdot)$, $f_{aa}^{(T)}(\cdot)$ and $f_{bb}^{(T)}(\cdot)$ are based on the periodograms of disjoint segments of the entire record length (Chapter 4).

Then if $L \to \infty$ as $T \to \infty$ (where L is the number of disjoint segments of the whole record), the estimates $|R_{ab}^{(T)}(\lambda)|^2$

$(a,b=N_1,N_2,\ldots,N_r)$ are asymptotically jointly normal with

$$\operatorname{Lim}_{T\to\infty} E\{\ |R_{ab}^{(T)}(\lambda)|^2\ \} = |R_{ab}(\lambda)|^2 \qquad \lambda\neq 0$$

$$\operatorname{Lim}_{T\to\infty} L\ \operatorname{cov}\{\ |R_{ab}^{(T)}(\lambda)|^2\ ,\ |R_{cd}^{(T)}(\lambda)|^2\ \}$$

$$= R_{ab}R_{dc}R_{bd}R_{ca} + R_{ba}R_{dc}R_{ad}R_{cb}$$

$$+ R_{ab}R_{cd}R_{bc}R_{da} + R_{ba}R_{cd}R_{ac}R_{db}$$

$$- |R_{cd}|^2\left\{R_{ab}R_{bd}R_{da}+R_{ab}R_{bc}R_{ca}+R_{ba}R_{ad}R_{db}+R_{ba}R_{ac}R_{cb}\right\}$$

$$- |R_{ab}|^2\left\{R_{dc}R_{bd}R_{cb}+R_{dc}R_{ad}R_{ca}+R_{cd}R_{bc}R_{db}+R_{cd}R_{ac}R_{da}\right\}$$

$$+ |R_{ab}|^2|R_{cd}|^2\left\{|R_{bd}|^2+|R_{bc}|^2+|R_{ad}|^2+|R_{ac}|^2\right\} \qquad (5.5.19)$$

$$\operatorname{Lim}_{T\to\infty} L\ \operatorname{var}\{\ |R_{ab}^{(T)}(\lambda)|^2\ \} = 2|R_{ab}(\lambda)|^2\left[1 - |R_{ab}(\lambda)|^2\right]^2 \qquad (5.5.20)$$

for $a,b,c,d=N_1,N_2,\cdots,N_r$ and $\lambda\neq 0$.

Proof:-

The proof follows from Theorem I.6 of Appendix I utilizing expression (3.3.22) of Chapter 3.

The above variance-covariance structure also allows one to estimate the correlation between two coherences at frequency λ by using the standard expression

$$\hat{\operatorname{corr}}\{|R_{ab}^{(T)}|^2,|R_{cd}^{(T)}|^2\} = \frac{\hat{\operatorname{cov}}\{|R_{ab}^{(T)}|^2\ ,\ |R_{cd}^{(T)}|^2\}}{[\hat{\operatorname{var}}\{|R_{ab}^{(T)}|^2\}\hat{\operatorname{var}}\{|R_{cd}^{(T)}|^2\}]^{1/2}} \qquad (5.5.21)$$

where $\hat{\operatorname{corr}}$ denotes the estimate of the correlation coefficient, and

$\hat{cov}\{\cdots\}$ and $\hat{var}\{\cdot\}$ are the estimates of the covariance and variance and may be obtained by inserting the respective estimates of the coherencies in expressions (5.5.19) and (5.5.20), respectively.

From the above Theorem it implies that under the null hypothesis $|R_{ab}(\lambda)|^2=|R_{cd}(\lambda)|^2$ at frequency λ, the variate $|R_{ab}^{(T)}(\lambda)|^2-|R_{cd}^{(T)}(\lambda)|^2$ is asymptotically normal with mean zero and variance, suppressing the dependence on λ, given by

$$\mathrm{var}\{|R_{ab}^{(T)}|^2-|R_{cd}^{(T)}|^2\} = \mathrm{var}\{|R_{ab}^{(T)}|^2\} + \mathrm{var}\{|R_{cd}^{(T)}|^2\} - 2\mathrm{cov}\{|R_{ab}^{(T)}|^2, |R_{cd}^{(T)}|^2\} \qquad (5.5.22)$$

Therefore we reject the null hypothesis of equal coherences at frequency λ at the 5% level of significance if

$$\left| \frac{|R_{ab}^{(T)}(\lambda)|^2 - |R_{cd}^{(T)}(\lambda)|^2}{[\hat{\mathrm{var}}\{|R_{ab}^{(T)}(\lambda)|^2 - |R_{cd}^{(T)}(\lambda)|^2\}]^{1/2}} \right| \geq 1.96 \qquad (5.5.23)$$

5.5.7 APPLICATIONS

We now turn to the application of the above procedure and test whether each of the sensory endings, the Ia and II, is equally associated with the static gamma motoneurons, ${}_1\gamma_s$ and ${}_2\gamma_s$.

From Figs.5.4.1a,c of Section 5.4.6, it is clearly seen that under the condition that both gammas are activated, the strength of coupling between the Ia discharge and the ${}_1\gamma_s$ (Fig.5.4.1a) is greater than the strength of coupling between the Ia and the ${}_2\gamma_s$ (Fig.5.4.1c). Comparing Fig.5.4.b with Fig.5.4.1d we also see that in the presence of the length change 'ℓ' the Ia-${}_1\gamma_s$ coupling remains stronger than the Ia-${}_2\gamma_s$ coupling. The difference between the coherences of these two pairs of processes is big enough that one may not feel the necessity for any test of significance.

However, examining Figs.5.4.2a,c and Figs.5.4.2(b,d), we find that the couplings of the II discharge with each of the gammas in the absence (Figs.5.4.2a,c) and in the presence (Figs.5.4.2b,d) of the length change are quite close to each other. Therefore the application of a test for equality of two coherences becomes crucial in order to be able to make inference about the strength of connectivity of the II ending with each of the static gamma inputs.

Fig.5.5.1 and Fig.5.5.2 illustrate the application of the test for equality of two coherences developed in Section 5.5.6. Figs.5.5.1a,b correspond to the estimates of the coherences between the II discharge and $_1\gamma_s$, and between the II discharge and $_2\gamma_s$ under the condition that $_1\gamma_s$ and $_2\gamma_s$ are both activated simultaneously. Fig.5.5.1c gives an estimate of the correlation coefficient at a given frequency λ between the two estimates given in Figs.5.5.1a,b at that frequency, and is based on expression (5.5.21) with appropriate modification (i.e., setting b=d). This figure suggests very weak, if any, association between the two coherences at each frequency. Fig.5.5.1d illustrates the test of equality of the two coherences given in Figs.5.5.1a,b. Based on expression (5.5.23) with appropriate change (b=d), the estimate in this figure corresponds to the standardised difference (difference divided by its estimated standard error) of the two coherences. The solid lines above and below the dotted line are the 95% points of the null distribution at a given frequency λ. Values lying outside these two points signify the frequencies at which the two coherences may differ significantly. Clearly the II ending has a stronger coupling with $_1\gamma_s$ than with $_2\gamma_s$ over an approximate range of frequencies 5-14 Hz.

Fig5.5.2 represents the estimates of the same parameters between the same processes as in Fig.5.5.1 but in this case the length change is also imposed on the spindle. The test-plot (Fig.5.5.2d)

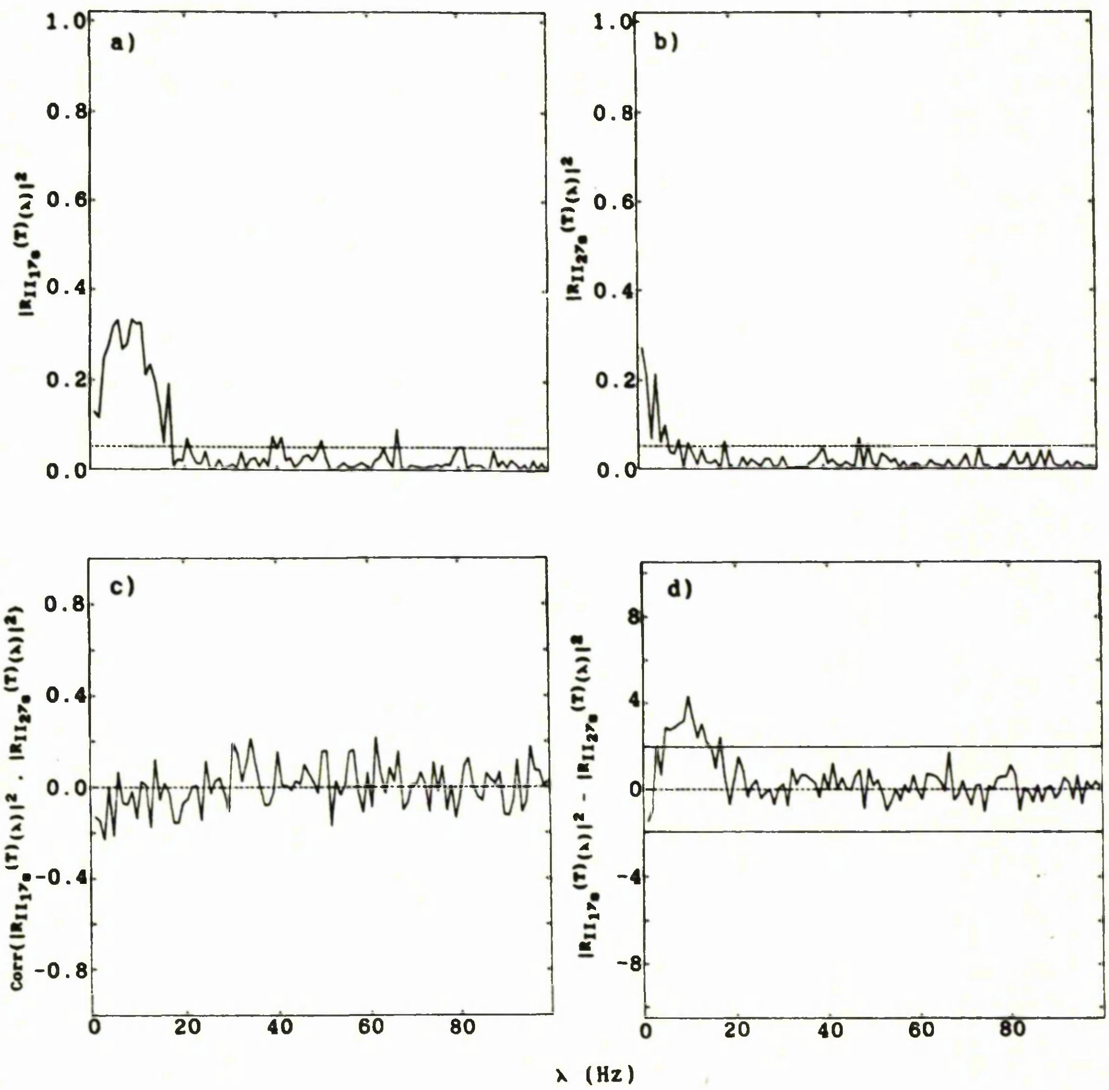

Fig.5.5.1 A test for the equality of two coherences

a,b) Estimated coherences of the II discharge with a static gamma input, $_1\gamma_s$, (a), and a second static gamma input, $_2\gamma_s$, (b) when both the static gamma inputs are applied to the spindle concurrently and independently

c) Estimated correlation coefficient at a given frequency between the estimates of two coherences illustrated in (a) and (b) at that frequency

d) Test-plot: The figure represents the standardised difference of the two estimates of the coherences given in (a) and (b)

The horizontal dotted lines in (a) and (b) are the upper limit of the 95% confidence interval (marginal) for the coherence under the hypothesis of zero coherence, whereas the solid lines below and above the dotted line in (d) represent the critical values for a two-sided test of the hypothesis of equal coherences at a given frequency at 5% level of significance.

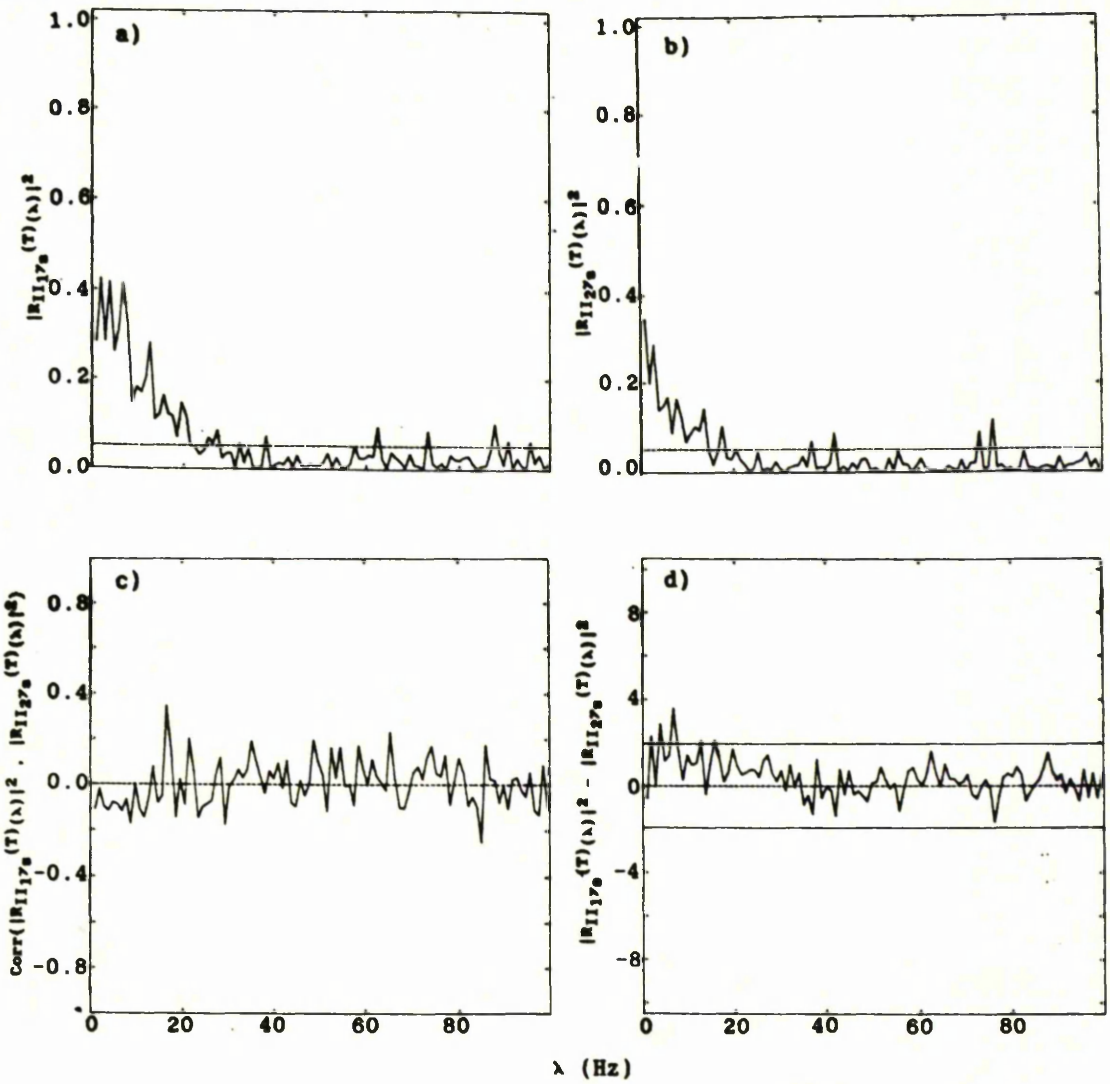

Fig.5.5.2 A test for the equality of two coherences

a,b) Estimated coherences of the II discharge with a static gamma input, ${}_1\gamma_s$, (a), and a second static gamma, ${}_2\gamma_s$, (b) when both the static gamma inputs are applied to the muscle spindle concurrently and independently in the presence of a length change *ℓ*

c) Estimated correlation coefficient at a given frequency between the estimates of two coherences illustrated in (a) and (b) at that frequency

d) Test-plot: The figure represents the standardised difference of the two estimates of the coherences given in (a) and (b)

The horizontal dotted lines in (a) and (b) are the upper limit of the 95% confidence interval (marginal)for the coherence under the hypothesis of zero coherence, whereas the solid lines below and above the dotted line in (d) represent the critical values for a two-sided test of the hypothesis of equal coherences at a given frequency at 5% level of significance.

reveals that the significant difference found in Fig.5.5.1d between the coherences given in Figs.5.5.1a,b is reduced to a narrower approximate range of frequencies 3-8 Hz. This suggests that the activation of the length change 'ℓ' brings the strength of coupling of the II ending with the ${}_1\gamma_s$ closer to that of the II with the ${}_2\gamma_s$.

We have been dealing, so far, with models having a single output. In reality, the muscle spindle (a point process system) receives a number of inputs and gives rise to at least two outputs, the Ia and II discharges. In order to analyse the more realistic picture of the spindle we need to develop a general multivariate model for a point process system with multiple-input and multiple-output. In the next section, developing such a model, we investigate the relationships between the inputs and the outputs in order to be able to identify the muscle spindle being acted upon by many inputs and giving rise to several outputs.

5.6 MULTIVARIATE POINT PROCESS SYSTEMS

Let $\underline{Z}(t)=\{\underline{M}(t),\underline{N}(t)\}$ be an (r+s) vector-valued stationary point process defined on the entire real line. Suppose also $\underline{Z}(t)$ satisfies the conditions of (strong) mixing and orderliness. The process $\underline{M}$ may be considered as an input to a linear time-invariant point process system corresponding to $\underline{N}(t)$, the output point process from the system.

Let the cumulant matrix of process $\underline{Z}$ be given by

$$Q_{\underline{ZZ}}(u) = \begin{bmatrix} Q_{\underline{MM}}(u) & Q_{\underline{MN}}(u) \\ Q_{\underline{NM}}(u) & Q_{\underline{NN}}(u) \end{bmatrix}$$

with entries $q_{k\ell}(u)$ satisfying the condition

$$\int |q_{k\ell}(u)|du < \infty \qquad k,\ell=M_1,\cdots,M_r,N_1,\cdots,N_s$$

The spectral density matrix of process $\underline{Z}$ may be written as

$$F_{\underline{ZZ}}(\lambda) = \begin{bmatrix} F_{\underline{MM}}(\lambda) & F_{\underline{MN}}(\lambda) \\ F_{\underline{NM}}(\lambda) & F_{\underline{NN}}(\lambda) \end{bmatrix}$$

where the entries $F_{\underline{MM}}(\lambda)$ and $F_{\underline{NN}}(\lambda)$ of $F_{\underline{ZZ}}(\lambda)$ are the rxr and sxs matrices of the spectral density functions of the processes $\underline{M}$ and $\underline{N}$, respectively, and $F_{\underline{NM}}(\lambda)$ is the sxr cross-spectral density matrix between $\underline{N}$ and $\underline{M}$. The matrix $F_{\underline{ZZ}}(\lambda)$ is defined as

$$F_{\underline{ZZ}}(\lambda) = \frac{1}{2\pi}\int \exp(-i\lambda u)\left[Q_{\underline{ZZ}}(u)+\delta(u)D_{\underline{Z}}\right]du$$

where $D_{\underline{Z}}$ is the (r+s)x(r+s) diagonal matrix of the mean intensities of the process $\underline{Z}$, and is given by

$$D_{\underline{Z}} = \begin{bmatrix} D_{\underline{M}} & 0 \\ 0 & D_{\underline{N}} \end{bmatrix}$$

The fact that the entries of $Q_{\underline{Z}\underline{Z}}(u)$ are real-valued implies that

$$\overline{F_{\underline{Z}\underline{Z}}(\lambda)} = F_{\underline{Z}\underline{Z}}(-\lambda) = F_{\underline{Z}\underline{Z}}{}^{T}(\lambda)$$

i.e., $F_{ZZ}(\lambda)$ is Hermitian

and so $F_{\underline{N}\underline{M}}(\lambda) = \overline{F_{\underline{M}\underline{N}}{}^{T}(\lambda)}$

ESTIMATION OF $F_{ZZ}(\lambda)$

Based on the disjoint sections of the entire record, T, (procedure 3 of Section 3.3.6), an estimate of $F_{ZZ}(\underline{\lambda})$ may be given by

$$F_{\underline{Z}\underline{Z}}{}^{(T)}(\lambda) = \begin{bmatrix} F_{\underline{M}\underline{M}}{}^{(T)}(\lambda) & F_{\underline{M}\underline{N}}{}^{(T)}(\lambda) \\ F_{\underline{N}\underline{M}}{}^{(T)}(\lambda) & F_{\underline{N}\underline{N}}{}^{(T)}(\lambda) \end{bmatrix} = \frac{1}{L} \sum_{j=0}^{L-1} I_{\underline{Z}\underline{Z}}{}^{(R)}(\lambda, j) \quad ; \ \lambda \neq 0 \qquad (5.6.1)$$

where

$$I_{\underline{Z}\underline{Z}}{}^{(R)}(\lambda, j) = (1/2\pi R)[d_{\underline{Z}}{}^{(R)}(\lambda, j)\overline{d_{\underline{Z}}{}^{(R)}(\lambda, j)^{T}}] \qquad (5.6.2)$$

and

$$d_{\underline{Z}}^{(R)}(\lambda,j) = \int_{t=jR}^{(j+1)R} \exp(-i\lambda t)d\underline{Z}(t) \qquad -\infty<\lambda<\infty \; ; \; j=0,1,\ldots,L-1$$

and R is such that T=LR.

The estimates $I_{\underline{Z}\underline{Z}}^{(R)}(\lambda,j)$; $j=0,1,\ldots,L-1$, $\lambda\neq 0$ are seen to be aysmptotically independent $W_{r+s}^{C}[1,F_{\underline{Z}\underline{Z}}(\lambda)]$ variates which follows from the fact that $d_{\underline{Z}}^{(R)}(\lambda,j) \sim N_{r+s}^{C}[\underline{0}\;,\;2\pi RF_{\underline{Z}\underline{Z}}(\lambda)]$, where W_2^C denotes the complex Wishart and N_2^C complex normal distributions.

From the above result it follows that as $T\to\infty$, but L remains fixed, the estimate given by expression (5.6.1) tends to $(1/L)W_{r+s}^{C}[L\;,\;F_{\underline{Z}\underline{Z}}(\lambda)]$, and is asymptotically normal if the limiting conditions are as $T\to\infty$, $L\to\infty$ but $(L/T)\to 0$ (Brillinger,1975a).

5.6.1 MULTIVARIATE POINT PROCESS LINEAR MODEL

Let $\underline{Z}(t)=\{\underline{M}(t),\ \underline{N}(t)\}$ be an (r+s) vector valued stationary point process which satisfies the conditions of (strong) mixing and orderliness. Corresponding to $\underline{M}(t)$, the input to a linear time invariant point process system, let $\underline{N}(t)$ be the output from the system. A graphical representation of this situation may be given by

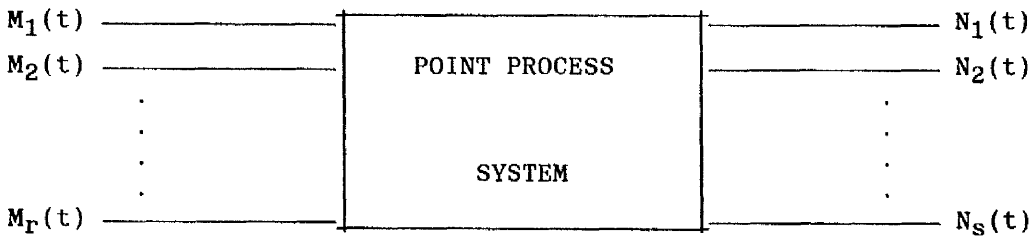

A general linear multivariate point process model relating $\underline{N}(t)$ to $\underline{M}(t)$ may be expressed by

$$E\{d\underline{N}(t)|\underline{M}\} = \left\{\alpha_{\underline{N}} + \int \alpha_{\underline{NM}}(t-u)d\underline{M}(u)\right\}dt \qquad (5.6.3)$$

where $\alpha_{\underline{N}}$ is an s vector-valued constant which gives the rate of $\underline{N}(t)$ in the case that $\underline{M}(t)$ is inactive. $\alpha_{\underline{NM}}(\cdot)=[\alpha_{jk}(\cdot)]$ $(j=N_1,N_2,\ldots,N_s\ ;\ k=M_1,M_2,\ldots,M_r)$ is an sxr matrix where $\alpha_{jk}(\cdot)$ be the response function corresponding to the jth component of $\underline{N}(t)$ and kth component of $\underline{M}(t)$. The above model says that the instantaneous intensity of the process $\underline{N}(t)$ at time t, given the location of all the points of the process $\underline{M}$, is a linear translation invariant function of the process $\underline{M}$. The locations of the points of $\underline{N}$ are affected by where the points of $\underline{M}$ are located.

The model (5.6.3) may be seen as a direct analogue of model in the case of multivariate time series and is given by Brillinger(1981). A model similar to (5.6.3) has been discussed by

Hawkes(1971) in the case of self-exciting and mutually exciting point processes. Systems with multiple-input and multiple-output, with and without feedback, have been considered in Schwalm(1971).

5.6.2 SOLUTION OF THE MODEL

We now turn to the solution of (5.6.3) for the vector-valued constant $\alpha_{\underline{N}}$ and the matrix-valued function $\alpha_{\underline{NM}}(\cdot)$.

Taking the expected value of (5.6.3) with respect to $\underline{M}$, we have

$$P_{\underline{N}} = \alpha_{\underline{N}} + \int \alpha_{\underline{NM}}(u)P_{\underline{M}}du \tag{5.6.4}$$

Now multiplying (5.6.3) by $d\underline{M}^T(t-u)$ ("T" denoting the transpose) and taking expected value with respect to $\underline{M}$, we obtain

$$P_{\underline{NM}}(u) = \alpha_{\underline{N}}P_{\underline{M}}^T + \int \alpha_{\underline{NM}}(t-v)\left[P_{\underline{MM}}(v-t+u)+\delta(v-t+u)D_{\underline{M}}\right]dv \tag{5.6.5}$$

where $\delta(\cdot)$ is the Dirac delta function.

Substituting the value of $\alpha_{\underline{N}}$ from (5.6.4) into (5.6.5) and simplifying, we get

$$P_{\underline{NM}}(u)-P_{\underline{N}}P_{\underline{M}}^T = \int \alpha_{\underline{NM}}(w)\delta(u-w)D_{\underline{M}}dw + \int \alpha_{\underline{NM}}(w)\left[P_{\underline{MM}}(u-w)-P_{\underline{M}}P_{\underline{M}}^T\right]dw$$

i.e.,
$$Q_{\underline{NM}}(u) = \alpha_{\underline{NM}}(u)D_{\underline{M}} + \int \alpha_{\underline{NM}}(w)Q_{\underline{MM}}(u-w)dw \tag{5.6.6}$$

From (5.6.6), it follows that in the case that the components of $\underline{M}$ are independent Poisson processes, $Q_{\underline{MM}}(\cdot)=0$ and so the response matrix $\alpha_{\underline{NM}}(\cdot)$ is simply identified by

$$\alpha_{\underline{NM}}(u) = Q_{\underline{NM}}(u)D_{\underline{M}}^{-1}$$

The solution of the equation (5.6.6) for $\alpha_{\underline{NM}}(\cdot)$, in general, requires some form of deconvolution, which may be avoided if we take the Fourier transform of this equation:

$$\frac{1}{2\pi}\int \exp(-i\lambda u)Q_{\underline{NM}}(u)du = \frac{1}{2\pi}\int \exp(-i\lambda u)\left[\alpha_{\underline{NM}}(w)D_{\underline{M}}+\int \alpha_{\underline{NM}}(w)Q_{\underline{MM}}(u-w)dw\right]du$$

i.e., $$F_{\underline{NM}}(\lambda) = A_{\underline{NM}}(\lambda)F_{\underline{MM}}(\lambda) \tag{5.6.7}$$

which implies that

$$A_{\underline{NM}}(\lambda) = F_{\underline{NM}}(\lambda)F_{\underline{MM}}^{-1}(\lambda) \tag{5.6.8}$$

where $A_{\underline{NM}}(\lambda)$ is the Fourier transform of $\alpha_{\underline{NM}}(u)$.

Let M_b' denote the set of all components of $\underline{M}$ omitting M_b.

For a=1,2,$\cdots$,s, the typical entry, $A_{N_aM_b}(\cdot)$, of $A_{\underline{NM}}(\cdot)$ is generally complex-valued and may be written, generalising Section 5.5.2, as .

$$A_{N_aM_b}(\lambda) = \frac{f_{N_aM_b.M_b'}(\lambda)}{f_{M_bM_b.M_b'}(\lambda)}$$

The amplitude (gain) and argument (phase) of this quantity may also be defined, respectively, as

$$G_{N_aM_b.M_b'}(\lambda) = |A_{N_aM_b}(\lambda)| = \left|\frac{f_{N_aM_b.M_b'}(\lambda)}{f_{M_bM_b.M_b'}(\lambda)}\right|$$

$$\Phi_{N_aM_b.M_b'}(\lambda) = \arg\{A_{N_aM_b}(\lambda)\} = \arg\{f_{N_aM_b.M_b'}(\lambda)\}$$

Both quantities are seen to be the partial gain and partial phase, respectively, between the point processes N_a and M_b with the linear effects of M_b' have been removed. Similar expressions in the case of ordinary multivariate time series are derived in Brillinger(1981).

5.6.3 MEAN SQUARED ERROR OF THE MODEL

With the same arguments as used for the mean squared error for the general linear point process model (Section 5.5.3), the computation of the M.S.E of model 5.6.1 may be achieved if we define the following process with stationary increments

$$d\underline{\epsilon}(t) = d\underline{N}(t) - \left[\alpha_{\underline{N}} + \int \alpha_{\underline{\underline{NM}}}(t-u)\,d\underline{M}(u)\right]dt$$

Clearly $E\{d\underline{\epsilon}(t)\} = 0$.

The cumulant density of $\underline{\epsilon}(\cdot)$ at two time instants t and t' is given by

$$Q_{\underline{\underline{\epsilon\epsilon}}}(t-t') = E[d\underline{\epsilon}(t)d\underline{\epsilon}^T(t')] - E[d\underline{\epsilon}(t)]E[d\underline{\epsilon}^T(t')]$$

$$= E\left[d\underline{N}(t) - \left\{\alpha_{\underline{N}} + \int \alpha_{\underline{\underline{NM}}}(t-u)\right\}dt\right]\left[d\underline{N}(t') - \left\{\alpha_{\underline{N}} + \int \alpha_{\underline{\underline{NM}}}(t'-v)\,d\underline{M}(v)\right\}dt'\right]^T$$

$$= \left[P_{\underline{\underline{NN}}}(t-t') + \delta(t-t')D_{\underline{N}}\right] - P_{\underline{N}}\alpha_{\underline{N}}^T - \alpha_{\underline{N}}P_{\underline{N}}^T + \alpha_{\underline{N}}\alpha_{\underline{N}}^T + \int \alpha_{\underline{N}}P_{\underline{M}}^T\alpha_{\underline{\underline{NM}}}^T(t'-v)\,dv$$

$$- \int P_{\underline{\underline{NM}}}(t-v)\alpha_{\underline{\underline{NM}}}^T(t'-v)\,dv - \int \alpha_{\underline{\underline{NM}}}(t-u)P_{\underline{M}}\alpha_{\underline{N}}^T\,du$$

$$+ \iint \alpha_{\underline{\underline{NM}}}(t-u)\left[P_{\underline{\underline{MM}}}(u-v) + \delta(u-v)D_{\underline{M}}\right]\alpha_{\underline{\underline{NM}}}^T(t'-v)\,du\,dv$$

where $[A]^T$ denotes the transpose of matrix A.

Substitution of the value of $\underline{\alpha_N}$ from expression (5.6.2) and some algebraic manipulation leads to

$$Q_{\underline{\underline{\epsilon\epsilon}}}(t-t')=\left[Q_{\underline{\underline{NN}}}(t-t')+\delta(t-t')D_{\underline{N}}\right]-\int Q_{\underline{\underline{NM}}}(t-v)\alpha_{\underline{\underline{NM}}}{}^{T}(t'-v)dv$$

$$-\int \alpha_{\underline{\underline{NM}}}(t-u)Q_{\underline{\underline{NM}}}(u-t')du$$

$$+\iint \alpha_{\underline{\underline{NM}}}(t-u)\left[Q_{\underline{\underline{MM}}}(u-v)+\delta(u-v)D_{\underline{M}}\right]\alpha_{\underline{\underline{NM}}}{}^{T}(t'-v)dudv$$

where $Q_{\underline{\underline{NM}}}(\cdot)=P_{\underline{\underline{NM}}}(\cdot)-P_{\underline{N}}P_{\underline{M}}{}^{T}$. With similar definition for $Q_{\underline{\underline{NN}}}(\cdot)$ and $Q_{\underline{\underline{MM}}}(\cdot)$. Now setting t-t'=u and making appropriate change of variable, we obtain

$$Q_{\underline{\underline{\epsilon\epsilon}}}(u)=\left[Q_{\underline{\underline{NN}}}(u)+\delta(u)P_{\underline{N}}\right]-\int Q_{\underline{\underline{NM}}}(u+v)\alpha_{\underline{\underline{NM}}}{}^{T}(v)dv-\int \alpha_{\underline{\underline{NM}}}(v)Q_{\underline{\underline{MN}}}(u-v)dv$$

$$+\iint \alpha_{\underline{\underline{NM}}}(w)\left[Q_{\underline{\underline{MM}}}(u+v-w)+\delta(u+v-w)D_{\underline{M}}\right]\alpha_{\underline{\underline{NM}}}{}^{T}(v)dwdv \qquad (5.6.9)$$

The Fourier transform of (5.6.9) leads to the frequency domain representation

$$F_{\underline{\underline{\epsilon\epsilon}}}(\lambda) = F_{\underline{\underline{NN}}}(\lambda)- F_{\underline{\underline{NM}}}(\lambda)\overline{A_{\underline{\underline{NM}}}(\lambda)} - A_{\underline{\underline{NM}}}(\lambda)F_{\underline{\underline{MN}}}(\lambda) + A_{\underline{\underline{NM}}}(\lambda)F_{\underline{\underline{MM}}}(\lambda)\overline{A_{\underline{\underline{NM}}}(\lambda)}$$

where $A_{\underline{\underline{NM}}}(\lambda)$ is given in (5.6.8). Now after substituting the value of $A_{\underline{\underline{NM}}}(\cdot)$, the above expression is seen to reduce to

$$F_{\underline{\underline{\epsilon\epsilon}}}(\lambda) = F_{\underline{\underline{NN}}}(\lambda) - F_{\underline{\underline{NM}}}(\lambda)F_{\underline{\underline{MM}}}(\lambda)^{-1}F_{\underline{\underline{MN}}}(\lambda) \qquad (5.6.10)$$

For s=1 this expression (5.6.10) reduces to (5.5.10).

The typical entry, $f_{\epsilon_a\epsilon_b}(\lambda)$, of the matrix $\mathbf{F}_{\underline{\epsilon\epsilon}}(\lambda)$ is the partial spectrum between processes N_a and N_b after removing the linear effects of the process $\underline{M}$. i.e.,

$$f_{\epsilon_a\epsilon_b}(\lambda) = f_{N_aN_b\cdot\underline{M}}(\lambda) \tag{5.6.11}$$

where a=b gives the partial auto-spectrum of N_a, and a≠b the partial cross-spectrum between N_a and N_b having removed the linear effects of $\underline{M}$. The partial coherence between N_a and N_b after removing the linear effects of process $\underline{M}$ may be written as

$$|R_{N_aN_b\cdot\underline{M}}(\lambda)|^2 = \frac{|f_{N_aN_b\cdot\underline{M}}(\lambda)|^2}{f_{N_aN_a\cdot\underline{M}}(\lambda)f_{N_bN_b\cdot\underline{M}}(\lambda)} \tag{5.6.12}$$

The partial phase of order-r measuring the phase difference between N_a and N_b after removing the linear effects of $\underline{M}$ may be defined as

$$\Phi_{N_aN_b\cdot\underline{M}}(\lambda) = \arg\{f_{N_aN_b\cdot\underline{M}}(\lambda)\} \tag{5.6.13}$$

whereas the partial gain of order r between N_a and N_b after removing the linear effects of process $\underline{M}$ is given as

$$G_{N_aN_b\cdot\underline{M}}(\lambda) = \left|\frac{f_{N_aN_b\cdot\underline{M}}(\lambda)}{f_{N_bN_b\cdot\underline{M}}(\lambda)}\right| \tag{5.6.14}$$

Expressions (5.6.11)-(5.6.14) may also be evaluated for partial parameters of order k≤r having removed the linear effects of k components of $\underline{M}$ by the appropriate changes to $\mathbf{F}_{\underline{NM}}(\lambda)$, $\mathbf{F}_{\underline{MM}}(\lambda)$ and $\mathbf{F}_{\underline{MN}}(\lambda)$ in expression (5.6.10). Once the basic auto- and cross-spectra have been computed all the partial spectra and related parameters may be found by simple algebraic combinations of these spectra.

The expression (5.6.10) may also be written as

$$F_{\underline{\epsilon\epsilon}}(\lambda) = F_{\underline{NN}}(\lambda)^{1/2}\left[I_s - F_{\underline{NN}}(\lambda)^{-1/2}F_{\underline{NM}}(\lambda)F_{\underline{MM}}(\lambda)^{-1}F_{\underline{MN}}(\lambda)F_{\underline{NN}}(\lambda)^{-1/2}\right]F_{\underline{NN}}(\lambda)^{1/2}$$

Thus we are led to measure the linear association of $\underline{N}(t)$ with $\underline{M}(t)$ by the s x s matrix

$$F_{\underline{NN}}(\lambda)^{-1/2}F_{\underline{NM}}(\lambda)F_{\underline{MM}}(\lambda)^{-1}F_{\underline{MN}}(\lambda)F_{\underline{NN}}(\lambda)^{-1/2} \qquad (5.6.15)$$

For s=1, this expression is seen to reduce to the multiple coherence of process N with process $\underline{M}$ given in expression (5.5.11).

Expression (5.6.15) may be called a measure of generalised coherence between two vector-valued processes $\underline{M}$ and $\underline{N}$. A plausible way of making use of this expression may be based on the same arguments as used for the multivariate correlation between two vector-valued random variables (see for example, Mardia et al, 1979), which leads to the quantity $F_{\underline{NN}}(\lambda)^{-1}F_{\underline{\epsilon\epsilon}}(\lambda)$ as a simple generalization of $1-|R_{N.\underline{M}}(\lambda)|^2$. We also note that $F_{\underline{\epsilon\epsilon}}(\lambda)$ ranges between zero, when the $\underline{N}(t)$ is perfectly predicted by $\underline{M}(t)$ based on model (5.16.1), and $F_{\underline{NN}}(\lambda)$ at the other extreme when no part of $\underline{N}(t)$ is explained by $\underline{M}(t)$. Now if we let

$$B(\lambda) = F_{\underline{NN}}(\lambda)^{-1}F_{\underline{\epsilon\epsilon}}(\lambda)$$

then $I-B(\lambda)$ varies between the identity matrix and the zero matrix. Any sensible measure of multivariate generalised coherence between $\underline{M}$ and $\underline{N}$ at frequency λ should range between 1 and zero, and this property is satisfied by two often-used coefficients

$$\mathrm{Tr}\{I-B(\lambda)\}/s$$

and $$\mathrm{Det}\{I-B(\lambda)\}$$

The application of these measures is left as a work of further research. For example, we must investigate the question of whether these measures will help in determining if a particular neurone is a member of a neuronal network, or if one neuronal network influences another.

5.6.4 ESTIMATION OF THE PARAMETERS RELATED TO THE MODEL

Estimates of the partial parameters defined in expressions (5.6.11)-(5.6.14) of Section 5.6.3 may be obtained by inserting the estimates of the respective parameters, i.e,

$$F_{\underline{\epsilon}\underline{\epsilon}}{}^{(T)}(\lambda) = F_{\underline{N}\underline{N}}{}^{(T)}(\lambda) - F_{\underline{N}\underline{M}}{}^{(T)}(\lambda)F_{\underline{M}\underline{M}}{}^{(T)}(\lambda)^{-1}F_{\underline{M}\underline{N}}{}^{(T)}(\lambda)$$

$$f_{\epsilon_a\epsilon_b}{}^{(T)}(\lambda) = F_{N_aN_b}{}^{(T)}(\lambda) - F_{N_a\underline{M}}{}^{(T)}(\lambda)F_{\underline{M}\underline{M}}{}^{(T)}(\lambda)^{-1}F_{\underline{M}N_b}{}^{(T)}(\lambda)$$

$$|R_{N_aN_b\cdot\underline{M}}{}^{(T)}(\lambda)|^2 = \frac{|f_{\epsilon_a\epsilon_b}{}^{(T)}(\lambda)|^2}{f_{\epsilon_a\epsilon_a}{}^{(T)}(\lambda)f_{\epsilon_b\epsilon_b}{}^{(T)}(\lambda)} = \frac{|f_{N_aN_b\cdot\underline{M}}{}^{(T)}(\lambda)|^2}{f_{N_aN_a\cdot\underline{M}}{}^{(T)}(\lambda)f_{N_bN_b\cdot\underline{M}}{}^{(T)}(\lambda)}$$

$$\Phi_{N_aN_b\cdot\underline{M}}{}^{(T)}(\lambda) = \arg\{f_{\epsilon_a\epsilon_b}{}^{(T)}(\lambda)\} = \arg\{f_{N_aN_b\cdot\underline{M}}{}^{(T)}(\lambda)\}$$

$$G_{N_aN_b\cdot\underline{M}}{}^{(T)}(\lambda) = \left|\frac{f_{\epsilon_a\epsilon_b}{}^{(T)}(\lambda)}{f_{\epsilon_b\epsilon_b}{}^{(T)}(\lambda)}\right| = \left|\frac{f_{N_aN_b\cdot\underline{M}}{}^{(T)}(\lambda)}{f_{N_bN_b\cdot\underline{M}}{}^{(T)}(\lambda)}\right|$$

for $a, b = 1, 2, \cdots, s$; $\underline{M} = \{M_1, M_2, \cdots, M_r\}$

5.6.5 PROPERTIES OF THE ESTIMATE OF THE PARTIAL COHERENCE OF ORDER-r

The density function of $|R_{N_aN_b\cdot\underline{M}}{}^{(T)}(\lambda)|^2$ is seen to be of the same form as that of the unconditioned coherence, and is given by expression (5.5.14) with replacement of $|R_{N.\underline{M}}(\lambda)|^2$, $|R_{N.\underline{M}}{}^{(T)}(\lambda)|^2$, L and r by $|R_{N_aN_b\cdot\underline{M}}(\lambda)|^2$, $|R_{N_aN_b\cdot\underline{M}}{}^{(T)}(\lambda)|^2$, L-r and 1, respectively. See, for example, Brillinger(1981) in the case of ordinary time series and Kendall and Stuart(1961, vol2) in the case of ordinary random variables.

5.6.6 A TEST FOR ZERO PARTIAL COHERENCE OF ORDER-r

A value of $|R_{N_aN_b.\underline{M}}(\lambda)|^2=0$ indicates that the apparent association between the processes N_a and N_b is entirely due to the presence of the common input $\underline{M}$. A test for zero partial coherence may easily be developed in the same way as that for the ordinary coherence. We note from the density function obtained above that under the hypothesis of zero partial coherence, the estimate $|R_{N_aN_b.\underline{M}}^{(T)}(\lambda)|^2$ has a Beta distribution with parameters 1 and L-r-1. Following both procedures described in section (4.4.3) for the test of zero coherence, we reject the hypothesis $|R_{N_aN_b.\underline{M}}(\lambda)|^2 = 0$ if

$$|R_{N_aN_b.\underline{M}}^{(T)}(\lambda)|^2 \geq z = 1-\left[1-\alpha\right]^{1/(L-r-1)} \tag{5.6.16}$$

such that

$$\Pr\{|R_{N_aN_b.\underline{M}}^{(T)}(\lambda)|^2 \leq z\} = \alpha$$

or, alternatively, we reject the hypothesis if

$$|R_{N_aN_b.\underline{M}}^{(T)}(\lambda)|^2 \geq \frac{C_\alpha}{L+C_\alpha-r-1}$$

where $C_\alpha = F_{2,2(L-r-1);\alpha}$ is the 100α% point of an F distribution with 2 and 2(L-r-1) degrees of freedom.

5.6.7 ASYMPTOTIC CONFIDENCE INTERVAL FOR THE PARTIAL COHERENCE OF ORDER-r

It follows from Theorem I.7 of Appendix I that the estimate $|R_{N_aN_b.\underline{M}}^{(T)}(\lambda)|^2$ is asymptotically unbiased estimate of $|R_{NaNb.M}(\lambda)|^2$ and distributed asymptotically normally with variance given by

$$\text{Lim}_{T\to\infty}\ \text{var}\{|R_{N_aN_b.\underline{M}}^{(T)}(\lambda)|^2\} = \frac{2}{L}\ |R_{N_aN_b.\underline{M}}(\lambda)|^2\left[1 - |R_{N_aN_b.\underline{M}}(\lambda)|^2\right]^2$$

Hence an approximate 95% confidence interval for the partial coherence $|R_{N_aN_b.\underline{M}}(\lambda)|^2$ at frequency λ may be obtained by using the expression (4.4.5) with replacement of $|R_{21}^{(T)}(\lambda)|^2$ by $|R_{N_aN_b.\underline{M}}^{(T)}(\lambda)|^2$.

An approximate 95% confidence interval for the partial coherence may also be obtained by applying the variance stabilizing transformation Tanh^{-1} (Kendall and Stuart, 1966). The transformed variate $\tanh^{-1}|R_{N_aN_b.\underline{M}}^{(T)}(\lambda)|$ is an asymptotically unbiased estimate of $\tanh^{-1}|R_{N_aN_b.\underline{M}}(\lambda)|$ and is asymptotically distributed normally with variance

$$\text{Lim}_{T\to\infty}\ \text{var}\{\ \tanh^{-1}|R_{N_aN_b.\underline{M}}^{(T)}(\lambda)|\ \} = 1/2L \qquad \lambda\neq 0$$

Hence an approximate 95% confidence interval for the partial coherence may be based on expression (4.4.8) with replacement of $|R_{21}^{(T)}(\lambda)|$ by $|R_{N_aN_b.\underline{M}}^{(T)}(\lambda)|$.

5.6.8 PROPERTIES OF THE ESTIMATES OF THE PARTIAL PHASE AND PARTIAL GAIN OF ORDER-r

From Brillinger(1972) and Brillinger(1981), it follows that the estimates $f_{\epsilon_a\epsilon_b}^{(T)}(\lambda)$, $\Phi_{N_aN_b.\underline{M}}^{(T)}(\lambda)$ and $G_{N_aN_b.\underline{M}}^{(T)}(\lambda)$, for $\lambda,\mu\neq 0$, $\lambda\neq\mu$, are asymptotically normal with

$$\text{Lim}_{T\to\infty}\ \text{cov}\{f_{\epsilon_a\epsilon_b}^{(T)}(\lambda), f_{\epsilon_c\epsilon_d}^{(T)}(\mu)\} = \frac{1}{L}\delta\left\{\lambda-\mu\right\}f_{\epsilon_a\epsilon_c}(\lambda)f_{\epsilon_b\epsilon_d}(-\lambda)$$

$$\text{Lim}_{T\to\infty}\ \text{cov}\{\Phi_{N_aN_b.\underline{M}}^{(T)}(\lambda), \Phi_{N_aN_b.\underline{M}}^{(T)}(\mu)\} = \frac{1}{2L}\delta\left\{\lambda-\mu\right\}\left[|R_{N_aN_b.\underline{M}}(\lambda)|^{-2} - 1\right]$$

$$= \text{Lim}_{T\to\infty}\ \text{cov}\{\ln G_{N_aN_b.\underline{M}}^{(T)}(\lambda), \ln G_{N_aN_b.\underline{M}}^{(T)}(\mu)\}$$

where $\delta\{\alpha\}=1$ if $\alpha=0$, and zero otherwise.

5.6.9 APPLICATIONS

In the first part of this section, the application of partial coherence of order 1 to the real data sets obtained on the muscle spindle is demonstrated. Part 2 presents the applications of partial phase of order 1 to simulated data followed by its application to the real data on the muscle spindle. In the last part of the section the extension of the partial coherence and partial phase to order 2 is demonstrated, first, by using simulated data and then by the spindle data when several inputs are under independent control.

5.6.9a APPLICATIONS OF PARTIAL COHERENCE OF ORDER-1

In the application of ordinary coherence (Section 4.7) we found that the spontaneous discharges of the Ia and the II sensory axons are independent of each other (Fig.4.7.2a). The activation of a stimulus to the spindle, however, imposes a coupling between these discharges. This is confirmed by the application of the partial coherence.

Figs. 5.6.1 and 5.6.2 illustrate the application of the partial coherence of order 1. Fig.5.6.1 corresponds to the situation where the spindle is acted upon by the static gamma '${}_1\gamma_s$' input alone, whereas Fig.5.6.2 corresponds to the one when the other gamma input '${}_2\gamma_s$' alone is activated.

Figs.5.6.1a-c clearly reveal a significant pairwise coupling between the Ia discharge and '${}_1\gamma_s$', between the II discharge and the ${}_1\gamma_s$, and between the Ia and the II discharges. Fig.5.6.1d corresponds to the estimated partial coherence between the Ia and II discharges after removing the linear effects of ${}_1\gamma_s$. The horizontal dotted line in this figure represents the 95% point of the null distribution of the estimate. The estimate clearly suggests that the apparent coupling beteween the discharges of the two sensory axons is a consequence of the common input ${}_1\gamma_s$.

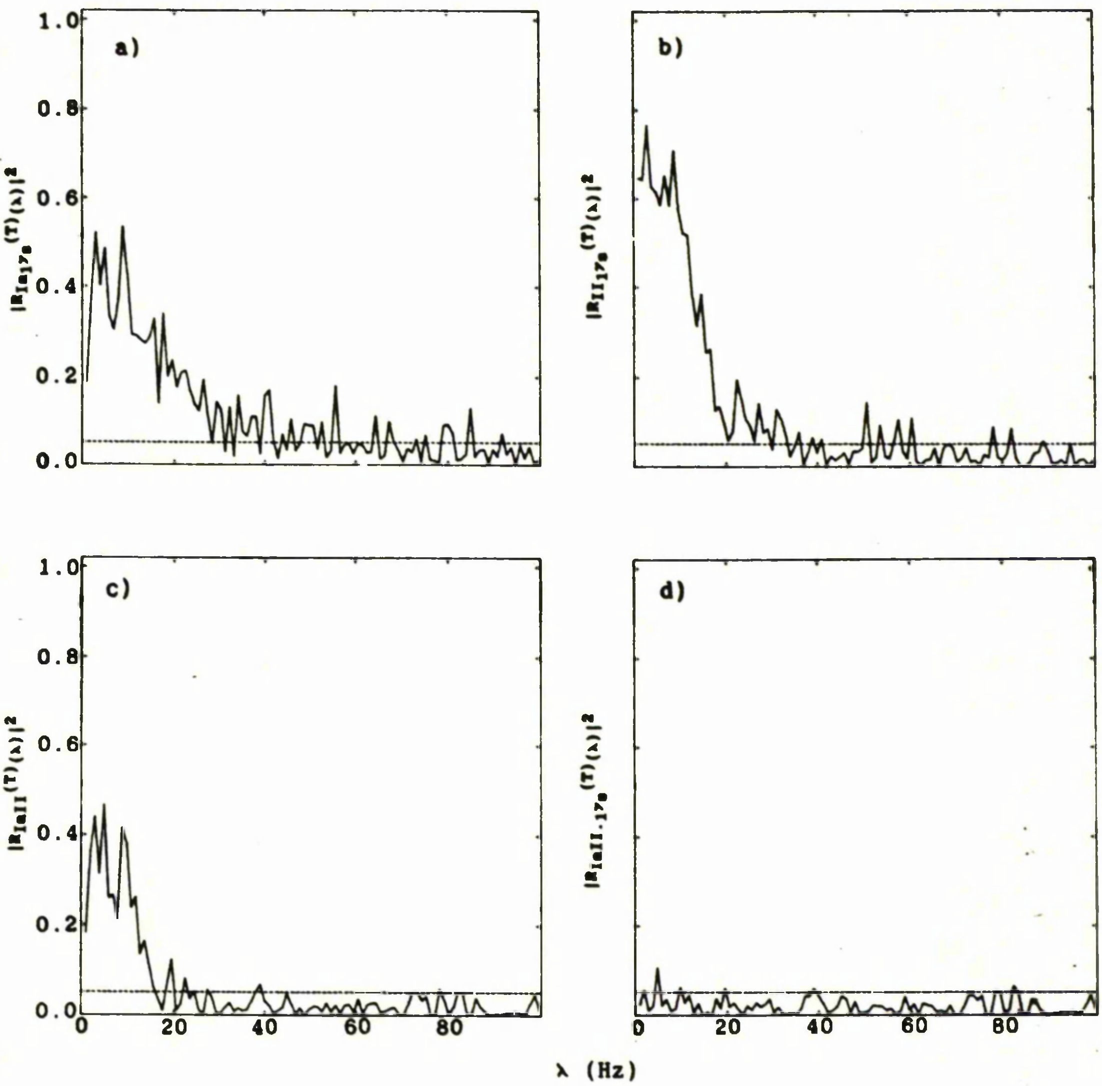

Fig.5.6.1 Illustration of the partial coherence of order-1

a) Estimated coherence (ordinary) between the Ia discharge and a static gamma input $_1\gamma_s$
b) Estimated coherence (ordinary) between the II discharge and a $_1\gamma_s$
c) Estimated coherece between Ia and II discharges in the presence of $_1\gamma_s$ alone
d) Estimated partial coherence between the Ia and II discharges after removing the linear effects of $_1\gamma_s$

The horizontal dotted line in each figure at a given frequency λ corresponds to the upper limit of the 95% confidence interval for the coherence at that frequency under the hypothesis of zero coherence.

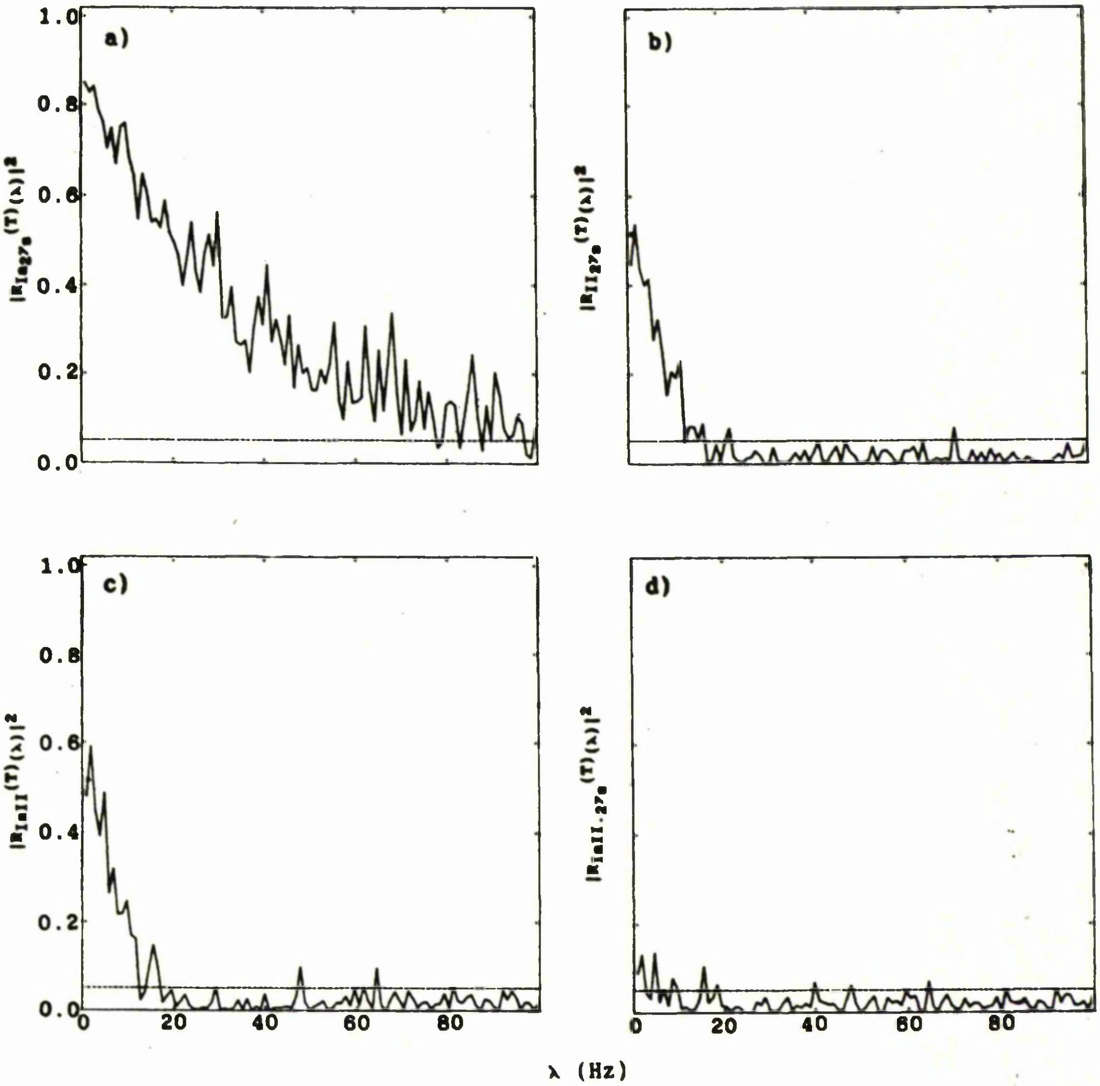

Fig.5.6.2 Illustration of the partial coherence of order-1

a) Estimated coherence (ordinary) between the Ia discharge and the second static gamma input, $_2\gamma_s$.
b) Estimated coherence (ordinary) between the II discharge and the $2\gamma s$
c) Estimated coherece between Ia and II discharges in the presence of $_2\gamma_s$ alone
d) Estimated partial coherence between the Ia and II discharges after removing the linear effects of $_2\gamma_s$

The horizontal dotted line in each figure at a given frequency λ corresponds to the upper limit of the 95% confidence interval for the coherence at that frequency under the hypothesis of zero coherence.

Figs.5.6.2a-d reveal features similar to those illustrated in Fig.5.6.1. The individual graphs (a-d) correspond to the estimates of

$|R_{Ia,2\gamma_s}(\lambda)|^2$, $|R_{II,2\gamma_s}(\lambda)|^2$, $|R_{Ia,II}(\lambda)|^2$ and $|R_{IaII\cdot 2\gamma_s}(\lambda)|^2$, respectively. Fig.5.6.2c clearly gives the evidence of a significant association between the Ia and II discharges over the range of frequencies (0-15) Hz. Fig.5.6.2d reveals that this association is a consequence of the common input $_2\gamma_s$. A few values in this estimate at low frequencies, however, show a non-zero partial coherence, and which may be attributed to either possible non-linear effects of $_2\gamma_s$ (Brillinger's letter, 3 May 1988) (this point will be discussed in more detail in Chapter 6) or to the presence of some other source of input (see part c of this section).

The above examples demonstrate how important and powerful tool the partial coherence is in investigating the connectivities between the processes.

In addition to affecting the strength of coupling between two processes, the common input may also alter the timing relations between these processes . This important information may be obtained from the partial phase which measures the phase angle between two processes after removing the linear effects of the common input. The application of partial phase of order 1 is presented in the following part of this section.

5.6.9b APPLICATION OF PARTIAL PHASE OF ORDER-1

In order to have a better understanding about how the partial phase works and how it may be interpreted, we generate a set of data in the following simulation and then apply the partial phase to this data set.

SIMULATION 1

Consider four independent Poisson processes $M_1(t)$, $M_2(t)$, $\epsilon_1(t)$ and $\epsilon_2(t)$. We construct two more processes $N_1(t)$ and $N_2(t)$ based on the superposition of the four using the following scheme.

$$N_1(t) = M_1(t) + M_2(t) + \epsilon_1(t)$$

$$N_2(t) = M_1^{d1}(t) + M_2^{d2}(t) + \epsilon_2(t)$$

where '+' denotes superposition (Cox and Lewis, 1972). $M_1^{d1}(\cdot)$ and $M_2^{d2}(\cdot)$ denote the delayed versions of processes $M_1(\cdot)$ and $M_2(\cdot)$, respectively, with d1 and d2 being the amounts of the delays. Let the times of occurrence of processes M_1, M_2, ϵ_1, ϵ_2 be, respectively, σ_{jk} $\{j=M_1,M_2,\epsilon_1,\epsilon_2$ and $k=1,2,\cdots,j(T)\}$.

Now considering M_1 and M_2 as the input processes to a linear time-invariant point process system with N_1 and N_2 the output processes we investigate the relationships between these processes. The discrete Fourier transforms of these four processes may be written as

$$d_{M_1}{}^{(T)}(\lambda) = \Sigma\exp(-i\lambda\sigma_{M_1k})$$

$$d_{M_2}{}^{(T)}(\lambda) = \Sigma\exp(-i\lambda\sigma_{M_2k})$$

$$d_{N_1}^{(T)}(\lambda) = \Sigma\exp(-i\lambda\sigma_{M_1k}) + \Sigma\exp(-i\lambda\sigma_{M_2k}) + \Sigma\exp(-i\lambda\sigma_{\epsilon_1k})$$

$$d_{N_2}^{(T)}(\lambda) = \Sigma\exp\{-i\lambda(\sigma_{M_1k}+d1)\} + \Sigma\exp\{-i\lambda(\sigma_{M_2k}+d2)\} + \Sigma\exp(-i\lambda\sigma_{\epsilon_2k})$$

Following the argument in Brillinger and Tukey(1984), we derive the following quantities

SPECTRA BETWEEN N_1 AND N_2

$$f_{N_2N_1}(\lambda) = \text{Lim}_{T\to\infty}\ E[d_{N_2}^{(T)}(\lambda)\overline{d_{N_1}^{(T)}(\lambda)}]$$

$$= \text{Lim}_{T\to\infty}\ E\{\Sigma\exp\{-i\lambda(\sigma_{M_1k}+d1)\}\Sigma\exp\{i\lambda\sigma_{M_1k}\}$$

$$+ \text{Lim}_{T\to\infty}\ E[\Sigma\exp\{-i\lambda(\sigma_{M_1k}+d1)\}][\Sigma\exp\{i\lambda\sigma_{M_2k}\}]$$

$$+ \text{Lim}_{T\to\infty}\ E[\Sigma\exp\{-i\lambda(\sigma_{M_1k}+d1)\}][\Sigma\exp\{i\lambda\sigma_{\epsilon_1k}\}]$$

$$+ \text{Lim}_{T\to\infty}\ E[\Sigma\exp\{-i\lambda(\sigma_{M_2k}+d2)\}][\Sigma\exp\{i\lambda\sigma_{M_1k}\}]$$

$$+ \text{Lim}_{T\to\infty}\ E[\Sigma\exp\{-i\lambda(\sigma_{M_2k}+d2)\}][\Sigma\exp\{i\lambda\sigma_{M_2k}\}]$$

$$+ \text{Lim}_{T\to\infty}\ E[\Sigma\exp\{-i\lambda(\sigma_{M_2k}+d2)\}][\Sigma\exp\{i\lambda\sigma_{\epsilon_2k}\}]$$

$$+ \text{Lim}_{T\to\infty}\ E[\Sigma\exp\{-i\lambda\sigma_{\epsilon_1k}\}][\Sigma\exp\{i\lambda\sigma_{M_1k}\}]$$

$$+ \text{Lim}_{T\to\infty}\ E[\Sigma\exp\{-i\lambda\sigma_{\epsilon_1k}\}][\Sigma\exp\{i\lambda\sigma_{M_2k}\}]$$

$$+ \text{Lim}_{T\to\infty}\ E[\Sigma\exp\{-i\lambda\sigma_{\epsilon_1k}\}][\Sigma\exp\{i\lambda\sigma_{\epsilon_2k}\}]$$

Since M_1, M_2, ϵ_1 and ϵ_2 are mutually independent, this implies that the pairwise cross-spectra between these processes are identically zero. Thus the above expression reduces to

$$f_{N_2N_1}(\lambda) = f_{M_1M_1}(\lambda)\exp(-i\lambda d1) + f_{M_2M_2}(\lambda)\exp(-i\lambda d2) \qquad (5.6.17)$$

Similarly it can also be shown that

$$f_{N_1N_1}(\lambda) = f_{M_1M_1}(\lambda) + f_{M_2M_2}(\lambda) + f_{\epsilon_1\epsilon_1}(\lambda)$$

$$f_{N_2N_2}(\lambda) = f_{M_1M_1}(\lambda) + f_{M_2M_2}(\lambda) + f_{\epsilon_2\epsilon_2}(\lambda)$$

and

$$\left.\begin{aligned} f_{N_2M_1}(\lambda) &= f_{M_1M_1}(\lambda)\exp(-i\lambda d1) \\ f_{N_2M_2}(\lambda) &= f_{M_2M_2}(\lambda)\exp(-i\lambda d2) \\ f_{N_1M_1}(\lambda) &= f_{M_1M_1}(\lambda) = f_{M_1N_1}(\lambda) \\ f_{N_1M_2}(\lambda) &= f_{M_2M_2}(\lambda) = f_{M_2N_1}(\lambda) \end{aligned}\right\} \qquad (5.6.18)$$

COHERENCE BETWEEN N_1 AND N_2

By definition

$$|R_{N_2N_1}(\lambda)|^2 = \frac{|f_{N_2N_1}(\lambda)|^2}{f_{N_1N_1}(\lambda)f_{N_2N_2}(\lambda)} \qquad (5.6.19)$$

substituting the values of the respective spectra from (5.6.17) and (5.6.18) and simplifying, we obtain, suppressing the dependence on λ

$$|R_{N_2N_1}|^2 = \frac{f_{M_1M_1}{}^2+f_{M_2M_2}{}^2+2f_{M_1M_1}f_{M_2M_2}\text{Cos}\lambda\{d1-d2\}}{\{f_{M_1M_1}+f_{M_2M_2}+f_{\epsilon_1\epsilon_1}\}\{f_{M_1M_1}+f_{M_2M_2}+f_{\epsilon_2\epsilon_2}\}} \tag{5.6.20}$$

Expression (5.6.20) shows that $|R_{N_2N_1}(\lambda)|^2$ should oscillate between 0 and 1 with a period of $2\pi/(d1-d2)$ if $d1 \neq d2$, and stable otherwise.

PHASE BETWEEN N_1 and N_2

By definition the phase between N_1 and N_2 is given by

$$\Phi_{N_2N_1}(\lambda) = \arg\{f_{N_2N_1}(\lambda)\}$$

$$= \tan^{-1}\left\{ \frac{\text{Im } f_{N_2N_1}(\lambda)}{\text{Re } f_{N_2N_1}(\lambda)} \right\}$$

Substituting the values of the real and imaginary parts of $f_{N_2N_1}(\lambda)$ from expression (5.6.17) and simplifying, we get

$$\Phi_{N_2N_1}(\lambda) = -\tan^{-1}\left\{ \frac{R(\lambda)\text{Sin}\lambda d1+\text{Sin}\lambda d2}{R(\lambda)\text{Cos}\lambda d1+\text{Cos}\lambda d2} \right\}$$

where

$$R(\lambda) = f_{M_1M_1}(\lambda)/f_{M_2M_2}(\lambda)$$

Now if the ratio $R(\lambda)=1$, i.e., both processes M_1 and M_2 are Poisson with the same mean rate then the phase simply becomes

$$\Phi_{N_2N_1}(\lambda) = -\left\{\frac{d1+d2}{2}\right\}\lambda \tag{5.6.21}$$

revealing that the Process N_2 is delayed by the process N_1 by an amount equal to the average of d1 and d2.

Similarly, with this condition the coherence between N_1 and N_2 (i.e., expression 5.6.20) reduces to

$$|R_{N_2N_1}(\lambda)|^2 = \frac{2P_{M_1}\{1 + \mathrm{Cos}\lambda(d1-d2)\}}{\{2P_{M_1}+P_{\epsilon_1}\}\{2P_{M_1}+P_{\epsilon_2}\}} \qquad (5.6.22)$$

where P_{M_1} is the mean intensity of process M_1.

PARTIAL CROSS SPECTRA

By definition

$$f_{N_2N_1.M_1}(\lambda) = f_{N_2N_1}(\lambda) - \frac{f_{N_2M_1}(\lambda)f_{M_1N_1}(\lambda)}{f_{M_1M_1}(\lambda)}$$

$$f_{N_2N_1.M_2}(\lambda) = f_{N_2N_1}(\lambda) - \frac{f_{N_2M_2}(\lambda)f_{M_2N_1}(\lambda)}{f_{M_2M_2}(\lambda)}$$

substitution of the values of the basic spectra into the above expressions from (5.6.17), (5.6.18) and some algebraic manipulation lead to

$$f_{N_2N_1.M_1}(\lambda) = f_{M_2M_2}(\lambda)\exp(-i\lambda d2) \qquad (5.6.23)$$
$$f_{N_2N_1.M_2}(\lambda) = f_{M_1M_1}(\lambda)\exp(-i\lambda d1) \qquad (5.6.24)$$

PARTIAL PHASES

From expression (5.6.20) and (5.6.21), it easily follows that

$$\Phi_{N_2N_1.M_1}(\lambda) = -\lambda d2$$

$$\Phi_{N_2N_1.M_2}(\lambda) = -\lambda d1$$

Fig.5.6.3 demonstrates the application of the partial phase of order 1 applied to the above simulated data with d1=-5, d2=-1, and M_1 and M_2 being Poisson with the same mean rate. Figs.5.6.3a,b are the estimated coherence and the phase between N_1 and N_2. The solid curve in the coherence plot corresponds to the derived coherence (expression 5.6.22), and is seen to be in a good agreement with the estimate. A weighted least squares line (through the origin) fitted to the phase curve (Fig.5.6.3b) is obtained by using the same procedure as developed in Section 4.6 of Chapter 4. The slope of this line gives a lead of process N_2 over Process N_1 with an approximate 95% confidence interval 2.98±0.14 msec.

Figs.5.6.3c,d represent the estimated partial coherence and partial phase between N_1 and N_2 having removed the linear effects of process N_1. The derived partial phase (solid line) can be seen to fit the estimate quite well. The estimated slope of the curve is found to be 1.01±0.02 msec. A comparison of this figure with Fig.5.6.3b suggests that the presence of the process M_1 increase the phase lead of N_2 over N_1. The partial phase between N_1 and N_2 after removing the linear effects of process M_2 (Fig.5.6.3f), however, reveals that the presence of M_2 decreases this lead. The estimated lead in this case is 4.99±0.24 msec.

The above example clearly shows that if the effects of the input processes are both additive and linear then the mathematical removal of an input process is equivalent to the physical removal of that process, and the partial parameters, in such situations, give a clear and simple interpretation.

With the help of the above simulation and interpretation, we now apply the partial phase of order 1 to the real data obtained from the muscle spindle and investigate some further characteristics of the Ia and II discharges in the presence of various stimuli.

Figs.5.6.4a,b are the estimates of the partial coherence

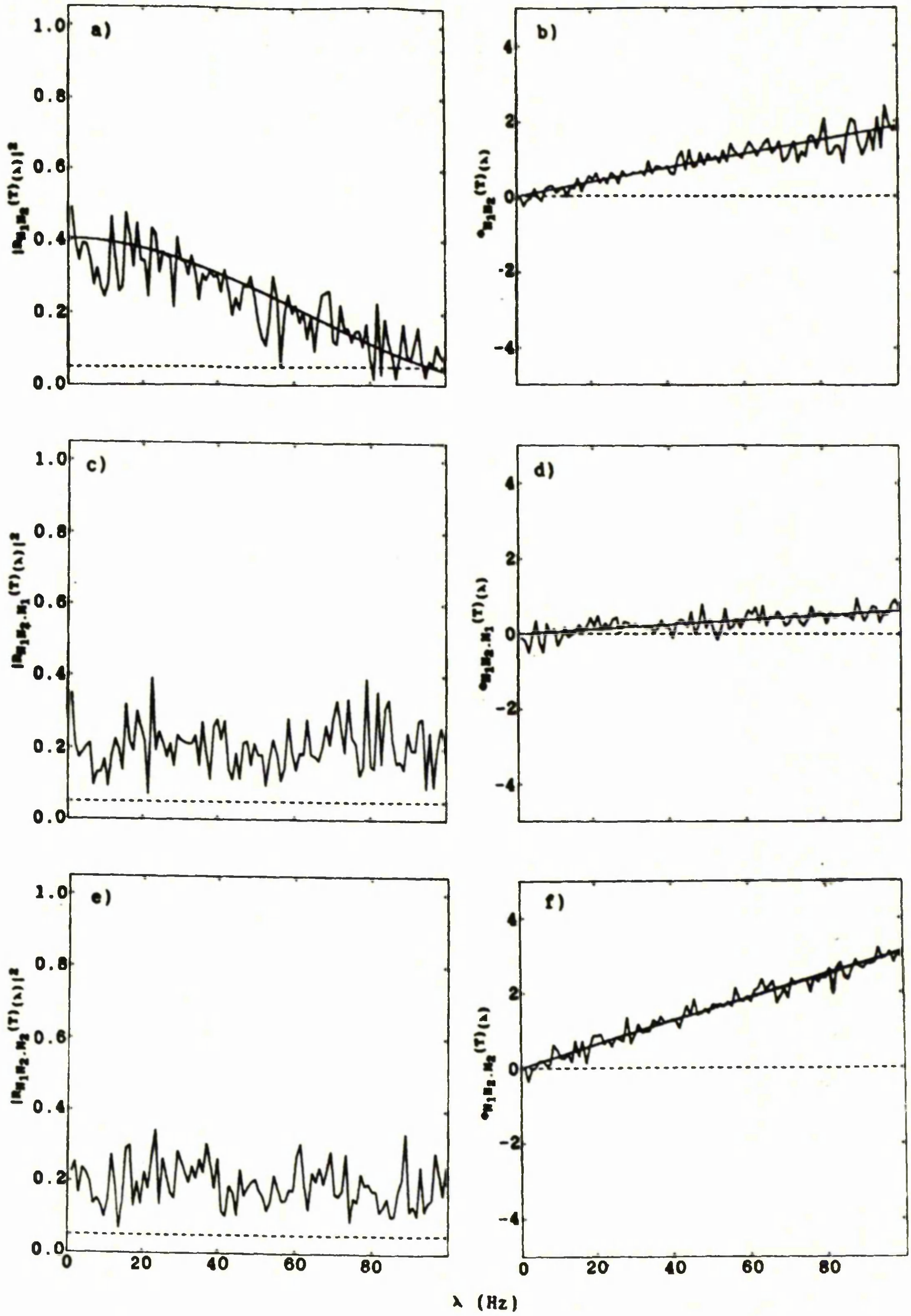

Fig.5.6.3 Illustration of partial phase of order-1 of simulated data

a,b) Estimated coherence (a) and phase (b) between processes N_1 and N_2

c,d,e,f) Estimated partial coherences (c,e) and partial phases (d,f) between N_1 and N_2 after removing the linear effects of M_1 (c,d) and M_2 (e,f)

The dotted lines in the coherence plots correspond to the upper limit of the 95% confidence interval (marginal) for the coherence under the hypothesis of zero coherence. The smooth curve in (a) represents the derived coherence between N_1 and N_2 whereas the solid lines in the phase plots (b,d,f) are the respective derived phase (slopes of which give the time delays) between N_1 and N_2.

and partial phase between the Ia and II discharges in the presence of both gamma static inputs $_1\gamma_s$ and $_2\gamma_s$, being applied independently. The weighted least squares line (dotted) fitted to the phase curve over the range of frequencies where the coherence (Fig.5.6.4a) is significantly different from zero gives a lead of the Ia over II discharge of 7.3±2.2 msec (same as Fig.4.7.4f). The partial phase between the Ia and II after removing the linear effects of $_2\gamma_s$ is presented in Fig.5.6.4d. The estimated slope of the least squares line (dotted) over the range of frequencies at which the corresponding partial coherence between the Ia and II (Fig.5.6.4c) is non-zero is equivalent to a lead of 3.9±2.2 msec. This lead is found not to be significantly different from the one obtained when $_1\gamma_s$ alone was present (Fig.4.7.4b). A close examination of the partial phase between the Ia and II discharges having removed the linear effects of $_1\gamma_s$ (Fig.5.6.4f) reveals that the phase curve is not linear over the entire range of frequencies at which the corresponding partial coherence (Fig.5.6.4e) is non-zero. This may be attributed to the fact that the variability of the estimate at a frequency depends on the coherence at that frequency and so the phase is not very well-defined at the frequencies where the coherence is not large enough (Bloomfield,1976), or it may be a possible indication of non-linear effects of $_1\gamma_s$ and $_2\gamma_s$. The phase curve, however, can be seen to be reasonably linear in the range 0-9 Hz. The slope of the weighted least squares line to the curve in this range gives a lead of the Ia over II discharge of 15.1±2.6 msec., which is not significantly different from the lead of the Ia over II in the presence of $_2\gamma_s$ alone (Fig.4.7.4d).

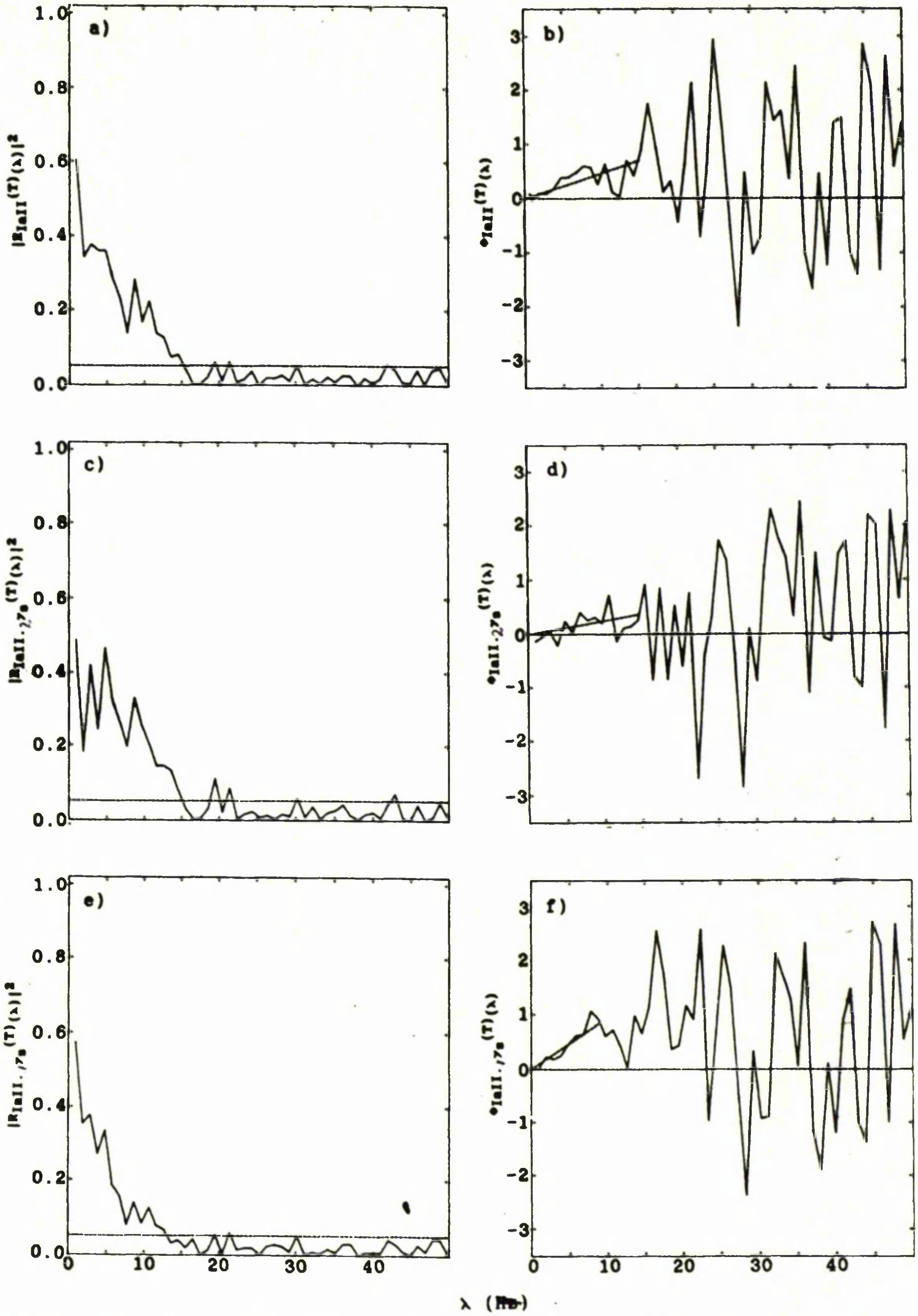

Fig.5.6.4 Illustration of partial phase of order-1 of the real data

a,b) Estimated coherence (a) and phase (b) between the Ia and II responses to the independent stimulation of both $_1\gamma_s$ and $_2\gamma_s$

c,d,e,f) Estimated partial coherences (c,e) and partial phases (d,f) between the Ia and II discharges after removing the linear effects of $_1\gamma_s$ (e,f) and $_2\gamma_s$ (c,d)

The dotted lines in the coherence plots correspond to the upper limit of the 95% confidence interval (marginal) for the coherence under the hypothesis of zero coherence. The smooth curve in (a) represents the derived coherence between N_1 and N_2 whereas the solid lines in the phase plots (b,d,f) are the respective derived phase (slopes of which give the time delays) between N_1 and N_2.

5.6.9c APPLICATIONS OF PARTIAL COHERENCE AND PARTIAL PHASE OF ORDER-2

The examples of this section describe further applications of partial coherence and partial phase of order 2, first to simulated data and then to real data on muscle spindles. The simulated data is constructed as follows

SIMULATION 2

Let $M_1(t)$, $M_2(t)$, $M_3(t)$, $\epsilon_1(t)$, $\epsilon_2(t)$ represent five independent Poisson processes with σ_{jk} the times of occurence of the k^{th} event of the j^{th} process for $j=M_1,M_2,M_3,\epsilon_1,\epsilon_2$ and $k=1,2,\cdots,j(T)$. These five processes are arranged according to the following scheme to form four observable processes M_1, M_2, N_1, N_2.

$$M_1(t) = M_1(t)$$

$$M_2(t) = M_2(t)$$

$$N_1(t) = M_1(t) + M_2(t) + M_3(t) + \epsilon_1(t)$$

$$N_2(t) = M_1^{d1}(t) + M_2^{d2}(t) + M_3^{d3}(t) + \epsilon_2(t)$$

where M_1^{d1}, M_2^{d2}, M_3^{d3} denote the delayed versions of M_1, M_2, M_3 with d1, d2, and d3 fixed time delays.

Considering N_1, N_2 as the outputs from a time-invariant point process system with M_1 and M_2 the inputs, we estimate the strength of association between N_1 and N_2 when contributions from M_1 and M_2 are taken into account first separately and then together.

By a similar procedure as used in Section 5.6.9b, the following quantities can easily be derived

$$f_{N_2N_1}(\lambda)=f_{M_1M_1}(\lambda)\exp\{-i\lambda d1\}+f_{M_2M_2}(\lambda)\exp\{-i\lambda d2\}+f_{M_3M_3}(\lambda)\exp\{-i\lambda d3\} \quad (5.6.25)$$

$$f_{N_1N_1}(\lambda)=f_{M_1M_1}(\lambda)+f_{M_2M_2}(\lambda)+f_{M_3M_3}(\lambda)+f_{\epsilon_1\epsilon_1}(\lambda) \quad (5.6.26)$$

$$f_{N_2N_2}(\lambda)=f_{M_1M_1}(\lambda)+f_{M_2M_2}(\lambda)+f_{M_3M_3}(\lambda)+f_{\epsilon_2\epsilon_2}(\lambda) \quad (5.6.27)$$

$$f_{N_2M_1}(\lambda)=f_{M_1M_1}(\lambda)\exp\{-i\lambda d1\} \quad (5.6.28)$$

$$f_{N_2M_2}(\lambda)=f_{M_2M_2}(\lambda)\exp\{-i\lambda d2\} \quad (5.6.29)$$

$$f_{N_1M_1}(\lambda)=f_{M_1M_1}(\lambda)=f_{M_1N_1}(\lambda) \quad (5.6.30)$$

$$f_{N_1M_2}(\lambda)=f_{M_2M_2}(\lambda)=f_{M_2N_1}(\lambda) \quad (5.6.31)$$

The partial spectra of order-1 follow by substitution of appropriate results of expressions (5.6.25)-(5.6.31) into the general expression of the partial spectrum of order-1 given as

$$f_{N_aN_b\cdot M_\ell}(\lambda)=f_{N_aN_b}(\lambda) - \frac{f_{N_aM_\ell}(\lambda)f_{M_\ell N_b}(\lambda)}{f_{M_\ell M_\ell}(\lambda)} \quad (5.6.32)$$

for $a,b,\ell=1,2$

Now as M_1 and M_2 are independent Poisson processes, the partial spectrum of order 2 based on expression (5.6.10) with r=2, and s=2 takes on a simple form

$$f_{N_aN_b\cdot M_1M_2}(\lambda)=f_{N_aN_b}(\lambda) - \frac{f_{N_aM_1}(\lambda)f_{M_1N_b}(\lambda)}{f_{M_1M_1}(\lambda)} - \frac{f_{N_aM_2}(\lambda)f_{M_2N_b}(\lambda)}{f_{M_2M_2}(\lambda)}$$

for a,b=1,2

The derived coherences and phases take particularly clear and easily interpretable forms if M_1 , M_2, and M_3 are chosen to be independent Poisson processes with the same mean rates, and if the delays d1, d2, and d3 are equally spaced, as well as small to avoid the spiraling effects (Brillinger and Tukey, 1984). This special case, in fact, occurs in a number of real data cases where delays predominate and the input processes are realizations of Poisson processes.

The derived coherence between N_1 and N_2, suppressing the dependence on λ, is given as

$$|R_{N_2N_1}|^2 = \frac{|f_{N_2N_1}|^2}{f_{N_1N_1}f_{N_2N_2}} \tag{5.6.33}$$

Where

$$|f_{N_2N_1}|^2 = f_{M_1M_1}{}^2 + f_{M_2M_2}{}^2 + f_{M_3M_3}{}^2 + 2f_{M_1M_1}f_{M_2M_2}\mathrm{Cos}\lambda\{d1-d2\}$$
$$+ 2f_{M_1M_1}f_{M_3M_3}\mathrm{Cos}\lambda\{d1-d3\} + 2f_{M_2M_2}f_{M_3M_3}\mathrm{Cos}\lambda\{d2-d3\}$$

and

$$f_{N_1N_1} = f_{M_1M_1} + f_{M_2M_2} + f_{M_3M_3} + f_{\epsilon_1\epsilon_1}$$

$$f_{N_2N_2} = f_{M_1M_1} + f_{M_2M_2} + f_{M_3M_3} + f_{\epsilon_2\epsilon_2}$$

Similarly the two derived partial coherences of order-1 are given as

$$|R_{N_2N_1.M_1}|^2 = \frac{f_{M_2M_2}{}^2+f_{M_3M_3}{}^2+2f_{M_2M_2}f_{M_3M_3}\mathrm{Cos}\lambda\{d2-d3\}}{[f_{M_2M_2}+f_{M_3M_3}+f_{\epsilon_1\epsilon_1}][f_{M_2M_2}+f_{M_3M_3}+f_{\epsilon_2\epsilon_2}]} \tag{5.6.34}$$

$$|R_{N_2N_1.M_2}|^2 = \frac{f_{M_1M_1}{}^2+f_{M_3M_3}{}^2 +2f_{M_1M_1}f_{M_3M_3}\mathrm{Cos}\lambda\{d1-d3\}}{[f_{M_1M_1}+f_{M_3M_3}+f_{\epsilon_1\epsilon_1}][f_{M_1M_1}+f_{M_3M_3}+f_{\epsilon_2\epsilon_2}]} \tag{5.6.35}$$

The phase between N_1 and N_2, in general, derived from $\arg\{f_{N_2N_1}(\lambda)\}$ is given by

$$\Phi_{N_2N_1}(\lambda) = -\tan^{-1}\left[\frac{f_{M_1M_1}\mathrm{Sin}\lambda d1+f_{M_2M_2}\mathrm{Sin}\lambda d2+f_{M_3M_3}\mathrm{Sin}\lambda d3}{f_{M_1M_1}\mathrm{Cos}\lambda d1+f_{M_2M_2}\mathrm{Cos}\lambda d2+f_{M_3M_3}\mathrm{Cos}\lambda d3}\right] \qquad (5.6.36)$$

If, however, M_1, M_2 ,and M_3 are Poisson processes with the same mean rate and the d1 ,d2 , d3 are equally spaced, then the above expression reduces to

$$\Phi_{N_2N_1}(\lambda) = -\left[\frac{d1+d2+d3}{3}\right]\lambda \qquad (5.6.37)$$

and the derived partial phases are

$$\Phi_{N_2N_1.M_1}(\lambda) = -\left[\frac{d1+d2}{2}\right]\lambda \qquad (5.6.38)$$

$$\Phi_{N_2N_1.M_2}(\lambda) = -\left[\frac{d1+d3}{2}\right]\lambda \qquad (5.6.39)$$

$$\Phi_{N_2N_1.M_1M_2}(\lambda) = -(d3)\lambda \qquad (5.6.40)$$

Simulating the above data with d1=-6,d2=-2, d3=+2 msec, the derived and estimated (ordinary and partial) coherences and phases between N_1 and N_2 are shown plotted on the same graph in Fig5.6.5, and clearly illustrate the close agreement between derived and estimated values for the respective parameters. In the presence of both processes M_1 and M_2 the coherence between N_1 and N_2 (Fig.5.6.5a) remains significant to about 65 Hz , while the estimated slope of the linear phase curve (Fig.5.6.5b) indicates a system dominated by a delay of 1.92±0.26 msec, with N_2 leading N_1. The partial coherence and partial phase between N_1 and N_2 allowing for process M_1, illustrated

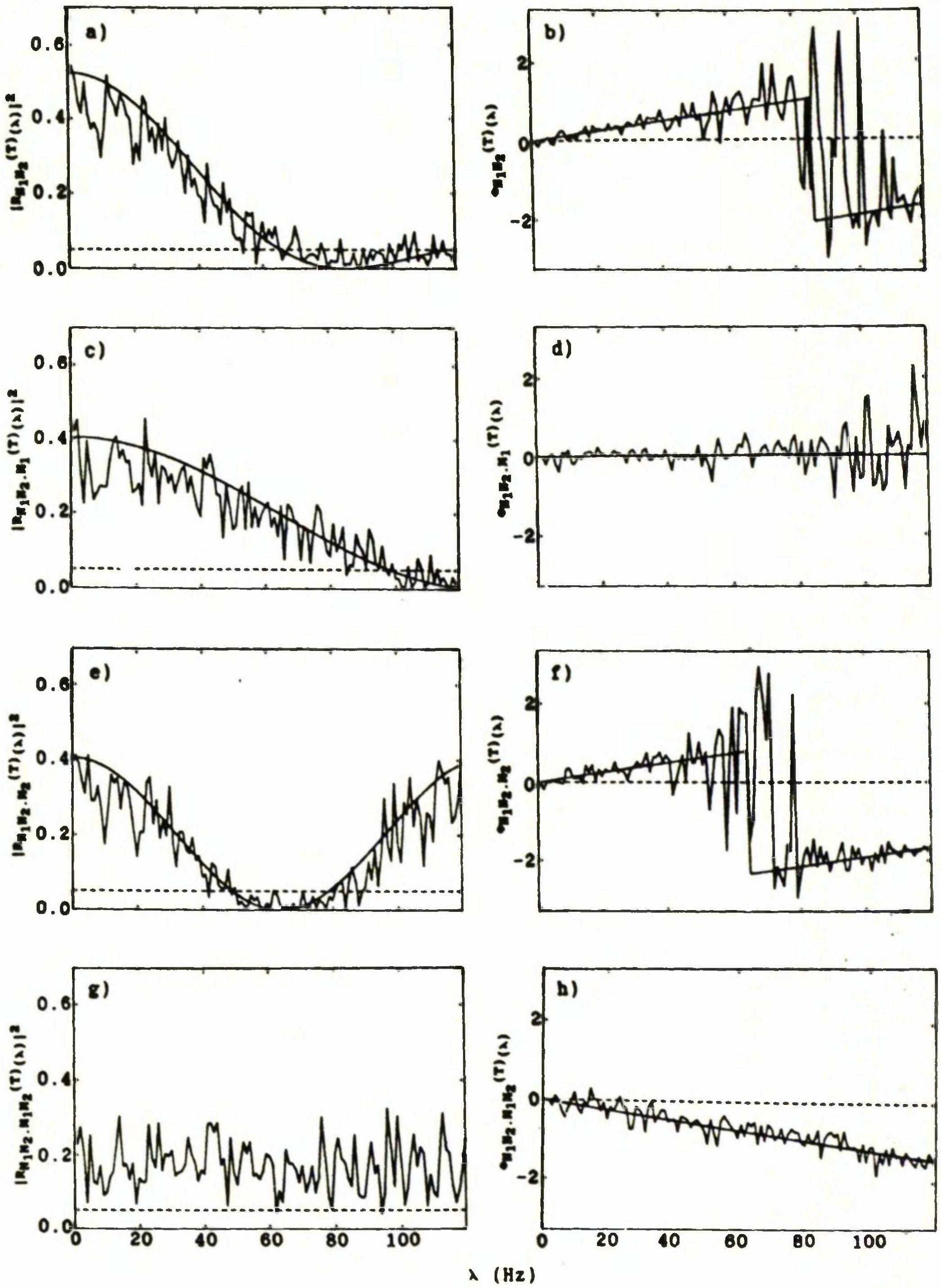

Fig.5.6.5 Illustration of partial phase of order 2 of simulated data

a,b) Estimated coherence (a) and phase (b) between processes N_1 and N_2

c,d,e,f) Estimated partial coherences (c,e) and partial phases (d,f) between N_1 and N_2 after removing the linear effects of M_1 (c,d) and M_2 (e,f)

g,h) Estimated partial coherence (g) and partial phase (h) between N_1 and N_2 after removing the linear effects of M_1 and M_2

The dotted lines in the coherence plots are the upper limit of the 95% confidence interval (marginal) for the coherence under the hypothesis of zero coherence whereas the solid smooth curves correspond to the derived coherences. The solid lines in the phase plots are the derived phase, the slopes of which represent the time delay between N_1 and N_2.

in Figs.5.6.5c,d , suggest that process M_2 alone synchronizes the processes N_1 and N_2. Accounting for the linear contribution of process M_2 to the relationship between N_1 and N_2 produces quite different consequences. The partial phase (Fig.5.6.5d) remains the same as the original phase (Fig.5.6.5b), whereas the partial coherence (Fig.5.6.5.e) becomes strikingly periodic. These results suggest that in the presence of both inputs, M_1 and M_2, process M_2 has a predominant effect on the coherence between N_1 and N_2, whereas process M_1 primarily affects the timing relation between N_1 and N_2.

The second-order partial coherence and partial phase between N_1 and N_2 are, respectively, given in Figs.5.6.5g,h. The partial coherence is small but significant over the entire range of frequencies, whereas the partial phase illustrates that the process N_2 is delayed by process N_1 with an estimated delay of 1.96±0.06 msec. These two measures taken together suggest the presence of another source of coupling between N_1 and N_2. This situation is most likely to occur when recording several processes simultaneously within the central nervous system.

Fig.5.6.6 is an illustration of the application of partial coherence of order-2 between the Ia and II discharges recorded from the same muscle spindle in the presence of independent static gamma inputs ${}_1\gamma_s$, ${}_2\gamma_s$, and an imposed dynamic length change ℓ. In the presence of all the three inputs, the coherence between the Ia and II discharges shown in Fig.5.6.6a (same as Fig.4.7.2f) reveals two distinct regions, (0-17) Hz and (30-60) Hz, of association. The partial coherence of order-2 after removing the linear effects of both static gamma axons (Fig.5.6.6b) shows a significant reduction of coherence in the low frequency range alone. This suggests that the coupling in the higher range is entirely a consequence of the presence of the length change. The coupling in the lower range, however, is not

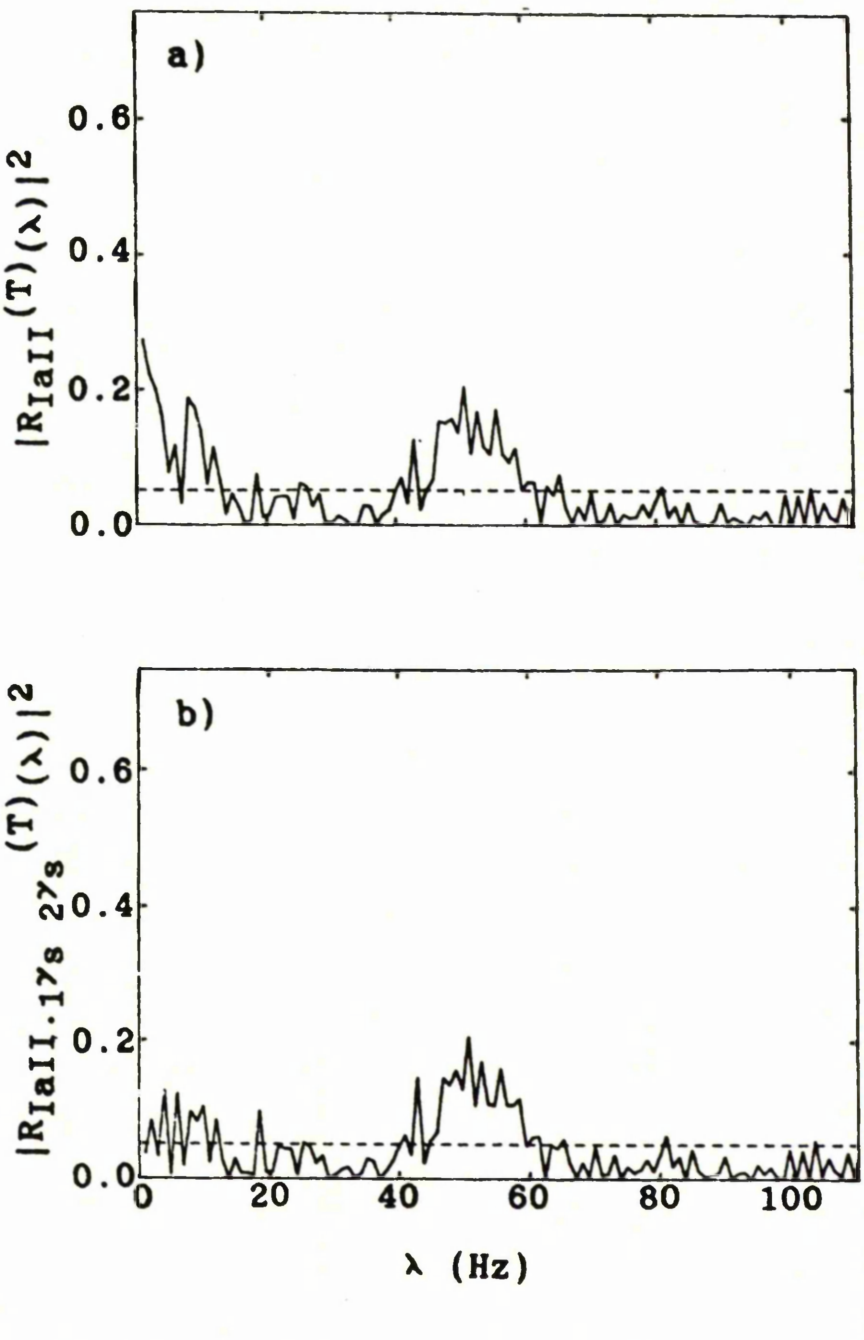

Fig.5.6.6 Illustration of partial coherence of order 2 of real data

a) Estimate of the coherence between the Ia and II discharges in the presence of two gamma inputs, $_1\gamma_s$ and $_2\gamma_s$, applied concurrently and independently, and a random length change ℓ

b) Estimate of the partial coherence between the Ia and II discharges after removing the linear effects of both gamma inputs

The dotted line in each figure corresponds to the upper limit of the 95% confidence interval (marginal) for the respective coherence under the hypothesis of zero coherence.

entirely accounted for by the linear contribution of the fusimotor inputs and, in addition, the length change, in the presence of gamma activity, may possibly contribute to the low frequency coupling. This may be examined by taking into account the contribution of the length input to the coherence at low frequencies.

5.7 SUMMARY AND CONCLUSIONS

In this chapter we have provided an extensive development and description of the wide range of applicability of a Fourier approach to measures of association and timing relation in the identification of point process systems and related problems.

The main features of the procedures are summarised in the following

1. The partial parameters, in the analysis of multivariate point processes, play an important role in assessing the association between the processes. In physiological context, they provide with a powerful tool in investigating the connectivities between any two cells that are subjected to be influenced directly or indirectly by a large number of other cells. Introducing the same idea, we defined and derived certain frequency domain partial parameters of order-1 followed by their extension to order-r. Estimation procedures of these parameters were considered.
2. A two-input single-output linear model was developed, and the identification of the muscle spindle, when it was acted upon by two point processes, ${}_1\gamma_S$ and ${}_2\gamma_S$, was carried out by using this model. The multiple coherence was discussed and applied to the data sets, which provided a useful measure of linear predictability of the output discharges from the two inputs, and led to the conclusion that both the static gamma inputs jointly increase the linear predictability of the Ia and II discharges.
3. In order to identify the spindle in more realistic situation, we extended the linear model to a general one in order to include "r" inputs. Estimates of the parameters related to the model were considered, and the properties of these estimates were examined. A test for the equality of two coherences under

the condition that the two pairs of processes are not independent was developed and demonstrated by illustrating the difference between the II-${}_1\gamma_s$ coupling and the II-${}_2\gamma_s$ coupling in the presence and absence of the length change, and it was found that the II-${}_1\gamma_s$ coupling is stronger than the coupling between the II discharge and ${}_2\gamma_s$. The presence of the length change was, however, seen to reduce the difference between the two couplings.

4. In the final part of this chapter we developed a regression type multivariate point process linear model. The main aim of this model was to study the association and timing relation between the outputs, and to investigate how these relations were altered by the presence of various stimuli. The partial phase provided a useful technique to assess the effect of one or many inputs on the timing relation between two outputs. This model also led to a generalised measure of association between vector-valued point processes, and which may prove a useful tool in finding relations between neuronal networks.
5. The applications of the procedures discussed were illustrated by a large number of examples on the simulated data followed by the real data obtained on the muscle spindle. In both cases the procedures seemed to work effectively.
6. From the concept of partial parameters, it does not necessarily mean that the mathematical removal is equivalent to the physical removal. Since the partial parameters are based on the removal of only linear time-invariant effects, the presence of non-linearities may cause problems in interpreting the results. So it becomes desirable to search for any possible non-linear features of the underlying processes.

CHAPTER 6

IDENTIFICATION OF NON-LINEAR POINT PROCESS SYSTEMS

6.1 INTRODUCTION

In the previous chapters we considered linear point process systems and their identification. Many biological systems are inherently non-linear even under "small-signal" conditions (Marmarelis and Ken-Ichi Naka, 1974). Figs.5.6.2, 5.6.4, and 5.6.6 of Chapter 5 also revealed some indication of possible non-linear interactive effects of the static gamma inputs on to the Ia and II discharges. It now, naturally, becomes desirable to extend the linear model to include higher order terms in order to be able to investigate the non-linear characteristics of the system.

The idea of characterizing a non-linear system from its response to a white noise stimulus is originally due to Wiener(1958), and has been refined and reformulated by many others, for example, Katzenelson and Gould (1962). Recent developments in the case of point processes can be seen in Brillinger(1975c) and Rigas(1983). In addition, Brillinger(1988) developed a new approach based on maximum likelihood estimation for the identification of non-linear systems with application to neuronal spike trains.

In this chapter certain higher order parameters, which provide useful information regarding the identification of a non-linear point process system, in both the time and frequency domains are defined. Plausible estimates and their properties are discussed. Asymptotic confidence intervals for the parameters of interest are constructed and illustrated by applying to both simulated and real data. In the final part of this Chapter we extend the linear model, presented in chapter 4, to a quadratic model and discuss the presence of any non-linearities in the muscle spindles.

6.2 HIGHER ORDER PARAMETERS IN THE TIME DOMAIN

Second-order time and frequency domain models can easily be extended to include higher order parameters for point processes allowing the assessment of the non-linear interactive effects between the increments within the processes, and between the processes.

Let $\underline{N}(t) = \{N_1(t), N_2(t), \cdots, N_r(t)\}$, $t \in R$, be an r vector-valued stationary point process with differential increments $\{dN_1(t), dN_2(t), \cdots, dN_r(t)\}$ and satisfying the conditions of orderliness and (strong) mixing. We define the third order product density, conditional density, and cumulant density functions as follows

6.2.1 THE THIRD ORDER PRODUCT DENSITY FUNCTION

The third order product density between processes N_a, N_b, and N_c at two lags u and v (Fig.6.2.1) is defined by

$$P_{abc}(u,v) = \text{Lim}_{\,h_1,\,h_2,\,h_3 \to 0} \Pr\{N_a \text{ event in } (t+u, t+u+h_1], \\ N_b \text{ event in } (t+v, t+v+h_2] \text{ and } N_c \text{ event in } (t, t+h_3]\}/h_1 h_2 h_3$$

for a, b, c = 1, 2, $\cdots$, r ; u, v, 0 distinct.

This parameter provides a measure of the probability of the simultaneous occurrence of N_a, N_b, and N_c separated by u and v time units. This situation is described graphically in Fig.6.2.1.

Now as the processes are assumed to be orderly, we have

$$P_{abc}(u,v)\,du\,dv\,dt = E\{dN_a(t+u)\,dN_b(t+v)\,dN_c(t)\}$$

Under (strong) mixing condition, this parameter satisfies the following limiting conditions

$$\text{Lim}_{\,u \to \infty} P_{abc}(u,v) = P_a P_{bc}(v)$$

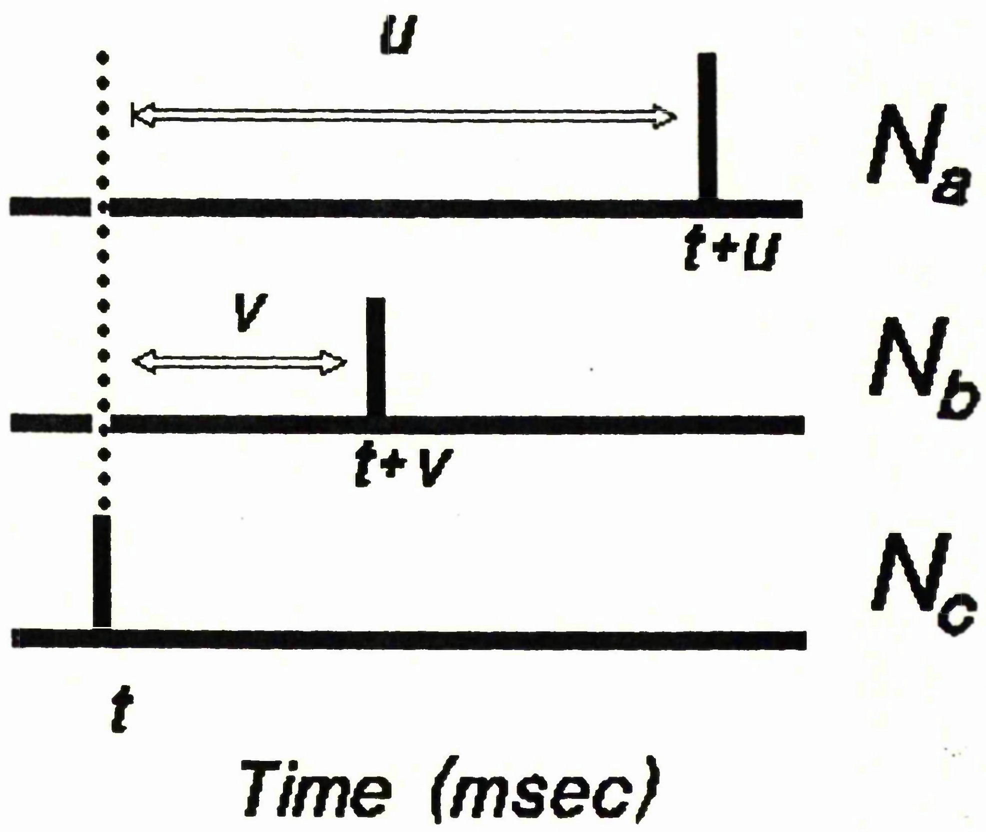

Fig.6.2.1

Diagrammatic representation of the convention used to represent the relative times of occurence of spikes from three processes N_a, N_b, and N_c.

$$\lim_{v\to\infty} P_{abc}(u,v) = P_{ab}(u)P_c$$

$$\lim_{u,v\to\infty} P_{abc}(u,v) = P_aP_bP_c \qquad (6.2.1)$$

where $P_{ab}(\cdot)$ is the second order product density between N_a and N_b, and P_c is the mean intensity of process N_c.

In the case a=b=c, the third order product density gives a measure of probability of simultaneous occurrence of three events of process N_a separated by time units u and v, with a similar interpretation for the case b=c, distinct from a or for any combination of N_a, N_b, and N_c.

6.2.2 THE THIRD ORDER CONDITIONAL DENSITY FUNCTION

By analogy with the second order cross intensity the third order conditional density between three processes N_a, N_b, and N_c may also be defined as

$$m_{abc}(u,v) = \lim_{h\to 0} \Pr\{N_a \text{ event in } (t,t+h] | N_b \text{ event at } t-v \text{ and } N_c \text{ event at } t-u\}/h \qquad (6.2.2)$$

The definition of the conditional density between three processes may be extended in a variety of ways depending on the process conditioned and the conditioning processes. For example, one may set up a definition with the following interpretation

$$\lim_{h_1,h_2\to 0} \Pr\{N_a \text{ event in } (t,t+h_1] \text{ and } N_b \text{ event in } (t-v,t-v+h_2] | N_c \text{ event at } t-u\}/h_1h_2$$

Under the condition of orderliness, expression (6.2.2) may be written as

$$m_{abc}(u,v)dt = E\{dN_a(t)\,|\,dN_b(t-v)=1, dN_c(t-u)=1\}$$

The strong mixing condition further allows the limiting relation

$$\text{Lim}_{\ v\to\infty}\ m_{abc}(u,v) = m_{ac}(u)$$

From the definition of conditional probability, $m_{abc}(u,v)$ is seen to be related to $P_{abc}(u,v)$ as

$$m_{abc}(u,v) = \frac{P_{abc}(u,u-v)}{P_{bc}(u-v)} \qquad (6.2.3)$$

In the case a=b=c, the third order conditional density, which may be called the third order auto-intensity, measures the probability of occurence of an N_a event given that two events of the same process have occured u and v time units before that event. A similar definition for the case b=c, distinct from c, or for any other combination.

6.2.3 THE THIRD ORDER CUMULANT DENSITY FUNCTION

Another parameter of particular importance is called the third order cumulant density function. This parameter measures the joint statistical dependence between the increments of three point processes N_a, N_b, N_c, and is defined as

$$q_{abc}(u,v)dudvdt = \text{cum}\{dN_a(t+u),\ dN_b(t+v),\ dN_c(t)\}$$

a, b, c, = 1, 2, $\cdots$, r and u,v,0 distinct.

Let $dN_a{}'(t+u) = dN_a(t+u) - P_a du$, with similar definitions for

$dN_b'(t+u)$ and $dN_c'(t)$. We may also define the third order cumulant function as

$$q_{abc}(u,v) = E\{dN_a'(t+u)dN_b'(t+v)dN_c'(t)\}/dudvdt$$

$$= P_{abc}(u,v)-P_{ac}(u)P_b-P_{bc}(v)P_a-P_{ab}(u-v)P_c+2P_aP_bP_c \qquad (6.2.4)$$

Under the (strong) mixing condition, we have the limiting relation as

$$\text{Lim}_{v\to\infty}\ q_{abc}(u,v) = 0$$

It also follows from the properties of the cumulants that if any subset of the processes N_a, N_b, N_c is independent of the remainder, then $q_{abc}(\cdot,\cdot)$ is identically zero (Brillinger, 1970). Expression (6.2.4) shows explicitly how the third order cumulant density, $q_{abc}(\cdot\cdot\cdot)$, differs from the third order product density, $P_{abc}(\cdot\cdot\cdot)$, by taking into account the lower order contributions to the third order product density. $P_{abc}(\cdot\cdot\cdot)$ used on its own for the assessment of the third order non-linear interactive effects could be misleading. This will be demonstrated by applying these parameters to simulated data and by constructing approximate asymptotic confidence intervals for both parameters in Section 6.2.6.

6.2.4 ESTIMATION OF THE PARAMETERS

Suppose that the point processes N_a, N_b, and N_c are realized in (0,T] with σ_j $j=1,2,\cdots,N_a(T)$; r_k $k=1,2,\cdots,N_b(T)$ and s_ℓ $\ell=1,2,\cdots,N_c(T)$ denoting the times of occurence of N_a, N_b, N_c events. An estimate of the third order product density may be obtained by (Brillinger, 1975b)

$$\hat{P}_{abc}(u,v) = \frac{J_{abc}^{(T)}(u,v)}{h^2T} \qquad (6.2.5)$$

and

$$\hat{P}_{abc}(u,u-v) = \frac{J_{abc}^{(T)}(u,u-v)}{h^2T} \qquad (6.2.6)$$

where

$$J_{abc}^{(T)}(u,v)=\#\{(\sigma_j,r_k,s_\ell) : u-(h/2)<\sigma_j-s_\ell<u+(h/2) \text{ and } v-(h/2)<r_k-s_\ell<v+(h/2)\} \qquad (6.2.7)$$

for some binwidth h. The symbol #{A} denotes the number of events in set A.

The variate $J_{abc}^{(T)}(u,v)$ is a histogram type of estimate, and is an extension of $J_{ab}^{(T)}(u)$ (see Chapter 4). This variate counts the number of differences (σ_j-s_ℓ) and (r_k-s_ℓ) which fall in two distinct bins of width h centred on u and v. The algorithm for computing $J_{ab}^{(T)}(u)$, discussed in Chapter 4, may easily be extended to one for a rapid computation of $J_{abc}^{(T)}(u,v)$. The same algorithm i.e., for $J_{abc}^{(T)}(u,v)$, however, may also be used to calculate $J_{abc}^{(T)}(u,u-v)$ if we note that

$$P_{abc}(u,v) = P_{cba}(-u,v-u)$$

i.e.,

$$P_{abc}(u,u-v) = P_{cba}(-u,-v)$$

Thus the computation of $J_{abc}^{(T)}(u,u-v)$ with an algorithm defined for $J_{abc}^{(T)}(u,v)$ may be carried out in the following two steps

1. Interchange process N_a with N_c and compute $J_{cba}^{(T)}(u,v)$

2. Reverse the signs of the lags, which gives $J_{abc}^{(T)}(u,u-v)$

For large T, the estimate $J_{abc}^{(T)}(u,v)$ is asymptotically Poisson with mean $h^2TP_{abc}(u,v)$ (Brillinger,1975b). Further, if $T\to\infty$, $h\to 0$ but $h^2T\to\infty$, this estimate is asymptotically normal with variance $h^2TP_{abc}(u,v)$ (since a Poisson variate with large mean is approximately normal). These results imply that as $T\to\infty$, $\hat{P}_{abc}(u,v)$ is asymtotically

$$(h^2T)^{-1}Po[h^2TP_{abc}(u,v)]$$

and if the limiting conditions are as $T\to\infty$, $h\to 0$ but $h^2T\to\infty$, $\hat{P}_{abc}(u,v)$ is asymptotically

$$N[P_{abc}(u,v)\ ,\ (h^2T)^{-1}P_{abc}(u,v)]$$

where $Po[\alpha]$ denotes a Poisson variate with mean α, and $N[\alpha,\beta]$ denotes a normal variable with mean α and variance β.

Estimates of the third order conditional density, $m_{abc}(u,v)$, and the third order cumulant density functions may be obtained by inserting the estimates of the third order and lower order product densities in expressions (6.2.3) and (6.2.4), respectively, i.e.,

$$\hat{m}_{abc}(u,v) = \frac{\hat{P}_{abc}(u,u-v)}{\hat{P}_{bc}(u-v)} \tag{6.2.8}$$

$$\hat{q}_{abc}(u,v) = \hat{P}_{abc}(u,v)-\hat{P}_{ac}(u)\hat{P}_b-\hat{P}_{bc}(v)\hat{P}_a-\hat{P}_{ab}(u-v)\hat{P}_c+2\hat{P}_a\hat{P}_b\hat{P}_c \tag{6.2.9}$$

and

$$\hat{q}_{abc}(u,u-v)=\hat{P}_{abc}(u,u-v)-\hat{P}_{ac}(u)\hat{P}_b-\hat{P}_{bc}(u-v)\hat{P}_a-\hat{P}_{ab}(v)\hat{P}_c+2\hat{P}_a\hat{P}_b\hat{P}_c \tag{6.2.10}$$

6.2.5 CONFIDENCE INTERVALS FOR THE THIRD ORDER PRODUCT AND CUMULANT DENSITY FUNCTIONS

Variance stabilizing transformation for a Poisson variate (Kendall and Stuart, 1966) leads to the variate $[\hat{P}_{abc}(u,v)]^{1/2}$ as

$$[\hat{P}_{abc}(u,v)]^{1/2} \sim N\{[P_{abc}(u,v)]^{1/2} \ , \ 1/(4h^2T)\}$$

Under the limiting condition (6.2.1), i.e., under the assumption that the increments of processes N_a, N_b, N_c are independent, an approximate 95% confidence interval for $[P_{abc}(u,v)]^{1/2}$ may be constructed as

$$[\hat{P}_a\hat{P}_b\hat{P}_c]^{1/2} \pm 1.96\ (4h^2T)^{-1/2} \tag{6.2.11}$$

The estimate $\hat{q}_{abc}(u,v)$, under the assumption of independence, and if $T\to\infty$, $h\to 0$ but $h^2T\to\infty$, is asymptotically normal with variance given by (Rigas, 1983), as $T\to\infty$

$$\operatorname{var}[\hat{q}_{abc}(u,v)] = \frac{2\pi}{T}\int\!\!\int_0^{2\pi} f_{aa}(\lambda_1)f_{bb}(\lambda_2)\overline{f_{cc}(\lambda_1+\lambda_2)}d\lambda_1 d\lambda_2 \tag{6.2.12}$$

Based on the disjoint sections of the entire record T (T=LR), an estimate of above variance may be obtained by inserting the respective estimates of the auto spectra in expression (6.2.12), i.e.,

$$\hat{\operatorname{var}}[\hat{q}_{abc}(u,v)] = \left[\frac{2\pi}{T}\right]\left[\frac{2\pi}{R}\right]^2 \sum_j \sum_k f_{aa}^{(T)}(\lambda_j)f_{bb}^{(T)}(\lambda_k)\overline{f_{cc}^{(T)}(\lambda_j+\lambda_k)}$$

for $\lambda_j = 2\pi j/R$, $j=1,2\cdots R$; $\lambda_k=2\pi k/R$ $k=1,2,\cdots,R$

Hence an approximate 95% confidence interval for $q_{abc}(u,v)$, under the hypothesis that processes are independent is given by

$$0 \pm 1.96\ \{\hat{\mathrm{var}}[\hat{q}_{abc}(u,v)]\}^{1/2} \qquad (6.2.13)$$

Any value lying outside this interval at lags u,v will signify a possible joint interactive effect (statistical dependence) between the three processes at those lags.

6.2.6 APPLICATIONS

Fig.6.2.2 illustrate the application of third order product density (Fig.6.2.2a), third order conditional density (Fig.6.2.2b), and third order cumulant density functions (Fig.6.2.2c) applied to a computer generated data using the following simple scheme

Let N_a be a Poisson process, then

$$N_b = N_a^{d1}$$

$$N_c = N_a^{d2}$$

where N_a^{d1} and N_a^{d2} are the delayed versions of process N_a with d1=-6 and d2=-16. The estimates given in Fig.6.2.2a-c are based on expressions, respectively, (6.2.6),(6.2.8) and (6.2.10) with h=1msec.

The simplicity of this simulation is the key factor in this example in order to demonstrate how these parameters reveal different information present in the processes under investigation. A large peak in the the estimated third order product density (Fig.6.2.2a) corresponds to the lags (16,6) at which the processes are jointly related. Small raised areas revealing the pairwise lower order dependencies are also clear in this estimate.

The estimate of the third order conditional density function clearly reveals different information suggesting that an N_a

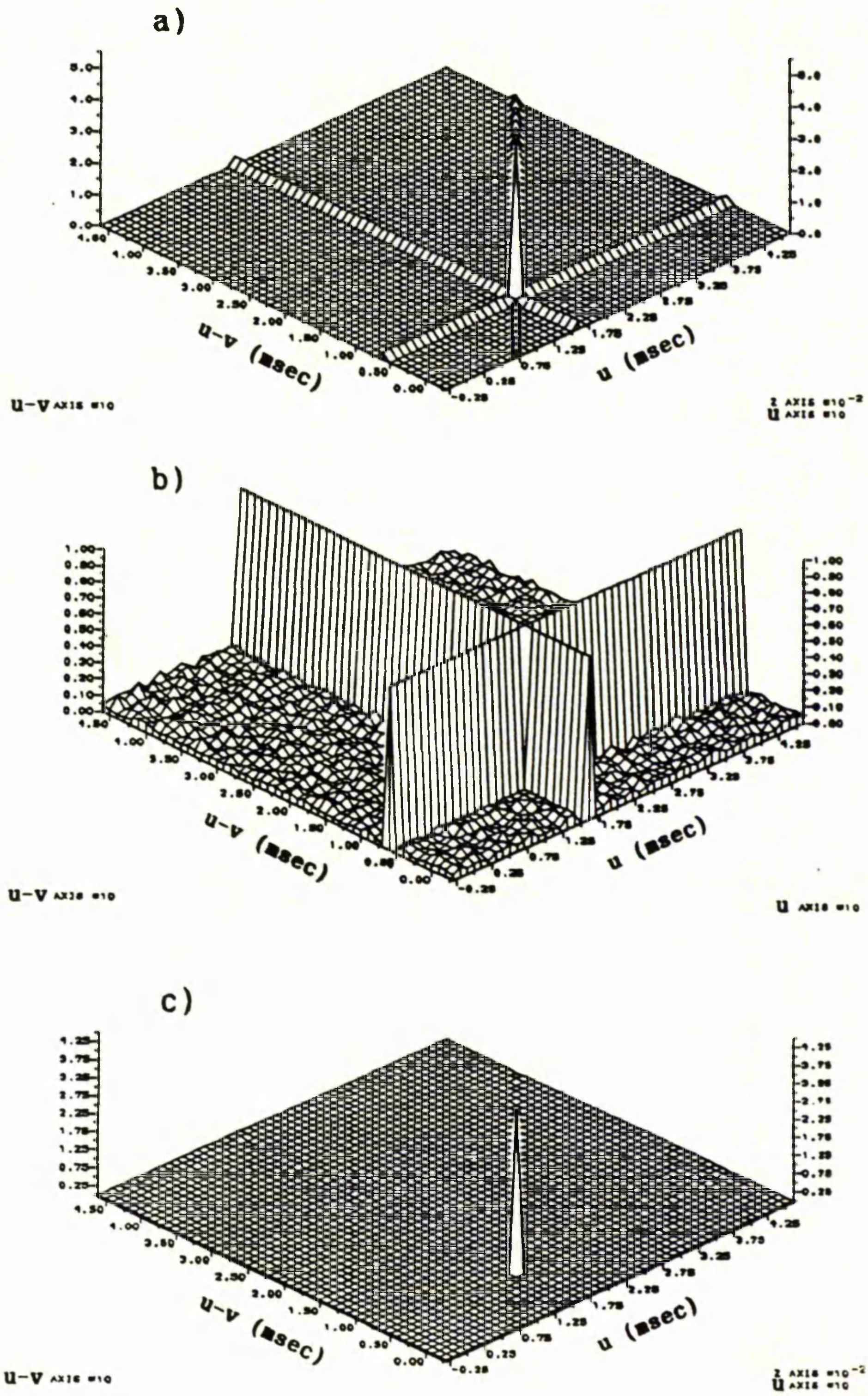

Fig.6.2.2 Illustration of third order time domain parameters

Estimates of the third order (a) product density, $P_{abc}(u,u-v)$, (b) conditional density, $m_{abc}(u,u-v)$, and (c) cumulant density $q_{abc}(u,u-v)$, functions of the simulated data. The lags u-v and u are, respectively, the times of an N_b and an N_c events relative to an N_a event.

event is certain, in this example, to occur after 6 msec of an N_b event or after 16 msec of an N_c event. So this estimate also contains the pairwise latency between N_a and N_b, and between N_a and N_c.

Fig.6.2.2c, which is the estimate of the third order cumulant density function, clearly shows the lags at which the joint dependence between the three processes occurs having removed all the lower order pairwise dependence or interaction, and suggests that a particular pattern of pair of N_b and N_c events (i.e N_c event 10 msec behind an N_b event) facilitates the process N_a by producing an N_a event after 6 msec.

We now turn to the application of the above procedures to the real data set on the muscle spindle. Figs.6.2.3-6.2.6 illustrate the application of the third order product density and the cumulant density functions. Fig.6.2.3a gives the estimate of $P_{Ia_1\gamma_{s1}\gamma_s}(u,u-v)$ in the presence of a second fusimotor input, $_2\gamma_s$, applied to the spindle independently of $_1\gamma_s$. The u and u-v axes correspond to two $_1\gamma_s$ spikes prior to a Ia spike. The inserts in Fig.6.2.3a, which show the third order product density plotted, respectively, for v=8 msec and v=13 msec, are similar to the kind of figures used by Windhorst and Schwestka(1982). The solid lines above and below the dotted line in these inserts represent an approximate 95% confidence limits, based on (6.2.11), for $[P_{Ia\,_1\gamma_s\,_1\gamma_s}(u,u-v)]^{1/2}$ under the hypothesis that the processes are independent. The values of the estimate lying outside these limits reveal significant interactive effects of the two $_1\gamma_s$ spikes on the Ia response. Based on the confidence limits at various lags , the regions where the $_1\gamma_s$ has a significant effect on the Ia response is shown in the contour plot (Fig.6.2.3b) by dark areas. A large ridge running parallel to the u axis at u-v=13 msec corresponds to the delay between the two processes, and is consistent with the Fig.4.2.2a of Chapter 4.

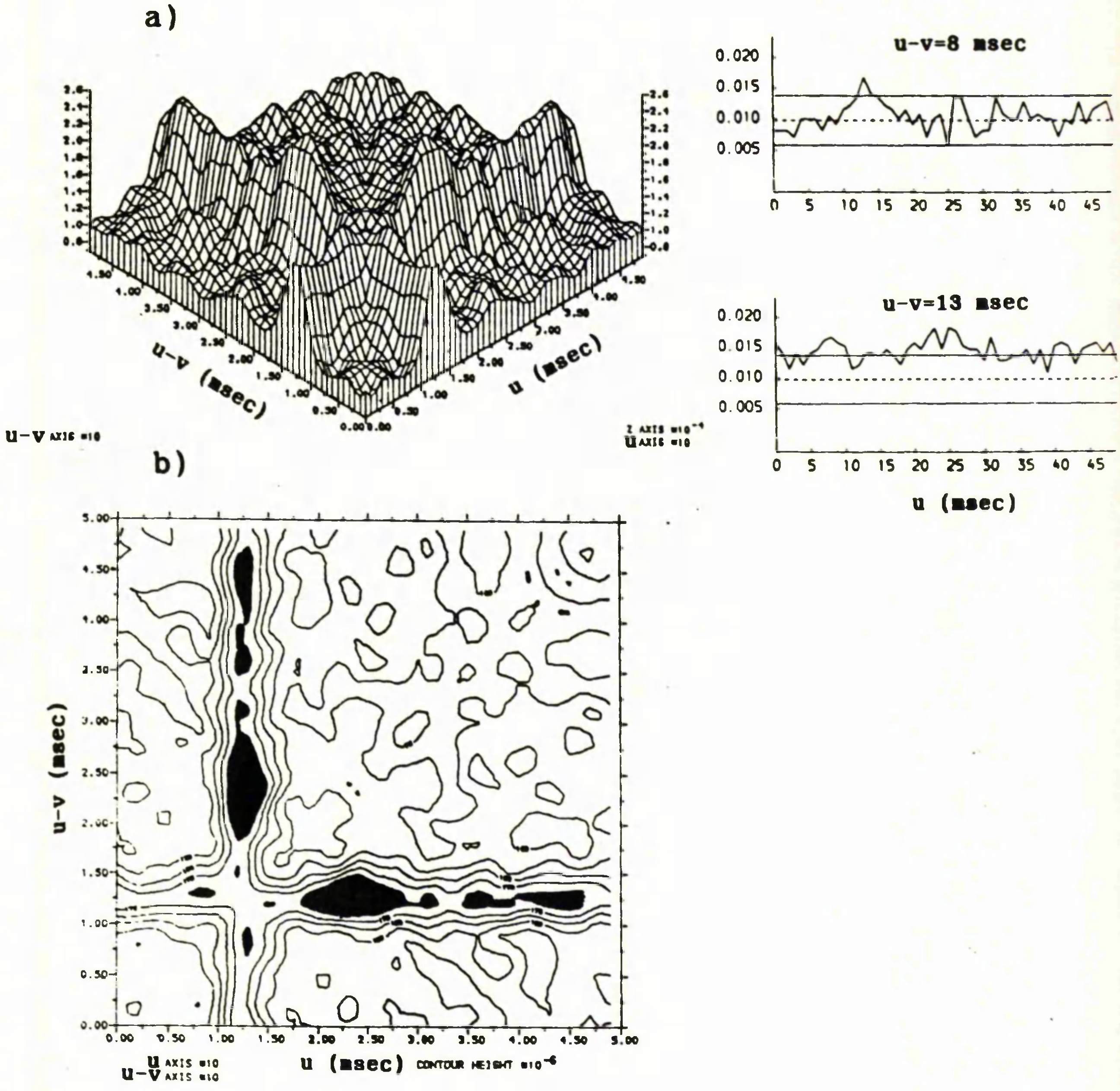

Fig.6.2.3

a) Estiamte of the third order product density function where u-v and u are the times of $_1\gamma_s$ spikes relative to a Ia spike. The two inserts are for u-v=8,13 msec and show the approximate 95% confidence interval for the product density function under the hypothesis that the two processes are independent.

b) Contour plot of the estimate illustrated in (a). The darkened area signifies a possible departure from the hypothesis of independent processes at the corresponding lags u and u-v.

The third order cumulant, $q_{Ia_1\gamma_s 1\gamma_s}(u,u-v)$, (Fig.6.2.4.a), however, reveals more clearly the complexity of the pattern of the interaction between two $_1\gamma_s$ spikes that alters the Ia response. The approximate 95% confidence limits shown in the inserts of this figure are based on expression (6.2.13). From these inserts, it is clearly seen that the large ridge which was present in the product density function (Fig.6.2.3a) has disappeared and an area of significant depression also seems to appear. This can be seen more clearly in the contour plot (Fig.6.2.4b). The depression (dotted region) at u=10-15 msec and v=10-15 msec suggest that synchronous firing of the static fusimotor input, $_1\gamma_s$, tends to decrease the probability of the Ia discharge after about 10-15 msec. A region of facilitation (darkened) at u=20-25 msec and u-v=10-15 msec can also be seen to reveal that two $_1\gamma_s$ spikes separated by 5-10 msec also interact which leads to a facilitation in the Ia response after 10-15 msec. These interpretations may be presented diagramatically as follows

Depression of the Ia response relative to static gamma input, $_1\gamma_s$

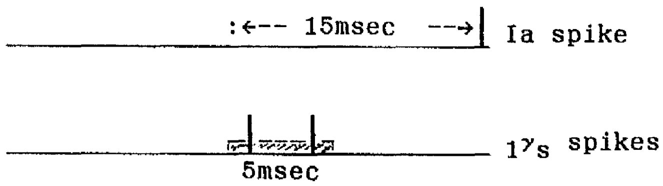

Facilitation of the Ia response relative to static gamma input, $_1\gamma_s$

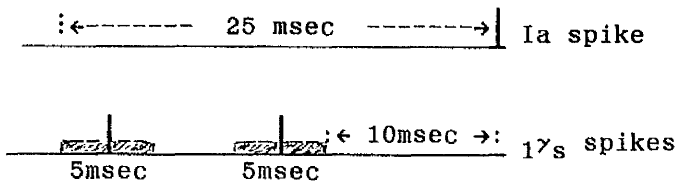

From the above interpretation, it seems that the interaction between

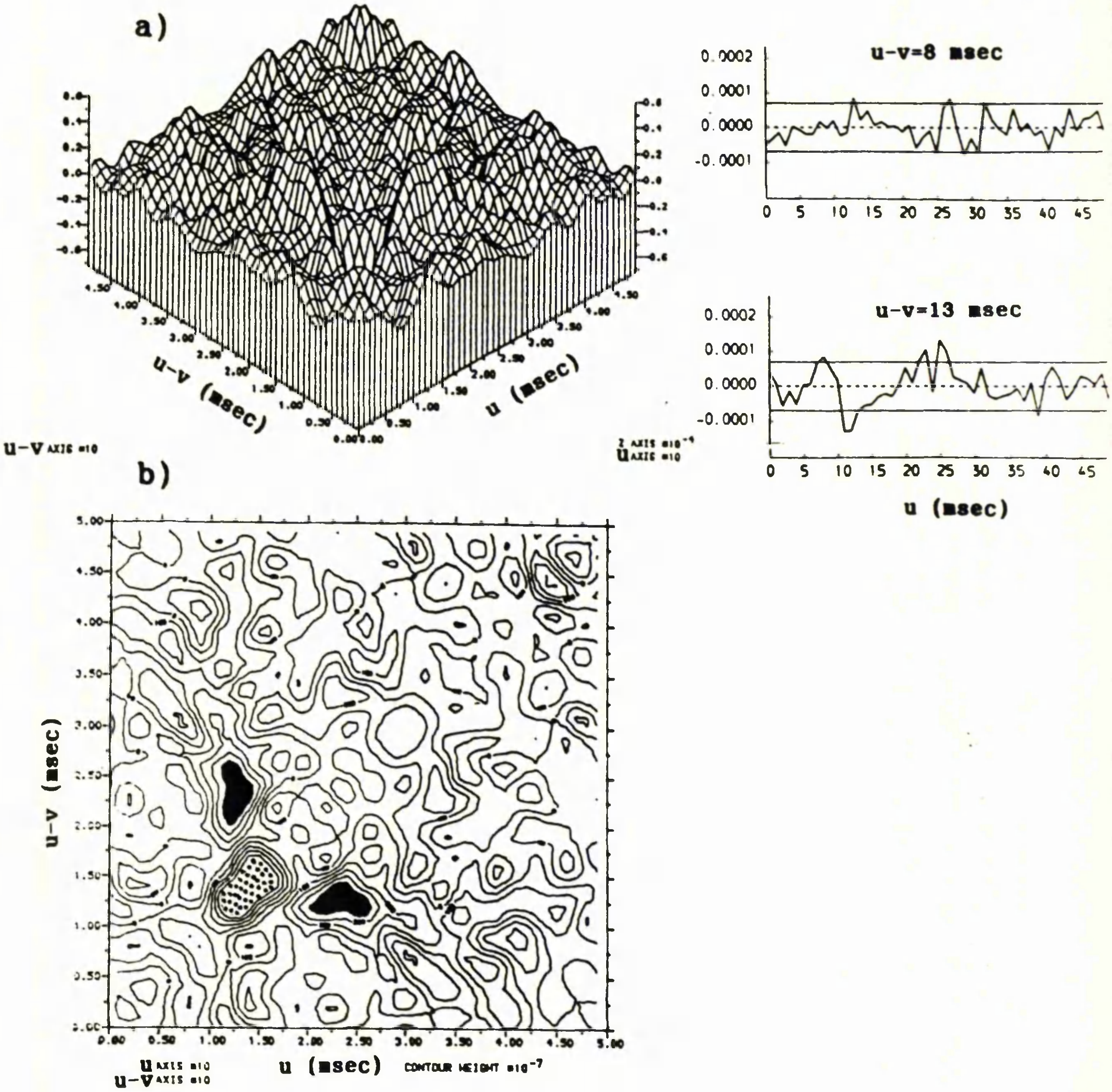

Fig.6.2.4

a) Estimate of the third order cumulant density function where u-v and u are the times of $_1\gamma_s$ spikes realtive to a Ia spike. The two inserts are for u-v=8,13 msec and show the approximate 95% confidence interval for the cumulant density function under the hypothesis that the two processes are independent.

b) Contour plot the estimate illustrated in (a). The dotted area represents a significant depression, whereas the darkened area corresponds to a significant excitation in the Ia discharge caused by the interaction of two $_1\gamma_s$ spikes at the the corresponding lags u and u-v.

two spikes of ${}_1\gamma_s$ has both types of effects, i.e., inhibitory as well as exitatory, on the Ia response depending on the pattern of the gamma spikes. This example clearly demonstrates how the pattern of the spikes is an important feature of the interaction which affects the Ia response.

Fig.6.2.5 corresponds to the estimates of the third order product density $P_{Ia\,{}_2\gamma_s\,{}_2\gamma_s}(u,u-v)$ (Fig.6.2.5a), the third order cumulant density $q_{Ia\,{}_2\gamma_s\,{}_2\gamma_s}(u,u-v)$ (Fig.6.2.5b) and its contour plot (Fig.6.2.5c). This figure reveals almost similar features as the Figs.6.2.3-6.2.4 but with a slight difference in the pattern of the ${}_2\gamma_s$ spikes suggesting that the interaction between a pair of ${}_2\gamma_s$ spikes when they occur close to each other causes a depression of the Ia response whereas when they are separated by 10-20 msec facilitate the Ia response after about 10 msec. In addition, another area of depression might appear at u=17-18 msec and u-v=13-14 msec.

A comparison between the non-linear interactive effects of both gamma static inputs, applied concurrently and independently, on the Ia response shows that the ${}_2\gamma_s$ has a broader region of interaction that alters the Ia response than that of ${}_1\gamma_s$.

A further example contrasting the third order product density and the third order cumulant density is presented in Fig.6.2.6 which describes the pattern of the activity from both fusimotor inputs, ${}_1\gamma_s$ and ${}_2\gamma_s$, applied concurrently and independently, that alters the Ia response from the same muscle spindle. Fig.6.2.6a is the estimate of the product density, $P_{Ia\ \gamma\ {}_1\gamma_s\,{}_2\gamma_s}(u,u-v)$, where u-v and u are, respectively, the times of ${}_1\gamma_s$ and ${}_2\gamma_s$ spikes prior to a Ia spike. This figure, which is not symmetrical about the main diagonal, may be seen as a combination of Fig.6.2.3a and Fig.6.2.5a. The two large ridges parallel to both axes correspond to the time delays of the Ia discharge over both gamma inputs.

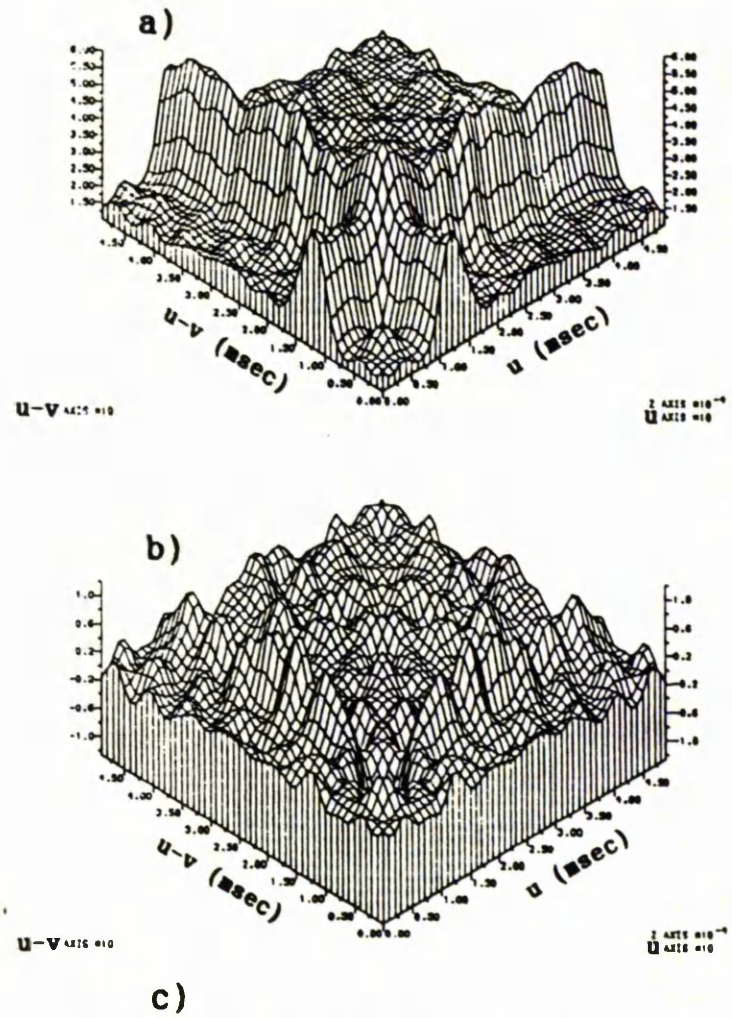

Fig.6.2.5

a) Estimated third order product density and (b) cumulant density functions. The lags u-v and u are the times of $_2\gamma_s$ spikes relative to a Ia spike.

c) Contour plot of the estimate illustrated in (b). The dotted area represents a significant depression whereas the darkened area corresponds to a significant excitaion in the Ia discharge caused by the interaction of two $_2\gamma_s$ spikes at the corresponding lags u and u-v.

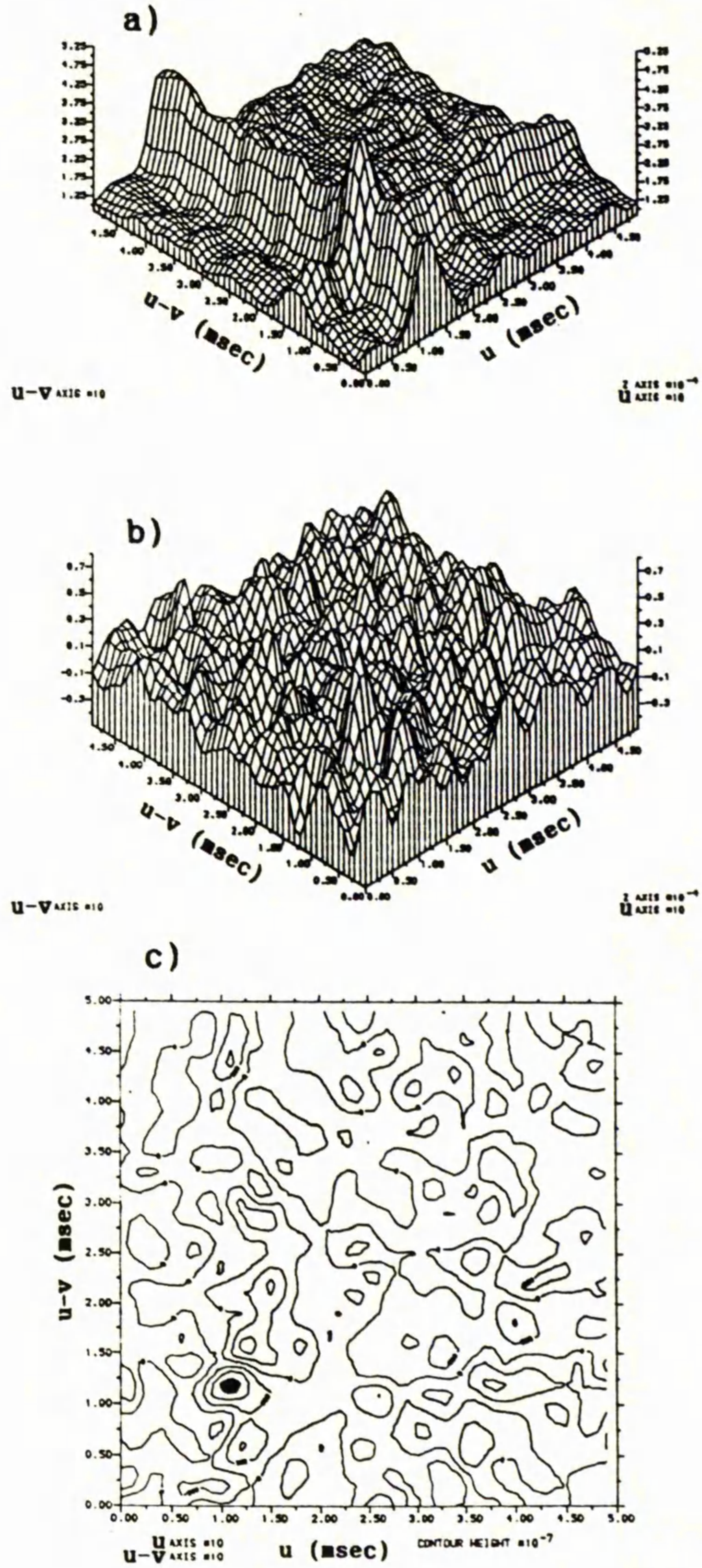

Fig.6.2.6

a) Estimated third order product density and (b) cumulant density functions. The lags u-v and u are the times of a ${}_1\gamma_s$ and a ${}_2\gamma_s$ spikes realtive to a Ia spike.

c) Contour plot of the estimate illustrated in (b). The darkened area represents a significant excitation in the Ia discharge caused by the interaction between ${}_1\gamma_s$ and ${}_2\gamma_s$ spikes at the corresponding lags u and u-v.

The cumulant, $q_{Ia_1\gamma_s 2\gamma_s}(u,u-v)$, (Fig.6.2.6b) and its contour plot in Fig.6.2.6c reveal a weak but significant interactive effect of both gamma inputs on the Ia whenever $_1\gamma_s$ spike proceeds $_2\gamma_s$ spike, but not in the reverse order, and which confirms that the order of the discharge of the two gamma inputs is also an important feature of the interaction between their effects on the Ia response.

6.3 FURTHER CONSIDERATIONS

The above procedures may easily be extended in order to assess a further high order non-linear interactive effects of one point process on the other. The product density and cumulant density functions of order-4 may reveal more interesting features of the system under investigation by providing useful informations about fourth order (cubic) interactions between the processes. The following is a brief discussion about the 4th order product density and cumulant density functions.

6.3.1 THE FOURTH ORDER PRODUCT DENSITY FUNCTION

Let $\underline{N}(t)=\{N_1(t),\ N_2(t),\ \cdots,\ N_r(t)\}$ be an r-vector valued stationary point process which satisfies the conditions of orderliness and (strong) mixing. The product density of order-4 of the components N_a, N_b, N_c, and N_d of $\underline{N}$ may be defined as

$$\begin{aligned} P_{abcd}(u,v,w)=\text{Lim}_{\,h_1,h_2,h_3,h_4\to 0}\ \Pr\{&N_a \text{ event in } (t+u,t+u+h_1],\\ &N_b \text{ event in } (t+v,t+v+h_2],\\ &N_c \text{ event in } (t+w,t+w+h_3], \text{ and}\\ &N_d \text{ event in } (t,t+h_4]\}/h_1h_2h_3h_4 \end{aligned}$$

which, under orderliness condition, may be written as

$$P_{abcd}(u,v,w)dudvdwdt = E\{dN_a(t+u)dN_b(t+v)dN_c(t+w)dN_d(t)\}$$

for a,b,c,d=1,2,$\cdots$,r and u,v,w,0 disdinct.

Under (strong) mixing condition, the 4th order product density function satisfies the limiting condition

$$\text{Lim}_{\,u,v,w\to\infty}\ P_{abcd}(u,v,w) = P_aP_bP_cP_d \qquad (6.3.1)$$

6.3.2 ESTIMATION OF THE FOURTH ORDER PRODUCT DENSITY FUNCTION

Let $\underline{N}(t)$ be observed in $(0,T]$ with σ_j $\{j=1,2,\cdots,N_a(T)\}$ r_k $\{k=1,2,\cdots,N_b(T)\}$, s_ℓ $\{\ell=1,2,\cdots,N_c(T)\}$, and τ_m $\{m=1,2,\cdots,N_d(T)\}$ being the respective observed times of the events of component processes N_a, N_b, N_c, and N_d. Extending the procedure of estimating $P_{abc}(u,v)$, an estimate of $P_{abcd}(u,v,w)$ may be obtained by

$$\hat{P}_{abcd}(u,v,w) = J_{abcd}{}^{(T)}(u,v,w)/h^3T \tag{6.3.2}$$

where

$$\begin{aligned} J_{abcd}{}^{(T)}(u,v,w) = \#\{(\sigma_j,r_k,s_\ell,\tau_m) \;:\; & u-(h/2) < \sigma_j-\tau_m < u+(h/2), \text{ and} \\ & v-(h/2) < r_k-\tau_m < v+(h/2), \text{ and} \\ & w-(h/2) < s_\ell-\tau_m < w+(h/2)\} \end{aligned}$$

where h is the binwidth parameter, and $\#\{A\}$ denotes the number of events in set A. The variate counts the number of differences $(\sigma_j-\tau_m)$ $(r_k-\tau_m)$ and $(s_\ell-\tau_m)$ which fall into three distinct bins of width h and centred on u, v, and w. The computation of this variate may easily be carried out by extending the algorithm for $J_{abc}{}^{(T)}(\cdots)$ discussed in Section 6.2.4.

With similar arguments given in Section 6.2.5, it can be shown that the variate $J_{abcd}{}^{(T)}(u,v,w)$ is asymptotically distributed as Poisson with mean $h^3TP_{abcd}(u,v,w)$ (Brillinger,1975a), and if the limiting conditions are as $T\to\infty$, $h\to 0$, but $h^3T\to\infty$, this variate is asymptotically normal with variance $h^3TP_{abcd}(u,v,w)$. This implies that under the same limiting conditions, $\hat{P}_{abcd}(u,v,w)$ is asymptotically normal with mean $P_{abcd}(u,v,w)$ and variance $(h^3T)^{-1}P_{abcd}(u,v,w)$.

6.3.3 CONFIDENCE INTERVALS FOR THE FOURTH ORDER PRODUCT DENSITY FUNCTION

Applying the square root transformation (Kendall and Stuart, 1966), the variate $[\hat{P}_{abcd}(u,v,w)]^{½}$ is seen to be asymptotically normal with mean $[P_{abcd}(u,v,w)]$ and a stabilised variance $[4h^3T]^{-1}$. Therefore an approximate 95% confidence interval for $[P_{abcd}(u,v,w)]^{½}$ may easily be set up as

$$[\hat{P}_{abcd}(u,v,w)]^{½} \pm 1.96[4h^3T]^{-½}$$

and under the limiting condition (6.3.1), i.e., under the hypothesis of independent processes, above confidence interval becomes as

$$[\hat{P}_a\hat{P}_b\hat{P}_c\hat{P}_d]^{½} \pm 1.96[4h^3T]^{-½} \qquad (6.3.3)$$

6.3.4 APPLICATION OF THE FOURTH ORDER PRODUCT DENSITY FUNCTION

Fig.6.3.1a demonstrates the application of the product density function of order-4, $P_{NNNN}(u,v,w)$, at w=15 msec of a Poisson process N. The computation of this estimate, based on expression (6.3.2), is carried out with h=2 msec. The two inserts in this figure give the approximate 95% confidence interval at v=22,40 msec under the hypothesis that the increments of the process are independent (i.e., a Poisson process), and are based on expression (6.3.3). These inserts clearly confirm the Poisson nature of the process. This can also be seen more clearly in the contour plot given in Fig.6.3.1b which reveals no obvious pattern, suggesting a Poisson process.

Fig.6.3.2 gives the estimate of the 4th order product density, $\hat{P}_{Ia\ {}_1\gamma_s\ {}_2\gamma_s\ {}_2\gamma_s}(u,v,w)$, with w fixed at 15 msec.
The computation of this estimate is carried out with h=5 msec.

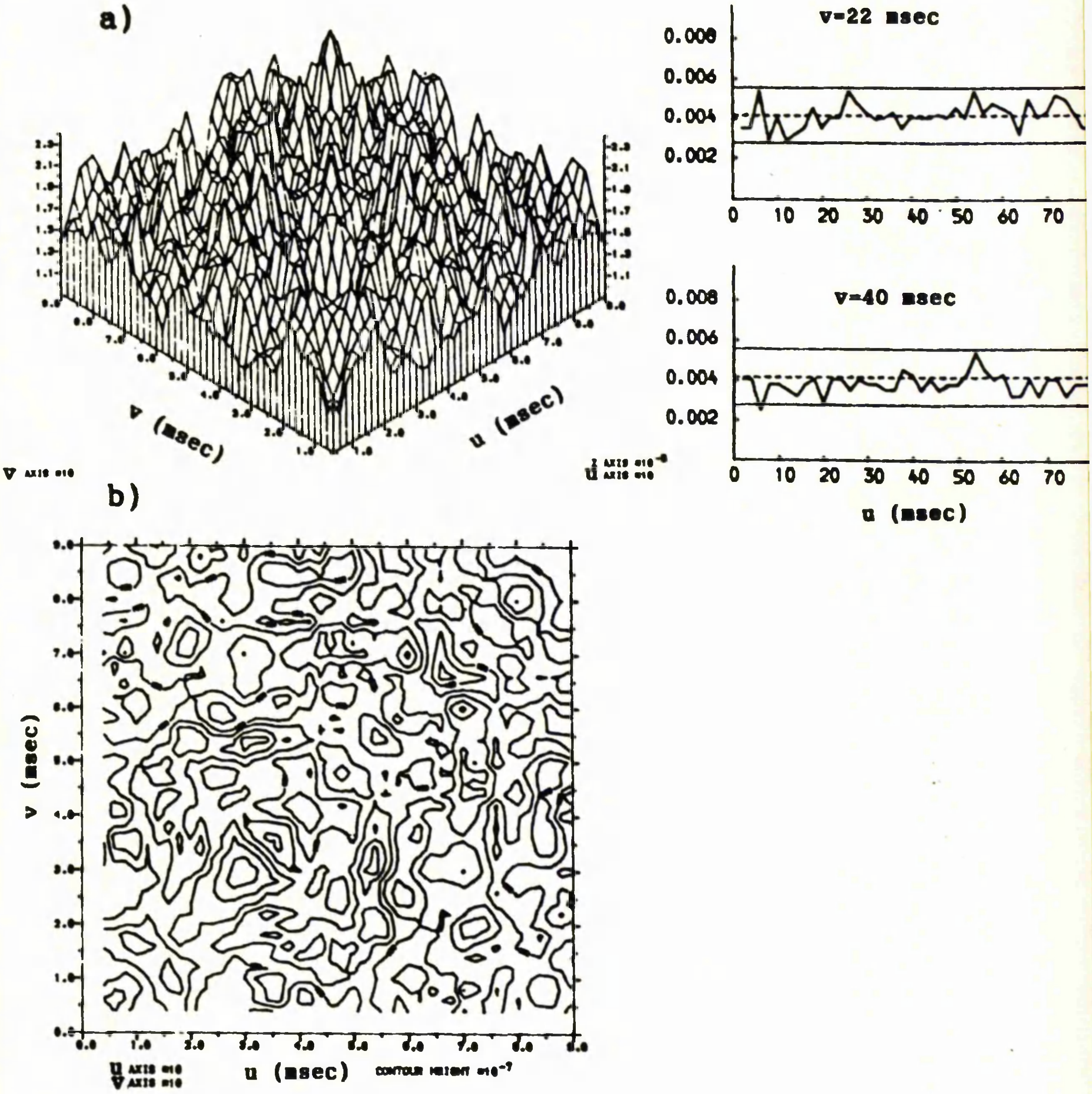

Fig.6.3.1 Illustration of the 4th order product density function

a) Estimate of $P_{NNNN}(u,v,w)$ at w=30 msec of a Poisson process. The computation of this estimate is carried out with h=2msec. The two inserts in this figure correspond to the estimate at w=30 msec and v=22,40 msec. The horizontal solid lines inserts give an approximate 95% confidence interval for the forth order product density function under the hypothesis of independent increments of the porocess. Fig.b gives the Contour plot of this estimate.

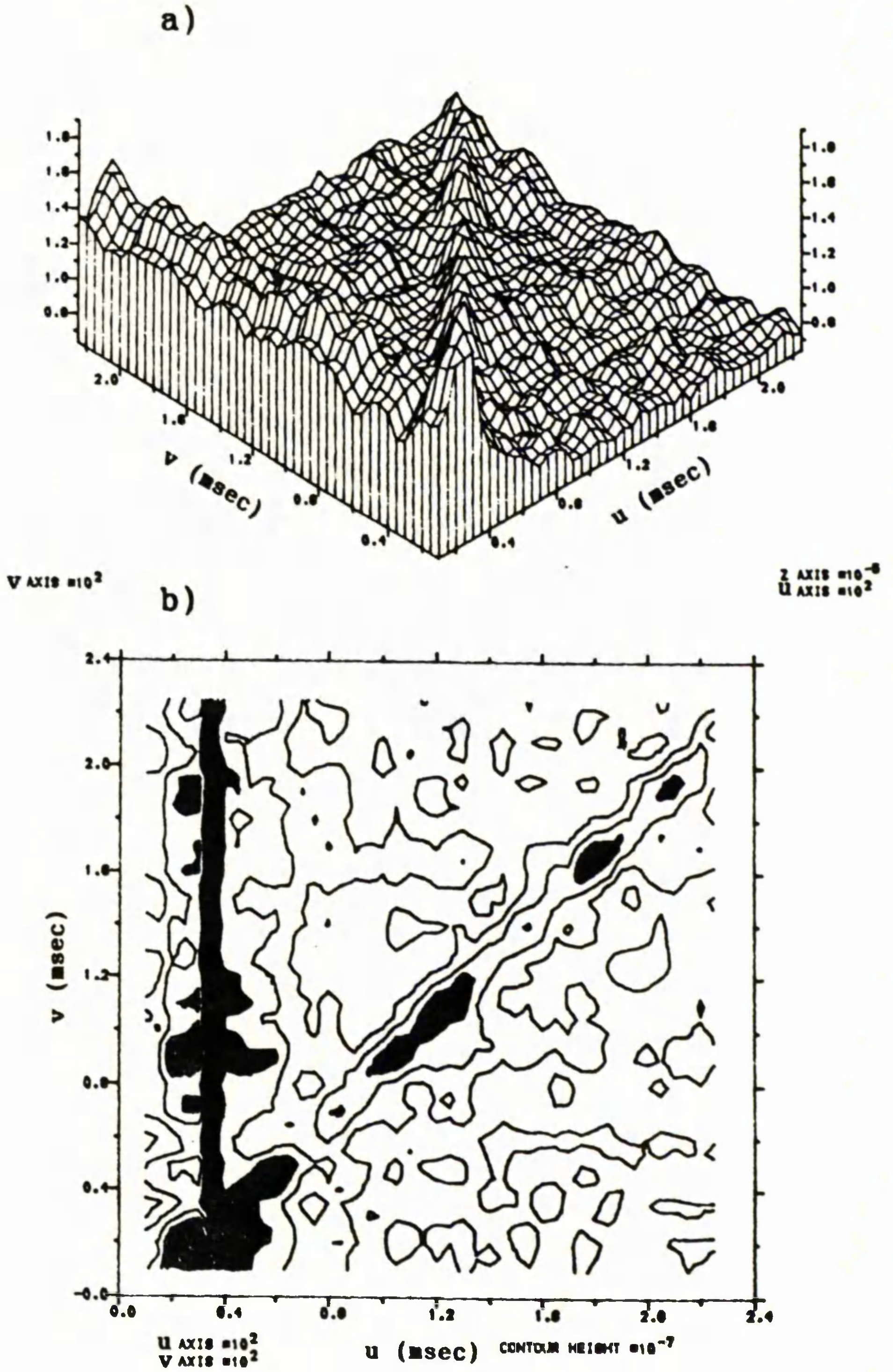

Fig.6.3.2 Illustration of the fourth order product density function

a) Estimate of $P_{Ia_1\gamma_s\ {}_2\gamma_s\ {}_2\gamma_s}(u,v,w)$ at w=15 msec where u,v, and w correspond to the timings of a Ia, a ${}_1\gamma_s$, and a ${}_2\gamma_s$ spike relative to a second ${}_2\gamma_s$ spike. The value of h is taken to be 5 msec. Fig.b gives the contour plot of this estimate. The area darkened in this plot signify a possible departure from the hypothesis of independent processes.

The lags u,v, and w may be explained diagrammatically as follows

```
:---------- u --------|
____________________________________ Ia
:----- v ----|
____________________________________ 1γs
|-- w --|
____________________________________ 2γs
```

The two ridges in the estimate, one parallel to the v axis at u=25 msec and the other diagonal at about u-v=15 msec are clearly seen. This suggests that the chance of a Ia spike, a $_1\gamma_s$ spike, and two $_2\gamma_s$ spikes occurring with the particular spacings, i.e., u=25, v=10 and w=15 msec is greater than it would be expected if the processes were independent. This result also confirms the previous conclusions obtained from Figs.6.2.4 and 6.2.5

6.3.4 <u>THE FOURTH ORDER CUMMULANT DENSITY FUNCTION</u>

As discussed in Section 6.3 about the validity of the third order product density in the assessment of third order non-linear interactive effects, the product density of order-4 could also be misleading in assessing the 4th order non-linear interactions because of the presence of the lower order interactions. The cumulant density function of order-4 may then be used for such an assessment.

The 4th order cumulant density function of processes N_a, N_b, N_c, and N_d may be defined as

$$q_{abcd}(u,v,w)dudvdwdt = \mathrm{cum}\{dN_a(t+u),\ dN_b(t+v),\ dN_c(t+w),\ dN_d(t)\}$$

a,b,c,d=1,2,$\cdots$,r, and u,v,w,0 distinct.

With the definition of zero mean point process, i.e., $dN_a'(t+u)=dN_a(t+u)-P_a du$, the 4th order cumulant density may be written as

$$q_{abcd}(u,v,w)dudvdwdt = E\{dN_a'(t+u)dN_b'(t+v)dN_c'(t+w)dN_d'(t)\}$$

$$-E\{dN_a'(t+u)dN_b'(t+v)\}E\{dN_c'(t+w)dN_d'(t)\}$$

$$-E\{dN_a'(t+u)dN_c'(t+w)\}E\{dN_b'(t+v)dN_d'(t)\}$$

$$-E\{dN_a'(t+u)dN_d'(t)\}E\{dN_b'(t+v)dN_c'(t+w)\}$$

or in terms of the product densities, the above cumulant density function may be written as (definition I.3 of Appendix I)

$$q_{abcd}(u,v,w) = P_{abcd}(u,v,w) - P_{abc}(u-w,v-w)P_d - P_{abd}(u,v)P_c$$

$$- P_{acd}(u,w)P_b - P_{bcd}(v,w)P_a + 2P_{ab}(u-v)P_cP_d$$

$$+ 2P_{ac}(u-w)P_bP_d + 2P_{ad}(u)P_bP_c + 2P_{bc}(v-w)P_aP_d$$

$$+ 2P_{bd}(v)P_aP_c + 2P_{cd}(w)P_aP_b - P_{ab}(u-v)P_{cd}(w)$$

$$- P_{ac}(u-w)P_{bd}(v) - P_{ad}(u)P_{bc}(v-w) - 6P_aP_bP_cP_d \qquad (6.3.4)$$

An estimate of $q_{abcd}(u,v,w)$ may be obtained by inserting the estimates of the 4th and lower order product densities, which have been discussed previously, in expression (6.3.4). The application of the cumulant function of order-4 with appropriate confidence intervals is left as a work of further research.

6.4 HIGHER ORDER PARAMETERS IN THE FREQUENCY DOMAIN

We now turn to the frequency domain parameters which provide useful information about the third order non-linear effects. The fundamental parameter called the third order spectrum is a further extension of the ordinary spectrum. In contrast with the ordinary specrtrum, which describes the linear mechanism, the third order spectrum describes the quadratic structure in the mechanism. We discuss this parameter in more detail in the following section.

6.4.1 THE THIRD ORDER SPECTRA

Let $\underline{N}(t)=\{N_1(t), \cdots, N_r(t)\}$ be an r-vector valued stationary point process which satisfies the conditions of orderliness and (strong) mixing, and is defined on the entire real line.

Further suppose that the third order cumulant density function between components N_a, N_b, and N_c, defined by (6.2.4) exists and satisfies the condition

$$\iint |q_{abc}(u,v)|dudv < \infty$$

By analogy with the second order cross-spectrum the third order spectrum between N_a, N_b and N_c is defined as the Fourier transform of the third order cumulant, i.e.,

$$(2\pi)^2 f_{abc}(\lambda,\mu) = \iint \exp\{-i(\lambda u+\mu v)\} q_{abc}(u,v)dudv \qquad -\infty<\lambda,\mu<\infty \quad (6.4.1)$$

The third order spectrum (6.4.1) is generally a complex function, and since $\underline{N}(t)$ is real-valued, we have

$$f_{abc}(\lambda,\mu) = \overline{f_{abc}(-\lambda,-\mu)} = f_{cba}(-\lambda-\mu,\mu)$$

With a=b=c, we have the bispectrum of the process N_a, and is defined by (Brillinger, 1975b)

$$(2\pi)^2 f_{aaa}(\lambda,\mu)= \iint \exp\{-i(\lambda u+\mu v)\}\mathrm{cum}\{dN_a(t+u),dN_a(t+v),dN_a(t)\}/dt$$

$$=q_a+\int \exp\{-i\lambda u\}q_{aa}(u)du+\int \exp\{-i\mu u\}q_{aa}(u)du$$

$$+\int \exp\{-i(\lambda+\mu)\}q_{aa}(u)du+\iint \exp\{-i(\lambda u+\mu v)\}q_{aaa}(u,v)dudv$$

In the case that N_a is a Poisson process, above expression reduces to

$$f_{aaa}(\lambda,\mu) = q_a/(2\pi)^2 = P_a/(2\pi)^2$$

where $q_a=P_a$ is the mean intensity of the process.

Similarly for b=c, and a distinct, the third order spectrum is called the cross-bispectrum between process N_a and N_b and is defined as

$$(2\pi)^2 f_{abb}(\lambda,\mu)=\iint \exp\{-i(\lambda u+\mu v)\}\mathrm{cum}\{dN_a(t+u),dN_b(t+v),dN_b(t)\}/dt$$

$$=\int \exp\{-i\lambda u\}q_{ab}(u)du+\iint \exp\{-i(\lambda u+\mu v)\}q_{abb}(u,v)dudv$$

and similarly,

$$(2\pi)^2 f_{aab}(\lambda,\mu)=\int \exp\{-i(\lambda+\mu)u\}q_{ab}(u)du+\iint \exp\{-i(\lambda u+\mu v)\}q_{aab}(u,v)dudv$$

For the case of a single time series the idea of higher order spectrum was developed by Shiryaev(1960). Tick(1961) considers the cross-bispectrum as providing the "frequency response" of a quadratic system involving a bivariate ordinary time series. Further considerations of the bispectrum of time series with application to a variety of real data can be seen in Hasselmann et al(1963), Godfrey(1965) and Brillinger and Rosenblatt(1967). Akaike(1966) has introduced a new notion of "mixed spectrum" which situates between the moment function and the spectrum, and relates the higher order spectra to linear theory of ordinary spectrum and cross-spectrum.

Theoretical developements of the higher order spectra in the case of point processes have been presented in Brillinger(1972).

6.4.2 <u>ESTIMATION OF THE THIRD ORDER SPECTRUM</u>

Let the point process $\underline{N}(t)$ be realised in $(0,T]$. Based on the periodograms of 'L' disjoint sections of the whole record length, T, where T=LR, an estimate of the cross-spectrum $f_{abc}(\lambda,\mu)$ between the components N_a,N_b,N_c of $\underline{N}$ may be obtained as

$$f_{abc}^{(T)}(\lambda,\mu) = \frac{1}{L}\sum_{j=0}^{L-1} I_{abc}^{(R)}(\lambda,\mu;j) \tag{6.4.2}$$

where $I_{abc}^{(R)}(\lambda,\mu;j)$ is the third order periodogram of the jth section at frequencies λ and μ, and is given by

$$I_{abc}^{(R)}(\lambda,\mu;j) = \frac{1}{(2\pi)^2R}\, d_a^{(R)}(\lambda;j)d_b^{(R)}(\mu;j)\overline{d_c^{(R)}(\lambda+\mu;j)}$$

where $d_a^{(R)}(\cdot;j)$, $d_b^{(R)}(\cdot;j)$ and $d_c^{(R)}(\cdot;j)$ are the Fourier-Steiltjes transforms of the jth section of processes N_a,N_b and N_c, respectively, and have been defined in Section 4.3.3 of Chapter 4.

Before we proceed on to the development of the point process quadratic model, we illustrate the application of the third order cross-spectrum $f_{abc}(\lambda,\mu)$ in order to demonstrate how this parameter may be interpreted in the assessment of third order non-linear interactive effects. Figs.6.4.1a,b,c give the second order auto spectra of three periodic spike trains at frequencies, respectively 10 Hz, 13 Hz, and 23 Hz. Figs.6.4.1d,e,f are the estimates of pairwise coherences (linear), and clearly suggest no significant linear association between any pair of them. Fig.6.4.1g is the modulus-squared of the estimated third order cross-spectrum, and is based on expression (6.4.2). A large and sharp peak at $(\lambda,\mu)=(10,13)$ Hz reveals that the interaction between the harmonics of processes N_a and N_b at frequencies, respectively, 10 and 13 Hz affects the harmonics of process N_c at frequency 23 Hz, and so the three processes are jointly interrelated even though no pair of these is linearly related.

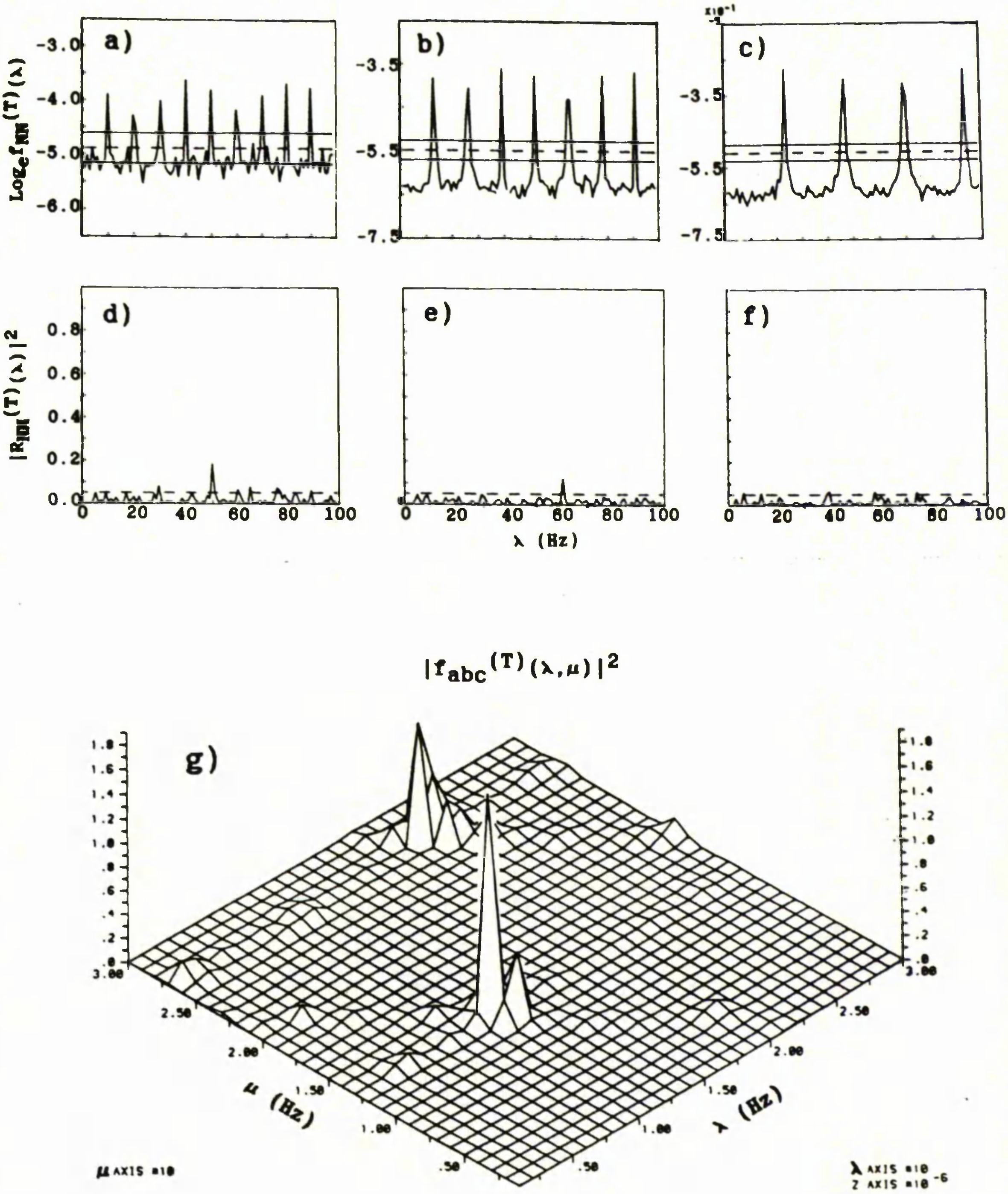

Fig.6.4.1 Illustration of third order frequency domain parameters

a,b,c) Log_e of the estimated second order auto-spectra of three periodic spike trains N_a, N_b, and N_c. The horizontal solid lines are the 95% confidence interval at a given frequency under the hypothesis that the process is Poisson.

d,e,f) Estimated pairwise coherences between N_a, N_b, and N_c. The dotted lines are the upper limits of the approximate 95% confidence intervals at a given frequency under the hypothesis of zero coherences.

g) Modulus-squared of the estimate of the third order corss-spectrum $f_{abc}(\lambda,\mu)$.

6.5 SINGLE-INPUT SINGLE-OUTPUT POINT PROCESS QUADRATIC MODEL

Let $\underline{N}(t)=\{N_1(t),N_2(t)\}$ be a stationary and orderly bivariate point process, corresponding to N_1 being input to the system with output N_2. Further suppose that the cumulants up to order-ℓ exist and satisfy the condition

$$\int\cdots\int |u_j|\,|q_{k_1k_2\ldots k_\ell}(u_1,u_2,\cdots,u_{\ell-1})|\,du_1du_2\cdots du_{\ell-1}<\infty$$

$k_1,k_2=1,2$, $\ell=2,3\ldots$, $j=1,2,\cdots,\ell-1$

The linear model discussed in Section 4.5.1 of Chapter 4 may be extended to a quadratic model in order to include the non-linear terms. To develop a model we proceed as follows:

Suppose that the input process N_1 corresponds to two events at times u_1 and u_2. In order to take into account the interaction between these events on the output N_2, the quantity given in expression (4.5.1) of Chapter 4 may be extended to

$$\mu_1(t) = \alpha_0+\alpha_1(t-u_1)+\alpha_1(t-u_2)+\alpha_2(t-u_1,t-u_2) \qquad (6.5.1)$$

where $\alpha_2(\cdot,\cdot)$ corresponds to the interactive effect of the two events on the output.

Similarly, if a number of events occurred at times $u_1,u_2,\cdots$, (6.5.1) becomes as

$$\begin{aligned}\mu_1(t) = {} & \alpha_0+\alpha_1(t-u_1)+\alpha_1(t-u_2)+\cdots \\ & +\alpha_2(t-u_1,t-u_2)+\alpha_2(t-u_1,t-u_3)+\cdots \\ & +\alpha_2(t-u_2,t-u_1)+\alpha_2(t-u_2,t-u_3)+\cdots \\ & +\cdots \end{aligned} \qquad (6.5.2)$$

Expression (6.5.2) may be written in more compact form as

$$\mu_1(t) = E\{dN_2(t)|N_1\}$$

$$=\alpha_0+\int\alpha_1(t-u)dN_1(u)+\iint\limits_{u\neq v}\alpha_2(t-u,t-v)dN_1(u)dN_1(v) \qquad (6.5.3)$$

The function $a_2(u,v)$ is called the second order kernel of the system, and gives the nonlinear effects of two input events occurring at two time instants u and v (see Krausz(1975) for more detail about physiological interpretation of this parameter).

Model (6.5.3) has been introduced and discussed in Brillinger(1975c).

6.5.1 SOLUTION OF THE MODEL

In order to solve (6.5.3) for α_0, $\alpha_1(\cdot)$ and $\alpha_2(\cdot\cdot\cdot)$, it is convenient to set it down in an alternative form.

Let $dN_1'(u)=dN_1(u)-P_1du$. Model (6.5.3) may now be written as

$$E\{dN_2(t)|N_1\}=s_0+\int s_1(t-u)dN_1'(u)+\iint\limits_{u\neq v}s_2(t-u,t-v)dN_1'(u)dN_1'(v) \qquad (6.5.4)$$

where the new parameters s_0, $s_1(\cdot)$, $s_2(\cdot\cdot\cdot)$ are connected with the old ones through the following relations

$$\alpha_0 = s_0-P_1\int s_1(u)du+P_1{}^2\iint\limits_{u\neq v}s_2(u,v)dudv \qquad (6.5.5)$$

$$\alpha_1(u) = s_1(u)-2P_1\int s_2(u,v)dv \qquad (6.5.6)$$

$$\alpha_2(u,v) = s_2(u,v) \tag{6.5.7}$$

Now taking expected value of (6.5.4) with respect to N_1, we obtain

$$P_2 = s_0+\iint_{u\neq v} s_2(u,v)q_{11}(u-v)dudv \tag{6.5.8}$$

Multiplying (6.5.4) by $dN_1{}'(t-w)$ and taking expected value, we obtain

$$q_{21}(w) = \int s_1(t-u)\left[q_{11}(u-t+w)+\delta(u-t+w)P_1\right]du$$

$$+\iint_{u\neq v} s_2(t-u,t-v)\left[q_{111}(u-t+w,v-t+w)+\delta(u-t+w)q_{11}(v-t+w)\right.$$

$$\left.+\delta(v-t+w)q_{11}(u-v)\right]dudv$$

$$= P_1s_1(w)+\int s_1(w-u)q_{11}(u)du+\iint_{u\neq v} s_2(w-u,w-v)q_{111}(u,v)dudv$$

$$+\int s_2(w,w-u)q_{11}(u)du+\int s_2(w-u,w)q_{11}(u)du \tag{6.5.9}$$

Multiplying (6.5.4) by $dN_1{}'(t-w)$ and $dN_1{}'(t-s)$ and taking expected value with respect to N_1, we get

$$q_{211}(s,s-w)+P_2q_{11}(s-w) =$$

$$s_0q_{11}(s-w)+\int s_1(t-u)\Big[q_{111}(u-t+s,s-w)+\delta(u-t+w)q_{11}(s-w)$$

$$+\delta(u-t+s)q_{11}(s-w)\Big]du+\int\int s_2(t-u,t-v)\Big[q_{1111}(u-t+s,v-t+s,s-w)$$

$$+\delta(v-t+w)q_{111}(u-t+s,s-w)+\delta(u-t+s)q_{111}(v-t+s,s-w)$$

$$+\delta(v-t+s)q_{111}(u-t+s,s-w)+\delta(u-t+w)\delta(v-t+s)q_{11}(u-t+s)$$

$$+\delta(v-t+w)\delta(u-t+s)q_{11}(s-w)+q_{11}(u-v)q_{11}(s-w)+q_{11}(u-t+w)q_{11}(v-t+s)$$

$$+P_1\delta(v-t+s)q_{11}(u-t+w0+P_1\delta(u-t+w)q_{11}(v-t+s)+P_1{}^2\delta(u-t+w)\delta(v-t+s)$$

$$+q_{11}(v-t+w)q_{11}(u-t+s)+P_1\delta(u-t+s)q_{11}(v-t+w)+P_1\delta(v-t+w)q_{11}(u-t+s)$$

$$P_1{}^2\delta(v-t+w)\delta(u-t+s)\Big]dudv$$

Substituting the value of s_0 from (6.5.8) and simplifying, we obtain

$$q_{211}(s,s-w) = \int s_1(s-u)q_{111}(u,s-w)du+s_1(w)q_{11}(s-w)+s_1(s)q_{11}(s-w)$$

$$+\iint_{u\neq v} s_2(s-u,s-v)q_{1111}(u,v,s-v)dudv+\int s_2(w,s-u)q_{111}(u,s-w)du$$

$$+\int s_2(s-u,w)q_{111}(u,s-w)du+\int s_2(s,s-u)q_{111}(u,s-w)du$$

$$+\int s_2(s-u,s)q_{111}(u,s-w)du+\iint_{u\neq v} s_2(w-u,s-v)q_{11}(u)q_{11}(v)dudv$$

$$+2s_2(w,s)q_{11}(s-w)+\iint\limits_{u\neq v} s_2(s-v,w-u)q_{11}(u)q_{11}(v)dudv$$

$$+P_1\int s_2(w-u,s)q_{11}(u)du+P_1\int s_2(w,s-u)q_{11}(u)du$$

$$+P_1\int s_2(w,s-u)q_{11}(u)du+P_1\int s_2(s,w-u)q_{11}(u)du$$

$$+P_1\int s_2(s-u,w)q_{11}(u)du+P_1{}^2s_2(w,s)+P_1{}^2s_2(s,w)$$

Setting s-w=t and since $s_2(u,v)=s_2(v,u)$, we have

$$q_{211}(s,t) = s_1(s-t)q_{11}(t)+s_1(s)q_{11}(t)+\int s_1(s-u)q_{111}(u,t)du$$

$$+\iint\limits_{u\neq v} s_2(s-u,s-v)q_{1111}(u,v,t)dudv+2\int s_2(s-t,s-u)q_{111}(u,t)du$$

$$+2\int s_2(s,s-u)q_{111}(u,t)du+2\iint\limits_{u\neq v} s_2(s-t-u,s-v)q_{11}(u)q_{11}(v)dudv$$

$$+2P_1\int s_2(s-t-u,s)q_{11}(u)du+2s_2(s-t,s)q_{11}(t)$$

$$+2P_1\int s_2(s-u,s-t)q_{11}(u)du+2P_1{}^2s_2(s-t,s) \qquad (6.5.10)$$

From equations (6.5.8)-(6.5.10), it is not all apparent how one can solve these for s_0, $s_1(\cdot)$, and $s_2(\cdot,\cdot)$. However, if we N_1 is chosen to be a Poisson process for which all the cumulants of order 2 or greater are identically zero, the system may be identified simply by

$$s_0 = P_2 \tag{6.5.11}$$

$$s_1(u) = q_{21}(u)/P_1 \tag{6.5.12}$$

$$s_2(u,v) = q_{211}(u,u-v)/2P_1{}^2 \tag{6.5.13}$$

6.5.2 MEAN SQUARED ERROR OF THE MODEL

For the mean squared error of the quadratic model (6.5.4), we define the following process with stationary increments

$$d\epsilon(t)=dN_2(t)-\left[s_0+\int s_1(t-u)dN_1'(u)+\iint_{u\neq v} s_2(t-u,t-v)dN_1'(u)dN_1'(v)\right]dt$$

where $E[dN_1'(t)] = E[d\epsilon(t)] = 0$

The cumulant density of process $\epsilon(t)$ at two time instants t and t' is defined as

$$q_{\epsilon\epsilon}(t-t')dtdt' = E[d\epsilon(t)d\epsilon(t')]-E[d\epsilon(t)]E[d\epsilon(t')]$$

$$=E\left\{dN_2(t)-\left[s_0+\int s_1(t-u)dN_1'(u)+\iint s_2(t-u,t-v)dN_1'(u)dN_2'(v)\right]dt\right\}$$

$$\left\{dN_2(t')-\left[s_0+\int s_1(t'-u)dN_1'(u)+\iint s_2(t'-u,t'-v)dN_1'(u)dN_1'(v)\right]dt'\right\}$$

$$= E\left\{dN_2(t)dN_2(t')\right\}-s_0E\left\{dN_2(t')\right\}dt-\int s_1(t-u)E\left\{dN_2(t')dN_1'(u)\right\}dt$$

$$-\iint s_2(t-u,t-v)E\left\{dN_2(t')dN_1'(u)dN_1'(v)\right\}dt$$

$$-s_0E\left\{dN_2(t)\right\}dt'+s_0 2dtdt'+s_0\int s_1(t-u)E\left\{dN_1'(u)\right\}dtdt'$$

$$+s_0\iint s_2(t-u,t-v)E\left\{dN_1'(u)dN_1'(v)\right\}dtdt'$$

$$-\int s_1(t'-u)E\left\{dN_2(t)dN_1'(u)\right\}dtdt'+s_0\int s_1(t'-u)E\left\{dN_1'(u)\right\}dtdt'$$

$$+\iint s_1(t-u)s_1(t'-w)E\left\{dN_1'(u)dN_1'(w)\right\}dtdt'$$

$$+\iiint s_1(t'-w)s_2(t-u,t-v)E\left\{dN_1'(w)dN_1'(u)dN_1(v)\right\}dtdt'$$

$$-\iint s_2(t'-u,t'-v)E\left\{dN_2(t)dN_1'(u)dN_1'(v)\right\}dtdt'$$

$$+s_0\iint s_2(t'-u,t'-v)E\left\{dN_1'(u)dN_1'(v)\right\}dtdt'$$

$$+\iiint s_1(t-w)s_2(t'-u,t'-v)E\left\{dN_1'(w)dN_1'(u)dN_1'(v)\right\}dtdt'$$

$$\begin{aligned}+\iiiint s_2(t-u,t-v)s_2(t'-w,t'-s)\Big[\Big\{&E[dN_1'(u)dN_1'(v)dN_1'(w)dN_1'(s)]\\ &-E[dN_1'(u)dN_1'(v)]E[dN_1'(w)dN_1'(s)]\\ &-E[dN_1'(u)dN_1'(w)]E[dN_1'(v)dN_1'(s)]\\ &-E[dN_1'(v)dN_1'(w)]E[dN_1'(u)dN_1'(s)]\Big\}\\ &+\Big\{E[dN_1'(u)dN_1'(v)]E[dN_1'(w)dN_1'(s)]\\ &+E[dN_1'(u)dN_1'(w)]E[dN_1'(v)dN_1'(s)]\\ &+E[dN_1'(v)dN_1'(w)]E[dN_1'(u)dN_1'(s)]\Big\}\Big]\end{aligned}$$

$q_{\epsilon\epsilon}(t-t')$

$$= P_{22}(t-t') + \delta(t-t')P_2 + s_0P_2 - \int s_1(t-u)q_{21}(t'-u)du$$

$$- \iint s_2(t-u,t-v)\left[P_{211}(t'-u,u-v)-P_1P_{21}(t'-u)-P_1P_{21}(t'-v)+P_2P_1{}^2\right]dudv$$

$$- s_0P_2 + s_0{}^2 + s_0\iint s_2(t-u,t-v)q_{11}(u-v)dudv$$

$$+ \iint s_1(t-u)s_1(t'-w)\left[q_{11}(u-w)+\delta(u-w)P_1\right]dwdu$$

$$+ \iiint s_1(t'-w)s_2(t-u,t-v)\left[q_{111}(w-v,u-v)+\delta(w-u)q_{11}(u-v)\right.$$

$$\left.+\delta(w-v)q_{11}(u-v)\right]dudvdw$$

$$+ \iint s_2(t'-u,t'-v)\left[P_{211}(t-u,u-v)-P_1P_{21}(t-u)-P_1P_{21}(t-v)+P_2P_1{}^2\right]dudv$$

$$+ s_0\iint s_2(t'-u,t'-v)q_{11}(u-v)dudv$$

$$+ \iiint s_1(t-w)s_2(t'-u,t'-v)\left[q_{111}(w-v,u-v)+\delta(w-u)q_{11}(w-v)\right.$$

$$\left.+\delta(w-v)q_{11}(w-u)\right]dudvdw$$

$$+ \iiiint s_2(t-u,t-v)s_2(t'-w,t'-s)\left[\left\{q_{1111}(u-s,v-s,w-s)\right.\right.$$

$$+\delta(u-w)q_{111}(v-s,w-s)+\delta(v-w)q_{111}(u-s,w-s)+\delta(u-s)q_{111}(v-s,w-s)$$

$$+\delta(v-s)q_{111}(u-s,w-s)+\delta(u-w)\delta(v-s)q_{11}(u-s)+\delta(v-w)(\delta(u-s)q_{11}(w-s)\Big\}$$

$$+\Big\{q_{11}(u-v)q_{11}(w-s)+[q_{11}(u-w)+\delta(u-w)P_1][q_{11}(v-s)+\delta(v-s)P_1]$$

$$+[q_{11}(v-w)+\delta(v-w)P_1][q_{11}(u-s)+\delta(u-s)P_1]\Big\}\Big]dsdwdudv$$

Substituting the value of s_0 from (6.5.8), and simplifying, we obtain

$$q_{\epsilon\epsilon}(t-t') = q_{22}(t-t')+\delta(t-t')P_2 - \int s_1(t-u)q_{21}(t'-u)du$$

$$- \iint s_2(t-u,t-v)q_{211}(t'-u,u-v)dudv - \int s_1(t'-u)q_{21}(t-u)du$$

$$+ \iint s_1(t-u)s_1(t'-w)q_{11}(u-w)dudw + P_1\int s_1(t-u)s_1(t'-u)du$$

$$+ \iiint s_1(t'-w)s_2(t-u,t-v)q_{111}(w-v,u-v)dudvdw$$

$$+ 2\iint s_1(t'-u)s_2(t-u,t-v)q_{11}(u-v)dudv$$

$$- \iint s_2(t'-u,t'-v)q_{211}(t-u,u-v)dudv$$

$$+ \iiint s_1(t-w)s_2(t'-u,t'-v)q_{111}(w-v,u-v)dudvdw$$

$$+ 2\iint s_1(t-u)s_2(t'-u,t'-v)q_{11}(u-v)dudv$$

$$+ \iiiint s_2(t-u,t-v)s_2(t'-w,t'-s)q_{1111}(u-s,v-s,w-s)dsdudvdw$$

$$+ 4\iiint s_2(t-u,t-v)s_2(t'-u,t'-w)q_{111}(v-w,u-w)dudvdw$$

$$+ 2\iint s_2(t-u,t-v)s_2(t'-u,t'-v)q_{11}(u-v)dudv$$

$$+ \iiiint s_2(t-u,t-v)s_2(t'-w,t'-s)q_{11}(u-v)q_{11}(w-s)dsdudvdw$$

$$+ 2\iiiint s_2(t-u,t-v)s_2(t'-w,t'-s)q_{11}(u-w)q_{11}(v-s)dsdudvdw$$

$$+ 2P_1\iiint s_2(t-u,t-v)s_2(t'-w,t'-v)q_{11}(u-w)dudvdw$$

$$+ 2P_1\iiint s_2(t-u,t-v)s_2(t'-u,t'-w)q_{11}(v-w)dudvdw$$

$$+ 2P_1^2\iint s_2(t-u,t-v)s_2(t'-v,t'-u)dudv$$

Above result holds in the case $N_1(t)$ being a general stationary point process. However, if $N_1(t)$ is is taken to be Poisson process for which the cumulants of order 2 or greater are identically zero, above expression reduces to

$$q_{\epsilon\epsilon}(t-t')$$

$$= q_{22}(t-t')+\delta(t-t')P_2 - \int s_1(t-u)q_{21}(t'-u)du - P_1\int s_1(t'-u)q_{21}(t-u)du$$

$$+ P_1\int s_1(t-u)s_1(t'-u)du - \iint s_2(t-u,t-v)q_{211}(t'-u,v-u)dudv$$

$$- \iint s_2(t'-u,t'-v)q_{211}(t-u,u-v)dudv$$

$$+ 2P_1{}^2 \iint s_2(t-u,t-v)s_2(t'-u,t'-v)dudv \qquad (6.5.13)$$

Substitution of the values of $s_1(\cdot)$ and $s_2(\cdot,\cdot)$ into expression (6.5.13) from (6.5.11)-(6.5.12), and a further simplification leads to

$$q_{\epsilon\epsilon}(t-t') = q_{22}(t-t')+\delta(t-t')P_2 - \frac{1}{P_1}\int q_{21}(t-u)q_{21}(t'-u)du$$

$$- \frac{1}{P_1{}^2}\iint q_{211}(t'-u,v-u)q_{211}(t-u,v-u)dudv$$

Setting $t-t'=w$, we have

$$q_{\epsilon\epsilon}(w) = q_{22}(w)+\delta(w)P_2 - \frac{1}{P_1}\int q_{21}(w+v)q_{21}(v)dv$$

$$- \frac{1}{2P_1{}^2}\iint q_{211}(w+u,v)q_{211}(u,v)dudv$$

$$= q_{22}(w)+\delta(w)P_2 - \frac{2\pi}{P_1}\int |f_{21}(\lambda_1)|^2 \exp(-i\lambda_1 w)d\lambda_1$$

$$- \frac{(2\pi)^2}{2P_1{}^2}\iint |f_{211}(\lambda_1,\lambda_2)|^2 \exp(-i\lambda_1 w)d\lambda_1 d\lambda_2 \qquad (6.5.14)$$

where $f_{21}(\lambda_1)$ is the cross spectrum of N_2 and N_1 at frequency λ_1 and $f_{211}(\lambda_1,\lambda_2)$ is the cross-bispectrum of output N_2 and input N_1 at frequencies λ_1 and λ_2, and has been discussed in Section 6.4.1

Now taking the Fourier transform of (6.5.14), we obtain

$$f_{\epsilon\epsilon}(\lambda) = f_{22}(\lambda) - \frac{|f_{21}(\lambda)|^2}{(P_1/2\pi)} - \frac{1}{2(P_1/2\pi)^2}\int |f_{211}(-\lambda,\mu)|^2 d\mu$$

or

$$f_{\epsilon\epsilon}(\lambda) = f_{22}(\lambda) - \frac{|f_{12}(\lambda)|^2}{(P_1/2\pi)} - \frac{1}{2(P_1/2\pi)^2}\int |f_{112}(\lambda-\mu,\mu)|^2 d\mu$$

$$= f_{22}(\lambda)\left\{1-\left[\frac{|f_{12}(\lambda)|^2}{(P_1/2\pi)f_{22}(\lambda)}+\frac{1}{2(P_1/2\pi)^2 f_{22}(\lambda)}\int |f_{112}(\lambda-\mu,\mu)|^2 d\mu\right]\right\}$$

Since N_1 is Poisson, i.e., $P_{11}(\lambda) = P_1/2\pi \quad -\infty < \lambda < \infty$, we can write the above expression as

$$f_{\epsilon\epsilon}(\lambda) = f_{22}(\lambda)\left\{1 - \text{Quad. Coh.}(\lambda)\right\} \tag{6.5.15}$$

where

$$\text{Quad. Coh.}(\lambda) = |R_{12}(\lambda)|^2 + \frac{1}{2(P_1/2\pi)^2 f_{22}(\lambda)}\int |f_{112}(\lambda-\mu,\mu)|^2 d\mu \tag{6.5.16}$$

The second term on the righ hand side of (6.5.16), may be called as the quadratic component of the quadratic coherence at frequency λ, gives a measure of the amount of quadratic effect the input N_1 has on the output N_2 at that frequency.

The inequality $0 \leq f_{\epsilon\epsilon}(\lambda) \leq f_{22}(\lambda)$ suggests that

$$0 \leq \text{Quad. Coh.}(\lambda) \leq 1$$

which implies that $f_{\epsilon\epsilon}(\lambda)$ at frequency λ will tend to zero as the quadratic coherence at that frequency tends to 1. Thus the quadratic coherence provides a measure of quadratic predictability of the output process N_2 from the input N_1.

Further, by analogy with the ordinary regression theory (i.e., fitting a second degree polynomial of Y on X ; e.g. Draper and Smith, 1981), expression (6.5.15) may be seen to be analogous with

$$R^2 = (\rho_{yx})^2 + (\rho_{yx^2.x})^2\{1-(\rho_{yx})^2\} \qquad (6.5.17)$$

where $(\rho_{yx^2.x})^2$ represents the quadratic contribution to the multiple correlation (R^2) allowing for the linear contribution.

6.5.3 ESTIMATION OF THE QUADRATIC COHERENCE

Based on the disjoint sections of the entire record, an estimate of the quadratic component of the quadratic coherence, given by

$$\text{Q.Comp.}(\lambda) = \frac{1}{2(P_1/2\pi)^2 P_{22}(\lambda)} \int_0^{\Omega} |f_{112}(\lambda-\mu,\mu)|^2 d\mu$$

where Ω is the Nyquist frequency (Hung et al, 1979), may be obtained by

$$\text{Q.Comp.}^{(T)}(\lambda_j) = \frac{1}{2(P_1/2\pi)^2 P_{22}(\lambda_j)R} \cdot \sum_{k=1}^{R/2} |f_{112}^{(T)}(\lambda_j-\mu_k,\mu_k)|^2 \qquad (6.5.18)$$

for $j = 0, 1, \cdots, (R/2)-1$. R is the record length of each section. $f_{112}^{(T)}(\cdot,\cdot)$ is the estimate of $f_{112}(\cdot,\cdot)$, and has been discussed in Section (6.4.2). R is the record length of each section.

The significance of the quadratic effects that the input has on the output may be assessed by constructing an asymptotic confidence interval for the estimate of the quadratic component of the quadratic coherence under the hypothesis of zero quadratic effects.

The construction of such interval requires an estimate of the variance of this estimate, and consequently this requires the development of second order properties of this estimate and its null distribution. An alternative possible way of constructing such interval may, however, be based on simulations.

6.5.4 APPLICATIONS

Figs.6.5.1 and 6.5.2 illustrate the application of the quadratic coherence of the Ia discharge with the static gamma inputs, ${}_1\gamma_s$ and ${}_2\gamma_s$. Before computing expression (6.5.18), the estimate $f_{112}^{(T)}(\lambda,\mu)$ is further smoothed with a two dimensional smoothing scheme of the following form

$$\hat{f}_{112}^{(T)}(\lambda_j,\mu_k) = \sum_{\ell=-1}^{+1}\ \sum_{m=-1}^{+1} a_{\ell m} f_{112}^{(T)}(\lambda_{j+\ell},\mu_{k+m}) \qquad (6.5.19)$$

for $\lambda_j=(2\pi j)/R$, $\mu_k=(2\pi k)/R$ $j,k=1,2,\cdots(R/2)$, R being the length of each disjoint segment. The weights a's satisfiy the condition $\Sigma\Sigma a_{\ell m}=1$.

Fig.6.5.1a gives an estimate of the quadratic component, based on estimate (6.5.19), of the quadratic coherence of two independent Poisson processes. Fig.6.5.1b correspond to the linear coherence of the Ia discharge with the static gamma input, ${}_1\gamma_s$. The horizontal dotted line in the figure gives the upper limit of the approximate 95% confidence interval for the coherence under the hypothesis that the two processes are independent. Fig.6.5.1c gives the estimate of quadratic component of the quadratic coherence of the

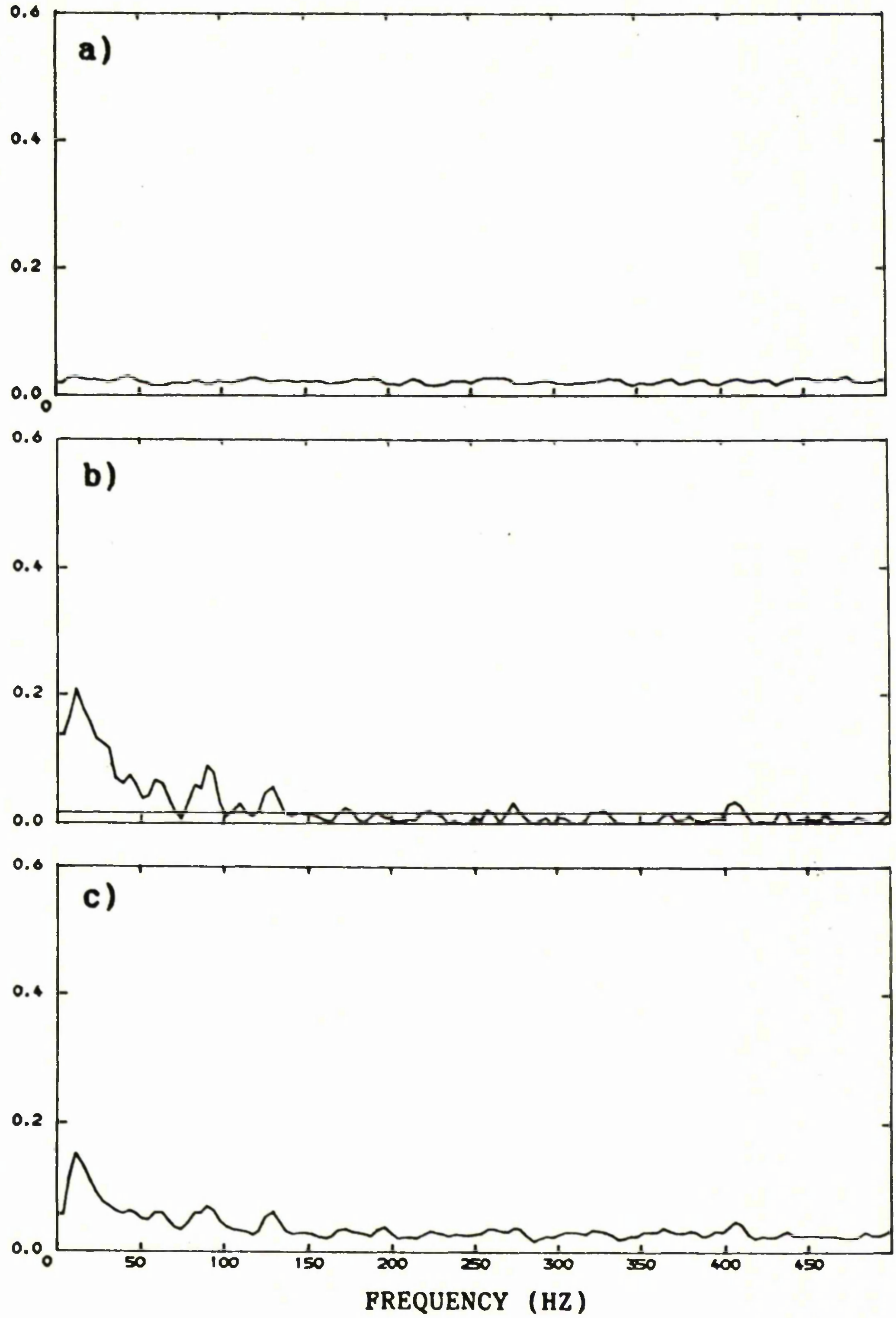

Fig.6.5.1 Application of the quadratic coherence

a) Estimated quadratic component of the quadratic coherence between two independent Poisson processes
b) Estimated linear coherence of the Ia discharge with the static gamma input, ${}_1\gamma_s$. The dotted line gives the upper limit of the approximate 95% confidence interval for the coherence under the hypothesis that the two processes are independent
c) Estimated quadratic component of the quadratic coherence of the Ia discharge with the static gamma input, ${}_1\gamma_s$

Ia discharge with the static gamma input, ${}_1\gamma_s$, and clearly suggests (compared with Fig.6.5.1a) the presence of quadratic effects that the static gamma input, ${}_1\gamma_s$, has on the Ia discharge at roughly the same frequencies where the linear coherence is significantly non-zero.

Fig.6.5.2 gives similar estimates as given by Fig.6.5.1 of the Ia discharge and the second static gamma input, ${}_2\gamma_s$. Fig.6.5.2.a is the quadratic component of the quadratic coherence of two independent Poisson processes. Fig.6.5.2b corresponds to the linear coherence of the Ia discharge with ${}_2\gamma_s$, and Fig.6.5.2.c represents the estimate of the quadratic component of the quadratic coherence of the Ia discharge with the 2nd static gamma input, ${}_2\gamma_s$. The peaks at low frequencies indicate possible significant quadratic effects of the ${}_2\gamma_s$ on to the Ia discharge.

The above results confirm the previous conclusions about the presence of non-linear features in the muscle spindle, obtained from Figs.6.2.4 and 6.2.5b. Further, a comparison of the Fig.6.5.1c with Fig.6.5.2c reveals that quadratic effects of ${}_1\gamma_s$ on the Ia discharge are relatively stronger than that of the ${}_2\gamma_s$ on the Ia discharge as compared to the correponding linear coherences.

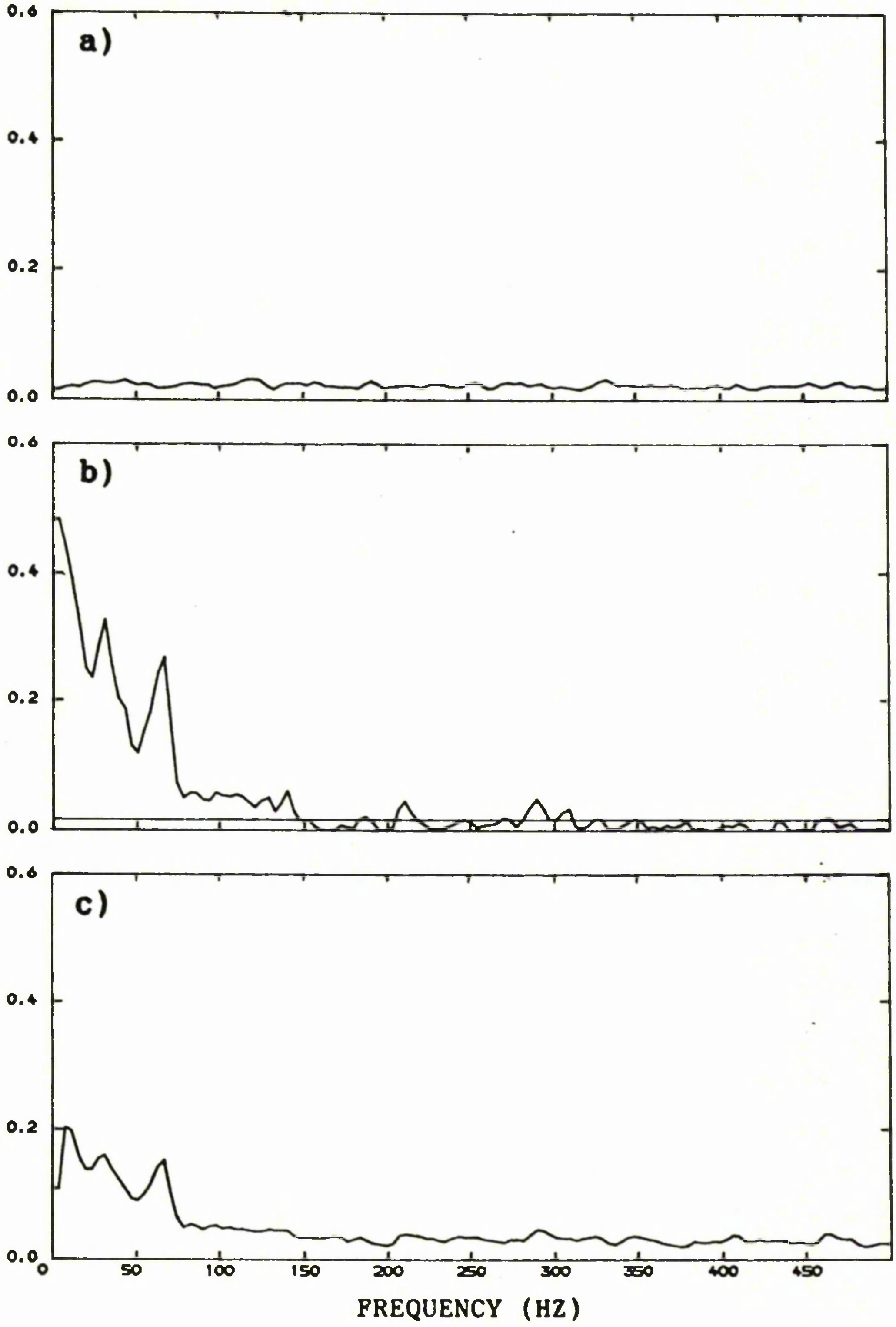

Fig.6.5.2 Application of the quadratic coherence

a) Estimated quadratic component of the quadratic coherence between two independent Poisson processes
b) Estimated linear coherence of the Ia discharge with the static gamma input, $_2\gamma_s$. The dotted line gives the upper limit of the approximate 95% confidence interval for the coherence under the hypothesis that the two processes are independent
c) Estimated quadratic component of the quadratic coherence of the Ia discharge with the static gamma input, $_2\gamma_s$

6.6 TWO-INPUTS SINGLE OUTPUT POINT PROCESS QUADRATIC MODEL

The quadratic model discussed in the previous section may easily be extended to a more complicated model in order to include one more input point process. The idea to develop such a model is to study the non-linear (quadratic) effects that both static gamma inputs jointly have on to the Ia discharge. Accounting for the interactive effects between the inputs M_1 and M_2, a quadratic model relating the output, N, to both inputs may be written as

$$E\{dN(t)|M_1,M_2\} = \Big\{S_0 + \int s_1(t-u)dM_1'(w) + \int s_2(t-w)dM_2'(w)$$

$$+ \iint s_{11}(t-u,t-v)dM_1'(u)dM_2'(v) + \iint s_{22}(t-u,t-v)dM_2'(u)dM_2'(v)$$

$$+ \iint s_{12}^*(t-u,t-v)dM_1'(u)dM_2'(v)\Big\}dt \qquad u \neq v \qquad (6.6.1)$$

where $s_{12}^*(\cdot,\cdot) = s_{21}^*(\cdot,\cdot) = s_{12}(\cdot,\cdot) + s_{21}(\cdot,\cdot)$ represents the effects of the interactions between the two inputs on the output (Marmarelis, 1975).

6.6.1 SOLUTION OF THE MODEL

Following the same procedure used to solve the model (6.5.3), the solution of (6.6.1) for s_0, $s_1(\cdot)$, $s_2(\cdot)$, $s_{11}(\cdot,\cdot)$, $s_{22}(\cdot,\cdot)$, and $s_{12}*(\cdot,\cdot)$ may be obtained as under:-

Take the expected value of (6.6.1) with respect to M_1 and M_2 to obtain

$$P_N = s_0 + \iint s_{11}(u,v)q_{M_1M_1}(u-v)dudv + \iint s_{22}(u,v)q_{M_2M_2}(u-v)dudv$$

$$+ \iint s_{12}*(u,v)q_{M_1M_2}(u-v)dudv \qquad (6.6.2)$$

Now multiplying (6.6.1) by $dM_1'(t-w)$ and taking the expected values with respect to M_1 and M_2, we obtain

$$q_{NM_1}(w) = \int s_1(t-u)\left[q_{M_1M_1}(u-t+w)+\delta(u-t+w)\right]du+\int s_2(t-u)q_{M_2M_1}(u-t+w)du$$

$$+\iint s_{11}(t-u,t-v)\left[q_{M_1M_1M_1}(u-t+w,v-t+w)+\delta(u-t+w)q_{M_1M_1}(v-t+w)\right.$$

$$\left.+\delta(v-t+w)q_{M_1M_1}(u-v)\right]dudv$$

$$+\iint s_{22}(t-u,t-v)q_{M_2M_2M_1}(u-t+w,v-t+w)dudv$$

$$+\iint s_{12}*(t-u,t-v)\left[q_{M_2M_1M_1}(v-t+w,u-t+w)+\delta(u-t+w)q_{M_2M_1}(v-u)\right]dudv \ .$$

A further simplification reduces the above expression to

$$q_{NM_1}(w) = P_{M_1}s_1(w) + \int s_1(w-u)q_{M_1M_1}(u)du + \int s_2(w-u)q_{M_2M_1}(u)du$$

$$+ \iint s_{11}(w-u,w-v)q_{M_1M_1M_1}(u,v)dud + 2\iint s_{11}(w,w-u)q_{M_1M_1}(u)du$$

$$+ \iint s_{22}(w-u,w-v)q_{M_2M_2M_1}(u,v)dudv + \iint s_{12}{}^{*}(w-u,w-v)q_{M_2M_1M_1}(v,u)dudv$$

$$+ \int s_{12}{}^{*}(w,w-v)q_{M_2M_1}(v)dv \quad . \qquad (6.6.3)$$

Similarly, multiplying (6.6.1) by $dM_2'(t-w)$ and taking the expected values with respect of M_1 and M_2, we obtain

$$q_{NM_2}(w) = \int s_1(w-u)q_{M_1M_2}(u)du + s_2(w)P_{M_2} + \int s_2(w-u)q_{M_2M_2}(w-u)du$$

$$+ \iint s_{11}(w-u,w-v)q_{M_1M_1M_2}(u,v)dudv + \iint s_{22}(w-u,w-v)q_{M_2M_2M_2}(u,v)dudv$$

$$+ 2\int s_{22}(w,w-v)q_{M_2M_2}(v)dv + \iint s_{12}{}^{*}(w-u,w-v)q_{M_1M_2M_2}(u,v)dudv$$

$$+ \int s_{12}{}^{*}(w-u,w)q_{M_1M_2}(u)du \qquad (6.6.4)$$

Now multiplying (6.6.1) by $dM_1'(t-w)dM_1'(t-s)$; $w \neq s$, and taking the expected values with respect of M_1 and M_2, we have

$$q_{NM_1M_1}(s,s-w)+P_N q_{M_1M_1}(s-w)$$

$$= s_0 q_{M_1M_1}(s-w) + \int s_1(t-u)\Big[q_{M_1M_1M_1}(u-t+s,s-w)+\delta(u-t+w)q_{M_1M_1}(s-w)$$

$$+\delta(u-t+s)q_{M_1M_1}(s-w)\Big]du + \int s_2(t-u)q_{M_2M_1M_1}(u-t+s,s-w)du$$

$$+\iint s_{11}(t-u,t-v)\Big[\Big\{q_{M_1M_1M_1M_1}(u-t+s,v-t+s,s-w)$$

$$+\delta(u-t+w)q_{M_1M_1M_1}(u-t+s,s-w)+\delta(v-t+w)q_{M_1M_1M_1}(u-t+s,s-w)$$

$$+\delta(u-t+s)q_{M_1M_1M_1}(v-t+s,s-w)+\delta(v-t+s)q_{M_1M_1M_1}(u-t+s,s-w)$$

$$+\delta(u-t+w)\delta(v-t+s)q_{M_1M_1}(u-t+s)+\delta(v-t+w)\delta(u-t+s)q_{M_1M_1}(s-w)\Big\}$$

$$+\Big\{q_{M_1M_1}(u-v)q_{M_1M_1}(s-w)+q_{M_1M_1}(u-t+w)q_{M_1M_1}(v-t+s)$$

$$+P_{M_1}\delta(v-t+s)q_{M_1M_1}(u-t+w)+P_{M_1}\delta(u-t+w)q_{M_1M_1}(v-t+s)$$

$$+P_{M_1}{}^2\delta(u-t+w)q_{M_1M_1}(v-t+s)+q_{M_1M_1}(v-t+w)q_{M_1M_1}(u-t+s)$$

$$+P_{M_1}\delta(u-t+s)q_{M_1M_1}(v-t+w)+P_{M_1}\delta(v-t+w)q_{M_1M_1}(u-t+s)$$

$$+P_{M_1}{}^2\delta(v-t+w)\delta(u-t+s)\Big\}\Big]dudv$$

$$+\iint s_{22}(t-u,t-v)\Big[q_{M_2M_2M_1M_1}(u-t+s,v-t+s,s-w)+q_{M_2M_2}(u-v)q_{M_1M_1}(s-w)$$

$$+q_{M_2M_1}(u-t+w)q_{M_2M_1}(v-t+s)+q_{M_2M_1}(v-t+w)q_{M_2M_1}(u-t+s)\Big]dudv$$

$$+\iint s_{12}{}^*(t-u,t-v)\Big[q_{M_2M_1M_1M_1}(v-t+s,u-t+s,s-w)$$

$$+\delta(u-t+s)q_{M_2M_1M_1}(v-t+s,s-w)+q_{M_2M_1}(v-u)q_{M_1M_1}(s-w)$$

$$+q_{M_2M_1}(v-t+w)q_{M_1M_1}(u-t+s)+P_{M_1}\delta(u-t+s)q_{M_2M_1}(v-t+w)$$

$$+q_{M_1M_1}(u-t+w)q_{M_2M_1}(v-t+s)+P_{M_1}\delta(u-t+w)q_{M_2M_1}(v-t+s)\Big]dudv$$

Substituting α_0, setting s-w=p and simplifying, we obtain

$$q_{NM_1M_1}(s,p)$$

$$= s_1(s-p)q_{M_1M_1}(p) + s_1(s)q_{M_1M_1}(p) + \int s_1(s-u)q_{M_1M_1M_1}(u,p)du$$

$$+ \int s_2(s-u)q_{M_2M_1M_1}(u,p)du + \iint s_{11}(s-u,s-v)q_{M_1M_1M_1M_1}(u,v,p)dudv$$

$$+ 2\iint s_{11}(s-p,s-u)q_{M_1M_1M_1}(u,p)du + 2\int s_{11}(s,s-u)q_{M_1M_1M_1}(u,p)du$$

$$+ \; 2\iint s_{11}(s-p-u,s-v)q_{M_1M_1}(u)q_{M_1M_1}(v)dudv$$

$$+ \; 2P_{M_1}\int s_{11}(s-p-u,s)q_{M_1M_1}(u)du \; + \; 2s_{22}(s-p,s)q_{M_1M_1}(p)$$

$$+ \; 2P_{M_1}\int s_{11}(s-u,s-p)q_{M_1M_1}(u)du \; + \; 2P_{M_1}{}^2 s_{11}(s-p,s)$$

$$+ \iint s_{22}(s-u,s-v)q_{M_2M_2M_1M_1}(u,v,p)dudv$$

$$+ \; 2\iint s_{22}(s-p-u,s-v)q_{M_2M_1}(u)q_{M_2M_1}(v)dudv$$

$$+ \iint s_{12}{}^*(s-u,s-v)q_{M_2M_1M_1M_1}(v,u,p)dudv$$

$$+ \int s_{12}{}^*(s,s-v)q_{M_2M_1M_1}(v,p)dv$$

$$+ \iint s_{12}{}^*(s-u,s-p-v)q_{M_2M_1}(v)q_{M_1M_1}(u)dudv$$

$$+ \iint s_{12}{}^*(s-p-u,s-v)q_{M_2M_1}(v)q_{M_1M_1}(u)dud$$

$$+ \; P_{M_1}\int s_{12}{}^*(s,s-p-v)q_{M_2M_1}(v)dv$$

$$+ \; P_{M_1}\int s_{12}{}^*(s-p,s-v)q_{M_2M_1}(v)dv \qquad (6.6.5)$$

Similarly, multiplying (6.6.1) by $dM_2'(t-w)dM_2'(t-s)$; $s \neq w$, taking expected values with respect to M_1 amd M_2, substituting the value of α_0, and making appropriate changes of variables as made to obtain (6.6.5), we get

$$q_{NM_2M_2}(s,p)$$

$$= s_2(s-p)q_{M_2M_2}(p) + s_2(s)q_{M_2M_2}(t) + \int s_1(s-u)q_{M_1M_2M_2}(u,p)du$$

$$+ \int s_2(s-u)q_{M_2M_2M_2}(u,p)dudv + \iint s_{11}(s-u,s-v)q_{M_1M_1M_2M_2}(u,v,p)dudv$$

$$+ 2\iint s_{11}(s-p-u,s-v)q_{M_1M_2}(u)q_{M_1M_2}(v)dudv$$

$$+ \iint s_{22}(s-u,s-v)q_{M_2M_2M_2M_2}(u,v,p)dudv$$

$$+ 2\int s_{22}(s-p,s-u)q_{M_2M_2M_2}(u,p)du + 2\int s_{22}(s-u,s)q_{M_2M_2M_2}(u,p)du$$

$$+ 2s_{22}(s-p,s)q_{M_2M_2}(t) + 2\iint s_{22}(s-p-u,s-v)q_{M_2M_2}(u)q_{M_2M_2}(v)dudv$$

$$+ 2P_{M_2}\int s_{22}(s-p-u,s)q_{M_2M_2}(u)du + 2P_{M_2}\int s_{22}(s-u,s-p)q_{M_2M_2}(u)du$$

$$+ 2P_{M_2}{}^2 s_{22}(s-p,s) + \iint s_{12}^*(s-u,s-v)q_{M_1M_2M_2M_2}(u,v,p)dudv$$

$$+ \int s_{12}^*(s-u,s-p)q_{M_1M_2M_2}(u,p)du + \int s_{12}^*(s-u,s)q_{M_1M_2M_2}(u,p)du$$

$$+ \iint s_{12}^{*}(s-p-u,s-v)q_{M_1M_2}(u)q_{M_2M_2}(v)dudv$$

$$+ P_{M_2}\int s_{12}^{*}(s-p-u,s)q_{M_1M_2}(u)du$$

$$+ \iint s_{12}^{*}(s-u,s-p-v)q_{M_2M_2}(v)q_{M_1M_2}(u)dudv$$

$$+ P_{M_2}\int s_{12}^{*}(s-u,s-p)q_{M_1M_2}(u)du \ . \qquad (6.6.6)$$

Finally, multiplying (6.6.1) by $dM_1'(t-w)dM_2'(t-s)$ and following the same steps as used to obtain (6.6.5) and (6.6.6), we have

$$q_{NM_1M_2}(s,p)$$

$$= s_1(s-p)q_{M_1M_2}(p) + \int s_1(s-u)q_{M_1M_1M_2}(u,p)du + s_2(s)q_{M_1M_2}(p)$$

$$+ \int s_2(s-u)q_{M_2M_1M_2}(u,p)du + \iint s_{11}(s-u,s-v)q_{M_1M_1M_1M_2}(u,v,p)dudv$$

$$+ 2\int s_{11}(s-p,s-p-u)q_{M_1M_2M_1}(u,p-s)du$$

$$+ \iint s_{11}(s-p-u,s-v)q_{M_1M_1}(u)q_{M_1M_2}(v)dudv$$

$$+ \iint s_{11}(s-u,s-p-v)q_{M_1M_1}(v)q_{M_1M_2}(u)dudv$$

$$+ 2P_{M_1}\int s_{11}(s-p,s-v)q_{M_1M_2}(v)dv + \iint s_{22}(s-u,s-v)q_{M_2M_2M_1M_2}(u,v,p)dudv$$

$$+ 2\int s_{22}(s,s-v)q_{M_2M_1M_2}(v,p)dv$$

$$+ \iint s_{22}(s-p-u,s-v)q_{M_2M_1}(u)q_{M_2M_2}(v)dudv$$

$$+ \iint s_{22}(s-u,s-p-v)q_{M_2M_1}(v)q_{M_2M_2}(u)dudv$$

$$+ 2P_{M_2}\int s_{22}(s,s-v)q_{M_2M_1}(u)du + \iint s_{12}*(s-u,s-v)q_{M_1M_2M_1M_2}(u,v,p)dudv$$

$$+ \int s_{12}*(s-p,s-v)q_{M_1M_2M_2}(p,v)dv + \int s_{12}*(s-u,s)q_{M_1M_1M_2}(u,p)du$$

$$+ s_{12}*(s-p,s)q_{M_1M_2}(t) + \iint s_{12}*(s-p-u,s-v)q_{M_1M_1}(u)q_{M_2M_2}(v)dudv$$

$$+ \iint s_{12}*(s-u,s-p-v)q_{M_2M_1}(v)q_{M_1M_2}(u)dudv$$

$$+ P_{M_2}\int s_{12}*(s-p-u,s)q_{M_1M_1}(u)du + P_{M_1}\int s_{12}*(s-p,s-v)q_{M_2M_2}(v)dv$$

$$+ P_{M_1}P_{M_2}s_{12}*(s-p,s) \qquad (6.6.7)$$

From expressions 6.6.2 to 6.6.7 , it is not all clear how to solve them for s_0, $s_1(\cdot)$, $s_2(\cdot)$, $s_{11}(\cdot,\cdot)$, $s_{22}(\cdot,\cdot)$, and $s_{12}*(\cdot,\cdot)$. However, if the inputs M_1 and M_2 are taken to be independent Poisson processes then all the cumulants for the processes M_1 and M_1 of order two or greater will identically be zero, and which lead to reduced expressions

$$P_N = s_0 \tag{6.6.8}$$

$$q_{NM_1}(w) = P_{M_1} s_1(w) \tag{6.6.9}$$

$$q_{NM_2}(w) = P_{M_2} s_2(w) \tag{6.6.10}$$

$$q_{NM_1M_1}(w,u) = 2P_{M_1} s_{11}(w-u,w) \tag{6.6.11}$$

$$q_{NM_2M_2}(w,u) = 2P_{M_2} s_{22}(w-u,w) \tag{6.6.12}$$

$$q_{NM_1M_2}(w,u) = P_{M_1} P_{M_2} s_{12}{}^*(w-u,w). \tag{6.6.13}$$

So the features of a non-linear (quadratic) system with a single output point process and two inputs (independent Poisson processes) may be identified by making a direct use of expressions (6.6.8)-(6.6.13).

6.7 SUMMARY AND CONCLUSIONS

In this chapter we have extended the linear point process identification procedures discussed in previous chapters to the case when the system is assumed to be non-linear.

The main features of this chapter are summarised as follows:

1. We first introduced and defined certain third order parameters in time domain. Their estimation was discussed, and asymptotic properties of these estimates were examined.
   The large sample properties of these estimates allowed to construct approximate asymptotic confidence intervals which provided a useful tool in the assessment of any significant non-linearities present in the underlying processes. The application of these procedures were demonstrated by a number of illustrations using first simulated data followed by the real data obtained on the muscle spindle. From the example, using simulated data, it is clear that the three time domain parameters, the third order product density, conditional and cumulant density functions provide different informations about the processes under investigation. The use of the product density or the conditional density on their own in order to assess the third order order non-linear effects could be misleading. The cumulant density is the one among these three which provides a measure of third order non-linear interactive effects of the processes. The results suggested a significant non-linear mechanism in the muscle spindles.
2. We further extended the third order (quadratic) time domain parameters to order-4 (cubic) in the hope to get more insight into the system. The examples, we demonstrated, clearly

suggested the usefulness of these procedures. These extensions will certainly help in further understanding about the neuromuscular control system. A difficulty in graphics, and consequently in interpreting the figures while going into higher dimensions might arise. But in the presence of a significant advancement in computers and computer graphics, this should not be a big problem. Recent developments in 4-D graphics may prove useful techniques in this connection.

3. We have also defined certain higher order parameters in the frequency domain, and illustrated by using simulated data which showed that in the absence of a linear association the processes could still be related in a quadratic fashion.
4. The linear model with single-input single-output point process, presented in Chapter 4, was extended to a quadratic one which led to the quadratic coherence as a measure of quadratic association between the two processes as well as a measure of predictability of the output from the input in a quadratic sense. The application of this measure confirmed the previous results obtained in the early part of this chapter about the non-linear features of the muscle spindle.
5. The final part of this chapter dealt with a non-linear system with two inputs and a single output. The model, studied in the previous section, was extended to include the second input process, and also taking into account the non-linear interactions between the two inputs. Under the assumption that the inputs are two independent Poisson processes, the model led to a simple solution involving the second and third order cross-cumulants between the output and inputs.

CHAPTER 7

FUTURE WORK

We, in the previous chapters, have provided an extensive development of statistical, mathematical, and computational procedures for treating multivariate point processes, identifying linear systems with multiple-input and multiple-output point processes, and measuring the association and timing relation between point processes. We also have made an attempt to carry out the identification of non-linear systems probed with Poisson processes. These procedures and their effectiveness have enabled us to answer a wide range of questions addressed in Chapter 1. However, there are many situations which arise in practice and require a further investigation about the underlying processes. For example, the effect of the length change, ℓ, under different conditions of other stimuli, on the sensory discharges from the same muscle spindle may be of interest.

The following list sets out several ways in which the work of this thesis may be extended.

1. Extend the point process models to include continuous inputs and outputs. This will involve, in part, the definition of hybrid parameters, such as covariance and cross-spectrum, as suggested by Jenkins(1963), between a continuous signal and a point process, and a consideration of their estimates and their properties.

2. Further investigation of higher order (order-4) cumulants and third order spectra and their applications.

3. Investigate the use of $Tr\{I-\underline{B}(\lambda)\}/s$ and $Det\{I-\underline{B}(\lambda)\}$, introduced in Chapter 5, in the analysis of neuronal networks. For example, can we determine if a particular neurone belongs to a network or if one neuronal network influences another.

4. Define and estimate partial parameters in the time domain, and compare them with the corresponding frequency domain ones, we developed and presented in this thesis. For example, partial product densities and partial cumulant densities together with the partial coherence and partial phase may provide a collection of powerful techniques in the assessment of connectivities and pattern of communication between the nerve cells.

5. Investigate the statistical properties of the estimate of the quadratic component of the quadratic coherence and construct appropriate confidence intervals for this parameter in order to assess the significance of the quadratic effects.

6. The idea of linear partial coherence may be extended to a higher order (non-linear) partial coherence. For example, the quadratic partial coherence may provide a useful tool in the assessment of connectivities between two nerve cells when they are assumed to be influenced by a third one in a quadratic fashion. Procedures for its estimation, and for appropriate confidence intervals must be developed.

APPENDIX I

Definition I.1 **INDECOMPOSABLE PARTITIONS**

Consider the following two way table

$$\begin{array}{cccc} (1,1) & (1,2) & \cdots & (1,J_1) \\ (2,1) & (2,2) & \cdots & (2,J_2) \\ \cdot & \cdot & \cdots & \cdot \\ \cdot & \cdot & \cdots & \cdot \\ \cdot & \cdot & \cdots & \cdot \\ (I,1) & (I,2) & \cdots & (I,J_I) \end{array} \qquad \text{I.1.A}$$

and a partition $P_1 \cup P_2 \cup \cdots \cup P_m$

We say that any two sets $P_{m'}$ and $P_{m''}$ of the partition **hook** if there exists $(i_1,j_1) \in P_{m'}$ and $(i_2,j_2) \in P_{m''}$ such that $i_1 = i_2$. We say that the sets $P_{m'}$ and $P_{m''}$ **communicate** if there exists a sequence of sets

$$P_{m'} = P_{m_1}, P_{m_2}, \cdots, P_{m_N} = P_{m''}$$

such that P_{m_n} and $P_{m_{n+1}}$ hook for n=1,2,...,N-1

We say that the partition is **indecomposable** if all sets communicate.

Example 1

suppose we have the following 4X4 table

(1,1)	(1,2)	(1,3)	(1,4)
(2,1)	(2,2)	(2,3)	(2,4)
(3,1)	(3,2)	(3,3)	(3,4)
(4,1)	(4,2)	(4,3)	(4,4)

One partition may be written as

$$\{(1,1),(1,2),(2,1)\} \cup \{(1,3),(2,2),(3,2),(2,4)\} \cup \{(1,4)\} \cup \{(2,3),(3,1),(3,4)\}$$

This partition contains 4 sets

$$P_1 = \{(1,1),(1,2),(2,1)\}$$

$$P_2 = \{(1,3),(2,2),(3,2),(2,4)\}$$

$$P_3 = \{(1,4)\}$$

$$P_4 = \{(2,3),(3,1),(3,3),(3,4)\}$$

Now P_1 and P_2 hook since for $(1,1)\epsilon P_1$ and $(1,3)\epsilon P_2$ first elements are identical. Similarly P_2 and P_3 hook, but P_3 and P_4 do not.

P_1 and P_2 communicate since they hook, and so do P_2 and P_3. P_3 and P_4 also communicate though they do not hook since for the sequence P_3, P_1, P_4 ; P_{m_n} and $P_{m_{n+1}}$ hook for n=1,2

Example 2

The partition

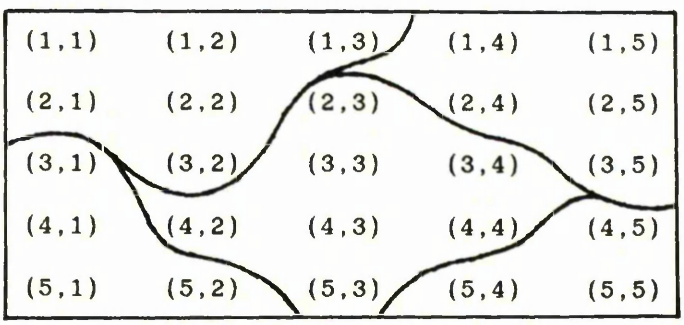

is an indecomposable, whereas

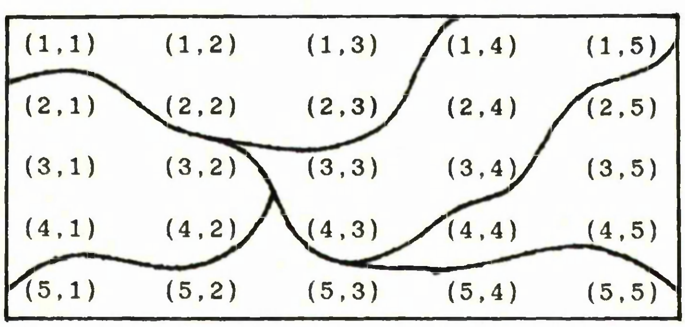

is not.

Definition I.2 **CUMULANTS**

Let $\underline{Y}=\{Y_1, Y_2, \cdots, Y_r\}$, where Y_k $(k=1,\cdots,r)$ are real or complex, be an r vector-valued random variable which satisfies the the condition

$$E|Y_k|^r < \infty \quad k=1,2,\cdots,r$$

The joint cumulant of order r, $\mathrm{cum}\{Y_1,Y_2,\cdots,Y_r\}$, of $\underline{Y}$ is defined as the coefficient of $(i)^r t_1\cdots t_r$ in the Taylor series expansion of

$$\log_e E[\exp\{i(Y_1t_1+\cdots+Y_rt_r)\}] \text{ about the origin}$$

and may be given by

$$\mathrm{cum}\{Y_1,Y_2,\cdots,Y_r\} = \Sigma\ (-1)^{p-1}(p-1)!\{E[\prod_{j=\nu_1} Yj]\} \cdots \{E[\prod_{j=\nu_p} Y_j]\}$$

where the summation extends over all partitions $(\nu_1,\cdots,\nu_p)$, $p=1,\cdots,r$ of the set $(1,\cdots,r)$

Cumulants provide measures of the joint statistical dependence of random variables and are useful tool for proving theorems. Cumulants are also known as semi-invariants (eg. Kendall and Stuart, 1958 ; Leonov and Shiryaev, 1959). Some of the properties of the cumulants include

i) $\mathrm{cum}\{a_1Y_1,\cdots,a_rY_r\} = a_1\cdots a_r\mathrm{cum}\{Y_1,\cdots,Y_r\}$

ii) $\mathrm{cum}\{Y_1,\cdots,Y_r\}$ is symmetric in its arguments

iii) If any subset of $(Y_1,\cdots,Y_r)$ is independent of the remaining Y's, then $\mathrm{cum}(Y_1,\cdots,Y_r) = 0$

iv) For the random variable $(Y_1,\cdots,Y_r,Z)$

$\mathrm{cum}\{Y_1,\cdots,Y_{r-1},Y_r+Z) = \mathrm{cum}\{Y_1,\cdots,Y_r) + \mathrm{cum}\{Y_1,\cdots,Y_{r-1},Z\}$

v) For some constant c and $r \geq 2$

$$\text{cum}\{Y_1+c, Y_2, \cdots, Y_r\} = \text{cum}\{Y_1, \cdots, Y_r\}$$

vi) If the random variables $(Y_1, \cdots, Y_r)$ and $(Z_1, \cdots, Z_r)$ are independent, then

$$\text{cum}\{Y_1+Z_1, \cdots, Y_r+Z_r\} = \text{cum}\{Y_1, \cdots, Y_r\} + \text{cum}\{Z_1, \cdots, Z_r\}$$

vii) $\text{cum}\{Y_k\} = E\{Y_k\}$; $k=1, \cdots, r$

viii) $\text{cum}\{Y_k, \bar{Y}_k\} = \text{var}\{Y_k\}$; $k=1, \cdots, r$

ix) $\text{cum}\{Y_k, \bar{Y}_\ell\} = \text{cov}\{Y_k, Y_\ell\}$; $k, \ell=1, \cdots, \ell$

The definition and properties of the cumulants of r vector-valued random variables can be found in Brillinger(1981), whereas the cumulants of univariate random variables are discussed in Kendall and Stuart(1966, Vol.1).

THEOREM I.1

Consider a two way table of random variables

$$X_{ij} \quad ; \; i=1,2,\cdots,I \; ; \; j=1,2,\cdots,J_i$$

Consider a set of I random variables

$$Y_i = \prod_{j=1}^{J_i} X_{ij} \qquad ; \; i=1,2,\cdots,I$$

The joint cumulant of Y_i ; $i=1,2,\cdots,I$ is given by

$$\text{cum}\{Y_1, Y_2, \cdots, Y_I\} = \sum_{\nu} \text{cum}\{X_{ij}, \; i,j \in \nu_1\} \cdots \text{cum}\{X_{ij}, \; i,j \in \nu_p\}$$

where the sum extends over all indecomposable partitions of the table I.1.A.

Proof:-

This theorem is given in Brillinger(1981) and its proof is a particular case of a result given by Leonov and Shiryaev(1959).

Example

Consider

$$\begin{matrix} X_{11} & X_{12} \\ X_{21} & X_{22} \end{matrix}$$

and define

$$Y_1 = X_{11}X_{12}$$

$$Y_2 = X_{21}X_{22}$$

All indecomposable partitions of (1,1), (1,2), (2,1), (2,2) are

{(1,1),(1,2),(2,1),(2,2)} , {(1,1)}{(1,2),(2,1),(2,2)}

{(1,2)}{(1,1),(2,1),(2,2)} , {(2,1)}{(1,1),(1,2),(2,2)}

{(2,2)}{(1,1),(1,2),(2,1)} , {(1,1),(2,1)}{(1,2),(2,2)}

{(1,1),(2,2)}{(2,1),(1,2)} , {(1,1)}{(2,1)}{(1,2),(2,2)}

{(1,1)}{(2,2)}{(2,1),(1,2)} , {(1,2)}{(2,2)}{(1,1),(2,1)}

{(1,2)}{(2,1)}{(1,1),(2,2)}

Therefore the cumulant of Y_1 and Y_2 is given as

$$\begin{aligned} \mathrm{cum}\{Y_1,Y_2\} = \; & \mathrm{cum}\{X_{11},X_{12},X_{21},X_{22}\} + \mathrm{cum}\{X_{11}\}\mathrm{cum}\{X_{12},X_{21},X_{22}\} \\ & + \mathrm{cum}\{X_{12}\}\mathrm{cum}\{X_{11},X_{21},X_{22}\} + \mathrm{cum}\{X_{21}\}\mathrm{cum}\{X_{11},X_{12},X_{22}\} \\ & + \mathrm{cum}\{X_{22}\}\mathrm{cum}\{X_{11},X_{12},X_{2}1\} + \mathrm{cum}\{X_{11},X_{21}\}\mathrm{cum}\{X_{12},X_{22}\} \\ & + \mathrm{cum}\{X_{11},X_{22}\}\mathrm{cum}\{X_{21},X_{12}\} + \mathrm{cum}\{X_{11}\}\mathrm{cum}\{X_{21}\}\mathrm{cum}\{X_{12},X_{22}\} \\ & + \mathrm{cum}\{X_{11}\}\mathrm{cum}\{X_{22}\}\mathrm{cum}\{X_{21},X_{12}\} \\ & + \mathrm{cum}\{X_{12}\}\mathrm{cum}\{X_{22}\}\mathrm{cum}\{X_{11},X_{21}\} \\ & + \mathrm{cum}\{X_{12}\}\mathrm{cum}\{X_{21}\}\mathrm{cum}\{X_{11},X_{22}\} \end{aligned}$$

Definition I.3

Let $\underline{N}(t)=\{N_1(t),N_2(t),\cdots,N_r(t)\}$, $t\in\mathbb{R}$, be an r vector-valued point process. Suppose that, for $t_1,t_2,\cdots,t_\ell$ real and distinct, the product density of order-ℓ given by

$$P_{a_1a_2\ldots a_\ell}(u_1,\cdots,u_\ell)=\text{Lim}_{h_1,h_2,\cdots,h_\ell\to 0}\Pr\{N_{a_1}\text{ event in }(t_1,t_1+h_1],\ N_{a_2}\text{ event in }(t_2,t_2+h_2],\ \ldots,\text{ and }N_{a_\ell}\text{ event in }(t_\ell,t_\ell+h_\ell]\}/h_1h_2\ldots h_\ell$$

$(a_1,\cdots,a_\ell=1,\cdots,r)$ exists. Then

$$E\{dN_{a_1}(t_1),\cdots,dN_{a_\ell}(t_\ell)\}$$

$$=\sum_{k=1}^{\ell}\sum_{\alpha_1,\ldots,\alpha_k=1}^{r}\left[\prod_{j\in\nu_1}\delta\{\alpha_1-a_j\}\right]\cdots\left[\prod_{j\in\nu_k}\delta\{\alpha_k-a_j\}\right]\left[\prod_{j\in\nu_1}\delta\{\tau_1-t_j\}\right]$$

$$\cdots\left[\prod_{j\in\nu_k}\delta\{\tau_\ell-t_j\}\right]P_{a_1\ldots a_k}(\tau_1,\cdots,\tau_k)d\tau_1\cdots d\tau_k$$

and

$$\text{cum}\{dN_{a_1}(t_1),\cdots,dN_{a_\ell}(t_\ell)\}$$

$$=\sum_{k=1}^{\ell}\sum_{\alpha_1,\ldots,\alpha_k=1}^{r}\left[\prod_{j\in\nu_1}\delta\{\alpha_1-a_j\}\right]\cdots\left[\prod_{j\in\nu_k}\delta\{\alpha_k-a_j\}\right]\left[\prod_{j\in\nu_1}\delta\{\tau_1-t_j\}\right]$$

$$\cdots\left[\prod_{j\in\nu_k}\delta\{\tau_\ell-t_j\}\right]q_{a_1\ldots a_k}(\tau_1,\cdots,\tau_k)d\tau_1\cdots d\tau_k$$

where the summation extends over all partitions $(\nu_1,\cdots,\nu_k)$ of the set $(1,\cdots,\ell)$, and $\delta\{\alpha\}=1$ if $\alpha=0$ and zero otherwise.

In relation to the product density functions we define the cumulant density function, $q_{a_1 \ldots a_\ell}(t_1, \ldots, t_\ell)$ as

$$q_{a_1 \ldots a_\ell}(t_1, \cdots, t_\ell) = \sum_{\alpha=1}^{\ell} (-1)^{\ell-1}(\ell-1)! \left[P_{a_j}(t_j); j \epsilon \nu_1\right] \ldots \left[P_{a_j}(t_j); t \epsilon \nu_\alpha\right]$$

with the inverse relation

$$P_{a_1 \ldots a_\ell}(t_1, \cdots, t_\ell) = \sum_{\alpha=1}^{\ell} \left[q_{a_j}(t_j); j \epsilon \nu_1\right] \ldots \left[q_{a_j}(t_j); t \epsilon \nu_\alpha\right]$$

where the summation extends over all partitions $(\nu_1, \cdots, \nu_\alpha)$ of the set $(1, \cdots, \ell)$

The above definitions are particular cases of more general situations when random interval functions are considered (e.g., Brillinger, 1972).

THEOREM I.2

Let $\{N_1(t), \cdots, N_r(t)\}$ be a r vector-valued stationary point process on $(0,T]$ with P_k , $k=1,\cdots,r$ the mean intensity and $q_{k\ell}(u)$, $k=1,\cdots,r$ the second order cumulant density function which satisfies the condition

$$\int |q_{k\ell}(u)|du < \infty$$

Let the periodogram be given by

$$I_{k\ell}^{(T)}(\lambda) = \frac{1}{2\pi T} d_k^{(T)}(\lambda)\overline{d_\ell^{(T)}(\lambda)} \qquad k,\ell=1,\cdots,r \qquad -\infty<\lambda<\infty \tag{I.1}$$

where

$$d_k^{(T)}(\lambda) = \int_0^T \exp(-i\lambda t)dN_k(t) \tag{I.2}$$

then

$$E\{I_{k\ell}^{(T)}(\lambda)\} = \frac{1}{2\pi T}\int\left[\frac{\sin(\lambda-\alpha)T/2}{(\lambda-\alpha)/2}\right]^2 f_{k\ell}(\alpha)d\alpha + \frac{P_kP_\ell}{2\pi T}\left[\frac{\sin\lambda T/2}{\lambda/2}\right]$$

Proof:-

$$E\{I_{k\ell}^{(T)}\} = \frac{1}{2\pi T}\int_0^T\int_0^T \exp\{-i(t-s)\lambda\}E\{dN_k(t)dN_\ell(s)\}$$

$$= \frac{1}{2\pi T}\int_0^T\int_0^T \exp\{-i(t-s)\}q_{k\ell}(t-s)dtds + \frac{P_kP_\ell}{2\pi T}\int_0^T\int_0^T \exp\{-i(t-s)\}dtds$$

setting t-s=u and s=v, we obtain

$$E\{I_{k\ell}^{(T)}(\lambda)\}=\frac{1}{2\pi T}\int_{-T}^{0}\int_{-u}^{T}\exp\{-i\lambda u\}q_{k\ell}(u)dudv+\frac{1}{2\pi T}\int_{0}^{T}\int_{0}^{T-u}\exp\{-i\lambda u\}q_{k\ell}(u)dudv$$

$$+\frac{P_kP_\ell}{2\pi T}\int_{-T}^{0}\int_{-u}^{T}\exp\{-i\lambda u\}dudv+\frac{P_kP_\ell}{2\pi T}\int_{0}^{T}\int_{0}^{T-u}\exp\{-i\lambda u\}dudv$$

$$=\frac{1}{2\pi T}\int_{-T}^{0}(T+u)\exp\{-i\lambda u\}\left\{\int_{-\infty}^{\infty}\exp\{i\alpha u\}f_{k\ell}(\alpha)d\alpha\right\}du$$

$$+\frac{1}{2\pi T}\int_{0}^{T}(T-u)\exp\{-i\lambda u\}\left\{\int_{-\infty}^{\infty}\exp\{i\alpha u\}f_{k\ell}(\alpha)d\alpha\right\}du$$

$$+\frac{P_kP_\ell}{2\pi T}\int_{-T}^{0}(T+u)\exp\{-i\lambda u\}du+\frac{P_kP_\ell}{2\pi T}\int_{0}^{T}(T-u)\exp\{-i\lambda u\}du$$

$$=\frac{1}{2\pi T}\int_{-\infty}^{\infty}\left\{\int_{0}^{T}(T-u)\exp\{i(\lambda-\alpha)u\}du+\int_{0}^{T}(T-u)\exp\{-i(\lambda-\alpha)u\}du\right\}f_{k\ell}(\alpha)d\alpha$$

$$+\frac{P_kP_\ell}{2\pi T}\left\{\int_{0}^{T}(T-u)\exp\{i\lambda u\}du+\int_{0}^{T}(T-u)\exp\{-i\lambda u\}du\right\}$$

$$=\frac{1}{2\pi T}\int_{-\infty}^{\infty}\left\{\int_{0}^{T}(T-u)2\cos(\lambda-\alpha)udu\right\}f_{k\ell}(\alpha)d\alpha+\frac{P_kP_\ell}{2\pi T}\int_{0}^{T}(T-u)2\cos\lambda udu$$

$$E\{I_{k\ell}^{(T)}(\lambda)\} = \frac{1}{2\pi T} \int_{-\infty}^{\infty} \frac{2}{(\lambda-\alpha)^2}\left[1-\cos(\lambda-\alpha)T\right] f_{k\ell}(\alpha)d\alpha + \frac{2P_kP_\ell}{2\pi T\lambda^2}\left[1-\cos\lambda T\right]$$

$$= \frac{1}{2\pi T} \int_{-\infty}^{\infty} \left[\frac{\sin(\lambda-\alpha)T/2}{(\lambda-\alpha)/2}\right]^2 f_{k\ell}(\alpha)d\alpha + \frac{P_kP_\ell}{2\pi T}\left[\frac{\sin\lambda T/2}{\lambda/2}\right]^2$$

COROLLARY I.2

Under the assumption of Theorem I.2 and if

$$\int |u|\,|q_{k\ell}(u)|\,du < \infty$$

then

$$E\{I_{k\ell}^{(T)}(\lambda)\} = f_{k\ell}(\lambda) + O(T^{-1})$$

Proof:-

The proof follows similarly as that of Theorem I.2, and by applying Lemma I.1.

Assumption I.1

Let $\underline{N}(t)=\{N_1(t),\cdots,N_r(t)\}$ be a stationary point process satisfying the conditions of (strong) mixing and orderliness, and defined on (0,T]. Further, suppose that the cumulant density function of order ℓ, $q_{k_1\ldots k_\ell}(u_1,\cdots,u_{\ell-1})$, exists and satisfies the condition

$$\int \cdots \int |u_j|\,|q_{k_1\ldots k_\ell}(u_1,\cdots,u_{\ell-1})du_1\cdots du_{\ell-1} < \infty$$

for $j=1,\cdots,\ell-1$; $k_1,\cdots,k_\ell=1,\cdots,r$

Lemma I.1

Let $\underline{N}(t)=\{N_1,\cdots,N_r\}$ be an r vector valued stationary point process defined on (0,T] and satisfies the conditions of (strong) mixing and orderliness. Further, suppose that the cumulant function of order ℓ exists and satisfies assumption I.1.

Let $d_{k_1}{}^{(T)}(\lambda_1)$, $\cdots$, $d_{k_\ell}{}^{(T)}(\lambda_\ell)$ be the Fourier transforms as given by expression (I.2). Then (Brillinger, 1981; Rigas,1983)

$$\text{cum}\{d_{k_1}{}^{(T)}(\lambda_1),\cdots,d_{k_\ell}{}^{(T)}(\lambda_\ell)\}$$

$$= (2\pi)^{\ell-1}\Delta^{(T)}\{\Sigma\lambda_j\}f_{k_1\ldots k_\ell}(\lambda_1,\ldots,\lambda_{\ell-1}) + O(1)$$

for $k_1,\cdots,k_\ell=1,\cdots,r$; where

$$\Delta^{(T)}\{\Sigma\lambda_j\} = \int_0^T \exp\{-i(\lambda_1+\cdots+\lambda_\ell)t\}dt$$

THEOREM I.3

Let $\underline{N}(t)=\{N_1(t),\cdots,N_r(t)\}$ be an r vector-valued stationary point process defined on $(0,T]$ with P_{k_1}; $k_1=1,\cdots,r$ the mean intensity and $q_{k_1\ell_1}(u)$; $k_1,\ell_1=1,\cdots,r$ the cumulant function which satisfies the condition

$$\int |u||q_{k_1\ell_1}(u)|du < \infty$$

Then for the periodogram given by the expression (I.1), we have

$$\mathrm{cov}\{I_{k_1\ell_1}{}^{(T)}(\lambda),I_{k_2\ell_2}{}^{(T)}(\mu)\}$$

$$=\frac{1}{T^2}\Big\{|\Delta^{(T)}(\lambda-\mu)|^2 f_{k_1k_2}(\lambda)f_{\ell_1\ell_2}(-\lambda)$$

$$+|\Delta^{(T)}(\lambda+\mu)|^2 f_{k_1\ell_2}(\lambda)f_{\ell_1k_2}(-\lambda)\Big\}+O(T^{-1})$$

where

$$\Delta^{(T)}(\lambda) = \int_0^T \exp(-i\lambda t)dt$$

Proof:-

From the definition of the periodogram, and the properties of the cumulants

$$\mathrm{cov}\{I_{k_1\ell_1}{}^{(T)}(\lambda),I_{k_2\ell_2}{}^{(T)}(\mu)\}$$

$$=\frac{1}{(2\pi T)^2}\mathrm{cum}\Big\{d_{k_1}{}^{(T)}(\lambda)d_{\ell_1}{}^{(T)}(-\lambda),d_{\ell_2}{}^{(T)}(\mu)d_{k_2}{}^{(T)}(-\mu)\Big\}$$

$$\operatorname{cov}\{I_{k_1\ell_1}^{(T)}(\lambda), I_{k_2\ell_2}^{(T)}(\mu)\}$$

$$= \frac{1}{(2\pi T)^2}\Big\{\operatorname{cum}\{d_{k_1}^{(T)}(\lambda), d_{\ell_1}^{(T)}(-\lambda), d_{\ell_2}^{(T)}(\mu), d_{k_2}^{(T)}(-\mu)\}$$

$$+\operatorname{cum}\{d_{k_1}^{(T)}(\lambda)\}\operatorname{cum}\{d_{\ell_1}^{(T)}(-\lambda), d_{\ell_2}^{(T)}(\mu), d_{k_2}^{(T)}(-\mu)\}$$

$$+\operatorname{cum}\{d_{\ell_1}^{(T)}(-\lambda)\}\operatorname{cum}\{d_{k_1}^{(T)}(\lambda), d_{\ell_2}^{(T)}(\mu), d_{k_2}^{(T)}(-\mu)\}$$

$$+\operatorname{cum}\{d_{k_2}^{(T)}(-\mu)\}\operatorname{cum}\{d_{k_1}^{(T)}(\lambda), d_{\ell_1}^{(T)}(-\lambda), d_{\ell_2}^{(T)}(\mu)\}$$

$$+\operatorname{cum}\{d_{\ell_2}^{(T)}(\mu)\}\operatorname{cum}\{d_{k_1}^{(T)}(\lambda), d_{\ell_1}^{(T)}(\lambda), d_{k_2}^{(T)}(-\mu)\}$$

$$+\operatorname{cum}\{d_{k_1}^{(T)}(\lambda), d_{k_2}^{(T)}(-\mu)\}\operatorname{cum}\{d_{\ell_1}^{(T)}(-\lambda), d_{\ell_2}^{(T)}(\mu)\}$$

$$+\operatorname{cum}\{d_{k_1}^{(T)}(\lambda), d_{\ell_2}^{(T)}(\mu)\}\operatorname{cum}\{d_{\ell_1}^{(T)}(-\lambda), d_{k_2}^{(T)}(-\mu)\}$$

$$+\operatorname{cum}\{d_{k_1}^{(T)}(\lambda)\}\operatorname{cum}\{d_{k_2}^{(T)}(-\mu)\}\operatorname{cum}\{d_{\ell_1}^{(T)}(-\lambda), d_{\ell_2}^{(T)}(\mu)\}$$

$$+\operatorname{cum}\{d_{k_1}^{(T)}(\lambda)\}\operatorname{cum}\{d_{\ell_2}^{(T)}(\mu)\}\operatorname{cum}\{d_{\ell_1}^{(T)}(-\lambda), d_{k_2}^{(T)}(-\mu)\}$$

$$+\operatorname{cum}\{d_{\ell_1}^{(T)}(-\lambda)\}\operatorname{cum}\{d_{\ell_2}^{(T)}(\mu)\}\operatorname{cum}\{d_{k_1}^{(T)}(\lambda), d_{k_2}^{(T)}(-\mu)\}$$

$$+\operatorname{cum}\{d_{\ell_1}^{(T)}(-\lambda)\}\operatorname{cum}\{d_{k_2}^{(T)}(-\mu)\}\operatorname{cum}\{d_{k_1}^{(T)}(\lambda), d_{\ell_2}^{(T)}(\mu)\}\Big\}$$

Substituting the values of the cumulants from lemma I.1 and simplifying, we obtain the required result

$$\operatorname{cov}\{I_{k_1\ell_1}^{(T)}(\lambda), I_{k_2\ell_2}^{(T)}(\mu)\}$$

$$= \frac{|\Delta^{(T)}(\lambda-\mu)|^2}{T^2} f_{k_1k_2}(\lambda) f_{\ell_1\ell_2}(-\lambda) + \frac{|\Delta^{(T)}(\lambda+\mu)|^2}{T^2} f_{k_1\ell_2}(\lambda) f_{\ell_1k_2}(-\lambda) + O(T^{-1})$$

$$= \left[\frac{\sin(\lambda-\mu)T/2}{T(\lambda-\mu)/2}\right]^2 f_{k_1k_2}(\lambda) f_{\ell_1\ell_2}(-\lambda) + \left[\frac{\sin(\lambda+\mu)T/2}{T(\lambda+\mu)/2}\right]^2 f_{k_1\ell_2}(\lambda) f_{\ell_1k_2}(-\lambda) + O(T^{-1})$$

Assumption I.2

Let $K(\alpha)$, $-\infty < \alpha < \infty$, be a real-valued and even function of bounded variation with

$$\int_{-\infty}^{\infty} K(\alpha)\,d\alpha = 1 \qquad \text{and} \qquad \int_{-\infty}^{\infty} |K(\alpha)|\,d\alpha < \infty$$

THEOREM I.4

Let $\underline{N}(t)$ be an r vector-valued point process defined on (0,T]. Suppose that the cumulants up to order ℓ exist and satisfy the assumption I.1.

Let $f_{k_1\ell_1}{}^{(T)}(\lambda)$ be an estimate of the spectrum of the processes N_{k_1} and N_{ℓ_1} for $k_1, \ell_1 = 1, \cdots, r$ given by

$$f_{k_1\ell_1}{}^{(T)}(\lambda) = \int K_{k_1\ell_1}{}^{(T)}(\lambda-\alpha) I_{k_1\ell_1}{}^{(T)}(\alpha)\,d\alpha$$

where $I_{k_1\ell_1}{}^{(T)}(\lambda)$ is the periodogram given by expression I.1.
The function $K^{(T)}(\alpha)$, defined by

$$K_{k_1\ell_1}{}^{(T)}(\alpha) = (b_T)^{-1} K_{k_1\ell_1}(b_T{}^{-1}\alpha)$$

is called the spectral window with b_T the bandwidth of the estimate, and the function $K_{k_1\ell_1}(\cdot)$ satisfies the assumption I.2.
Then if $b_T \to 0$ and $b_T T \to \infty$ as $T \to \infty$, we have

(i) $\quad \text{Lim}_{\,T\to\infty}\ E\{f_{k_1\ell_1}{}^{(T)}(\lambda)\} = f_{k_1\ell_1}(\lambda)$

and

(ii) $\quad \text{Lim}_{\,T\to\infty}\ b_T T\ \text{cov}\{f_{k_1\ell_1}{}^{(T)}(\lambda), f_{k_2\ell_2}{}^{(T)}(\mu)\}$

$$= \left[\delta\{\lambda-\mu\} f_{k_1k_2}(\lambda) f_{\ell_1\ell_2}(-\lambda) + \delta\{\lambda+\mu\} f_{k_1\ell_2}(\lambda) f_{\ell_1k_2}(-\lambda)\right]$$

$$2\pi \int K_{k_1\ell_1}(\beta) K_{k_2\ell_2}(\beta)\,d\beta$$

where $\delta\{\alpha\}=1$ if $\alpha=0$ and zero otherwise.

Proof:-

(i)

$$E\{f_{k_1\ell_1}^{(T)}(\lambda)\} = (b_T)^{-1}\int K_{k_1\ell_1}\left[b_T^{-1}(\lambda-\alpha)\right]E\{I_{k_1\ell_1}^{(T)}(\alpha)\}d\alpha$$

Substituting the value of $E\{I_{k_1\ell_1}^{(T)}(\alpha)\}$ from Corollary I.2

$$E\{f_{k_1\ell_1}^{(T)}(\lambda)\} = (b_T)^{-1}\int K_{k_1\ell_1}\left[b_T^{-1}(\lambda-\alpha)\right]f_{k_1\ell_1}(\alpha)d\alpha + O(b_T^{-1}T^{-1})$$

$$= (b_T)^{-1}\int K_{k_1\ell_1}(\lambda-\beta b_T)b_T d\beta + O(b_T^{-1}T^{-1})$$

Under the limiting conditions of $b_T\to 0$, $b_T T\to\infty$ as $T\to\infty$, above expression reduces to the required result, i.e.,

$$\text{Lim}_{\,T\to\infty}\; E\{f_{k_1\ell_1}^{(T)}(\lambda)\} = f_{k_1\ell_1}(\lambda) \quad ; \quad k_1,\ell_1=1,\cdots,r$$

(ii)

$$\text{cov}\{f_{k_1\ell_1}^{(T)}(\lambda), f_{k_2\ell_2}^{(T)}(\mu)\}$$

$$=b_T^{-2}\left\{\iint K_{k_1\ell_1}\left[b_T^{-1}(\lambda-\alpha_1)\right]K_{k_2\ell_2}\left[b_T^{-1}(\mu-\alpha_2)\right]\right.$$

$$\left.\text{cov}\{I_{k_1\ell_1}^{(T)}(\alpha_1), I_{k_2\ell_2}^{(T)}(\alpha_2)\}\right\}d\alpha_1 d\alpha_2$$

From Theorem I.3, it implies that

$$\mathrm{cov}\{f_{k_1\ell_1}{}^{(T)}(\lambda), f_{k_2\ell_2}{}^{(T)}(\mu)\}$$

$$= b_T{}^{-2}\iint K_{k_1\ell_1}\left[b_T{}^{-1}(\lambda-\alpha_1)\right]K_{k_2\ell_2}\left[b_T{}^{-1}(\mu-\alpha_2)\right]$$

$$\left[\frac{\sin(\alpha_1-\alpha_2)T/2}{T(\alpha_1-\alpha_2)/2}\right]^2 f_{k_1k_2}(\alpha_1)f_{\ell_1\ell_2}(-\alpha_1)d\alpha_1 d\alpha_2$$

$$+b_T{}^{-2}\iint K_{k_1\ell_1}\left[b_T{}^{-1}(\lambda-\alpha_1)\right]K_{k_2\ell_2}\left[b_T{}^{-1}(\mu-\alpha_2)\right]$$

$$\left[\frac{\sin(\alpha_1+\alpha_2)T/2}{T(\alpha_1+\alpha_2)/2}\right]^2 f_{k_1\ell_2}(\alpha_1)f_{\ell_1k_2}(-\alpha_2)+O(T^{-1})+O(b_T{}^{-2}T^{-2})$$

Setting $\beta_1=b_T{}^{-1}(\lambda-\alpha_1)$, $\beta_2=\alpha_1-\alpha_2$ in the first term ; and $\beta_1=b_T{}^{-1}(\lambda-\alpha_1)$, $\beta_2=\alpha_1+\alpha_2$ in the second term of the above expression, we obtain,

$$\mathrm{cov}\{f_{k_1\ell_1}{}^{(T)}(\lambda), f_{k_2\ell_2}{}^{(T)}(\mu)\}$$

$$= b_T{}^{-1}T^{-2}\iint K_{k_1\ell_1}\left[\beta_1\right]K_{k_2\ell_2}\left[b_T{}^{-1}(\mu-\lambda+\beta_2)+\beta_1\right]$$

$$\left[\frac{\sin\beta_2 T/2}{\beta_2/2}\right]^2 f_{k_1k_2}(\lambda-b_T\beta_1)f_{\ell_1\ell_2}(-\lambda+b_T\beta_1)d\beta_1 d\beta_2$$

$$+b_T^{-1}T^{-2}\iint K_{k_1\ell_1}\left[\beta_1\right]K_{k_2\ell_2}\left[b_T^{-1}(\mu+\lambda-\beta_2)+\beta_1\right]$$

$$\left[\frac{\sin\beta_2 T/2}{\beta_2/2}\right]^2 f_{k_1\ell_2}(\lambda-\beta_1 b_T)f_{\ell_1 k_2}(-\lambda+\beta_1 b_T)+O(T^{-1})+O(b_T^{-2}T^{-2})$$

Now as $T\to\infty$, $\frac{1}{2\pi T}\left[\frac{\sin\beta_2 T/2}{\beta_2/2}\right]^2\to\delta(\beta_2)$ (Papoulis, 1962), and we have

$$\operatorname{Lim}_{T\to\infty}\ b_T T\ \operatorname{cov}\{f_{k_1\ell_1}{}^{(T)}(\lambda),f_{k_2\ell_2}{}^{(T)}(\mu)\}$$

$$=2\pi\iint K_{k_1\ell_1}\left[\beta_1\right]K_{k_2\ell_2}\left[\beta_1\right]\delta\{\lambda-\mu-\beta_2\}\delta(\beta_2)f_{k_1k_2}(\lambda)f_{\ell_1\ell_2}(-\lambda)d\beta_1 d\beta_2$$

$$+\ 2\pi\iint K_{k_1\ell_1}\left[\beta_1\right]K_{k_2\ell_2}\left[\beta_1)\right]\delta\{\lambda+\mu-\beta_2\}\delta(\beta_2)f_{k_1\ell_2}(\lambda)f_{\ell_1k_2}(-\lambda)d\beta_1 d\beta_2$$

or

$$\operatorname{Lim}_{T\to\infty}\ b_T T\ \operatorname{cov}\{f_{k_1\ell_1}{}^{(T)}(\lambda),f_{k_2\ell_2}{}^{(T)}(\mu)\}$$

$$=\left\{\delta\{\lambda-\mu\}f_{k_1k_2}(\lambda)f_{\ell_1\ell_2}(-\lambda)\ +\ \delta\{\lambda+\mu\}f_{k_1\ell_2}(\lambda)f_{\ell_1k_2}(-\lambda)\right\}$$

$$2\pi\int K_{k_1\ell_1}(\beta)K_{k_2\ell_2}(\beta)d\beta$$

In the case that the same window (taper), $K^{(T)}(\cdot)$, is used then the above expression is further reduced to

$$\operatorname{Lim}_{T\to\infty}\ b_T T \operatorname{cov}\{f_{k_1\ell_1}{}^{(T)}(\lambda), f_{k_2\ell_2}{}^{(T)}(\mu)\}$$

$$= \left\{\delta\{\lambda-\mu\} f_{k_1k_2}(\lambda) f_{\ell_1\ell_2}(-\lambda) + \delta\{\lambda+\mu\} f_{k_1\ell_2}(\lambda) f_{\ell_1k_2}(-\lambda)\right\} 2\pi \int K^2(\beta)\,d\beta$$

THEOREM I.5

Let $\underline{N}(t)=\{N_1, N_2, \cdots, N_r\}$ be an r-vector valued stationary point process satisfying the conditions of (strong) mixing and orderliness. Let $q_{k_1k_2\ldots k_\ell}(u_1,u_2,\ldots,u_{\ell-1})$ be the ℓth order cumulant density function satisfying assumption I.1

Further, suppose that the estimate of the coherence $|R_{ab}(\lambda)|^2$ at frequency λ $(a,b=N_1, N_2, \cdots, N_r)$ is given by

$$R_{ab}^{(T)}(\lambda) = \frac{f_{ab}^{(T)}(\lambda)}{[f_{aa}^{(T)}(\lambda)f_{bb}^{(T)}(\lambda)]^{\frac{1}{2}}} \tag{I.3}$$

where

$$f_{ab}^{(T)}(\lambda) = \int K^{(T)}(\lambda-\alpha)I_{ab}^{(T)}(\alpha)d\alpha \tag{I.4}$$

The function $K^{(T)}(\cdot)$ is the spectral window with

$$K^{(T)}(\alpha) = b_T K(b_T^{-1}\alpha)$$

where $K(\cdot)$ satisfies the assumption I.2. The parameter b_T is the bandwidth of the estimate. Then the estimates $R_{ab}^{(T)}(\lambda)$, $\lambda\neq0$, $(a,b=N_1,N_2,\cdots,N_r)$ given by expression (I.3) are asymptotically jointly normal with

$$E\{R_{ab}^{(T)}(\lambda)\} = R_{ab}(\lambda) + O(b_T) + O(b_T^{-1}T^{-1}) \tag{I.5}$$

$$\begin{aligned}\operatorname{cov}\{R_{ab}^{(T)}(\lambda),R_{cd}^{(T)}(\lambda)\} = \Big[&R_{ac}R_{db} - \tfrac{1}{2}R_{dc}R_{ac}R_{cb} - \tfrac{1}{2}R_{dc}R_{ad}R_{db} \\ &- \tfrac{1}{2}R_{ab}R_{ac}R_{da} - \tfrac{1}{2}R_{ab}R_{bc}R_{db} + \tfrac{1}{4}R_{ab}R_{dc}R_{ac}R_{ca} \\ &+ \tfrac{1}{4}R_{ab}R_{dc}R_{ad}R_{da} + \tfrac{1}{4}R_{ab}R_{dc}R_{bc}R_{cb} \\ &+ \tfrac{1}{4}R_{ab}R_{dc}R_{bd}R_{db}\Big](b_T T)^{-1}2\pi\int K^2(\alpha)d\alpha + O(b_T^{-2}T^{-2})\end{aligned} \tag{I.6}$$

Proof:- The proof of this Theorem can be seen in Brillinger(1981)

THEOREM I.6

Let $\underline{N}(t)$ be an r-vector valued point process. Further, let the estimate of the coherence $|R_{ab}(\lambda)|^2$ at frequency λ be given by

$$|R_{ab}^{(T)}(\lambda)|^2 = \frac{|f_{ab}^{(T)}(\lambda)|^2}{f_{aa}^{(T)}(\lambda)f_{bb}^{(T)}(\lambda)} \qquad \lambda\neq 0 \qquad (I.7)$$

where the spectral estimate $f_{ab}^{(T)}(\lambda)$ is given by expression (I.4).

Under the conditions of Theorem I.5, we have

$$E\{|R_{ab}^{(T)}(\lambda)|^2\} = |R_{ab}(\lambda)|^2 + O(b_T) + O(b_T^{-1}T^{-1})$$

$$\begin{aligned}\mathrm{cov}\{|R_{ab}^{(T)}(\lambda)|^2, |R_{cd}^{(T)}(\lambda)|^2\} = \Big[&R_{ab}R_{dc}R_{bd}R_{ca} + R_{ba}R_{dc}R_{ad}R_{cb} \\ &+ R_{ab}R_{cd}R_{bc}R_{da} + R_{ba}R_{cd}R_{ac}R_{db} \\ &- |R_{cd}|^2\Big\{R_{ab}R_{bd}R_{da}+R_{ab}R_{bc}R_{ca}+R_{ba}R_{ad}R_{db}+R_{ba}R_{ac}R_{cb}\Big\} \\ &- |R_{ab}|^2\Big\{R_{dc}R_{bd}R_{cd}+R_{dc}R_{ad}R_{ca}+R_{cd}R_{bc}R_{db}+R_{cd}R_{ac}R_{da}\Big\} \\ &+|R_{ab}|^2|R_{cd}|^2\Big\{|R_{bd}|^2+|R_{bc}|^2+|R_{ad}|^2+|R_{ac}|^2\Big\}\Big]2\pi\int K^2(\alpha)d\alpha(b_TT)^{-1} \\ &+ O(b_T^{-2}T^{-2})\end{aligned}$$

$$\mathrm{var}\{|R_{ab}^{(T)}(\lambda)|^2\} = |R_{ab}|^2\Big[1 - |R_{ab}|^2\Big]^2 4\pi\int K^2(\alpha)d\alpha(b_TT)^{-1} + O(b_T^{-2}T^{-2})$$

where the dependence on λ on the right hand side of the above equations has been suppressed for convenience.

Proof:-

From Theorem I.1, and the asymptotic normality of $R_{ab}^{(T)}$ $(a,b=N_1,N_2,\cdots,N_r)$, it follows that

$$\mathrm{cov}\{|R_{ab}{}^{(T)}|^2, |R_{cd}{}^{(T)}|^2\} = \mathrm{cum}\{|R_{ab}{}^{(T)}|^2, |R_{cd}{}^{(T)}|^2\}$$

$$= \mathrm{cum}\{R_{ab}{}^{(T)}R_{ba}{}^{(T)}, R_{cd}{}^{(T)}R_{dc}{}^{(T)}\}$$

$$= \mathrm{cum}\{R_{ab}{}^{(T)}, R_{cd}{}^{(T)}\}\mathrm{cum}\{R_{ba}{}^{(T)}, R_{dc}{}^{(T)}\}$$
$$+ \mathrm{cum}\{R_{ab}{}^{(T)}, R_{dc}{}^{(T)}\}\mathrm{cum}\{R_{ba}{}^{(T)}, R_{cd}{}^{(T)}\}$$
$$+ \mathrm{cum}\{R_{ab}{}^{(T)}\}\mathrm{cum}\{R_{dc}{}^{(T)}\}\mathrm{cum}\{R_{ba}{}^{(T)}, R_{cd}{}^{(T)}\}$$
$$+ \mathrm{cum}\{R_{ba}{}^{(T)}\}\mathrm{cum}\{R_{dc}{}^{(T)}\}\mathrm{cum}\{R_{ab}{}^{(T)}, R_{cd}{}^{(T)}\}$$
$$+ \mathrm{cum}\{R_{ab}{}^{(T)}\}\mathrm{cum}\{R_{cd}{}^{(T)}\}\mathrm{cum}\{R_{ba}{}^{(T)}, R_{dc}{}^{(T)}\}$$
$$+ \mathrm{cum}\{R_{ba}{}^{(T)}\}\mathrm{cum}\{R_{cd}{}^{(T)}\}\mathrm{cum}\{R_{ab}{}^{(T)}, R_{dc}{}^{(T)}\}$$

Now from the properties of the cumulants (Definition I.2), we have

$$\mathrm{cov}\{|R_{ab}{}^{(T)}|^2, |R_{cd}{}^{(T)}|^2\} = \mathrm{Cov}\{R_{ab}{}^{(T)}, R_{dc}{}^{(T)}\}\mathrm{cov}\{R_{ba}{}^{(T)}, R_{cd}{}^{(T)}\}$$
$$+ \mathrm{cov}\{R_{ab}{}^{(T)}, R_{cd}{}^{(T)}\}\mathrm{cov}\{R_{ba}{}^{(T)}, R_{dc}{}^{(T)}\}$$
$$+ E\{R_{ab}{}^{(T)}\}E\{R_{dc}{}^{(T)}\}\mathrm{cov}\{R_{ba}{}^{(T)}, R_{dc}{}^{(T)}\}$$
$$+ E\{R_{ba}{}^{(T)}\}E\{R_{dc}{}^{(T)}\}\mathrm{cov}\{R_{ab}{}^{(T)}, R_{dc}{}^{(T)}\}$$
$$+ E\{R_{ab}{}^{(T)}\}E\{R_{cd}{}^{(T)}\}\mathrm{cov}\{R_{ba}{}^{(T)}, R_{cd}{}^{(T)}\}$$
$$+ E\{R_{ba}{}^{(T)}\}E\{R_{cd}{}^{(T)}\}\mathrm{cov}\{R_{ab}{}^{(T)}, R_{cd}{}^{(T)}\} .$$

Substituting the expected values and the covariances from expressions (I.5) and (I.6) into above equation.

$$\mathrm{cov}\{R_{ab}{}^{(T)}, R_{dc}{}^{(T)}\} = \Big[R_{ad}R_{cb} - \tfrac{1}{2}R_{cd}R_{ad}R_{db} - \tfrac{1}{2}R_{cd}R_{ac}R_{cb} - \tfrac{1}{2}R_{ab}R_{ad}R_{ca}$$
$$- \tfrac{1}{2}R_{ab}R_{bd}R_{cb} + \tfrac{1}{4}R_{ac}R_{cd}R_{ad}R_{da} + \tfrac{1}{4}R_{ab}R_{cd}R_{bd}R_{ca}$$
$$+ \tfrac{1}{4}R_{ab}R_{cd}R_{bd}R_{db} + \tfrac{1}{4}R_{ab}R_{cd}R_{bc}R_{cb}\Big]\Big[2\pi\int K^2(\alpha)d\alpha(b_T T)^{-1}\Big]$$
$$+ O(b_T{}^{-2}T^{-2})$$

$$= A_I O(b_T{}^{-1}T^{-1}) + O(b_T{}^{-2}T^{-2}) \quad \text{(say)} \qquad (I.8)$$

$$\mathrm{cov}\{|R_{ab}^{(T)}|^2, |R_{cd}^{(T)}|^2\}$$

$$=\left[A_1 O(b_T^{-1}T^{-1})+O(b_T^{-2}T^{-2})\right]\left[A_2 O(b_T^{-1}T^{-1})+O(b_T^{-2}T^{-2})\right]$$

$$+\left[A_3 O(b_T^{-1}T^{-1})+O(b_T^{-2}T^{-2})\right]\left[A_4 O(b_T^{-1}T^{-1})+O(b_T^{-2}T^{-2})\right]$$

$$+\left[R_{ab}+O(b_T)+O(b_T^{-1}T^{-1})\right]\left[R_{dc}+O(b_T)+O(b_T^{-1}T^{-1})\right]\left[A_4 O(b_T^{-1}T^{-1})+O(b_T^{-2}T^{-2})\right]$$

$$+\left[R_{ba}+O(b_T)+O(b_T^{-1}T^{-1})\right]\left[R_{dc}+O(b_T)+O(b_T^{-1}T^{-1})\right]\left[A_1 O(b_T^{-1}T^{-1})+O(b_T^{-2}T^{-2})\right]$$

$$+\left[Rab+O(b_T)+O(b_T^{-1}T^{-1})\right]\left[R_{cd}+O(b_T)+O(b_T^{-1}T^{-1})\right]\left[A_2 O(b_T^{-1}T^{-1})+O(b_T^{-2}T^{-2})\right]$$

$$+\left[R_{ba}+O(b_T)+O(b_T^{-1}T^{-1})\right]\left[R_{cd}+O(b_T)+O(b_T^{-1}T^{-1})\right]\left[A_3 O(b_T^{-1}T^{-1})+O(b_T^{-2}T^{-2})\right]$$

where $A_2, A_3, \ldots$ have the similar definition as A_1 in (I.8). A further simplification of the above expression produces

$$\mathrm{cov}\{|R_{ab}^{(T)}|^2, |R_{cd}^{(T)}|^2\} = \Big[R_{ab}R_{dc}A_4+R_{ba}R_{dc}A_1+R_{ab}R_{cd}A_2$$

$$+ R_{ba}R_{cd}A_3\Big]2\pi\int K^2(\alpha)d\alpha(b_T T)^{-1} + O(b_T^{-2}T^{-2})$$

Substitution of the values of A_1, A_2 etc. gives

$$\mathrm{cov}\{|R_{ab}^{(T)}|^2, |R_{cd}^{(T)}|^2\} = \Big\{R_{ab}R_{dc}R_{bd}R_{ca}-\tfrac{1}{2}R_{ab}|R_{cd}|^2R_{bd}R_{da}$$

$$- \tfrac{1}{2}R_{ab}|R_{cd}|^2R_{bc}R_{ca} -\tfrac{1}{2}|R_{ab}|^2R_{dc}R_{bd}R_{c}-\tfrac{1}{2}|R_{ab}|^2R_{dc}R_{ad}R_{ca}$$

$$+ \tfrac{1}{4}|R_{ab}|^2|R_{cd}|^2|R_{bc}|^2+\tfrac{1}{4}|R_{ab}|^2|R_{cd}|^2|R_{bd}|^2$$

$$+ \tfrac{1}{4}|R_{ab}|^2|R_{cd}|^2|R_{ad}|^2+\tfrac{1}{4}|R_{ab}|^2|R_{cd}|^2|R_{ac}|^2$$

$$+ R_{ba}R_{dc}R_{ad}R_{cb}-\tfrac{1}{2}R_{ba}|R_{cd}|^2R_{ad}R_{db}-\tfrac{1}{2}R_{ba}|R_{cd}|^2R_{ac}R_{cb}$$

$$- \tfrac{1}{2}|R_{ab}|^2R_{dc}R_{ad}R_{ca}-\tfrac{1}{2}|R_{ab}|^2R_{dc}R_{bd}R_{cb}$$

$$+ \tfrac{1}{4}|R_{ab}|^2|R_{cd}|^2|R_{ad}|^2+\tfrac{1}{4}|R_{ab}|^2|R_{cd}|^2|R_{ac}|^2$$

$$+ \tfrac{1}{4}|R_{ab}|^2|R_{cd}|^2|R_{bd}|^2+\tfrac{1}{4}|R_{ab}|^2|R_{cd}|^2|R_{bc}|^2$$

$$+ R_{ab}R_{cd}R_{bc}R_{da}-\tfrac{1}{2}R_{ab}|R_{cd}|^2R_{bc}R_{ca}-\tfrac{1}{2}R_{ab}|R_{cd}|^2R_{bd}R_{da}$$

$$- \tfrac{1}{2}|R_{ab}|^2R_{cd}R_{bc}R_{db}-\tfrac{1}{2}|R_{ab}|^2R_{cd}R_{ac}R_{da}$$

$$+ \tfrac{1}{4}|R_{ab}|^2|R_{cd}|^2|R_{bc}|^2+\tfrac{1}{4}|R_{ab}|^2|R_{cd}|^2|R_{bd}|^2$$

$$+ \tfrac{1}{4}|R_{ab}|^2|R_{cd}|^2|R_{ac}|^2+\tfrac{1}{4}|R_{ab}|^2|R_{cd}|^2|R_{ad}|^2$$

$$+ R_{ba}R_{cd}R_{ac}R_{db}-\tfrac{1}{2}R_{ba}|R_{cd}|^2R_{ac}R_{cb}-\tfrac{1}{2}R_{ba}|R_{cd}|^2R_{ad}R_{db}$$

$$- \tfrac{1}{2}|R_{ab}|^2R_{cd}R_{ac}R_{da}-\tfrac{1}{2}|R_{ab}|^2R_{cd}R_{bc}R_{db}$$

$$+ \tfrac{1}{4}|R_{ab}|^2|R_{cd}|^2|R_{ac}|^2+\tfrac{1}{4}|R_{ab}|^2|R_{cd}|^2|R_{ad}|^2$$

$$+ \tfrac{1}{4}|R_{ab}|^2|R_{cd}|^2|R_{bc}|^2+\tfrac{1}{4}|R_{ab}|^2|R_{cd}|^2|R_{bd}|^2\Big\}2\pi\int K^2(\alpha)d\alpha(b_TT)^{-1}$$

$$+ O(b_T{}^{-2}T^{-2})$$

A further little algebraic manipulation leads to the required result

$$\mathrm{cov}\{|R_{ab}{}^{(T)}|^2,|R_{cd}{}^{(T)}|^2\} = \Big[R_{ab}R_{dc}R_{bd}R_{ca}+R_{ba}R_{dc}R_{ad}R_{cb}$$

$$+ R_{ab}R_{cd}R_{bc}R_{da} + R_{ba}R_{cd}R_{ac}R_{db}$$

$$-|R_{cd}|^2\Big\{R_{ab}R_{bd}R_{da}+R_{ab}R_{bc}R_{ca}+R_{ba}R_{ad}R_{db}+R_{ba}R_{ac}R_{cb}\Big\}$$

$$-|R_{ab}|^2\Big\{R_{dc}R_{bd}R_{cb}+R_{dc}R_{ad}R_{ca}+R_{cd}R_{bc}R_{db}+R_{cd}R_{ac}R_{da}\Big\}$$

$$+|R_{ab}|^2|R_{cd}|^2\Big\{|R_{bd}|^2+|R_{bc}|^2+|R_{ad}|^2+|R_{ac}|^2\Big\}\Big]2\pi\int K^2(\alpha)d\alpha(b_TT)^{-1}$$

$$+O(b_T{}^{-2}T^{-2}) \qquad (I.9)$$

Now for the variance, we set c=a , d=b in expression (I.9) which reduces to

$$\mathrm{var}\{|R_{ab}^{(T)}|^2\} = \Big[2|R_{ab}|^2 - 4|R_{ab}|^2|R_{ab}|^2$$

$$+ 2|R_{ab}|^2|R_{ab}|^2|R_{ab}|^2\Big]2\pi(b_T^{-1}T^{-1})\int K^2(\alpha)d\alpha$$

$$+ O(b_T^{-2}T^{-2})$$

$$= |R_{ab}|^2\Big[1 - |R_{ab}|^2\Big]^2 4\pi\int K^2(\alpha)d\alpha(b_T^{-1}T^{-1})$$

$$+ O(b_T^{-2}T^{-2}) \qquad \text{(I.10)}$$

COROLLARY I.6.1

Under the conditions of Theorem I.6 and if $b_T \to 0$, $b_T T \to \infty$ as $T \to \infty$, we have, for $\lambda \neq 0$,

$$\lim_{T\to\infty} E\{|R_{ab}^{(T)}(\lambda)|^2\} = |R_{ab}(\lambda)|^2$$

$$\lim_{T\to\infty} b_T T\,\mathrm{cov}\{|R_{ab}^{(T)}(\lambda)|^2, |R_{cd}^{(T)}(\lambda)|^2\}$$

$$= \Big[R_{ab}R_{dc}R_{bd}R_{ca}+R_{ba}R_{dc}R_{ad}R_{cb}$$

$$+ R_{ab}R_{cd}R_{bc}R_{da}+R_{ba}R_{cd}R_{ac}R_{db}$$

$$+ |R_{cd}|^2\Big\{R_{ab}R_{bd}R_{da}+R_{ab}R_{bc}R_{ca}+R_{ba}R_{ad}R_{db}+R_{ba}R_{ac}R_{cb}\Big\}$$

$$+ |R_{ab}|^2\Big\{R_{dc}R_{bd}R_{cb}+R_{dc}R_{ad}R_{ca}+R_{cd}R_{bc}R_{db}+R_{cd}R_{ac}R_{da}\Big\}$$

$$+ |R_{ab}|^2\Big\{|R_{bd}|^2+|R_{bc}|^2+|R_{ad}|^2+|R_{ac}|^2\Big\}\Big]2\pi\int K^2(\alpha)d\alpha$$

$$\lim_{T\to\infty} b_T T\,\mathrm{var}\{|R_{ab}^{(T)}|^2\} = |R_{ab}|^2\Big[1 - |R_{ab}|^2\Big]^2 4\pi\int K^2(\alpha)d\alpha$$

THEOREM I.7

Let $\underline{Z}(t)=\{\underline{M}(t),\ \underline{N}(t)\}$ be an r+s vector-valued stationary point process satisfying assumption I.1 of Appendix I and has the spectral density matrix $F_{\underline{Z}\underline{Z}}(\lambda)$. Suppose $F_{\underline{M}\underline{M}}(\lambda)$ is the spectral density matrix of $\underline{M}(t)$, and is non-singular. Let $K(\alpha)$ satisfying the assumption I.2 of Appendix I. Let the estimate of the partial coherence between the components $,N_a$ and N_b, $(a,b=1,\cdots,s)$, of $\underline{N}(t)$ after removing the linear effects of $\underline{M}(t)$ be given by

$$|R_{N_aN_b\cdot\underline{M}}{}^{(T)}(\lambda)|^2 = \frac{|f_{\epsilon_a\epsilon_b}{}^{(T)}(\lambda)|^2}{f_{\epsilon_a\epsilon_a}{}^{(T)}(\lambda)f_{\epsilon_b\epsilon_b}{}^{(T)}(\lambda)} \qquad \lambda\neq 0 \qquad \text{(I.11)}$$

where

$$f_{\epsilon_a\epsilon_b}{}^{(T)}(\lambda)= f_{N_aN_b}{}^{(T)}(\lambda)-F_{N_a\underline{M}}{}^{(T)}(\lambda)[F_{\underline{M}\underline{M}}{}^{(T)}(\lambda)]^{-1}F_{\underline{M}N_b}{}^{(T)}(\lambda)$$

then the estimate given by expression (I.11) is asymptotically unbiased and normally distributed with

(i) $\quad \mathrm{cov}\{|R_{N_aN_b\cdot\underline{M}}{}^{(T)}(\lambda)|^2, |R_{N_cN_d\cdot\underline{M}}{}^{(T)}(\lambda)|^2\} \sim$ expression (I.9)

(ii) $\quad \mathrm{var}\{|R_{N_aN_b\cdot\underline{M}}{}^{(T)}(\lambda)|^2\} \sim$ expression (I.10)

Proof:-

The proof follows in the same manner as that of Theorem I.6 and by applying a result of Theorem 8.7.1 given by Brillinger(1981, p309).

APPENDIX II

II.1 An algorithm for rapid computation of $J_{N_1N_2}{}^{(T)}(u)$

Let N_1 and N_2 be two spike trains realised on (0,T]. Suppose r_j, $j=1,2,\cdots,N_1(T)$, and s_k, $k=1,2,\cdots,N_2(T)$, are the observed times of the N_1 and N_2 spikes, respectively. The algorithm for a fast computation of the variate $J_{N_1N_2}{}^{(T)}(u)$ with binwidth h may be described as follows:-

1. Store the ordered times r_j and s_k in two separate arrays.
2. Initialize an array JT(NN:NP) of dimension NP-NN+1 to zero. {i.e., (NN,NP) is the interval for the lag "u" in which the estimate is required. It may be set, for example, (-100,100)}
3. Initialize two indicators "a" and "b" to 1 for the first spikes of N_1 and N_2 processes, respectively.
4. For the b^{th} spike of the N_2 process, increment "a" by 1 until it reaches the N_1 spike for which the lag value given by

   $$u = \text{integral part of } (r_a - s_b)/h$$

   lies inside the interval (NN,NP). Retain the indicator "a"
5. Compute the lag value "u" corresponding to the b^{th} spike of N_2 and a^{th} spike of N_1 processes, and set

   $$JT(u) = JT(u)+1.$$

   Repeat step 5 for the subsequent N_1 spikes until $u \geq NP$.
6. Increment "b" by 1 and go to step 4 if $b \leq N_2(T)$, or stop otherwise.

REFERENCES

REFERENCES

ABRAMOWITZ, M. and STEGUN, I.A. (1964): Handbook of Mathematical Functions. National Bureau of Standards, Washington.

AKAIKE, H. (1966): Notes on higher order spectra. Ann. Inst. Statist. Mathematics, 18, 123-126.

BARTLETT, M.S. (1963): The spectral analysis of point processes. Jl. R. Statist. Soc. B. 25, 164-280.

BARTLETT, M. S. (1966): An Introduction to Stochastic Processes, 2nd edn. Cambridge Univ. Press, Cambridge.

BESSOU, P. and PAGES, B. (1975): Cinematographic analysis of contractile events produced in intrafusal fibres by stimulation of static and dynamic fusimotor axons. J. Physiol. 252, 397-427.

BHAT, U.N. (1969): Sixty years of queueing theory. Management, Sci. 15, 280-294.

BLACKMAN, R.B. and TUKEY, J.W. (1959): The Measurement of Power Spectra From the Point of View of Communication Engineering. Dover Publications, Inc., New York.

BLOOMFIELD, P. (1976): Fourier Analysis of Time Series: An Introduction. 1st edn. Wiley, New York.

BOX, G.E.P. (1954) Some theorems on quadratic forms applied in the study of analysis of variance problems. Ann. Math. Statist., 25, 290-302.

BOX, G.E.P and Jenkins, G.M. (1970): Time Series Analysis, Forecasting and Control. Holden-Day, San Francisco, California.

BOYD, I.A. (1962): The structure and innervation of the nuclear bag muscle fibre system and the nuclear chain muscle fibre system in mammalian muscle spindles. Phil. Trans. R. Soc. B., 245, 83-136.

BOYD, I.A. (1980): The isolated mammalian muscle spindle. Trends in Neurosciences, 3, 258-265.

BRACEWELL, R.N. (1986): The Fourier Transform and Its Applications. McGraw-Hill, New York.

BRIGHAM, E.O (1974): The Fast Fourier Transform. Prentice-Hall, New Jersey.

BRILLINGER, D.R. (1970): The identification of polynomial systems by means of higher order spectra. J. Sound. Vib., 12, 301-313.

BRILLINGER, D.R. (1972): The spectral analysis of stationary interval functions. Proc. Seventh Berkeley Symp. Prob. Statist. eds. Le Cam, L., Neyman, J. and Scott, E.L. pp. 483-513. Univ. of California Press, Berkeley.

BRILLINGER, D.R. (1974a): Fourier analysis of stationary processes. Proc. IEEE., 62, 1628-1643.

BRILLINGER, D.R. (1974b): Cross-spectral analysis of processes with stationary increments including the G/G/∞ queue. Ann. Probab., 2, 815-827.

BRILLINGER, D.R. (1975a): Statistical inference for stationary point processes. In Stochastic Processes and Related Topics, Vol. 1 ed. Puri, M.I. pp. 55-79. Academic Press, New York.

BRILLINGER, D.R. (1975b): Estimation of product densities. Comp. Sci. Statist., Ann. Symp. Interface 8th. pp 431-438. UCLA, Los Angeles.

BRILLINGER, D.R. (1975c): The identification of point process systems. Ann. Probab., 3, 909-929.

BRILLINGER, D.R. (1976a): Estimation of second order intensities of a bivariate stationary point process. Jl. R. Statist. Soc., B, 38, 60-66.

BRILLINGER, D.R. (1976b): Measuring the association of point processes: a case history. Am. Math. Monthly, 86, 16-22.

BRILLINGER, D.R. (1978): Comparative aspects of the study of ordinary time series and of point processes. In Developments in Statistics, Vol. 1. pp. 33-134. ed. Krishnaiah, P.R. Academic Press, New York.

BRILLINGER, D.R. (1981): Time Series: Data Analysis and Theory, 2nd edn. Holden-Day, San Francisco, California.

BRILLINGER, D.R. (1983): The finite Fourier transform of a stationary process. In Handbook of Statistics, eds. D.R. Brillinger and P.R. Krishnaiah. Elsevier, Amsterdam.

BRILLINGER, D.R. (1986): Some statistical methods for random process data from seismology and neurophysiology. Technical report No. 84. Dept. of Statistics, Univ. of California, Berkeley.

BRILLINGER, D.R. (1988): The maximum likelihood approach to the identification of neuronal firing systems. Ann. Biomedical Engineering, 16, 3-16.

BRILLINGER, D.R., BRYANT, H.L.,JR., and SEGUNDO, J.P. (1976): Identification of synaptic interactions. Biol. Cyber. 22, 213-228.

BRILLINGER, D.R. and ROSENBLATT, M. (1967): Asymptotic theory of k-th order spectra. In Spectral Analysis of Time Series. ed. Harris, B. pp 153-188. New York: Wiley.

BRILLINGER, D.R. and TUKEY, J.W. (1984): Spectrum analysis in the presence of noise: Some issues and examples. In the collected works of J.W. Tukey, Vol.3, ed. D.R Brillinger. pp. 1002-1141. Monterey, California: Wadsworth.

BRYANT, H.L.,JR., RUIZ MARCOS, A. and SEGUNDO. J.P. (1973): Correlation of neuronal spike discharges produced by monosynaptic connections and common inputs. J. Neurophys., 36, 205-225.

COX, D.R. (1965): On estimation of the intensity function of a stationary point process. Jl. R. Statist. Soc. B., 27, 322-337.

COX, D.R. and ISHAM, V. (1980): Point Processes. Chapman and Hall, London.

COX, D.R. and LEWIS, P.A.W. (1966): The Statistical Analysis of Series of Events. Chapman and Hall, London.

COX, D.R. and Lewis, P.A.W. (1972): Multivariate point processes. Proc. 6th Berkeley Symp. Math. Statist. Prob., 2, 401-448.

CRAMÈR, H. and LEADBETTER, M.R. (1967): Stationary and Related Stochastic Processes. Wiley, New York.

DALEY, D.J. and VERE-JONES, D. (1988): An Introduction to the Theory of Point Processes. Springer, New York.

DOOB, J.L. (1953): Stochastic Processes. Wiley, New York.

DRAPER, N. and SMITH, H. (1966): Applied Regression Analysis. Wiley, New York.

EDGLEY, S.A. and JANKOWSKA, E. (1987): An interneural relay for group I and II muscle afferents in the midlumbar segments of cat spinal cord. J. Physiol. 389, 647-674.

EMONET-DÈNAND, F., LAPORTE, Y., MATTHEWS, P.B.C. and PETIT, J. (1977): On the subdivision of static and dynamic fusimotor axons on the primary endings of the cat muscle spindle. J. Physiol. 268, 827-860.

FEINBERG, S.E. (1974): Stochastic models for single neurone firing trains: a survey. Biometrics, 30, 399-427.

GENTLEMAN, W.M. and SANDE, G. (1966): Fast Fourier transforms - for fun and profit. AFIPS. 1966 Fall joint computer conference, 28, 563-578. Spartan, Washington.

GODFREY, M.D. (1965): An exploratory study of the bi-spectrum of economic time series. Applied Statistics, 14, 48-69.

GOODMAN, N.R. (1963): Statistical analysis based upon a certain multivariate complex Gaussian distribution (an introduction) Ann. Math. Statist. 34, 152-177.

HALLIDAY, D.M. (1986): Application of Point Process System Identification Techniques to Complex Physiological Systems. Ph.D Thesis, Univ. of Glasgow.

HARRIS, T.E., (1978): On the use of windows for harmonic analysis with discrete Fourier transforms, Proc. IEEE, 66, 51-83.

HASSELMANN, K., MUNK, W. and MacDONALD, G.(1963): Bispectra of Ocean waves. In Time Series Analysis, ed. M. Rosenblatt. Wiley, New York.

HAWKES, A.G. (1971): Spectra of some self-exciting and mutually exciting point processes. Jl. R. Statist. Soc. 58, 1, 83-90.

HEIGHT, F.A. (1967): Handbook of the Poisson Distribution. Wiley, New York.

HUNG, G., BRILLINGER, D.R. and STARK, L. (1979): Interpretation of kernels. II. Some signed 1st and 2nd-degree (main diagonal) kernels of the human pupillary system. Math. Biosci. 46, 159-187.

JENKINS, G.M. (1963): Contribution to a discussion of paper by M.S. Bartlett. Jl. R. Statist. Soc., B, 25, 290-291.

JENKINS, G.M. and Watts, D.G. (1968): Spectral Analysis and its applications. Holden-Day, San Francisco.

JOHANSSON, H. (1981): REFLEX control of γ-motoneurones. pp. 55-57. Umeå Univ. Medical Dissertation, Dept. of Physiology, Univ. of Umeå, Umeå, Sweden.

KATZENELSON, J. and GOULD, L.A. (1962): The design of non-linear filters and control systems, I. Inform. Control, 5, 108-143.

KATZNELSON, Y. (1968); Introduction to Harmonic Analysis. Wiley, New York.

KENDALL, M.G. and STUART, A. (1961): The advanced Theory of Statistics, Vol. 2. Griffen, London.

KENDALL, M.G. and STUART, A. (1966): The Advanced Theory of Statistics, 2nd edn. Vol. 1. Griffin, London.

KENDALL, D.G. (1975): The genealogy of genealogy branching processes before (and after) 1873,

Bull. London Math. Soc., 7, 225-253.

KHINTCHINE, A.Y. (1960): Mathematical Methods in the Theory of Queueing. Griffin, London.

KOOPMANS, L.H. (1974): The Spectral Analysis of Time Series. Academic Press, New York.

KOOPMANS, L.H. (1983): A spectral analysis primer. In Handbook of Statistics, Vol. 3. eds. D.R. Brillinger and P.R. Krishnaiah. pp. 169-184, Elsevier, Amsterdam.

KRAUSZ, H.I. (1975): Identification of non-linear systems using random impulse train inputs. Biol. Cybernetics, 19, 217-230.

LEONOV, V.P. and SHIRYAEV, A.N. (1959): On a method for the calculation of semi-invariants. Theor. Prob. Appl., 4, 319-329.

LEWIS, P.A.W. (1970): Remarks on the theory, computation and application of the spectral analysis of series of events. J. Sound Vib., 12, 353-375.

LEWIS, P.A.W. (1972): Stochastic Point Processes. Wiley, New York.

LOTKA, A.J. (1957): Elements of Mathematical Biology. Dover, New York.

MACLAIN, C.G., McWILLIAM, P.N., MURRAY-SMITH, D.J. and ROSENBERG, J.R. (1977): A possible mode of action of static fusimotor axons as revealed by system identification techniques. Brain Res. 135, 351-357.

MARDIA, K.V., KENT, J.T. and BIBBY, J.M. (1982): Multivariate Analysis. Academic Press, London.

MARMARELIS, P.Z. and NAKA, K-I. (1974): Identification of multiple-input biological systems. IEEE Trans. Boimedical Engineering, 21, 2, 88-101.

MARMARELIS, P.Z. (1975): Contribution to a discussion of paper by D.R. Brillinger. Ann. Probab., 3, 924-927.

MATTHEWS, P.B.C. (1962): The differentiation of two types of fusimotor fibre by their effects on the dynamic response of muscle spindle primary endings. Q. Jl. Exp. Physiol., 47, 324-333.

MATTHEWS, P.B.C. (1981): Review lecture: Evolving views on the internal operation and functional role of the muscle spindle. J. Physiol., 320, 1-30.

MATTHEWS, P.B.C. and STEIN, R.B. (1969): The regurarity of the primary and secondary muscle spindle afferent discharges. J. Physiol., 202, 59-82.

MOOD, A.M., GRAYBILL, F.A., BOES, D.C. (1985): Introduction to the Theory of Statistics. London: McGraw-Hill.

NYQUIST, H. (1928): Certain topics in telegraph transmission theory. Trans. AIEE, 617-649.

PAPOULIS, A. (1962): The Fourier Integral and its Applications. McGraw-Hill, New York.

PARZEN, E. (1957): On consistent estimate of the spectrum of a stationary time series. Ann. Math. Statist., 28, 329-348.

PARZEN, E. (1961): Mathematical considerations in the estimation of spectra. Technometrics, 3, 167-190.

PRIESTLEY, M.B. (1987): Spectral Analysis and Time Series. Academic Press, London.

RAMAKRISHNAN, A. (1950): Stochastic processes relating particles distributed in a continuous infinity of states. Proc. Cambridge Phil. Soc. 46, 596-602.

RAMIREZ, R.W. (1974): The Fourier transform's errors are predictable, therefore manageable. Electronics, 47, 96-103.

RAO, C.R. (1984): Linear Statistical Inference and its Applications. Wiley, New York.

RIGAS, A.G. (1983): Point Processes and Time Series Analysis: Theory and Applications to Complex Physiological Problems. Ph.D. Thesis, University of Glasgow.

SAMPATH, G. and SRINIVASAN, S.K. (1977): Stochastic spike trains of single neurones. In Lecture Notes in Biomathematics, Vol. 16, ed. Levin, S. pp 1-188. Springer-Verlag, Berlin.

SCHWALM, D. (1971): Identification of multiple-input multiple-output linear systems by correlation methods. Int. J. Control, 13, 6, 1131-1135.

SHEPHERD, G.M. (1974): The Synaptic Organisation of the Brain, 1st edn. pp. 79-110. Oxford University Press, London.

SHIRYAEV, A.N. (1960): Some problems in the spectral theory of higher-order moments, I. Theory Probab. Applic, 5, p. 265 ·

SRINIVASAN, S.K. (1974): Stochastic Point Processes and their Applications. Griffen, London.

TICK, L.J. (1961): The estimation of transfer functions of quadratic systems. Technometrics, 3, 563-567.

TICK, L.J. (1963): Conditional Spectra, Linear Systems, and Coherency. In Time Series Analysis, ed. Rosenblatt, M. pp. 197-203. Wiley, New York.

TUKEY, J.W. (1959): The estimation of power spectra and related quantities. In On Numerical Approximation. pp. 389-411. Univ. of Wisconsin Press, Madison.

TUKEY, J.W. (1977): Exploratory Data Analysis. Addison-Wesley, U.S.A.

TUKEY, J.W. (1978): Can we predict where "time series" should go next? In Directions in Time Series. eds. D.R. Brillinger and G.C. Tiao. Hayward: Inst. Math. Statist.

WEISBERG, S. (1985): Applied Linear Regression, 2nd edn. Wiley, New York.

WELCH, P.D. (1972): The use of fast Fourier transform for the estimation of power spectra: A method based on time averaging over short, modified periodograms. In Digital Signal Processing, eds. L.R. Rabiner and C.M Rader, IEEE Press, New York.

WESTERGAARD, H. (1968): Contributions to the History of Statistics. Agathon, New York.

WIENER, N. (1958): Non-linear Problems in Random Theory. MIT Press, Cambridge.

WINDHORST, U., and SCHWESTKA, R. (1982): Interactions between motor units in modulating discharge patterns of primary muscle spindle endings. Exptl. Brain Res, 45, 417-427.